UNIVERSITY OF CALIFORNIA
RIVERSIDE

Physical and Chemical Characterization of Particulate and Gas Phase Emissions From Biomass Burning

A Dissertation submitted in partial satisfaction
of the requirements for the degree of

Doctor of Philosophy

in

Mechanical Engineering

by

Seyedehsan Hosseini

December 2012

Dissertation Committee:

Dr. Heejung Jung, Chairperson
Dr. David Cocker
Dr. Marko Princevac
Dr. David Weise

The Dissertation of Seyedehsan Hosseini is approved:

_____

_____

_____

_____

Committee Chairperson

University of California, Riverside

Acknowledgements

Although only my name is on the cover of this dissertation, I could have never finished this thesis and explored the hidden angles of my research without help of many people. My deepest gratitude is to my advisors Dr. Heejung Jung, Dr. David Cocker, and Dr. Wayne Miller for giving me the freedom to explore on my own and guidance to correct my mistakes, teaching me to have confidence to manage projects, question thoughts and express ideas. Their recommendations and instructions have enabled me to assemble and finish the dissertation effectively; I cannot thank them enough.

Next, I would like to thank Dr. David Weise and Dr. Marko Princevac for being a part of my final thesis committee. Dr. Weise gave me tremendous insight into the statistical analysis of data. Dr. Princevac accompanied me during a few of my major field experiments without his help, I could have faced major problem.

My special thanks go to William A. Welch for sharing his field experience with me, providing me hands-on training, and being with me in every single field test that I had.

I will always be grateful to Kathy Cocker, Kurt Bumiller, and Charles Bufalino for accepting me as a member of CECERT family and their help with the test-preparation of laboratory and field experiments. I would also like to thank graduate and undergraduate students (Maryam Hajbabaei, Varalakshmi Jayaram, Poornima Dixit, Li Qi, Ping Tang, Xiaochen Tang, Ajay Chowdry, Harshit Agrawal, M Yusuf Khan, Nicholas Gysel, Daniel Short, Michael Giordano, Shunsuke Nakao, James Gutierrez, and Charles Wardle) for their technical and analytical support.

A special thanks to the U.S. Department of Defense Strategic Environmental Research and Development Program (SERDP) for providing the financial support without which none of this research could have happened.

Finally, I would like to thank my family and friends here and back home for their moral and emotional support I needed to complete my dissertation. Thanks Mom, Dad, Elham, Mehrnoosh, Mehran, and Maryam…

The text of Chapter 3 of this dissertation, in part or in full, is a reprint of the material as it appears in the Journal of Atmospheric Chemistry and Physics, Volume 10, August 2010, doi:10.5194/acp-10-8065-2010

Dedication

I dedicate this work to my parents Masoomeh Irandoost and Jalil Hosseini for their endless love, encouragement, and support all through my life. You taught me perseverance, strength and commitment…

ABSTRACT OF THE DISSERTATION

Physical and Chemical Characterization of Particulate and
Gas Phase Emissions From Biomass Burning

by

Seyedehsan Hosseini

Doctor of Philosophy, Graduate Program in Mechanical Engineering
University of California, Riverside, December 2012
Dr. Heejung Jung, Chairperson

Biomass burning is a dynamic combustion process during which large concentrations of particles and trace gases are released into the atmosphere. Trace gases emitted by fires include significant amounts of carbon monoxide, nitrogen oxides, volatile organic compounds, and long-lived greenhouse gases such as carbon dioxide and methane. This work surveys 18 different vegetation types of southeast (SE) and southwest (SW) U.S. commonly present in prescribed burns. The work provides key factors for prediction of Particulate Matter (PM) and gas phase emissions, and serves as a basis for atmospheric models used for land management. It was found that EC/TC ratio is the best surrogate for prediction of hydrocarbon emissions, performing better than the commonly used Modified Combustion Efficiency (MCE). The emissions factors were observed to decrease exponentially with elemental carbon to total carbon ratio (EC/TC ratio) used as an indirect measure of fire intensity. No regional/vegetation type dependency was observed for hydrocarbon emissions; the emissions tend to change with MCE and fire intensity. PM emission factors were found to correlate with EC/TC ratio or MCE. Metals, anion, and cation emissions were affected most directly by fuel composition.

Table of Contents

List of Figures

List of Tables

List of Abbreviations

%	percentage
°C	degree Centigrade
°F	degree Fahrenheit
1yr	1 year herbaceous
2yr	2 year herbaceous
Ace	Acenaphthene
Acy	Acenaphthylene
AK	Alaska
AMS	Aerodynamic Mass Spectrometer
ANOVA	Analysis of Variance
Ant	Anthracene
APS	Aerodynamic Particle Sizer
ASE	Automated Solvent Extractor
ATOFMS	Aerosol Time-Of-Flight Mass Spectrometer
AZ	Arizona
B[a]A	Benz[a]anthracene
B[a]P	Benzo[a]pyrene
B[b]F	Benzo[b]fluoranthene
B[ghi]P	Benzo[ghi]perylene

B[k]F	Benzo[k]fluoranthene
BTEX	Benzene/Toluene/Ethylbenzene/Xylenes
cas	California sagebrush
CE	Combustion Efficiency
cea	Ceanothus
CFO	Critical Flow Orifice
CFR	Code of Federal Regulations
chg	Chaparral Grass
Chr	chyrsene
chs	Chamise/Scrub oak
CL	Camp Lejeune
cos	Coastal sage scrub
CV	Coefficient of Variation
CPC	Condensation Particle Counter
cuh	Chipped understory hardwood
D[ah]A	Dibenz[ah]anthracene
DMM	Dekati® Mass Monitor
DMPS	Differential Mobility Particle Sizer
DNPH	2,4-Dinitrophenylhydrazine
DoD	Department of Defense
DR	Dilution Ratio

duf	Alaskan duff
EC	Elemental Carbon
EC/TC ratio	Elemental Carbon to Total Carbon ratio
EEPS	Engine Exhaust Particle Sizer
EF	Emission Factor
ER	Emission Ratio
FB	Fort Benning
FHL	Fort Hunter-Ligget
FHUA	Fort Huachuca
Fla	Fluoranthene
Fle	Fluorene
FM	Fuel Moisture
FMPS	Fast Mobility Particle Sizer
FS	Forest Service
FSL	Forest Sciences Laboratory
FTIR	Fast Fourier Transform InfraRed
GC-FID	Gas Chromatograph-Flame Ionization Detector
GC-MS	Gas Chromatograph-Mass Spectrometer
GLM	General Linear Model
GMD	Geometric Mean Diameter
HPLC	High Performance Liquid Chromatograph

HR-TOF-MS	Aerodyne High Resolution Time of Flight Aerosol Mass Spectrometer
IC	Ion Chromatography
ID	Internal Diameter
IMPROVE	Interagency Monitoring of Protected Visual Environments
Ind	indeno[1,2,3-cd]pyrene
LC	Liquid Chromatograph
LDPE	Low Density Polyethylene
LG	Levoglucosan
LHS	Left Hand Side
lit	Pine litter
lit	FB GA litter
LV	Levoglucosan
MAN	Manzanita
man	Manzanita
MC	Moisture Content
MCE	Modified Combustion Efficiency
mch	Maritime chaparral
MEK	MethylEthylKetone
mes	Masticated mesquite
MOUDI	Micro Orifice Uniform Deposit Impactor
MT	Montana

MW	Molecular Weight
Nap	Naphthalene
NICC	National Interagency Coordination Center
NIFC	National Interagency Fire Center
NIOSH	National Institute for Occupational Safety and Health
nm	nanometer
NMHC	Non-Methane Hydrocarbon
NO_x	Nitrogen oxides (NO and NO_2)
oas	Oak savanna
oaw	Oak woodland
OC	Organic Carbon
OM	Organic Matter
OP-FTIR	Open Path - Fast Fourier Transform InfraRed
OVOC	Oxygenated Volatile Organic Compound
PAH	Poly Aromatic Hydrocarbons
PCASP	Passive Cavity Aerosol Spectrometer Probe
PCASP	Passive Cavity Aerosol Spectrometer Probe
PE	Polyethylene
Ph	phenanthrene
PM	Particulate Matter
PM_{10}	Aerosol particles with aerodynamic diameters less than 10 μm

$PM_{2.5}$	Aerosol particles with aerodynamic diameters less than 2.5 μm
PN	Particle Number
poc	Pocosin
PSD	Particle Size Distribution
PTR-MS	Proton-transfer-Reaction mass spectrometry
PTV	Programmable Temperature Vaporizer
PUF/XAD	Polyurethane Foam/XAD
Py	Pyrene
RHS	Right Hand Side
SCAQMD	South Coast Air Quality Management District
SE	Southeast
SERDP	Strategic Environmental Research and Development Program
SMPS	Scanning Mobility Particle Sizer
SOA	Secondary Organic Aerosol
SVOC	Semi Volatile Organic Carbons
SW	Southwest
TC	Total Carbon
TDS	Thermal Desorption Spectroscopy
TEM	Transmission Electron Microscopy
UCR	University of California, Riverside
uh	Understory hardwood

USDA	United States Department of Agriculture
USFS	United States Forest Service
VAFB	Vandenberg Air Force Base
VOC	Volatile Organic Compound
XRF	X-ray Fluorescence
µm	micrometer

Chapter One: Introduction

Biomass burning is recognized as the largest source of Particulate Matter (PM) and the second largest source of trace gases in the atmosphere (Crutzen and Andreae, 1990, Yokelson et al., 1996, Akagi et al., 2011). The addition of PM and trace gases into the atmosphere can significantly alter its chemical composition and balance and result in serious effects on the earth's climate (Simpson et al., 2006, Lapina et al., 2006). The emissions from biomass burning include aerosols, long-lived greenhouse gases (carbon dioxide, methane) and short-lived greenhouse gases (ozone, VOC mainly composed of OVOC (Christian et al., 2004;Christian et al., 2003), nitrous oxides, carbon monoxide and nitrogen oxides (NO_x). The composition and amount of each compound in the complex mixture of emissions depend upon a wide range of parameters related to fuel type, fuel composition, chemical composition, packing ratio, fuel moisture, relative amount of smoldering and flaming, wind direction and speed, and slope (Andreae and Merlet, 2001, Akagi et al., 2011).

Unlike greenhouse gases that can only influence the outgoing radiation, aerosols can lead to both heating/cooling effects depending on a variety of parameters such as particle size distribution, particle morphology and composition of particles. The aerosols can directly influence the climate by adsorbing/scattering solar and earth radiation; they can also affect the climate through acting as cloud condensation nuclei, thus enforcing heating or cooling effects (indirect effect). Particles that are emitted directly from a fire are called primary particles; however, in-situ formation of condensable vapors through oxidation process of

existing VOCs leads to formation of Secondary Organic Aerosols (SOA) (Kroll and Seinfeld, 2008). As a result, the amount of PM can change as the smoke ages through heterogeneous chemistry and gas-particle phase reactions (Mühle et al., 2007, Phuleria et al., 2007). The secondary PM formation can contribute to 60-70% total PM in many rural and urban areas. Concentration of ozone as a reactive oxidant in photochemical processes in the atmosphere can significantly change. For example, large-scale savanna wildfires in Africa can result in regional ozone level of 60-100 ppb, which is similar to the ozone level of polluted urban areas (Fishman et al., 1992, Fishman et al., 1990).

Prescribed burning accounts for a significant fraction of emissions from biomass burning and is defined as a vegetation management tool used to mimic the natural role of fire in managing wildlife habitat, maintaining/restoring ecosystem health, and mitigating wildfire risk by reducing wildland fuel accumulation (Chandler et al., 1983, Wade et al., 1989, Biswell, 1999). The possibility of using prescribed burning as tool in reducing carbon dioxide emissions is investigated by Narayan et al., 2007 and Wiedinmyer and Hurteau, 2010. While an advantageous tool, emissions from prescribed burning can deteriorate air quality by degrading visibility and increasing ambient concentrations of fine particulate matter and ozone levels. Smoke aerosols can alter the radiation budget of the earth, cloud properties and climate (Reid et al., 1998, Haywood et al., 2003, Kaufman and Fraser, 1997, Hobbs et al., 1997). Prescribed burning as a subcategory of biomass burning can considerably change the chemical and physical properties of the atmosphere through short- and long-range transport (Crutzen and Andreae, 1990, Fishman et al., 1992, Fishman et al., 1990, Warneke et al., 2009, Warneke et al., 2010). Epidemiological studies have linked mass concentration of $PM_{2.5}$ to

human morbidity and mortality (Pope III et al., 2009). There is growing evidence of the role of particle size distribution and its adverse effect on human health following transport and deposition of particles (Pope et al., 2006).

Between 2002 and 2011 the annual average area treated with prescribed burning was 599 kHa in the southeastern U.S. (SE: Alabama, Arkansas, Florida, Georgia, Louisiana, Mississippi, North Carolina, South Carolina, Tennessee, and Virginia) and 134 kHa in the southwestern U.S. (SW: Arizona, California, Colorado, New Mexico, Nevada, and Utah) (NIFC, 2012). During the same period, wildfires burned an average of 854 kHa yr-1 in the SW and 215 kHa yr-1 in the SE (NIFC, 2012). In California, approximately 15 kHa is annually treated using prescribed burning.

To acquire a burn permit, land managers are required to assess the effect of prescribed burns and provide air quality assessment to regulators. Smoke dispersion models and chemistry transport models are the necessary tools for simulating the local and regional air quality impact of prescribed burns, however, existence of reliable emission factors that are obtained experimentally based on appropriate combustion parameters are crucial to the accuracy of the predictions.

This study provides insight into physical and chemical properties of emissions from combustion of vegetation types and fuels that are commonly found in the southeast and southwest US and are managed through prescribed burning by Department of Defense (DoD) land managers. A total of 9 different fuel types were collected from SW that included chamise and scrub oak-Figure 1.1, and ceanothus-Figure 1.2 from Ft. Hunter Liggett,

maritime chaparral-Figure 1.3, coastal sage scrub-Figure 1.4, manzanita-Figure 1.6, and California sagebrush-Figure 1.5 from Vandenberg AFB, and oak savannah-Figure 1.7, oak woodland-Figure 1.8, and masticated mesquite-Figure 1.9 from Ft. Huachuca. From the south east, 6 U.S. fuel types were collected, namely, 1 year herbaceous, 2 year herbaceous, pocosin, chipped and unchipped hardwood from Camp Lejuene, 'litter' from Ft. Benning, and Alaskan duff. Samples were harvested in January 2009 and shipped to Missoula, MT to be burned in the laboratory.

The experiments were conducted in February 2009 at the large-scale combustion facility of U.S. Department of Agriculture (USDA) Forest Service, Fire Sciences Laboratory, Missoula, MT. This laboratory allowed us to use a sophisticated suite of instrumentation that is hard to set up in the field.

Chapter 2 investigates the effect of inclusion of low-density polyethylene in piled silvicultural debris on smoke emissions. The results clearly demonstrated that only 3M-octane increased with increasing MCE. The statistical analysis revealed that fluoranthene, pyrene, indeno(1,2,3-cd) pyrene, and M-cyclo pentane were also affected, however no increasing or decreasing trend with increase of polyethylene could be attributed to them.

Chapter 3 explored the size distribution of smoke from 77 burns of SW and SE fuels combusted at the FSL in Missoula, MT. The effect of instantaneous MCE on the geometric mean diameter and discussion of how the instantaneous MCE along with geometric mean diameter can be used to better differentiate between combustion phases are discussed in this chapter.

Detailed chemical and physical characterizations of PM from laboratory combustion of SW and SE fuels are presented in chapter 4. We used Modified Combustion Efficiency (MCE) to calculate relative amount of flaming and smoldering (Ward, D.E. and Radke, 1993). We presented fuel moistures, emission factors of PM mass, aerodynamic particle size distributions by Multiple Orifice Uniform Deposit Impactor (MOUDI), particle number emission factors by Condensation Particle Counter (CPC) and Dekati Mass Monitor (DMM). We also reported emission factors of EC/TC components of PM, particle inorganics by X-Ray Fluorescence spectrometry (XRF) (Na through Pb), inorganic ionic species (Cl^-, K^+, SO_4^{2-}, Na^+, etc.), levoglucosan, and particle-phase Polycyclic Aromatic Hydrocarbons (PAH). We also discussed PAH diagnostic ratios of biomass burning.

Chapter 5 expands on the chapter 4 by investigating emissions of gas-phase PAHs, carbonyls, and select volatile organic compounds. We used statistical analysis to find any regional or fuel type dependency of emission factors, calculated the best linear fit for the plots of emission factors and MCE, and compared them with the same plots vs. EC/TC ratio. We also explored how MCE and EC/TC affected the emission factors, and pointed to the weaknesses of MCE.

Chapter 6 defines a carbon ratio (EC/TC ratio) and demonstrates how it could be used as a surrogate of fire intensity. From 1991, that Ward and Hardy introduced CE and shortly after MCE, this combustion parameter has been widely used for characterization and categorization of fire regimes (smoldering/flaming) and emission factors. However, for many compounds such as gas-phase PAHs and levoglucosan, MCE could not play a fair role similar to what it did for CO, formaldehyde, acetic acid, etc. We will show the ability of

EC/TC in representation of emission factors of the same compounds and compare the results with MCE plots.

Chapter 7 summarizes the results of this study and presents conclusions.

1.1. References

Akagi, S. K., Yokelson, R. J., Wiedinmyer, C., Alvarado, M. J., Reid, J. S., Karl, T., Crounse, J. D., and Wennberg, P. O.: Emission factors for open and domestic biomass burning for use in atmospheric models, Atmos. Chem. Phys., 11, 4039-4072, 10.5194/acp-11-4039-2011, 2011.

Andreae, M. O., and Merlet, P.: Emission of trace gases and aerosols from biomass burning, Global biogeochemical cycles, 15, 955-966, 2001.

Biswell, H.: Prescribed burning in California wildlands vegetation management, Univ of California Pr, 1999.

Chandler, C., Cheney, P., Thomas, P., Trabaud, L., and Williams, D.: Fire in forestry. Volume 1. Forest fire behavior and effects. Volume 2. Forest fire management and organization, John Wiley & Sons, Inc., 1983.

Christian, T., Kleiss, B., Yokelson, R., Holzinger, R., Crutzen, P., Hao, W., Saharjo, B., and Ward, D.: Comprehensive laboratory measurements of biomass-burning emissions: 1. Emissions from Indonesian, African, and other fuels, J. Geophys. Res, 108, 4719, 2003.

Christian, T., Kleiss, B., Yokelson, R., Holzinger, R., Crutzen, P., Hao, W., Shirai, T., and Blake, D.: Comprehensive laboratory measurements of biomass-burning emissions: 2. First intercomparison of open-path FTIR, PTR-MS, and GC-MS/FID/ECD, J. Geophys. Res., 109, D02311, 2004.

Crutzen, P. J., and Andreae, M. O.: Biomass burning in the tropics: Impact on atmospheric chemistry and biogeochemical cycles, Science, 250, 1669-1678, 1990.

Fishman, J., Watson, C. E., Larsen, J. C., and Logan, J. A.: Distribution of Tropospheric Ozone Determined From Satellite Data, J. Geophys. Res., 95, 3599-3617, 10.1029/JD095iD04p03599, 1990.

Fishman, J., Brackftt, V. G., and Fakhruzzaman, K.: Distribution of tropospheric ozone in the tropics from satellite and ozonesonde measurements, Journal of Atmospheric and Terrestrial Physics, 54, 589-597, 10.1016/0021-9169(92)90099-7, 1992.

Haywood, J., Osborne, S., Francis, P., Keil, A., Formenti, P., Andreae, M., & Kaye, P.:. The mean physical and optical properties of regional haze dominated by biomass burning aerosol measured from the C-130 aircraft during safari 2000, J. Geophys. Res, 108, 8473, 2003.

Hobbs, P., Reid, J., Kotchenruther, R., Ferek, R., & Weiss, R.: Direct radiative forcing by smoke from biomass burning, Science, 275(5307), 1777, 1997.

Kaufman, Y. & Fraser, R.: The effect of smoke particles on clouds and climate forcing, Science, 277(5332), 1636, 1997.

Kroll, J. H., and Seinfeld, J. H.: Chemistry of secondary organic aerosol: Formation and evolution of low-volatility organics in the atmosphere, Atmospheric Environment, 42, 3593-3624, 10.1016/j.atmosenv.2008.01.003, 2008.

Lapina, K., Honrath, R. E., Owen, R. C., Val Martín, M., and Pfister, G.: Evidence of significant large-scale impacts of boreal fires on ozone levels in the midlatitude Northern

Hemisphere free troposphere, Geophys. Res. Lett., 33, L10815, 10.1029/2006gl025878, 2006.

Materna, B. L., Jones, J. R., Sutton, P. M., Rothman, N., and Harrison, R. J.: Occupational exposures in California wildland fire fighting, The American Industrial Hygiene Association Journal, 53, 69-76, 1992.

Mühle, J., Lueker, T. J., Su, Y., Miller, B. R., Prather, K. A., and Weiss, R. F.: Trace gas and particulate emissions from the 2003 southern California wildfires, J. Geophys. Res., 112, D03307, 10.1029/2006jd007350, 2007.

Narayan, C., Fernandes, P. M., van Brusselen, J., and Schuck, A.: Potential for CO_2 emissions mitigation in Europe through prescribed burning in the context of the Kyoto Protocol, Forest Ecology and Management, 251, 164-173, 10.1016/j.foreco.2007.06.042, 2007.

Pope III, C., Ezzati, M., & Dockery, D.: Fine-particulate air pollution and life expectancy in the united states, New England Journal of Medicine, 360(4), 376–386, 2009.

Phuleria, H. C., Sheesley, R. J., Schauer, J. J., Fine, P. M., and Sioutas, C.: Roadside measurements of size-segregated particulate organic compounds near gasoline and diesel-dominated freeways in Los Angeles, CA, Atmospheric Environment, 41, 4653-4671, 10.1016/j.atmosenv.2007.03.031, 2007.

Pope, C. A., Young, B., and Dockery, D.: Health effects of fine particulate air pollution: lines that connect, Journal of the Air & Waste Management Association, 56, 709-742, 2006.

Ramdahl, T. & Becher, G.: Characterization of polynuclear aromatic hydrocarbon derivatives in emissions from wood and cereal straw combustion, Analytica Chimica Acta, 144, 83–91, 1982.

Reid, J. S., Hobbs, P. V., Ferek, R. J., Blake, D. R., Martins, J. V., Dunlap, M. R., and Liousse, C.: Physical, chemical, and optical properties of regional hazes dominated by smoke in Brazil, Journal of Geophysical Research, 103, 32059-32032, 1998.

Reinhardt, T. E., and Ottmar, R. D.: Baseline measurements of smoke exposure among wildland firefighters, Journal of occupational and environmental hygiene, 1, 593-606, 2004.

Roberts, R. & Corkill, J.: Grass seed field smoke and its impact on respiratory health, Journal of environmental health, 60, 1–8, 1998.

Roberts, J. M., Veres, P. R., Cochran, A. K., Warneke, C., Burling, I. R., Yokelson, R. J., Lerner, B., Holloway, J. S., Fall, R., and de Gouw, J.: Isocyanic acid in the atmosphere: Sources, concentrations and sinks, and potential health effects, PNAS, 108, 8966-8971, doi: 10.1073/pnas.1103352108, 2011.

Simpson, I. J., Rowland, F. S., Meinardi, S., and Blake, D. R.: Influence of biomass burning during recent fluctuations in the slow growth of global tropospheric methane, Geophys. Res. Lett., 33, L22808, 10.1029/2006gl027330, 2006.

Wade, D. D., Lunsford, J. D., Dixon, M. J., and Mobley, H. E.: A guide for prescribed fire in southern forests, Technical publication R8-TP-US Department of Agriculture, Forest Service, Southern Region, 1989.

Warneke, C., Bahreini, R., Brioude, J., Brock, C. A., de Gouw, J. A., Fahey, D. W., Froyd, K. D., Holloway, J. S., Middlebrook, A., Miller, L., Montzka, S., Murphy, D. M., Peischl, J., Ryerson, T. B., Schwarz, J. P., Spackman, J. R., and Veres, P.: Biomass burning in Siberia and Kazakhstan as an important source for haze over the Alaskan Arctic in April 2008, Geophys. Res. Lett., 36, L02813, 10.1029/2008gl036194, 2009.

Warneke, C., Froyd, K. D., Brioude, J., Bahreini, R., Brock, C. A., Cozic, J., de Gouw, J. A., Fahey, D. W., Ferrare, R., Holloway, J. S., Middlebrook, A. M., Miller, L., Montzka, S., Schwarz, J. P., Sodemann, H., Spackman, J. R., and Stohl, A.: An important contribution to springtime Arctic aerosol from biomass burning in Russia, Geophys. Res. Lett., 37, L01801, 10.1029/2009gl041816, 2010.

Wiedinmyer, C., and Hurteau, M. D.: Prescribed Fire As a Means of Reducing Forest Carbon Emissions in the Western United States, Environmental Science & Technology, 44, 1926-1932, 10.1021/es902455e, 2010.

Yokelson, R. J., Griffith, D. W. T., and Ward, D. E.: Open-path Fourier transform infrared studies of large-scale laboratory biomass fires, J. Geophys. Res, 101, 067-21080, 1996.

Figure 1.1. . Chamise and scrub oak fuel type – Ft. Hunter-Liggett, Photo taken 1/13/2009. Photo by USDA Forest Service

Figure 1.2. Ceanothus fuel type – Ft. Hunter-Liggett, Photo taken 1/13/2009. Photo by USDA Forest Service

Figure 1.3. Maritime chaparral fuel type – Vandenberg AFB, Photo taken 1/14/2009. Photo by USDA Forest Service

Figure 1.4. Coastal sage scrub fuel type – Vandenberg AFB, Photo taken 1/14/2009. Note the presence of black sage (Salvia mellifera). Photo by USDA Forest Service

Figure 1.5. California sagebrush fuel type – Vandenberg AFB, Photo taken 1/14/2009. Photo by USDA Forest Service

Figure 1.6. Manzanita fuel type – Vandenberg AFB. Photo taken 1/14/2009. Photo by USDA Forest Service

Figure 1.7 Emory oak savanna fuel type – Ft. Huachuca. Photo taken 1/21/2009. Photo by USDA Forest Service

Figure 1.8. Emory oak woodland fuel type – Coronado National Forest. Photo taken 1/21/2009 on National Forest because active training prevented access to stands at Ft. Huachuca. Photo by USDA Forest Service

Figure 1.9. Masticated mesquite, desert broom fuel type – Ft. Huachuca. Photo taken 1/21/2009. Photo by USDA Forest Service

Chapter Two: Effect of low-density polyethylene on smoke emissions from debris pile burning

2.1. Abstract

Effect of adding low-density polyethylene (LDPE) to piled silvicultural debris on smoke emissions was examined in a laboratory experiment. 2 kg mixtures of LDPE and wood containing 0, 0.25, and 2.5% LDPE by mass were burned. Gaseous and particulate emissions were sampled during the entire flaming and mixed combustion phases and during a portion of the smoldering phase. An analysis of variance (ANOVA) coupled with general linear model accounting for effects of Modified Combustion Efficiency (MCE), LDPE content and block effect was performed on measured individual compounds. MCE ranging between 0.982 and 0.992 was introduced as a covariate to assist ANOVA better identify the EF differences due to PE inclusion. Out of the 195 compounds analyzed by ANOVA, only EF of 2M-octane showed increase with increasing PE content. Inclusion of PE had an effect on EFs of pyrene and fluoranthene, but no statistical evidence of a linear trend was found. Particulate emission factors showed a marginally significant linear relationship with MCE ($0.05<$p-value0.10). Based on the results of the current and previous studies and literature reviews, inclusion of small mass proportions of LDPE in piled silvicultural debris does not appear to change the emissions produced when low moisture content wood is burned.

2.2. Introduction

Mechanical cutting and piling of woody shrubs and suppressed trees in forests is a common silvicultural practice to reduce fire hazard in the United States (Wenger, 1984). These piles are burned during periods of low fire danger to dispose of the material. In order to improve consumption of the piled debris when it is burned, low-density polyethylene plastic (LDPE) is placed over part or all of the pile to keep the piled debris dry. This practice is designed to dispose of hazardous fuels while minimizing noxious pollutants due to incomplete combustion. LDPE, also known as agricultural plastic, has been used for many years to conserve moisture and reduce weeds in row crops (Linak et al 1989).

In the western United States, silvicultural activities generate approximately 15,000 piles per year (McCorison, 2010), equal to 9000 Mg per year assuming an average of 600 kg fuel per pile. Assuming that the piles are "clean" (91% combustion efficiency) and that 100 percent of the debris is consumed, this level of burning might produce 99 Mg of particulate matter of which 59 Mg are particulate matter less than 2.5 μm in size (Hardy 1998). Current air quality regulations permit the use of burning to dispose of silvicultural piles; however, inclusion of LDPE in silvicultural piles can result in a designation of the pile as waste. Waste burning is not permitted in many areas.

Due to the widespread presence of polyethylene (and other plastics) in municipal waste and the use of combustion as a waste disposal mechanism, several studies have examined the pyrolysis and combustion products of PE (Kolb et al., 1965, Paabo and Levin 1987, Shemwell and Levendis, 2000, Wheatley et al., 1993, Conesa et al., 1994). Paabo and Levin

concluded in their literature review that "the toxicity of the combustion products from various samples of polyethylenes are not highly or unusually toxic." Linak et al. (1989) measured emissions produced by burning unused and used black agricultural plastic under simulated pile and forced air convection burning conditions. They found little difference in the variety and quantity of organic compounds between the burning techniques. Mutagenicity of organic extractives from particulate matter was similar to that from residential wood smoke. Salvador et al (2004) examined the combustion rate and production of polyaromatic hydrocarbons (PAHs) from cardboard and polyethylene mixtures compressed into fuel bricks of various densities and burned in a cone calorimeter. Percentage of LDPE in the mixtures was 0, 5, 10, 20, 33, 70, or 100. Brick density and size of the fuel elements had no effect on PAH emissions. The percentage of LDPE in the brick controlled the PAH emissions; PAH emissions were high when the percentage of LDPE in the composite fuel exceeded 30. Wrobel and Reinhardt (2003) performed a review of bench-scale studies of combustion and pyrolysis of PE and wood.to estimate the impact of PE in silvicultural burn piles on emissions. They concluded that the literature did not provide "an unequivocal answer to whether burning PE plastic would have any greater impact on air quality than the burning of biomass" and suggested that empirical studies be performed to determine the effect of LDPE on emissions from burning piled debris.

We report results of a laboratory study designed to simulate "an experimental burn using the same type of fuel with and without PE sheeting and to quantify the emissions."

2.3. Experimental Techniques and Procedure

2.3.1. Experimental design and fuel description

Wrobel and Reinhardt (2003) report dimensions for a typical silvicultural pile as 2.4 m in diameter and height and containing approximately 600 kg of woody debris. Assuming a cylindrical debris pile with exposed surface area of 23.4 m^2, the mass of a 4 mm LDPE sheet covering the pile was estimated as 0.87 kg. This yields a mass ratio of PE to woody debris of approximately 0.001. In order to determine if inclusion of PE in debris piles has any effect on smoke emissions, mass ratios of 0, 0.0025, and 0.025, were selected to cover the range of possible mass ratios. Idealized debris piles were composed of a 2 kg mixture of 0, 5, or 50 g of PE and manzanita wood (*Arctostaphylos sp.*). The 4 mm PE was shredded to provide homogeneous mixture. Moisture content of two 5 g samples of manzanita wood was determined using a Computrac XL1000 moisture analyzer. Density of the PE and manzanita was assumed 900 and 700 kg/m^3, respectively. Elemental composition of LDPE was assumed from the literature. Elemental composition of the manzanita wood was determined using ultimate analysis. Approximately 5 g of the fuel sample was finely ground and analyzed with a Thermo Fisher Scientific FlashEA 1112 Series Elemental Analyzer.

The experiments were conducted in the fire laboratory at the U.S. Forest Service Pacific Southwest Research Station facility in Riverside. All fires were burned on the same day. Three replications of the three polyethylene treatments (0, 5, 50 g) were arranged in a randomized complete block experimental design to control for possible effects due to changing ambient conditions throughout the day. The fire laboratory is a 12.2 × 12.2 × 11.1

m (L×W×H) metal building with an unconditioned environment. Total air volume of the building is approximately 1380 m^3; a high volume (2.4 m^3 s^{-1}) of air is introduced at low velocity into the building through ducts located along the base of the walls to vent smoke through openings in the roof. Each mixture was burned in a 30 cm diameter mesh walled basket, ignited with a small quantity of ethanol, and the smoke was collected using a small hood and ducting of galvanized steel as shown in Figure 2.1. The entrance to the 0.2 m diameter × 3 m long sampling duct was a 0.30 to 0.20 m reducer. Holes made in a capped tee formed the ports of the sampling duct. The L-shaped sampling probe was oriented with the flow with the sampling opening in downstream direction to limit large particles from entering the sampling probe. A 0.2 m single-speed duct fan inducted 7 m/s airflow inside the duct. Each test lasted 10 minutes after which the fire was extinguished.

The design of the experiment can be represented a fixed effects linear model, which assumes that the effects of various factors on the measured emission factor are, additive:

$$EF_{ij} = \mu + MCE_{ij} + \beta_i + \tau_j + \epsilon_{ij} \qquad \text{Eq. 2.1}$$

where EF_{ij} is the observed emission factor for a particular chemical species, μ is the overall mean emission factor, MCE_{ij} is the modified combustion efficiency, β_i is the effect due to block i (i=1,2,3), τ_j is the effect due to polyethylene (j=1,2,3; 0, 5, 50 g) and ε_{ij} is random error distributed $N\left(0,\sigma^2\right)$. The general linear model (PROC GLM) routine in SAS 9.3 (SAS Institute 2002) was used to estimate the general linear model terms and to test various hypotheses using analysis of variance (ANOVA) with $\alpha = 0.05$ as the significance level.

MCE was included as a covariate because it has been shown to be linearly related to EF (Ward and Radke 1993). Inclusion of the covariate reduces the unexplained variance thus improving the ability of ANOVA to detect differences due to the polyethylene treatment. Similarly, inclusion of the block effect β_j reduces unexplained variance as well. The key hypothesis tests performed are testing to determine if the presence of polyethylene affected EF. The initial hypothesis tested in the analysis of variance is that there is no effect due to polyethylene stated as follows

$$H_0 : \tau_1 = \tau_2 = \tau_3 = 0$$
$$H_1 : \tau_i \neq 0 \text{ for at least one } i \qquad \text{Eq. 2.2}$$

In PROC GLM, we used Type III sum of squares to test the null hypothesis H_0. These sum of squares are also called "independent" sums of squares in that the sum of squares calculated for an effect in Eq. 2.1 is not influenced by other terms in the model. Pairwise comparisons of the treatment effect (τ_j) were performed if the null hypothesis was rejected to determine which of the polyethylene effects differed from each other. The Bonferroni option was used to keep the experiment-wise Type 1 error rate at $\alpha = 0.05$. A Type 1 occurs when we falsely reject the null hypothesis. The general analysis of variance table for the experiment illustrates the sources of variation in the dependent variable (EF_{ij}) and the general form of the statistics used to test the significance of the terms (Table 2.1).

2.3.2. Sampling Media and Instrumentation

A multi-gas analyzer (PG-250, Horiba) was used to measure NO_x, CO, and CO_2 concentrations. Carbonyls were collected at 1.0 LPM onto 2,4-dinitrophenylhydrazine

(DNPH) coated silica cartridges (Water Corp., Milford, MA) . Volatile organic compounds (VOC) were collected at 100 mL min^{-1} onto pre-baked 6 mm OD Gerstel Carbotrap™ 300 Multi Bed glass thermal desorption (TDS) tubes (GERSTEL). Both the DNPH cartridge and TDS tube were located downstream of a Teflon® filter. PAHs) were collected sequentially; first on a quartz filter and then in a column packed with polyurethane foam (PUF) and XAD-4 resin. Particulate matter (PM) was collected on a 47 mm Quartz (2500QAT-UP Tissuquartz™ -Pall Corp.) filter and a pre-weighed Teflon® (2μm pore, Teflo® Company) filters. The quartz filter was preconditioned at 600°C for 5 hours in an oven. The flow rates through Teflon and quartz filters were measured to be 15.6 and 20.1 liter per minute (LPM), respectively.

Particle size distributions (5.6 to 560nm) were measured at 1 Hz using an Engine Exhaust Particle Sizer (EEPS) (TSI, Model 3090). Prior to entering the EEPS, the exhaust sample was diluted with a two stage ejector (TD-110H, Air-Vac Engineering Co.) diluter (Khalek et al., 2000) to a final dilution ratio of 17. Dilution air was cleaned in a series of units that removed water, hydrocarbons and particles (Agrawal et al., 2009).

2.3.3. Off-line Analytical Methods

Samples collected at the test facility were returned to a laboratory for subsequent analysis of carbonyls, VOCs, PAHs, PM mass and composition using the following protocols (Table 2.2):

Carbonyls. DNPH cartridges were analyzed for carbonyls following a modified SAE 930142 HP protocol (Siegel et al., 1993). The cartridges were extracted with acetonitrile and

injected into Agilent 1200 series high performance liquid chromatograph (HPLC) equipped with a diode array detector. The column used was Deltabond AK resolution (200cm × 4.6mm I.D.) with an upstream guard column.

C_3-C10. CarboTrap™ 300 Multi Bed tubes were injected into an Agilent® 6980 GC-FID system via a Gerstel® Thermal Desorption System (TDS) by ramping the injector from -40 to 250 °C at a rate of 6 °C/min. Chromatographic separation and hydrocarbon quantification followed the methods outlined in the SAE 930142 HP protocol (Siegl et al 1993).

PAHs and C_{10}-C_{30} hydrocarbons. Quartz filters and PUF/XAD resin were analyzed according to a modified EPA TO-13A protocol. Both substrates were spiked with deuterated standards and extracted with methylene chloride using a Dionex® Automated Solvent Extractor (ASE-200) (60 min, 250 °C). The extracts were Roto-evaporated and further concentrated with ultra-high pure nitrogen or helium stream. Samples were introduced to an Agilent® 5973 GC-MS using a programmable temperature vaporizer (PTV) large volume inlet (7683 Series).

Elemental and organic carbon: A 1.5 cm^2 quartz filter punch was analyzed for elemental and organic carbon with a Sunset Laboratory (Forest Grove, OR) Thermal/Optical Aerosol Analyzer according to the NIOSH 5040 reference method (NIOSH 5040, 1999).

Particulate mass: The PM mass was determined from the Teflon filter pre- and post-weights. Both tare and final weights were measured with a Cahn C-35 (Madison, WI)

microbalance in a temperature and humidity controlled room following the Code of Federal Regulations (40 CFR Part 1065). Table 2.2 provides summary of offline analysis methods.

2.4. Results and discussion

2.4.1. Fire and Smoke Characteristics

The nine simulated debris piles were burned on Nov 04, 2008. Mean moisture content of the manzanita wood was 30% (dry weight basis), which resulted in good combustion once ignited. Initially, the smoke was observed to be white in color indicating the presence of water vapor. During the early stage of the burn (< 60 s) the PE typically melted and combusted. Approximately three minutes after ignition, the opacity of the white smoke was greatly reduced and the smoke plume became transparent with active flaming up to 2 m in height. Based on fire video records, the presence of PE appeared to decrease the duration of the initial phase (before flaming phase dominated); however, a student t-test conducted on the duration of initial phase results in a marginal significance a p-value of 0.068. After 10 minutes of the burn the amount of visible smoke was reduced significantly and sampling ceased. The 10-minute period captured emissions from the flaming and mixed phases and some of the smoldering phase. While the presence of PE may have reduced the time until the flaming phase was dominant, the PE treatments did not significantly affect MCE.

2.4.2. Fuel Composition Analysis

The carbon content (mass basis) of manzanita wood and polyethylene was determined to be 41.3 % and 86%, respectively (Table 2.3). Using 41 and 86% carbon content for manzanita wood and PE, respectively, addition of 50 g of PE to 1.95 kg of manzanita wood added 43 g

carbon to the 820 g carbon in the wood. The difference between carbon content of the mixture and the wood is less than 1%; therefore, we assume that the fuel composition of the simulated debris pile did not significantly change due to addition of 5 or 50 g of PE.

2.4.3. Emission Factors

Emission factors are normally calculated and reported based on the amount of emissions per unit mass of fuel burned. A common measure of fire combustion efficiency is the Modified Combustion Efficiency (MCE) (Eq. 2.3) (Yokelson et al., 1996),

$$\mathrm{MCE} = \frac{\Delta \mathrm{CO_2}}{\Delta \mathrm{CO_2} + \Delta \mathrm{CO}} \qquad \text{Eq. 2.3}$$

where ΔCO_2 and ΔCO refers to the difference between the measured and background values. MCE was used to find correlation with $PM_{2.5}$ emissions. In this study we did not measure the amount of residual carbon in the char; therefore emission factors are calculated based on the amount of carbon dioxide released over the entire 10 min measurement period. Our data show that basing the calculations on CO_2 is a reasonable approach given that carbon from other sources – carbon monoxide, hydrocarbons, and PM – is much smaller (<1%) than the carbon released as carbon dioxide.

Jenkins and Ebeling (1985) reported that the carbon content of manzanita is 48.2%. The carbon content of manzanita wood and foliage has also been reported as 48 and 53% (McMeeking et al., 2009, Burling et al., 2010) suggesting differing proportions of wood and foliage, different species or individual vegetation, site differences, or collection time, etc. A carbon content of 41.3% was determined by ultimate analysis of the manzanita for this study (Burling et al., 2010, Hosseini et al., 2010, Hosseini et al., 2012). Because all the emission

factors in this study were based on kg CO_2, a factor of 1.8 can be used to convert all the emission factors from per kg CO_2 to per kg fuel.

To our knowledge, many of these compounds are reported for this fuel type for the first time. These values are the EF_{ij} (Eq. 2.1) which were then subjected to analysis of variance and hypothesis testing to determine the significance of the independent terms (RHS) in Eq. 2.1. ANOVA was used to test the significance of the effects in Eq. 2.1 on the EF for each of these 195 compounds (Table 2.4)

2.4.3.1. Carbon Monoxide and Nitric Oxides

Gas phase emissions were integrated over each burn and normalized against fire-average integrated CO_2. As shown in Table 2.5, average CO emission factors were 13.5±2.4, 12.6±2.6, and 9.9±1.4 g/kg CO_2 for 0, 0.25, and 2.5 wt% PE, respectively (average ± standard error). While the CO emissions reduced 7 and 27% at 0.25 and 2.5 wt% PE, the average values were not significantly different. We attribute this to better combustion efficiency of these burns (referred to a higher MCE as shown in Table 2.5). Note that the multi-gas analyzer got saturated for a portion of 0 wt% PE tests for CO. Therefore, actual CO emission factors in case of 0% PE should be higher than reported here and the reduction of CO emissions with inclusion of PE against 0wt% PE burn should be higher than we are reporting. The coefficients of variation (CVs) for this study were 18, 21, and 14%; the high values reflect the difficulty of replicating burn conditions. Note that reduction of CO emission factor due the use of PE cover for actual silvicultural piles is very effective due to the fact that fuel without PE is exposed to moisture which causes more smoldering

combustion and ultimately CO emissions. In this study, we did not consider moisture effects caused by PE cover.

Table 2.5 presents NO_x emission factors as NO of 1.53±0.09, 1.83±0.05 and 1.95±0.07 g/kg CO_2 for 0, 0.25 and 2.5 of PE, respectively. NO emissions increased 19 and 28% at 0.25 and 2.5%. NO_x is predominantly released during the flaming phase of the burns. Past research suggested that NO_x emissions in biomass burning depend on fuel nitrogen content (Andreae and Merlet, 2001, McMeeking et al., 2009). However, Burling et al., 2010 showed that for a specific fuel type, NO_x emissions normalized to fuel nitrogen is correlated with modified combustion efficiency (MCE). Since the fuel nitrogen content was (~1 wt.%) and Linak et al. (1989) measured no NO_x formation from combustion of agricultural plastic, it is inferred that the increase in NO_x formation might be due to increase in combustion efficiency with addition of PE. However, no significant difference in the

2.4.3.2. Gaseous C_3-C_{12}

In addition to criteria pollutants, emission factors for selected volatile and semi-volatile hydrocarbons with carbon numbers between C_3-C_{13} were measured (Table 2.8 and Table 2.9). Overall, the results show that propane, trans-2 pentene, 2-methyl-propene made up ~19-30% of the total aliphatic hydrocarbons. These emission factors fall within the lower range of the values reported in the literature. For example, EF of butane in this study was 5.0-8.5 mg/kg fuel burned, while McDonald et al., 2000a reported 1.7-17.4 mg/kg fuel for wood combustion (ponderosa pine, oak, etc.) in fireplace/woodstove and Schauer et al., 2001 reported 28.9 mg/kg fuel burned for Australian woods. Pentene ranged between 4.4-

9.9 mg/kg compared to 8.69-13.12 mg/kg of McDonald et al., 2000a and 4.7 mg/kg of Schauer et al., 2001. Our EFs are lower most likely due to high MCE values of the burns in the current study and more complete combustion of the fuel. An ANOVA analysis indicated that only 3M-octane was significantly affected and increased by the increase in PE content ($p<0.01$) and the emissions of the rest of alkanes, cycloalkanes, alkenes, and cyclo-alkenes were independent of the amount of PE added to the fuel.

2.4.3.3. Diolefins

Diolefins were 1-3% of total VOCs mass and emission factors of 1,3- butadiene are in the range of 2.6 -15.7 mg/kg CO_2 released with an average of 7.21 mg/kg CO_2 (Table 2.9).In mg/kg fuel burned, the 1,3-butadiene emission value is almost half of the lower range of McDonald et al., 2000a for 2.5wt% PE (28.7 vs. 62 mg/kg fuel burned) and a factor of ten smaller for the other two cases. The 0.25% PE case is one-third of 1,3-butadiene EF of 117 mg/kg fuel burned reported by Schauer et al., 2001. No trend with increasing PE content is observed. No statistically significant trend or difference with increasing PE content was recognized in this group.

2.4.3.4. Monocyclic aromatics

Emission factors of mono-cyclic-aromatic hydrocarbons are also presented in Table 2.9. For this group, benzene is about 70% of the total monocyclic aromatic fraction, a value consistent with the findings of Schauer (2001) in which there were no PE added to the wood. Although the average values decreased with increasing PE content, no significant differences were observed between different treatment groups.

Emission factors of benzene, toluene and xylene isomers (*m*, *p* and *o*) are shown in Table 2.8. The measured mass for the sum of BTEX group (210-270 mg/kg fuel burned) is comparable with lower range values reported by McDonald et al., (2000a) and Hedberg et al., (2002) of 420-1608 and 215-7481 mg per kg fuel burned, respectively. The average toluene/benzene ratio for this study was 0.24, 0.25, and 0.24 for 0, 0.25%, and 2.5% PE, respectively comparable with 0.26-0.58 reported by McDonalds et al. The same ratio from the study of Hedberg et al, 2002 was 0.4 inferring relatively higher toluene in that study.

PAH EFs are divided into two sub-categories of particle-phase and gas-phase PAHs (Table 2.7). Among gas-phase PAHs, naphthalene, acenaphthylene, phenanthrene are the most abundant, and among particle-phase PAHs benzo(ghi)perylene, benzo(a)pyrene, indeno(1,2,3-cd)pyrene had the highest emission rates. The sum of gas phase PAHs decreased with increasing PE content; however, no significant difference was observed. ANOVA analysis revealed that the particle phase fluoranthene and pyrene were affected by inclusion of PE ($0.01<p<0.05$), however no statistical evidence of increasing/decreasing trend could be found for these compounds. The differences in treatment values of EFs of Fluorene, Phenanthrene, and anthracene were marginally significant ($0.05<$p-value<0.10). It is worth to note that Jenkins et al., (1996) showed that a more robust vigorous fire might lead to lower formation rate of PAH due to the shortening of initial smoldering phase.

2.4.3.5. Carbonyls

Only formaldehyde, acetaldehyde, and hexanal made up the 50% of the aldehyde and ketones for this study (Table 2.6). Inclusion of PE in the wood did not affect the ratio of

carbonyls to VOCs. Formaldehyde was emitted at the highest rate of all carbonyls with the average emission factor of 372±138, 594±288, and 265±79 mg/kg CO_2 for 0, 0.25 and 2.50% PE, respectively. Emission factors for acetaldehyde, and hexanal were next highest rates. Aldehydes and ketones were not affected by addition of PE.

2.4.3.6. Particulate Matter:

The fire average $PM_{2.5}$ emission factors for the three cases of 0.0, 0.25, and 2.50 wt% PE are presented in Table 2.5. On average, the PM emission factors did not show any decreasing or increasing pattern with increasing PE content and were 1.97±0.50, 1.85±0.37, and 2.01±0.50 g/kg CO_2 for cases of 0.0, 0.25 and 2.5wt% PE, respectively. Considering the variations, different PE contents didn't show any pattern of increasing or decreasing PM mass emission factors of the particulate matter mass and the differences can be attributed to observed variations in MCE ($0.05<$p-value<0.10).

The particulate matter mass emission factors are plotted against MCE in Figure 2.3. As can be seen, the calculated MCEs are very high (ranged between 0.983 and 0.993) due to the fact that flaming/mixed phase was dominant during the 10 min measurement time. The EF_{PM} was weakly correlated to MCE ($R^2=0.50$) with all data points but when we excluded one outlier the correlation became much better ($R^2=0.93$).

Reconstructed mass of particulate matter (PM) based on EC/OC versus PM mass from gravimetric measurements of Teflon filters is shown in Figure 2.4. This was done assuming PM mass is equal to mass of organic matter (OM) added to mass of elemental carbon (EC) ($EF_{PM} = EF_{OC} \times \text{factor} + EF_{EC}$). Using OM-to-OC ratio of 1.55 as suggested by McMeeking

et al. 2009 and Leving et al., 2010 resulted in a best linear fit with slope of 1.00 and coefficient of variation of 0.87 between the two variables of gravimetric PM mass EF and constructed PM mass EF. The factor used is also within the range suggested by Reid et al., 2005 for biomass burning.

2.4.3.7. PM size distributions

Figure 2.5 represents the particle number size distributions obtained by EEPS. These two contour graphs are for two typical burns. Hosseini et al., (2010) showed that the Geometric Mean Diameter (GMD) of the particle size distribution is a function of instantaneous modified combustion efficiency, and that GMD decreases from flaming to smoldering phase. For 0% PE case intermittent increase of GMD is shown until 80s reflecting sporadic flame spread. From 80 to ~200s GMD shows continuous and smooth decrease due to more stable flame spread and combustion phase change into vigorous flaming phase. Flaming phase reduces GMDs for two reasons: First due to strong buoyant flow resulting in higher entrainment and therefore less particle growth, second better oxidation of hydrocarbons which can lead to larger particles unless oxidized. Total particle concentrations decreases as the combustion progresses from flaming to smoldering phase. For 2.5 wt% PE case GMD increases smoothly in a shorter time span reflecting stable flame spread due to the inclusion of shredded PE sheets. Past 100s total particle concentrations decrease as combustion progresses from flaming to smoldering phase. Overall inclusion of PE shortened flame spread period and advent of flaming phase, which may have led to better combustion efficiency or MCE (p-value of 0.07).

2.5. Summary and Conclusions

In this study, the effects of adding polyethylene plastic to piled silvicultural debris on smoke emissions were examined using a simplified laboratory experiment. Shredded LDPE was mixed with manzanita wood to produce 2 kg piles containing 0, 0.25, and 2.5% LDPE by mass. The piles were ignited and gaseous and particulate emissions were sampled during the entire flaming and mixed combustion phases and during a portion of the smoldering phase.

Based on analysis of variance, the PE treatment affected emissions of only 2 of the 195 compounds (Table 2.4). τ_j increased as the amount of polyethylene increased for 3M-Octane (Eq. 2.1). Increase in polyethylene content had an effect on the emissions of fluoranthene and pyrene in particle form, but there was no statistical evidence of a linear trend in the effect. MCE was a significant covariate for three compounds as well and ranged from 0.982 to 0.992. Although CO emissions reduced 7 and 27% and NO_x emissions increased 19 and 28% at 0.25 and 2.5 wt% PE, the variations in the data was such that the statistical tests could not detect differences due to increase in PE content. We attributed this to better combustion efficiency when PE is added to debris piles. Particulate emission factors also showed statistically marginal significance in relation with MCE regardless of PE content. The rest of PAHs and Carbonyls did not show any trend with PE contents. Diolefins were 1-3% of total VOCs mass and showed no trend with PE contents.

In summary, changes in criteria pollutant concentrations and selected compounds could be attributed to improve in combustion efficiency with addition of small amount of PE. These results support the conclusion of an earlier study in which negligible effect of LDPE on

PAH emissions was observed in compressed mixtures of cardboard and LDPE until LDPE comprised more than 30% of the mass of the mixture. Based on the results of this study, previous studies and literature reviews, inclusion of small proportions (of total mass) of low density polyethylene in piled silvicultural debris does not appear to significantly change the emissions produced when low moisture content wood is burned. The study did not examine the influence of LDPE on emissions of wet woody fuels nor did it quantify effects on burning rates.

2.6. Acknowledgements

We appreciate the persistence of Mike McCorison, the Forest Service's southern California air resource specialist in bringing this problem to light and seeking support for the work. The financial support provided by the Hazardous Fuels programs of the Angeles, Cleveland, Los Padres, and San Bernardino National Forests and by SERDP project SI-1648 "New Tools for Estimating and Managing Local/Regional Air Quality Impacts of Prescribed Burns" helped make this project possible. The logistical support provided by Forest Service technicians Joey Chong and David Kisor prior to and during the experimental phase of this project is also appreciated.

2.7. References

Andreae, M. O., and Merlet, P.: Emission of trace gases and aerosols from biomass burning, Global Biogeochemical Cycles, 15, 955-966, 2001.

Bowes, P. C.: Smoke and toxicity hazards of plastics in fire, Annals of Occupational Hygiene, 17, 143, 1974.

Burling, I., Yokelson, R. J., Griffith, D. W., Johnson, T. J., Veres, P., Roberts, J., Warneke, C., Urbanski, S., Reardon, J., and Weise, D.: Laboratory measurements of trace gas emissions from biomass burning of fuel types from the southeastern and southwestern united states, 2010.

Christian, T. J., Kleiss, B., Yokelson, R. J., Holzinger, R., Crutzen, P. J., Hao, W. M., Saharjo, B. H., and Ward, D. E.: Comprehensive laboratory measurements of biomass-burning emissions: 1. Emissions from Indonesian, African, and other fuels, J. Geophys. Res, 108, 4719, 2003.

Conesa, J. A., Font, R., Marcilla, A., and Garcia, A. N.: Pyrolysis of polyethylene in a fluidized bed reactor, Energy & fuels, 8, 1238-1246, 1994.

Elomaa, M., and Saharinen, E.: Polycyclic aromatic hydrocarbons (pahs) in soot produced by combustion of polystyrene, polypropylene, and wood, Journal of applied polymer science, 42, 2819-2824, 1991.

EPA. 1995. Section 13.1, Wildfires and Prescribed Burning. In: Compilation of Air Pollutant Emission Factors, Volume 1: Stationary Point and Area Sources, Fifth Edition, AP-42. U.S.

Environmental Protection Agency, Office of Air Quality Planning and Standards. Research Triangle Park, North Carolina.

Fine, P. M., Cass, G. R., and Simoneit, B. R. T.: Chemical characterization of fine particle emissions from fireplace combustion of woods grown in the northeastern United States, Environmental Science & Technology, 35, 2665-2675, 2001.

Hardy, C.C.: Guidelines for estimating volume, biomass, and smoke production for piled slash. General Technical Report PNW-364, Portland, OR: U.S. Department of Agriculture, Forest Service, Pacific Northwest Research Station. 28 p. http://treesearch.fs.fed.us/pubs/26244

Harshit Agrawal, Quentin G.J. Malloy, William A. Welch, J. Wayne Miller, David R. Cocker III, In-use gaseous and particulate matter emissions from a modern ocean going container vessel, Atmospheric Environment, Volume 42, Issue 21, July 2008, Pages 5504-5510, ISSN 1352-2310, 10.1016/j.atmosenv.2008.02.053.

Hedberg, E., Kristensson, A., Ohlsson, M., Johansson, C., Johansson, P. A., Swietlicki, E., Vesely, V., Wideqvist, U., and Westerholm, R.: Chemical and physical characterization of emissions from birch wood combustion in a wood stove, Atmospheric Environment, 36, 4823-4837, 2002.

Hosseini, S., Li, Q., Cocker, D., Weise, D., Miller, A., Shrivastava, M., Miller, J., Mahalingam, S., Princevac, M., and Jung, H.: Particle size distributions from laboratory-scale biomass fires using fast response instruments, Atmospheric Chemistry and Physics, 10, 8065-8076, 2010.

Jenkins, B.M., and Ebeling, J.M.: Thermochemical properties of biomass fuels, California Agriculture, p. 14-16, May-June, 1985.

Jenkins, B. M., Jones, A. D., Turn, S. Q., and Williams, R. B.: Emission factors for polycyclic aromatic hydrocarbons from biomass burning, Environmental Science & Technology, 30, 2462-2469, 1996.

Khalek, I., Kittelson, D. B., and Brear, F.: Nanoparticle growth during dilution and cooling of diesel exhaust: Experimental investigation and theoretical assessment, 2000.

Kolb, B., Kemmner, G., Kaiser, K. H., Cieplinski, E. W., and Ettre, L. S.: Pyrolysis-gas chromatography with linearly programmed temperature packed and open tubular columns. The thermal degradation of polyolefins, Fresenius' Journal of Analytical Chemistry, 209, 302-312, 1965.

Levin, E., McMeeking, G., Carrico, C., Mack, L., Kreidenweis, S., Wold, C., Moosm¸ller, H., Arnott, W., Hao, W., and Collett Jr, J.: Biomass burning smoke aerosol properties measured during fire laboratory at Missoula experiments (flame), Journal of Geophysical Research, 115, D18210, 2010.

Li, C. T., Lee, W. J., Mi, H. H., and Su, C. C.: PAH emissions from the incineration of waste oily sludge and PE plastic mixtures, Science of the total environment, 170, 171-183, 1995.

Linak, W.P., Perry, E., Williams, R.W., Ryan, J.V., and DeMarini, D.M.: Chemical and biological characterization of products of incomplete combustion from the simulated field

burning of agricultural plastic, Journal of the Air Pollution Control Association, 39, 836-846, 1989.

McCorison, M. personal communication, U.S. Forest Service, April, 2010

McDonald, J. D., Zielinska, B., Fujita, E. M., Sagebiel, J. C., Chow, J. C., and Watson, J. G.: Fine particle and gaseous emission rates from residential wood combustion, Environmental science & technology, 34, 2080-2091, 2000a.

Mcdonald, J. D., Zielinska, B., Fujita, E. M., Sagebiel, J. C., Chow, J. C., and Watson, J. G.: Fine Particle and Gaseous Emission Rates from Residential Wood Combustion Fine Particle and Gaseous Emission Rates from Residential Wood Combustion, Environmental Science & Technology, 10.1021/es9909632, 2000b.

McMeeking, G. R., Kreidenweis, S. M., Baker, S., Carrico, C. M., Chow, J. C., Collett Jr, J. L., Hao, W. M., Holden, A. S., Kirchstetter, T. W., and Malm, W. C.: Emissions of trace gases and aerosols during the open combustion of biomass in the laboratory, Journal of Geophysical Research, 114, D19210, 2009.

Paabo, M.; Levin, B.C.: A literature review of the chemical nature and Toxicity of the decomposition products of polyethylenes, Fire and materials, 11, 55-70, 1987

Reid, J. S., Koppmann, R., Eck, T. F., and Eleuterio, D. P.: A review of biomass burning emissions part ii: Intensive physical properties of biomass burning particles, Atmos. Chem. Phys, 5, 799-825, 2005.

Salvador, S., Quintard, M., and C. David.: Combustion of a substitution fuel made of cardboard and polyethylene: influence of the mix characteristics—experimental approach, Fuel, 83, 451-462, 2004.

Schauer, J. J., Kleeman, M. J., Cass, G. R., and Simoneit, B. R. T.: Measurement of emissions from air pollution sources. 3. C-1-c-29 organic compounds from fireplace combustion of wood, Environmental Science & Technology, 35, 1716-1728, 2001.

Shemwell, B. E., and Levendis, Y. A.: Particulates generated from combustion of polymers (plastics), Journal of the Air & Waste Management Association, 50, 94-102, 2000.

Siegl, W.O., Richert, J.F.O., Jensen, T.E., Schuetzle, D., Swarin, S.J., Loo, J.F., Prostak, A., Nagy, D., Schlenker, A.M., 1993. Improved emissions speciation methodology for phase II of the auto/oil air quality improvement research program—hydrocarbons and oxygenates. SAE Paper 930142.

Siegl, W. O., Richert, J. F. O., Jensen, T. E., Schuetzle, D., Swarin, S. J., Loo, J. F., Prostak, A., Nagy, D., and Schlenker, A. M.: Improved emissions speciation methodology for phase ii of the auto/oil air quality improvement research program - hydrocarbons and oxygenates, in, Copyright 1993 Society of Automotive Engineers, Inc., 1993.

Wang, Z., Wang, J., Richter, H., Howard, J. B., Carlson, J., and Levendis, Y. A.: Comparative study on polycyclic aromatic hydrocarbons, light hydrocarbons, carbon monoxide, and particulate emissions from the combustion of polyethylene, polystyrene, and poly (vinyl chloride), Energy & fuels, 17, 999-1013, 2003.

Wenger, K.F.: Forestry Handbook, 2nd ed. Wiley and Sons, 1335 p., 1984

Wheatley, L., Levendis, Y. A., and Vouros, P.: Exploratory study on the combustion and PAH emissions of selected municipal waste plastics, Environmental science & technology, 27, 2885-2895, 1993.

Wrobel, C., and Reinhardt, T.: Review of potential air emissions from burning polyethylene plastic sheeting with piled forest debris, 2003.

Yokelson, R. J., Griffith, D. W. T., and Ward, D. E.: Open-path Fourier transform infrared studies of large-scale laboratory biomass fires, J. Geophys. Res, 101, 67-21080, 1996.

(a) 0.25 wt% PE (b) 2.50 wt% PE

Figure 2.1. figure (a) represents a picture of the fuel bed containing manzanita mixed with 0.25 wt% PE. In figure (b) the fuel bed containing manzanita mixed with 2.50 wt% is shown.

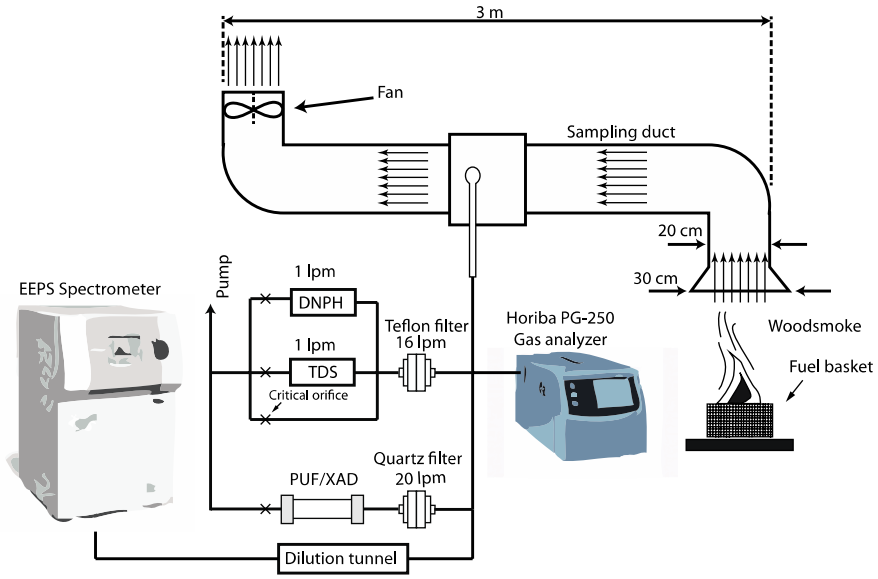

Figure 2.2. Schematic illustration of experimental setup

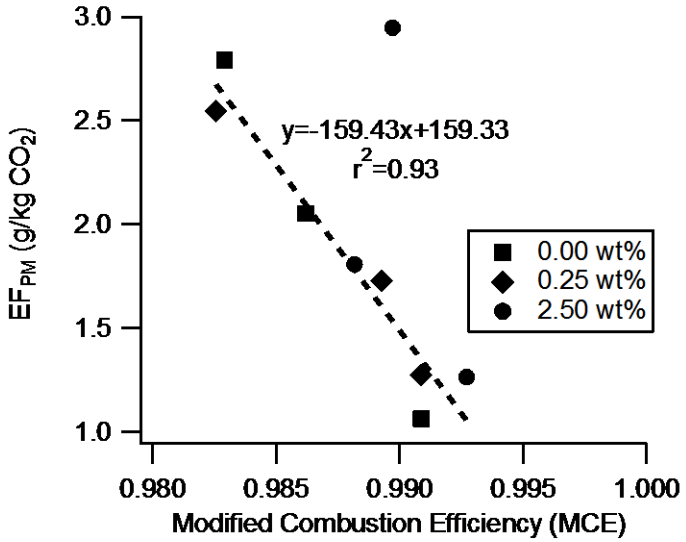

Figure 2.3. Particulate matter mass emission factor (g/ kg CO_2) as function of Modified Combustion Efficiency (MCE)- R^2 is calculated excluding the outlier point (including all points R^2=0.50).

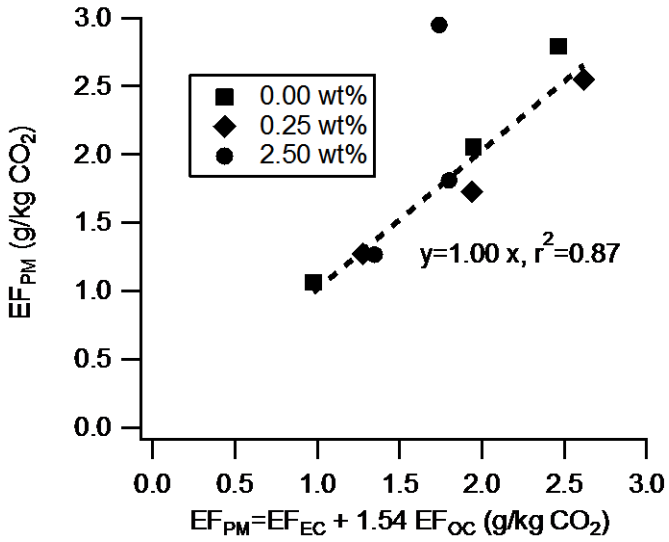

Figure 2.4. EF_{PM}.is plotted versus re-constructed PM mass based on the emission factors of Elemental Carbon (EC) and Organic Carbon (OC); Solid line shows the regression line with slope 1 and correlation coefficient of 0.87.

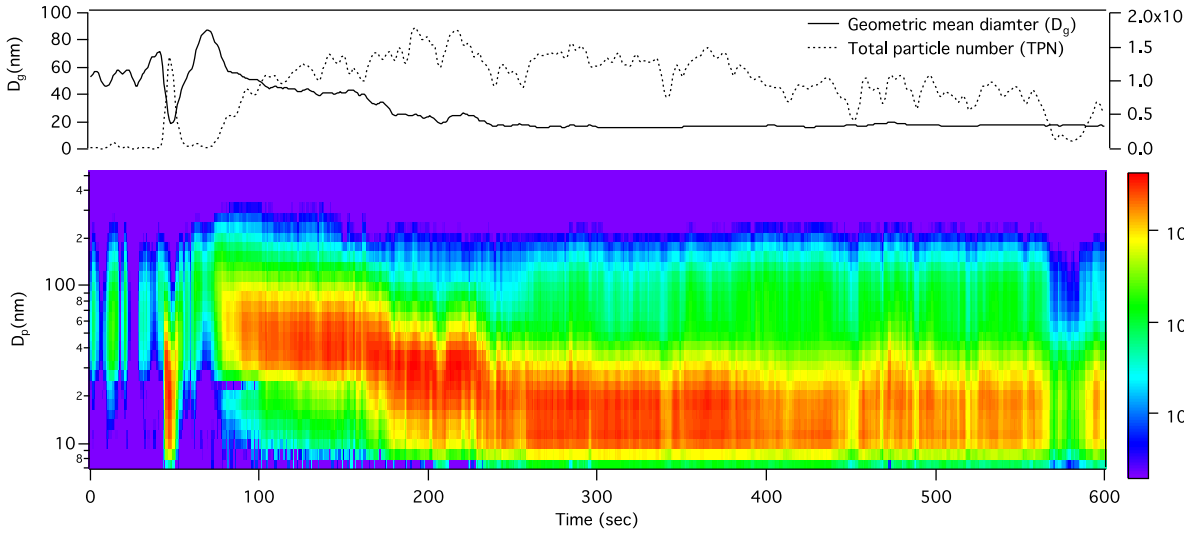

(a) 0.0 wt% PE

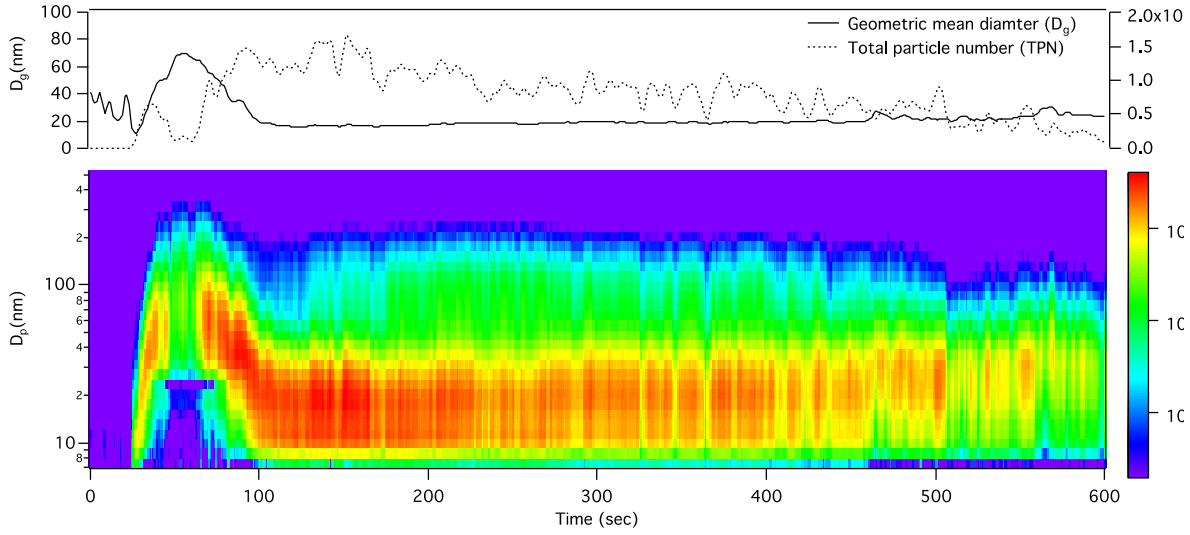

(b) 2.5 wt% PE

Figure 2.5. Contour graphs shown for two different PE contents; (a) 0.0 wt% (b) 2.5 wt% PE. The data is captured using a Model 3090 Engine Exhaust Particle Sizer (EEPS)

Table 2.1. General form of analysis of variance used to test effect of polyethylene plastic on emission factors produced by the burning of manzanita wood.

Source	df[1]	Sum of squares	Mean square	F-statistic
Model	5	SS(model)	$MS(model) = SS(model) / df$	$\frac{MS(model)}{MS(error)}$
MCE	1	SS(MCE)	$MS(MCE) = SS(MCE) / df$	$\frac{MS(MCE)}{MS(error)}$
Block	2	SS(β)	$MS(\beta) = SS(\beta) / df$	$\frac{MS(\beta)}{MS(error)}$
Polyethylene	2	SS(τ)	$MS(\tau) = SS(\tau) / df$	$\frac{MS(\tau)}{MS(error)}$
Error	3	SS(error)	$MS(error) = SS(error) / df$	
Total Corrected	8	SS(total)		

[1] Degrees of freedom. The interested reader is referred to any general statistics text (e.g. Cox 2012) for further explanation of the composition of an analysis of variance table.

Table 2.2. Summary of sampling media, analytes and method of analysis

Sample	Analyte	Method
Teflon Filters	PM mass	Code of Federal Regulation (40 CFR Part 1065)
Quartz Filters	PAHs and EC/OC	NIOSH 5040 (1996), EPA TO-13A protocol
DNPH cartridges	Carbonyls	SAE 93142 HP protocol
TDS tubes	VOCs C4-C12	Improved Emissions Speciation Methodology for Phase II of the Auto/Oil Air Quality Improvement Research Program- Hydrocarbons and Oxygenates (Siegl et al 1993)
PUF/XAD cartridges	PAHs / alkanes	EPA TO-13A protocol

Table 2.3. Mass-based fuel component and fuel bed elemental composition.

Element	Fuel[1]			
	PE[2]	Manzanita	5g PE pile[3]	50 g PE pile
C	86.00	41.30	41.41	42.42
N	0.00	1.00	1.00	0.98
O	0.01	42.70	42.59	41.64
H	13.90	5.74	5.76	5.94
S	0.40	0.20	0.20	0.20

[1] Elemental composition determined using a Thermo Fisher Scientific FlashEA 1112 Series Elemental Analyzer. Values are percentage of total mass.
[2] Mean of published information.
[3] Estimated mass-weighted composition. Example: $\frac{5(86)+1995(41.3)}{2000} = 41.41$

Table 2.4. Chemical species for which polyethylene plastic and modified combustion efficiency had an effect on emissions produced by burning manzanita wood

Chemical species	MCE[1]	PE treatment	Trend[2]
PM mass(particle)	M		
Acetone(gas)	M		
Anthracene(particle)	M		
Benzo(a)pyrene(particle)	M		
Dibenzo(a,h)anthra. (particle)	M		
Fluorene (gas)		M	
Phenanthrene(gas)		M	
Anthracene(gas)		M	
Fluoranthene(gas)		*	
Pyrene(gas)		*	

Chemical species	MCE[1]	PE treatment	Trend[2]
Indeno(1,2,3-cd)pyrene (gas)		M	
Propane(gas)	M		
3,3-DM-Pentane (gas)	M		
3,3-DM-Hexane(gas)	*		
E-CycHexane(gas)	M		
3M-Octane(gas)		**	I
M-CycPentane(gas)	*	M	
1M-3E-Benzene(gas)	M		

[1]MCE- test of significance of modified combustion efficiency as a covariate, Means- test of equality of means for polyethylene levels

$$Prob > F - value = \begin{cases} **, p < 0.01 \\ *, 0.01 < p < 0.0.5 \\ M, 0.05 < p < 0.1 \end{cases}$$

[2]Test to determine if mean EF responds to change in amount of polyethylene,

$$\begin{cases} I, PE_{50} - PE_0 > 0, p < 0.05 \\ D, PE_{50} - PE_0 < 0, p < 0.05 \end{cases}$$

Table 2.5. Emission factor of gases CO and NOx and also Particulate Matter (PM) mass, Elemental Carbon (EC), and Organic Carbon (OC) in g per kg CO_2.

Species	**0 wt% PE**	**0.25 wt% PE**	**2.50 wt% PE**	**Other ref. (g/kg fuel burned)**
MCE	0.9867±0.0023	0.9876±0.0025	0.9902±0.0013	0.948±0.007[a], 0.930±0.029[b]
CO	13.5±2.4	12.6±2.6	9.9±1.4	64.3±8.0[a]
NO_x as NO	1.531±0.093	1.827±0.054	1.955±0.066	2.67±0.21 [a]
PM mass	1.97±0.50	1.85±0.37	2.01±0.50	3.61±1.17 [a*], 23.5±25.9[b], 3.3-11.4[c], 2.5-9.0[d], 0.1-2.5[e], 5.1-9.5[f]
EC	0.379±0.062	0.536±0.199	0.575±0.166	0.51±0.18 [a], 0.35±0.31[b], 0.22-3.56[c], 1.4-3.2[f]
OC	0.91±0.24	0.91±0.14	0.97±0.38	0.85±0.71 [a], 14.8±17.3[b], 2.34-8.37[c], 43.7-56.0[f]

[*]MCE, Modified Combustion Efficiency [a] based on a study done on southwestern and southeastern fuels of the same fuel type (Manzanita), at Forest Service Fire Lab, Missoula, Montana [b] $PM_{2.5}$: McMeeking et al., 2009, the same fuel type and the same lab; most of the fuel masses were between 100-250 g [c] Fine et al., 2001, red maple, northern red oak, paper birch, eastern white pine, eastern hemlock, and balsam fir grown in northern U.S. [e] $PM_{2.5}$: Hedberg et al., 2002, birch wood combustion in a woodstove [f] Schauer et al., 2001, residential fireplace combustion of pine, oak, and eucalyptus

Table 2.6. Emission factor of aldehydes and ketones through analysis of the DNPH cartridges. Units are in mg per kg CO_2.

Species	**0 wt% PE**	**0.25 wt% PE**	**2.50 wt% PE**	**Other ref. (mg/kg fuel burned)**
Acetone	50±18	40±11	46±14	366 [b], 749[c], 73.9±16.2[d]
Formaldehyde	206±77	330±160	147±44	113-245[a], 422[b], 1165[c], 174.8±52.5[d]
Acetaldehyde	127±55	208±86	87±25	301-425 [a], 86 [b], 1704 [c], 92.7±21.9[d]
Propionaldehyde	19.9±8.5	30.8±11.7	13.8±5.5	80-150 [a],7.6, 255 [c], 7.5±15.1[d]
Crotonaldehyde (butenal)	12.5±5.0	19.8±8.6	9.9±3.8	276[c]
MEK	3.9±1.3	6.0±2.3	2.7±1.4	8.3 [b], 215[c]
Methacrolein	23.5±10.3	26.9±10.2	15.2±8.0	1.8 [a], 23[c]
Butyraldehyde	5.4±1.9	7.9±2.8	5.9±3.3	19-36 [b], 96[c], 52.1±18.2[d]
Benzaldehyde	8.4±3.3	12.5±4.6	7.8±0.9	12 [b]
Valeraldehyde	4.0±1.1	6.4±2.0	2.8±1.6	7-18 [a],1.1 [b], 85.9±37.4[d]
Tolualdehyde	4.5±2.7	6.6±1.4	2.4±0.2	0.9 [b]
Hexanal	120±47	183±74	91±36	34.6 [b], 89.0±37.5[d]
Acrolein	33±14	62±40	20±9	46-91 [a], 63[c]
Sum	618±109	940±201	452±65	

[a] McDonald et al., 2000a (fireplace softwood, hardwood, and woodstove), Cottonwood, birch, aspen, and oak. [b] Hedberg et al., 2002, birch wood combustion in a woodstove [c] Schauer et al., 2001, residential fireplace combustion of pine, oak, and eucalyptus [d] based on a study done on southwestern and southeastern fuels; manzanita (wood+foliage) at Forest Service Fire Lab, Missoula, MT

Table 2.7. Gaseous emission factors of Poly Aromatic Hydrocarbons (PAH) for the laboratory combustion of Manzanita mixed with PE, the units are in mg per kilogram CO_2 released.

Species	**0 wt% PE**	**0.25 wt% PE**	**2.50 wt% PE**	**Other ref. (mg/kg fuel burned)**
Particle-phase Poly Aromatic Hydrocarbons (PAH)				
Naphthalene	71±23	38±6	53±35	21-54[a], 18.34±14.05[d], 38.1±31.9[f]
Acenaphthylene	43±33	12±4	8±4	5-9[a], 1.01-2.66[e], 14.2±12.2[f]
Acenaphthene	0.82±0.45	0.54±0.12	0.31±0.15	0.41-0.89[a], 0.18-2.51[e], 0.2±0.1[f]
Fluorene	3.4±1.7	2.3±1.0	1.3±0.5	2.15-3.50[a], 0.05-0.92[e], 0.2±0.1[f]
Phenanthrene	10.5±7.0	5.7±2.1	3.4±0.7	1.99-3.94[e], 5.8±1.8[f]
Anthracene	1.15±0.48	0.94±0.31	0.35±0.19	0.32-1.27[e], 6.3±1.4[f]
Fluoranthene	1.02±0.21	1.11±0.36	1.02±0.18	0.52-2.86[e], 1.2±0.2[†]
Pyrene	1.03±0.20	2.17±1.16	1.12±0.05	0.45-1.47[e], 1.1±0.5[†]
Benz(a)anthracene	0.039±0.018	0.048±0.035	0.021±0.011	0.21-0.40[e], 0.04±0.06[†]
Chrysene	0.029±0.010	0.027±0.018	0.015±0.005	0.75-1.14[c], 0.21-0.34[e], 0.04±0.05
Benzo(b)fluoranthene	0.059±0.025	0.063±0.056	0.018±0.015	0.40-0.79[c], 0-0.05[e], 0.09±0.12[f]
Benzo(k)fluoranthene	0.008±0.002	0.024±0.005	0.022±0.009	0.29-0.67[c],0-0.13[e], 0.02±0.01[f]
Benzo(a)pyrene	0.032±0.006	0.076±0.058	0.040±0.023	0.25-0.71[c], 0.03±0.03[†]
Indeno(1,2,3cd)pyrene	0.013±0.001	0.053±0.037	0.017±0.008	n.d.[e], 0.03±0.04[†]
Dibenzo(a,h)anthra.	0.013±0.006	0.055±0.035	0.015±0.008	n.d.[e], 0.05±0.07[†]
Benzo(ghi)perylene	0.043±0.016	0.148±0.112	0.031±0.009	0-0.002[e], n.d.[†]
Sum	132±41	63±7	68±35	
Gas-phase Poly Aromatic Hydrocarbons (PAH)				

Species	0 wt% PE	0.25 wt% PE	2.50 wt% PE	Other ref. (mg/kg fuel burned)
Fluorene	0.056±0.015	0.124±0.019	0.108±0.011	27.4[b], 73-269[d], 0.04±0.06[f]
Phenanthrene	0.122±0.035	0.247±0.015	0.202±0.021	10-17[a], 99.1[b], 0.21±0.20[f]
Anthracene	0.0101±0.0024	0.0287±0.0061	0.0153±0.0012	19.3b, 1-50[d], 0.04±0.03[f]
Fluoranthene	0.095±0.021	0.278±0.061	0.134±0.008	1.75-3.99[a], 19.3[b], 286-1083[d], 0.22±0.14[f]
Pyrene	0.116±0.031	0.273±0.027	0.163±0.006	1.49-3.39a, 25.5b, 1.87-2.70c, 222-1080[d], 0.74±0.84[f]
Benz(a)anthracene	0.112±0.040	0.357±0.092	0.131±0.046	0.31-0.56[a], 3.5[b], 127-249[d], 0.23±0.08[f]
Chrysene	0.096±0.033	0.287±0.070	0.142±0.028	0.28-0.61[a], 4.1[b], 107-253[d],0.18±0.16[f]
Benzo(b)fluoranthene	0.26±0.12	0.40±0.18	0.21±0.04	0.51-1.05[a*], 6.1[b], 36-157[d], 0.67±1.00[f]
Benzo(k)fluoranthene	0.081±0.036	0.112±0.037	0.083±0.019	0.51-1.05[a*], b.d.[b], 3.23±2.91[f]
Benzo(a)pyrene	0.18±0.08	0.57±0.19	0.50±0.34	0.15-0.34[a], 0.09±0.10[f]
Indeno(1,2,3-cd)pyrene	0.21±0.10	0.67±0.19	0.45±0.27	0.07-0.19[a], 3.6[b], 39-164[d], 0.06±0.03[f]
Dibenzo(a,h)anthra.	0.04±0.01	0.22±0.12	0.30±0.24	b.d.[b], 3-11[d], 0.02±0.01[f]
Benzo(ghi)perylene	0.28±0.13	0.80±0.20	0.63±0.39	0.07-0.22[a], 2.6[b], 0.44[c], 25-70[d], 0.11±0.07[f]
Sum	1.66±0.23	4.36±0.42	3.07±0.63	

b.d. and **n.d.** indicate compound was below detection limit or not detected in that study. [a] McDonald et al., 2000a (fireplace softwood, hardwood, and woodstove), cottonwood, birch, aspen, and oak [b] Hedberg et al., 2002, birch wood combustion in a woodstove [c] Schauer et al., 2001, residential fireplace combustion of pine, oak, and eucalyptus [d] Fine et al., 2001, red maple, northern red oak, paper birch, eastern white pine, eastern hemlock, and balsam fir grown in northern

U.S. [e] Jenkins et al., 1996, included here of this study are wood from almond, walnut, and fir trees [f] based on a study done on southwestern and southeastern fuels; ; manzanita (wood+foliage) at Forest Service Fire Lab, Missoula, MT

Table 2.8. Emission factor of Volatile Aromatic Compounds in mg per kg CO_2; results from analysis of Thermal Desorption Spectroscopy (TDS) tubes.

Species	0 wt% PE	0.25 wt% PE	2.50 wt% PE	Other ref. (mg/kg fuel burned)
Benzene	105±70	102±13	83±22	225-110[a], 1500[b], 383[c], 411.8± 67.1 [d]
Toluene	25±20	26±6	20±8	130-320[a], 740[b], 158[c], 148.9± 22.9[d]
m&p-xylene	6.6±6.0	4.1±2.0	5.6±4.1	41-72[a], 125[b], 60[c], 34.8± 4.3[d]
o-Xylene	2.20±1.76	1.53±0.50	1.39±0.59	16-27[a], 20[b], 18[c], 9.0 ± 4.2
Styrene	9.2±8.0	8.3±3.3	7.6±3.3	40-117[a]
Indane	0.016±0.008	0.048±0.024	0.050±0.032	0-0.12[a]
Sum	148±74	142±15	118±24	

[a] Mcdonald et al., 2000b (fireplace softwood, hardwood, and woodstove), Cottonwood, birch, aspen, and oak. [b] Hedberg et al., 2002, birch wood combustion in a woodstove [c] Schauer et al., 2001, residential fireplace combustion of pine, oak, and eucalyptus [d] based on a study done on southwestern and southeastern fuels; manzanita (wood+foliage) at Forest Service Fire Lab, Missoula, MT

Table 2.9. Estimated emission factors of alkanes, cycloalkanes, alkenes, cycloalkenes, diolefins, and monocyclic aromatic hydrocarbons produced by the burning of manzanita wood-polyethylene plastic mixtures in mg/kg CO_2.

Species	0 wt% PE	0.25 wt% PE	2.50 wt% PE	Other ref. (mg/kg fuel)
		Alkanes		
Propane	14±6	45±33	9±4	107-167[a], 169[b]
2M-Propane	2.42±1.02	1.22±0.51	2.14±0.89	
2M-Propene	7.4±5.0	13.5±4.9	11.4±7.3	
Butane	4.7±2.7	2.8±1.9	3.3±3.0	1.68-17.36 [a], 25.9 [b]
2,2-DM-Propane	3.5±1.5	3.5±0.9	1.4±0.8	
Pentane	5.9±3.1	5.8±1.8	2.5±1.6	8.69-13.12 [a], 4.7 [b]
2,2-DM-Butane	3.3±1.6	8.7±4.2	1.8±1.3	

Species	0 wt% PE	0.25 wt% PE	2.50 wt% PE	Other ref. (mg/kg fuel)
CycPentane	3.1±2.8	0.1±0.1	0.6±0.6	
2,3-DM-Butane	7.6±6.1	11.3±10.0	1.9±1.4	
2M-Pentane	2.14±1.13	1.56±0.66	3.00±0.31	
3M-Pentane	1.69±0.46	2.01±0.15	2.56±0.97	
Hexane	2.5±2.0	3.2±2.3	5.5±4.9	6.01-12.30 [a]
2,2-DM-Pentane	0.14±0.07	0.26±0.10	0.26±0.19	
2M-Butane	3.5±1.9	5.9±3.6	11.7±9.2	
2,4-DM-Pentane	0.91±0.80	0.67±0.53	0.30±0.27	
2,2,3-TM-Butane	0.33±0.13	0.42±0.26	0.59±0.56	
3,3-DM-Pentane	1.49±1.34	0.70±0.51	0.22±0.10	
CycHexane	0.28±0.06	0.27±0.15	0.96±0.83	
2M-Hexane	0.63±0.52	1.88±1.19	0.36±0.24	
2,3-DM-Pentane	0.26±0.19	0.22±0.08	0.59±0.32	
3M-Hexane	0.30±0.24	0.44±0.08	0.56±0.48	
c-1,3-DM-CycPentane	0.05±0.01	0.06±0.01	0.80±0.46	
3E-Pentane	0.59±0.52	0.27±0.14	0.30±0.17	
2,2,4-TM-Pentane	0.40±0.39	0.42±0.26	0.48±0.30	
Heptane	0.32±0.23	0.34±0.07	0.72±0.62	3.71-5.36 [a], 28.9 [b]
2,2-DM-Hexane	0.180±0.093	0.136±0.081	0.087±0.059	
2,5-DM-Hexane	0.202±0.192	0.089±0.033	0.103±0.043	
2,4-DM-Hexane	0.07±0.06	0.04±0.02	0.56±0.54	
3,3-DM-Hexane	0.028±0.018	0.061±0.045	0.041±0.023	
2,3,4-TM-Pentane	0.04±0.03	12.29±12.18	0.11±0.06	
2,3,3-TM-Pentane	0.08±0.05	0.06±0.03	0.07±0.02	
2,3-DM-Hexane	1.62±1.59	0.67±0.09	1.15±0.48	
2M-Heptane	0.79±0.78	0.29±0.09	0.35±0.26	

Species	0 wt% PE	0.25 wt% PE	2.50 wt% PE	Other ref. (mg/kg fuel)
4M-Heptane	0.087±0.046	0.274±0.128	0.229±0.103	
3M-Heptane	0.10±0.06	0.12±0.06	0.51±0.40	
2,2,5-TM-Hexane	0.29±0.28	0.24±0.14	0.46±0.14	
Octane	0.09±0.06	0.34±0.15	0.79±0.46	2.54-14.94 [a], 1.7 [b]
2,3,5-TM-Hexane	0.22±0.22	0.19±0.17	0.15±0.02	
2,4-DM-Heptane	0.094±0.047	0.060±0.041	0.075±0.007	
E-CycHexane	0.017±0.009	0.060±0.044	0.047±0.007	
3,5-DM-Heptane	0.017±0.009	0.023±0.023	0.067±0.047	
2,3-DM-Heptane	0.010±0.010	0.012±0.012	0.066±0.066	
2M-Octane	0.38±0.30	1.13±1.03	1.09±0.43	
3M-Octane	0.024±0.013	0.098±0.031	0.225±0.028	
Nonane	0.19±0.14	0.17±0.06	0.38±0.21	1.09-5.13 [a], 3.9 [b]
2,2-DM-Octane	0.120±0.109	0.220±0.051	0.216±0.090	
2,4-DM-Octane	0.130±0.119	0.096±0.039	0.054±0.036	
Decane	0.53±0.47	0.38±0.11	0.20±0.08	0.92-2.10 [a]
Undecane	0.387±0.288	0.303±0.089	0.195±0.067	1.29-2.92 [a]
Dodecane	0.08±0.04	0.23±0.09	0.15±0.05	0.93-2.54 [a]
Tridecane	0.31±0.28	0.28±0.11	0.21±0.10	0.40-1.60 [a]
Sum	74±12	128±38	70±14	
		Cycloalkanes		
M-CycPentane	0.36±0.14	0.18±0.09	0.34±0.17	
t-1,2-DM-CycPentane	0.073±0.009	0.187±0.110	0.146±0.068	
M-CycHexane	0.19±0.18	0.24±0.08	0.16±0.11	
1c,2t,3-TM-CycPentane	0.027±0.018	0.049±0.012	0.040±0.023	
c-1,3-DM-	0.08±0.07	0.67±0.48	0.33±0.30	

Species	0 wt% PE	0.25 wt% PE	2.50 wt% PE	Other ref. (mg/kg fuel)
CycHexane				
t-1,4-DM-CycHexane	0.014±0.014	0.096±0.031	0.164±0.113	
t-1,3-DM-CycHexane	0.051±0.027	0.074±0.036	0.060±0.010	
c-1,2-DM-CycHexane	0.087±0.072	0.011±0.011	0.065±0.065	
Sum	0.88±0.25	1.50±0.51	1.31±0.40	
		Alkenes		
1-Butene	6.8±5.5	11.2±5.0	13.4±9.0	84-148 [a], 90.7 [b]
t-2-Butene	2.03±0.44	4.16±0.77	2.07±1.33	66.5 [b]
c-2-Butene	0.168±0.099	0.182±0.028	0.113±0.042	35.4 [b]
3M-1-Butene	5.5±4.5	1.9±0.2	1.4±0.6	6.9 [b]
1-Pentene	10.4±7.3	0.7±0.3	2.0±1.4	10-19 [a], 8.6 [b]
2M-1-Butene	6.0±5.0	3.4±2.0	0.9±0.2	13.8 [b]
t-2-Pentene	9.4±6.3	5.9±2.1	18.1±11.8	16.0 [b]
3,3-DM-1-Butene	1.5±0.7	8.0±4.3	16.8±12.4	
c-2-Pentene	1.4±0.3	3.7±1.2	3.8±2.9	10.4 [b]
2M-2-Butene	12.7±11.5	2.4±1.5	1.6±1.3	13.4 [b]
4M-1-Pentene	5.3±5.2	2.8±2.2	1.6±0.1	
3M-1-Pentene	1.97±1.42	3.70±0.84	0.17±0.09	
4M-c-2-Pentene	5.7±5.6	14.2±10.2	0.4±0.2	
4M-t-2-Pentene	9.3±6.2	4.9±1.9	4.7±2.6	
2M-1-Pentene	1.4±1.0	2.4±2.1	0.7±0.2	
1-Hexene	3.1±2.0	5.5±4.9	3.7±3.1	11-20 [a]
t-3-Hexene	1.14±0.44	2.88±1.48	0.48±0.40	
c-3-Hexene	0.81±0.50	1.63±1.18	0.07±0.01	
t-2-Hexene	0.30±0.17	0.62±0.50	0.96±0.85	8.6 [b]

Species	0 wt% PE	0.25 wt% PE	2.50 wt% PE	Other ref. (mg/kg fuel)
3M-t-2-Pentene	0.12±0.09	0.95±0.81	0.82±0.72	
2M-2-Pentene	0.10±0.06	0.77±0.59	0.45±0.23	6.9 [b]
c-2-Hexene	0.61±0.35	0.54±0.13	0.15±0.01	
3M-c-2-Pentene	0.17±0.05	0.39±0.31	0.08±0.05	
3,4-DM-1-Pentene	0.33±0.24	0.09±0.05	0.05±0.03	
3M-1-Hexene	0.65±0.27	1.28±0.66	0.57±0.34	
1-Heptene	0.91±0.69	0.55±0.34	2.54±0.90	3.71-5.36 [a]
t-3-Heptene	0.17±0.13	0.70±0.58	0.10±0.05	
2M-2-Hexene	0.17±0.10	0.17±0.11	1.17±0.77	
3M-t-3-Hexene	0.26±0.13	0.32±0.06	0.38±0.24	
t-2-Heptene	0.11±0.11	0.14±0.07	0.43±0.16	
3E-c-2-Pentene	0.17±0.14	0.32±0.06	0.42±0.25	
2,4,4-TM-1-Pentene	0.220±0.153	0.047±0.024	0.335±0.069	
2,3-DM-2-Pentene	0.121±0.121	0.151±0.094	0.173±0.071	
c-2-Heptene	0.09±0.09	0.06±0.03	0.36±0.31	
2,4,4-TM-2-Pentene	0.040±0.040	0.144±0.035	0.342±0.208	
1-Octene	0.08±0.05	0.26±0.09	0.74±0.38	0.43-1.49 [a]
t-4-Octene	0.31±0.19	0.17±0.06	0.49±0.38	
t-2-Octene	0.09±0.05	0.11±0.03	0.58±0.51	
c-2-Octene	0.30±0.27	0.12±0.06	0.20±0.15	
1-Nonene	0.93±0.69	0.94±0.41	2.11±1.19	0-0.49 [a]
Sum	91±20	88±14	85±20	
		Cycloalkenes		
CycPentene	0.29±0.08	0.61±0.12	0.31±0.23	
3M-CycPentene	0.23±0.13	0.18±0.03	0.50±0.27	
1M-CycPentene	0.47±0.37	0.23±0.10	0.54±0.45	

Species	0 wt% PE	0.25 wt% PE	2.50 wt% PE	Other ref. (mg/kg fuel)
CycHexene	0.41±0.28	0.27±0.13	0.97±0.72	
Sum	1.40±0.49	1.29±0.21	2.32±0.92	
		Diolefins		
1,3-Butadiene	2.6±1.6	15.7±6.0	3.4±2.8	62-196[a], 117[b]
2M-1,3-Butadiene	0.7±0.3	3.4±1.8	5.4±4.9	
CycPentadiene	1.40±1.27	0.07±0.03	0.99±0.85	26-127[a]
Sum	4.7±2.0	19.1±6.2	9.8±5.7	
		Monocyclic aromatic hydrocarbons		
Toluene	25±20	26±6	20±8	130-320 [a]
m&p-xylene	6.6±6.0	4.1±2.0	5.6±4.1	40-72 [a]
Styrene	9.2±8.0	8.3±3.3	7.6±3.3	35-117 [a]
o-Xylene	2.20±1.76	1.53±0.50	1.39±0.59	16-27 [a]
Benzene	105±70	102±13	83±22	225-1190 [a]
Indan	0.016±0.008	0.048±0.024	0.050±0.032	0.12-0.49 [a]
Sum	148±74	142±15	118±24	
Ethyl Benzene	5.2±4.3	4.4±1.7	4.2±1.7	
i-PropBenzene	0.27±0.27	0.18±0.10	0.08±0.02	
n-PropBenzene	0.70±0.70	0.41±0.26	0.44±0.36	
1M-3E-Benzene	0.43±0.43	0.37±0.15	0.14±0.03	
1M-4E-Benzene	0.09±0.05	0.15±0.07	0.46±0.26	
1,3,5-TM-Benzene	0.43±0.32	0.47±0.34	0.32±0.11	
1M-2E-Benzene	0.69±0.66	0.12±0.07	0.57±0.42	
1,2,4-TM-Benzene	0.3±0.2	3.1±1.0	2.6±1.9	
i-ButylBenzene	0.056±0.030	0.195±0.112	0.025±0.025	

Species	0 wt% PE	0.25 wt% PE	2.50 wt% PE	Other ref. (mg/kg fuel)
s-ButylBenzene	0.39±0.38	0.05±0.02	0.04±0.04	
1M-3-i-PropBenzene	0.036±0.026	0.317±0.150	0.052±0.026	
1,2,3-TM-Benzene	0.44±0.37	0.21±0.08	0.43±0.31	
1M-4-i-PropBenzene	0.162±0.124	0.047±0.012	0.051±0.033	
1M-2-i-PropBenzene	0.264±0.244	0.101±0.048	0.071±0.007	
1,3-DE-Benzene	0.11±0.11	0.42±0.29	0.11±0.08	
1,4-DE-Benzene	0.05±0.04	0.07±0.00	1.65±1.57	
1M-3-n-PropBenzene	0.15±0.08	0.67±0.43	0.27±0.10	
1M-4-n-PropBenzene	0.10±0.08	0.16±0.13	0.21±0.14	
1,2-DE-Benzene	0.08±0.04	0.28±0.25	0.05±0.03	
1M-2-n-PropBenzene	0.049±0.026	0.123±0.069	0.115±0.065	
1,4-DM-2-E-Benzene	0.16±0.14	0.35±0.31	0.13±0.08	
1,3-DM-4-E-Benzene	0.13±0.11	0.35±0.33	0.02±0.02	
1,2-DM-4-E-Benzene	0.24±0.22	0.28±0.23	0.09±0.05	
1,3-DM-2-E-Benzene	0.32±0.25	0.25±0.09	0.30±0.23	
1,2-DM-3-E-Benzene	0.13±0.12	0.14±0.11	0.18±0.10	
1,2,4,5-TetM-Benzene	0.062±0.043	0.093±0.048	0.062±0.062	
2-M-ButylBenzene	0.04±0.04	0.34±0.32	0.01±0.01	
1,2,3,5-TetM-Benzene	0.065±0.055	0.091±0.057	0.013±0.013	
tert-1-But-2-M-Benzene	0.040±0.026	0.078±0.060	0.045±0.007	
1,2,3,4-TetM-Benzene	0.104±0.055	0.118±0.059	0.029±0.015	
n-Pent-Benzene	0.26±0.24	0.16±0.08	0.10±0.03	
tert-1-But-3,5-DM-Benzene	0.072±0.053	0.057±0.039	0.051±0.033	
Sum	11.6±4.5	14.1±2.2	12.9±3.1	

[a] Mcdonald et al., 2000b (fireplace softwood, hardwood, and woodstove), Cottonwood, birch, aspen, and oak. [b] Schauer et al., 2001, residential fireplace combustion of pine, oak, and eucalyptus

Chapter Three: Particle Size Distributions from Laboratory-Scale Biomass Fires Using Fast Response Instruments

3.1. Abstract

Particle size distribution from biomass combustion in an important parameter as it affects air quality, climate modeling and health effects. To date particle size distributions reported from prior studies vary not only due to difference in fuels but also due to difference in experimental conditions. This study reports characteristics of particle size distribution in a well-controlled repeatable lab scale biomass fires for southwestern United States fuels with focus on chaparral. The combustion laboratory at the United States Department of Agriculture-Forest Service's Fire Science Laboratory (USDA-FSL), Missoula, MT provided repeatable combustion and dilution environment ideal for measurements. For a variety of fuels tested, the major mode of particle size distribution was in the range of 29 to 52 nm, which is attributable to dilution of the fresh smoke. Comparing mass size distribution from FMPS and APS measurement 51-68 % of particle mass was attributable to the particles ranging from 0.5 to 10 μm for PM_{10}. Geometric mean diameter rapidly increased during flaming and gradually decreased during mixed and smoldering phase combustion. Most of fuels gave unimodal distribution during flaming phase and strong bimodal distribution during smoldering phase. The mode of combustion (flaming, mixed and smoldering) could

be better-distinguished using slopes in MCE vs. geometric mean diameter than only using MCE values.

3.2. Introduction

Biomass combustion encompasses a wide range of sources including wildland fire, prescribed burning, agricultural residue/waste burning, residential wood combustion, and power generation. Since the 1970s, considerable effort has been devoted to characterizing the products associated with biomass combustion in general. In the United States, intentional biomass burning (prescribed burning) is regulated by the Clean Air Act. Prescribed burning is the planned use of fire under specified environmental and meteorological conditions to accomplish specific vegetation management objectives. These objectives include the removal of hazardous fuel accumulations, wildlife habitat improvement, forest regeneration, and mimicking the natural role of fire. In order to utilize prescribed burning, managers must provide estimates of the quantity of certain combustion products that will be produced before air quality regulators issue burn permits. These products of combustion include particulate matter (PM) released into the atmosphere (Chi, 1979, Levine, 1996, Goldammer, 2009). Particles can affect the radiation budget of the earth depending on their size distribution, morphology and their chemical composition. There is growing evidence of the role of particle size distribution and its adverse effect on human health following transport and deposition of particles (Pope and Dockery, 2006). Currently in the United States, the production of particles smaller than 2.5 μm is regulated due to the adverse impacts on human health and visibility.

Particle size distribution from biomass combustion evolves due to condensation/coagulation within the plume and photochemical aging downstream of the fire. The particle size distribution can also differ by combustion phase (ignition/flaming/smoldering), fuel condition (live, dead and varying moisture content), fuel configuration (dense vs. light and plain vs. sloped terrain), and fuel type (foliage, log, branch). Due to the importance of particle size distribution and its impact on air quality, climate modeling and health effects, particle size distributions from diverse biomass combustion conditions have been reported (S. Janhall et al., 2009, Hays et al., 2005, Capes et al., 2008).

Particle size distributions from biomass burning have been studied for a variety of fuels (P. Le Canut, 1996, Posfai et al., 2003, Posfai et al., 2004, Capes et al., 2008). A wide variety of instruments have been used to measure particle size distribution; Laser Optical Particle Counter, Aerosol Time-Of-Flight Mass Spectrometer (ATOFMS), Differential Mobility Particle Sizer (DMPS)(Hedberg et al., 2002, Sullivan et al., 2008), Scanning Mobility Particle Sizer (SMPS)(Hays et al., 2002, Hays et al., 2005), Transmission Electron Microscopy (TEM) analysis (Posfai et al., 2003, Posfai et al., 2004, Chakrabarty et al., 2006), Micro Orifice Uniform Deposit Impactor (MOUDI) (Hays et al., 2005, Engling et al., 2009), and Passive Cavity Aerosol Spectrometer Probe (PCASP) (Capes et al., 2008).

Previous studies have shown a wide variation in particle size distribution due to differing combustion and measurement conditions. Hays et al. (2002) reported unimodal distribution using a SMPS. They used open combustion of a fuel to simulate combustion of fuel in the field. They reported geometric mean diameters between 0.1-0.2 μm. Due to the use of a small enclosure (28 m^3), their particles must have grown by condensation and coagulation

within the enclosure. Le Canut et al. (1996) measured particle size distribution using a laser optical particle counter in their airborne study during a savanna fire. They reported two mass modes: one in 0.2-0.3 μm and the other above 2 μm. Chakrabarty et al. (2006) measured particle size distribution from laboratory combustion of eight different fuels using SMPS and image analysis. Projected area equivalent diameter peaks ranged from 30 to 200 nm for wet (moisture content (MC) = 20 % on dry mass basis) and dry (MC = 5-10 %) fuels. Major mode diameter ranged 40-45 nm for three burns out of six burns (see their figure 12) for dry fuels they tested. To authors' knowledge, none of previous studies captured the temporal evolution of size distribution due to the relatively slow response rate of the instruments. For example, the SMPS requires 2 min to measure one size distribution. Janhäll et al. (2009) parameterized particle number emissions by applying complicated fittings to published experimental data. They pointed out that well-defined laboratory experiments should help validate their finding and enable a better understanding of particle emission/formation mechanisms.

A study to characterize smoke emissions from prescribed burns in chaparral and Madrean oak woodlands in the southwestern United States was initiated in 2008. Detailed characterization of gaseous and particulate emissions is being made in laboratory and field settings. Changes in and transport of emissions from the source downwind are being measured and modeled for inclusion in air quality models such as CMAQ (Byun, 2006). The objective of this paper is to characterize particle size distribution from the laboratory component of the study. A suite of fast-response online instruments were applied to measure evolution of particle size distribution from fire ignition to extinction to capture

transient and integrated characteristics of particle size distribution from biomass burning. To the best of our knowledge, current study reports fast time-dependent (1s interval) size distribution of the particle-phase emissions and their characteristics from biomass burning in detail for the first time.

3.3. Experimental

3.3.1. Combustion Lab Facility

Experiments were conducted in the combustion laboratory at the USDA Forest Service's Fire Science Laboratory (FSL), Missoula, MT. A detailed description of the characteristics of the facility can be found in Christian et al (2004). The facility measures 12.5 m by 12.5 m and is 22 m in height. The combustion laboratory is exhausted via a 3.6 m diameter hood attached to a 1.6 m stack located in the center. Figure 3.1 shows a schematic of the lab. The base of the hood is above the fuel bed. The stack extends from 2 m above the floor to all the way up through the ceiling. The lab is slightly pressurized with pre-conditioned outside air to precisely control the temperature, and relative humidity. This ensures entrainment of all the produced emissions, making the conditions ideal for determining emissions factors. The air velocity in the chimney was set at either 1.5 m/s or 3 m/s by controlling the exhaust fan speed to maintain proper entrainment of fresh air.

3.3.2. Particle Measurement System

The sampling platform (Figure 3.1) is located 17 m above the floor surrounding the stack; this is where all particle measurement instruments were placed Figure 3.2 shows schematics of sampling system. First sampling flow was taken from the isokinetic sampling port

installed at the height of the sampling platform at the stack. The sample flow was diluted using a mini dilution tunnel at 1:13.5 ratio. The diluted aerosol flow directed to a PM10 impactor, then distributed to Fast Mobility Particle Sizer (FMPS –model 3091, TSI), an Aerodynamic Particle Sizer (APS- model 3321, TSI) and Condensation Particle Counter (CPC Model 3775, TSI). Other online and offline instruments were used for physical and chemical characterization of the particles but are not reported here.

The Fast Mobility Particle Sizer Spectrometer (FPMS, TSI Model 3091) is capable of measuring mobility diameter of the particles. The instrument is made of two concentric cylinders (Classification columns), a corona diffusion charger, and 32 electrometers, which covers range of 5 nm to 560 nm. The stream containing positively charged particles flows along with sheath air. The high voltage between the two cylinders carries the particles from the side that they are introduced to the other side that has the electrometers. Close the top of the column, the particles with higher electrical mobility are collected, and further upstream the particles with lower electrical mobility are collected (TSI manual[1]). Electrical mobility, Z is defined as below

$$Z = \frac{neC}{3\pi\mu_g D_m} \qquad \text{Eq. 3.1}$$

Where n, e, C, μ_g, D_m are number of charge, unit charge of an electron, slip correction factor, gas viscosity and particle mobility diameter.

[1] http://www. tsi.com/uploadedFiles/Product_Information/Literature/Spec_Sheets/3091FMPS.pdf

The aerodynamic diameter D_a is the diameter of the unit density (ϱ_p=1 g/cc) sphere that has the same settling velocity as the particle (Hinds, 1982). The Aerodynamic Particle Sizer (APS, TSI Model 3321) is capable of measuring particle size distributions in the size range of 0.5 to 20 μm. The sample particles are accelerated as the carrier gas flows through a converging nozzle. Due to the inertia, particles cannot accelerate as fast as the gas and the velocity lags that of the gas. Particle size is related to this velocity lag and that is measured at the nozzle exit when particles pass through two partially overlapping laser beams. The time of flight between the two laser beams is then used to calculate the aerodynamic diameter (Rader et al, 1990, Wang and John, 1987). Chen et al. (1985) found a unique calibration curve existed between a particle Stokes number and its velocity normalized by the gas velocity.

The Stokes number is defined as

$$St = \frac{\rho_p D_p^2 V_g C}{9 \mu_g W} \qquad \text{Eq. 3.2}$$

where ϱ_p, D_p, V_g, C, μ_g, W are particle density, particle diameter, gas velocity, slip correction factor, gas viscosity and diameter of the nozzle at the exit. The APS measured aerodynamic diameter requires correction for non-Stokesian effects when particle Reynolds diameter becomes greater than 0.5 (Wang and John, 1987). A conversion of aerodynamic diameter into mobility diameter requires a correction factor involving dynamic shape factor and density of particles (Stöber, 1971). The particle Reynolds numbers are reported as 0.65, 4.8, 24 and 103 for diameters of 1.0, 2.1, 5, and 15 μm by Wang and John (1987) for the APS at the nozzle flow velocity of 150 m/s. Current study does not aim to measure shape factor and density of particles for a conversion from aerodynamic to mobility diameter.

3.3.3. Gas Measurement System

Every molecule has its own specific IR radiation absorption pattern. Researchers have used this fact in Fast Fourier Transform InfraRed (FTIR) spectroscopy. If a beam of IR is passed through smoke, and the IR spectrum is recorded, the acquired graph will have peaks that are due to molecules present in the smoke (Yokelson et al. 1997, Goode et al. 1999). The OP-FTIR instrument used in this study included a Bruker Matrix-M IR Cube spectrometer and a thermally stable open white cell. The white cell was positioned on the sampling platform approximately 17 m above the fuel bed so that the open white cell spanned the stack directly in the rising emissions stream. The white cell path length was set to 58 m. Several extensive tests were performed to optimize the many sampling parameters, including duty cycle, sample frequency, and spectrometer options and chose a spectral resolution of 0.67 cm-1 and spectra were acquired every 1.5 seconds (four co-added spectra in 1.5 seconds) beginning several minutes prior to the fire and continuously until the end of the fire. A pressure transducer and two temperature sensors were located adjacent to the optical path and were logged on the instrument computer and used for spectral analysis.

The Open-Path Fourier Transform infrared (OP-FTIR) spectrometer was used to monitor concentrations of CO and CO_2 for this study. These concentrations were used to calculate a Modified Combustion Efficiency (MCE). MCE is defined as the amount of carbon released as CO_2 divided by the amount of carbon released as CO_2 plus CO (Ward et al., 1996, Ward, 1993).

$$MCE = \frac{\Delta CO_2}{\Delta CO_2 + \Delta CO} \qquad \text{Eq. 3.3}$$

$$\Delta x = x_{measured} - x_{background}$$

Since CO_2 and CO account for about 95 % of carbon released during biomass combustion, the MCE is a good surrogate for true combustion efficiency. Ward et al. (1993) classified combustion conditions into three phases by MCE: flaming when MCE > 0.97, mixed when 0.97 ≥ MCE > 0.85 and smoldering when 0.85 ≥ MCE > 0.75.

3.3.4. Experimental Fires

Fuel characterization and fuel bed configuration are very important parameters to determine particle emissions and formations. Yet many previous studies are lacking this critical information in their publications(Reid et al., 2005). In the present work, a total of 44 burns, composed of 8 different types of wildland fuels (Table 3.1), were conducted. The fuels were collected from California (Ft. Hunter-Liggett, Vandenberg Air Force Base) and Arizona (Ft. Huachuca). The fuel types selected for study are composed primarily of living vegetation. The chaparral fuel type is actually mixtures of shrub species that grow together in the Mediterranean climate of California and Baja California. Many of the shrub species in this climate have developed similar physical characteristics to minimize water loss such as leaves with waxy cuticles, which pyrolyze at low temperatures (Susott, 1982). The shrub canopies are relatively porous which facilitates fire spread. Fires burning in these fuel beds are typically intense with relatively high rates of energy release. In the Madrean oak fuel types, the woodland type consists of oak trees with an understory of shrub species related to chaparral species and the savanna type consists of oak trees with an understory of native and

introduced grasses. Fuels were harvested from the three locations and shipped to Missoula where they were stored for several weeks prior to the experiments. During this time, the fuels lost most of the moisture that was present at the time of harvest.

A small amount of isopropyl alcohol (generally less than 50 cc) was used initially to get a quick even ignition of the fuel bed. Eighteen of 44 of the southwestern fuel beds (chamise, ceanothus, manzanita, and California sagebrush – see Table 3.1) were ignited in this manner using a propane torch. No alcohol was used to enhance ignition in the remaining fuel beds. With the exception of the masticated mesquite fuel type which was created by mowing down and grinding the shrubs , the natural fuel beds tend to have a vertical orientation in the natural setting (Figure 3.3-a). We attempted to burn the fuels in a vertical orientation with limited success so the fuels were oriented horizontally (Figure 3.3-b). Average consumption (mass basis) of the chamise/scrub oak fuels oriented vertically was 30 %. Consumption of horizontally oriented fuel beds increased to 90 %. Bulk characteristics of the fuel beds are found in Table 3.2. Average moisture content (oven-dry mass basis, ASTM D4442-07) of the fuel beds at the time of burning ranged from 4 to 33 %, which is similar to fuel moistures in dead fuels. Moisture content in these live fuels seldom decreases below 50 % in the field. The initial oven-dry mass in the fuel beds ranged from 670 to 4630 g. Bulk density of the fuel beds ranged from 5.8 to 14 kg/m3 and the packing ratio (defined as the ratio of fuel bed bulk density to fuel particle density) ranged from 0.010 to 0.024. These packing ratios are similar to those reported for laboratory fire spread experiments (Weise et al., 2005), but they are 1 to 2 orders of magnitude larger than packing ratios observed in the field which indicates the fuel beds were less porous than natural fuel

beds. While our initial intent was to burn fuel beds similar to those found naturally, the fuel beds in the lab experiment were much drier with higher bulk densities than the fuel types they represent.

3.4. Results and Discussion

3.4.1. Particle size distribution from 7 to 520 nm measured by FMPS

Figure 3.4-a shows averaged particle size distribution for different fuels as measured by FMPS. The size distribution is averaged over the time from ignition to the end of sampling (absolute CO concentration 1ppm) and over at least three burn replicates for each fuel type. Averaged size distributions were unimodal for many fuel types. Interestingly, a few fuel types showed bimodal distributions, with the minor (meaning lower concentration) mode around 10 nm. The major mode varies from 29 to 52 nm for fuels tested. This is a very narrow range considering diverse fuels tested. Consistent technique was used to minimize experimental errors in order to detect differences between species. The similarity of the size distribution among fuels tested can be attributable to the systematic burning and sampling method. The combustion facility in Missoula was designed to divert all the generated smoke into the chimney. This allows enough dilution of the particles so that particle sizes measured and reported in this facility are smaller than those from other studies are. Chakrabarty et al. (2006) used the same combustion facility in Missoula for their experiment. They reported particle Count Median Diameter (CMD) varying from 30 to 70 nm for dry fuels (sagebrush, poplar wood, ponderosa pine wood, ponderosa pine needles, white pine needles, Montana grass, dambo grass, tundra core) but they found the CMD increases to 120-140 nm for wet

fuels (tundra core and Montana grass) from their SEM measurement. Hays et al. (2005) measured size distribution from open burning of agricultural biomass (wheat straw). The open burning was conducted in an enclosure and the particles were diluted from 1:25 to 36 and measured by a SMPS. They reported a bimodal distribution and suggested that one mode is characterized by nucleation while the other represents an accumulation mode. The modes in their size distributions were around 100 nm. Their measured SMPS scans take 60 to 120 s. Considering characteristics of biomass burning this is not fast enough to capture the transient phenomena. The background particle size distribution was obtained by averaging size distributions measured before ignition for seven burns, which were conducted consecutively in one experimental day and plotted with averaged size distributions in log scale as shown in Figure 3.4-b. Figure 3.4-b also shows that particle concentration decreased sharply above 200 nm.

While some other studies report combustion conditions of biomass burn only by using integrated or averaged MCE over the whole burn, we attempted to segregate the mode of combustion during each burn using instantaneous MCE value and other indicators (i.e. slopes in MCE vs. geometric mean diameter curve). The average size distributions of Figure 3.4-ab were segregated into three burning conditions: flaming, mixed and smoldering by MCE. This division was done by plotting geometric mean diameter change as a function of MCE instead of using only Ward and Radke's criteria by MCE value. Details of this will be discussed in later section. The majority of particles were emitted during flaming therefore the shapes of size distribution during flaming were similar to that of the average of the whole burn (Figure 3.4-c). (Note our presentation of data in Figure 3.4 is time based while

some studies report particle emission per fuel mass.) Mixed phase, which consists of flaming and smoldering, shows unimodal distribution with the mode ranges from 30 to 50 nm (Figure 3.4-d). The particle concentration was lower than that of flaming by factor of 5 roughly. The change between flaming and mixed mode could be observed clearly from our video recording of all burns. The size of flames was decreased noticeably at the beginning of the mixed phase compared to the flaming phase. The flame was still clearly visible during the mixed phase.

Size distribution during smoldering showed a bimodal distribution for all fuel types at around 10 nm (Figure 3.4-e). A possible explanation for this is nucleation of volatile particles as the burnt gas temperature cooled down. The particle concentration during smoldering was two orders of magnitude lower than during the flaming phase. Note that this is time-based not fuel mass-based. Analysis of fuel mass-based results will be reported in another paper. Figure 3.4-f shows background particle size distribution change during a day. The background concentrations (Figure 3.4-f) are much lower than our measured particle concentration during the burn (Figure 3.4-cde), which ensures that background particles did not interfere our measurements. Figure 3.4-g shows variation of FMPS number distribution measurement for the fuel of oak savanna. Thick solid line represents average of six burns and shaded area shows variation. Table 3.3 shows the geometric diameter and standard deviation of size distributions for fuels tested. Similarity between geometric mean diameters for the nine fuel types is illustrated in Table 3.4. Notice that the standard deviations of the distributions are similar. Several of the chaparral fuel types had similar geometric mean diameters and the two Madrean oak fuel types were similar.

3.4.2. Particle size distribution from 0.5 to 20 μm measured by APS

Figure 3.5-a shows time and cycle averaged particle size distributions from APS measurement. This was done to determine whether large particle concentrations were higher than background levels aerosol by number and by volume. It has been reported that mass mean diameter is as large as 0.5 μm (or 500 nm) for aged particles from biomass burning (Reid et al., 2005). Most of these previous measurements were performed optically by aircraft measurement. Particles larger than 100 nm in mobility diameter was reported by previous studies, which measured size distribution in the field. However smaller particle mode was reported for particles measured in the lab (Hays et al., 2005, Keshtkar and Ashbaugh, 2007). This can be attributed to immediate dilution that prevents further coagulation and condensation. Regardless, particles larger than 0.5 μm were measured using APS to determine whether there was any noticeable number or mass of particles in this size range from freshly diluted biomass smoke. The particle number distribution (Figure 3.5-a) showed that the concentrations are orders of magnitude lower compared to the concentrations of small particles measured by FMPS. Log conversion of Figure 3.5-a illustrated that the smoke particle distributions were greater than background. Background distributions (Figure 3.5-f) measured between each burn during a day show that they do not vary much compared to that of small size particles (Figure 3.4-f). This validated that our APS measurements were not interfered by background particle size distribution. The average size distributions of Figure 3.5 were separated by combustion phases using the same method used with the FMPS size distribution. Particles larger than 0.5μm were emitted mostly during

flaming and mixed phases of combustion. Emissions during the smoldering phase were lower by at least a factor of 4 in comparison to peak concentrations.

The mass distributions were compared between large and small particles measured by APS and FMPS. The number of fractal-like particles for the size greater than 0.5 μm was insignificant based on our TEM measurement (images not shown in this paper). A range of particle densities was chosen to assess uncertainties in mass distribution taking into account of non-Stokesian effects. Figure 3.6 shows that the mass larger than 0.5 μm attribute to 51 to 68 % of total volume measured by APS and FMPS when particle density range of 0.8~2.5 was assumed for non-Stokesian correction with the APS measurement. Note that the dilution was applied for all online aerosol measurement. Relative Humidity (RH) of dilution air was maintained at 16.5±4 %. Note the size distribution by APS is in aerodynamic diameter while that by FMPS is in mobility diameter.

3.4.3. Evolution of particle size distribution (FMPS+APS)

It is extremely difficult to identify what determines evolution of particle distribution from biomass burning due to the large variability in fuel composition, fuel humidity, fuel bed arrangement and the nature of turbulent combustion. Therefore, most previous studies reported either time-integrated results or snap shots of transient phenomenon. In order to understand the evolution of particle size distribution, it is instructive to examine Figure 3.7 that shows the evolution of particle size distribution for a burn from initial ignition until extinction. This temporal resolution is possible due to the fast scanning ability of the FMPS and the APS (1 scan per second). The data showed that particle concentration reached a

maximum during the flaming phase (confirmed by CO and CO_2 data) and diminished to lower concentration in either unimodal or bimodal distributions. Right after ignition CO_2 concentration increases and that leads to increase in MCE. After the MCE reaches nearly one it starts to decrease because $\Delta CO_2/ \Delta CO$ decreases as shown in Figure 3.7-a. During smoldering phase, $\Delta CO_2/ \Delta CO$ increases again mainly due to decrease in Δ CO, which leads to increase of MCE value. The MCE value reaches plateau toward the end of smoldering phase. During flaming phase significant amount of particle emissions occurs for the size range both instruments (FMPS and APS) measure. It is important to note that emissions of ultrafine particle (Dp<100 nm) reduces significantly as the combustion phase progresses from flaming, mixed to smoldering phase. On the other hand high concentration of particles between 0.5 and 1 μm range persist during flaming, mixed phase and even past smoldering until 400s in Figure 3.7-b. It is noteworthy that near the end of smoldering phase ultrafine particles show bimodal distribution clearly (see Figure 3.7-c). Values of peak concentration measured by FMPS were at least three to four orders of magnitude higher than APS concentrations during the flaming and mixed phases. Likewise, the evolution of geometric mean diameter was plotted for a few burns as illustrated in Figure 3.8. These results revealed that the geometric mean diameter increases rapidly during flaming phase and decreased during mixed and smoldering phases. In Figure 3.9, MCE was plotted as a function of geometric diameter for three different fuels. Ward and Radke (1993)'s MCE criteria gives a guideline to distinguish different phase of combustion but it fails to give accurate distinction at specific MCE value. For example, smoldering mode starts at different MCE value of 0.82, 0.76 and 0.83 for different burns at Figure 3.9-abc. As the combustion

of biomass is always dynamic instead of being steady state, either combustion or emissions parameters should evolve at different rate and/or direction at different phase of combustion. When we plotted MCE value against geometric mean diameter, we found that the distinction between different phases of combustions could be more clearly seen. This was also confirmed by comparing video records of the burn with Figure 3.9. The geometric mean diameter increased rapidly during flaming condition when MCE was > 0.97. However, the MCE value for the mixed phase could become smaller than what Ward and Radke (1993) define. The geometric mean diameter decreased during both mixed and smoldering conditions. While the MCE decreased as the mixed phase proceeded, the MCE value increased as the smoldering phase proceeded. As a result, one can distinguish mixed phase combustion from smoldering phase combustion based on the slope change in MCE vs. geometric mean diameter graph..

3.5. Conclusions

This paper presented particle size distributions measured by a suite of fast-response online instruments for laboratory-scale biomass fires for a variety of southwestern U.S. fuel types. The instruments measured evolution of particle size distribution from fire ignition to extinction to capture transient and integrated characteristics of the particle size distribution. Time-averaged particle size distributions were segregated into three combustion phases: flaming, mixed and smoldering. The major mode of particle size distribution was in the range of 29 to 52 nm for the cycle-averaged distribution. These are much smaller diameters compared to previous studies. The difference from previous studies was attributed to dilution of the fresh smoke in the current study. Time-averaged particle concentrations were

highest during the flaming phase and gradually decreased during mixed and smoldering phases. Comparing mass size distribution from the FMPS and APS measurements, 51-68 % of particle mass was attributable to the particles ranging from 0.5 to 10 μm for PM10. Geometric mean diameter rapidly increased during flaming combustion and gradually decreased during mixed and smoldering phase combustion. Particle size distribution was unimodal for most fuel types during the flaming phase and strongly bimodal during the smoldering phase. The slopes of the linear plots of MCE versus geometric mean diameter appear to better separate the combustion phases than simply using the value of MCE. Given the wide use of MCE alone to define combustion phases, additional measurement of particulate matter from biomass burning using fast response instruments is recommended.

3.6. Acknowledgements

Funding for this study was provided by the U.S. Department of Defense Strategic Environmental Research and Development Program as projects SI-1647, SI-1648, and SI-1649. We appreciate the assistance of personnel at USMC Camp Lejeune, US Army Ft. Huachuca, Ft. Hunter-Liggett, Ft. Benning, and Vandenberg Air Force Base in selecting fuel types for study and fuel samples for burning. Authors are grateful to Drs. Robert Yokelson and Ian Burling for FTIR data and Dr. Wei Min Hao, Shawn Urbanski, Cyle Wold, Joey Chong, Trevor Maynard and Emily Lincoln for their help.

3.7. References

Byun, D. W., and K. L. Schere: Review of Governing equations, Computational Algorithms, and Other Components of the Models-3 Community Multi-scale Air Quality (CMAQ) Modeling Systems, Applied Mechanics Reviews, 59, 51-77, 2006.

Capes, G., Johnson, B., McFiggans, G., Williams, P. I., Haywood, J., and Coe, H.: Aging of biomass burning aerosols over West Africa: Aircraft measurements of chemical composition, microphysical properties, and emission ratios, J Geophys Res-Atmos, 113, 2008.

Chakrabarty, R. K., Moosmuller, H., Garro, M. A., Arnott, W. P., Walker, J., Susott, R. A., Babbitt, R. E., Wold, C. E., Lincoln, E. N., and Hao, W. M.: Emissions from the laboratory combustion of wildland fuels: Particle morphology and size, J Geophys Res-Atmos, 111, 2006.

Chen, B. T., Cheng, Y. S., and Yeh, H. C., Performance of a TSI Aerodynamic Particle Sizer. Aerosol Sci. Technol. 4:89–97, 1985.

Chi, C. T., D.A. Horn, R.B. Reznik, D.L. Zanders, R.E. Opferkuch, J.M. Nyers, J.M. Pierovich, L.G. Lavdas, C.K. Mcmahon, R.M. Nelson, R.W. Johansen, and P.W. Ryan: Source assessment: prescribed burning, state of the art. , U.S. Environmental Protection Agency, Washington D.C., 1979.

Christensen, N. L.: Vegetation of the southeastern coastal plain, in: North American Terrestrial Vegetation, edited by: M.G. Barbour, W. D. B., Cambridge University Press, United Kingdom, 1999.

Christian, T. J., Kleiss, B., Yokelson, R. J., Holzinger, R., Crutzen, P. J., Hao, W. M., Shirai, T., and Blake, D. R.: Comprehensive laboratory measurements of biomass-burning emissions: 2. First intercomparison of open-path FTIR, PTR-MS, and GC- MS/FID/ECD, J Geophys Res-Atmos, 109, 2004.

Countryman, C. M.: Physical characteristics of some northern California brush fuels., USDA Forest Service, Pacific Southwest Forest and Range Experiment Station, General Technical Report 1982.

Engling, G., Lee, J. J., Tsai, Y. W., Lung, S. C. C., Chou, C. C. K., and Chan, C. Y.: Size-Resolved Anhydrosugar Composition in Smoke Aerosol from Controlled Field Burning of Rice Straw, Aerosol Sci Tech, 43, 662-672, 2009.

Goldammer, J. G., M. Statheropoulos, and M.O. Andreae: Goldammer, J.G., M. Statheropoulos, and M.O. Andreae. (2009) "Impacts of vegetation fire emissions on the environment, human health, and security: a global perspective" in Bytnerowicz, A., M. Arbaugh, A. Riebau, and C. Andersen (eds.), Wildland Fires and Air Pollution. Elsevier, 2009.

Goode, J. G., R. J. Yokelson, R. A. Susott, and D. E. Ward, Trace gas emissions from laboratory biomass fires measured by Fourier Transform InfraRed spectroscopy: Fires in grass and surface fuels, J. Geophys.Res., 104, 21,237– 21,245. 1999.

Hays, M. D., Geron, C. D., Linna, K. J., Smith, N. D., and Schauer, J. J.: Speciation of gas-phase and fine particle emissions from burning of foliar fuels, Environ Sci Technol, 36, 2281-2295, 2002.

Hays, M. D., Fine, P. M., Geron, C. D., Kleeman, M. J., and Gullett, B. K.: Open burning of agricultural biomass: Physical and chemical properties of particle-phase emissions, Atmos Environ, 39, 6747-6764, 2005.

Hedberg, E., Kristensson, A., Ohlsson, M., Johansson, C., Johansson, P. A., Swietlicki, E., Vesely, V., Wideqvist, U., and Westerholm, R.: Chemical and physical characterization of emissions from birch wood combustion in a wood stove, Atmos Environ, 36, 4823-4837, 2002.

Hinds, W.C., Aerosol Technology: Properties, Behavior, and Measurement of Airborne Particles, Wiley Interscience, New York ,1982.

Keeley, J. E.: Chaparral, in: North American Terrestrial Vegetation, edited by Barbour, M. G. and Billing, W. D., Cambridge University Press, N.Y., 397–448, 1999.

Janhall, S., Andreae, M. O., and Poschl, U.: Biomass burning aerosol emissions from vegetation fires: particle number and mass emission factors and size distributions, Atmos. Chem. Phys., 10, 1427–1439, 2010.

Keshtkar, H., and Ashbaugh, L. L.: Size distribution of polycyclic aromatic hydrocarbon particulate emission factors from agricultural burning, Atmos Environ, 41, 2729-2739, 2007.

Levine, J. S.: Biomass Burning and Global Change, MIT Press, 1996.

Le Canut, P., Andreae, M. O., Harris, G. W., Wienhold, F. G., and Zenker, T.: Airborne studies of emissions from savanna fires in southern Africa, J. Geophys. Res.-Atmos., 8483,doi:10.1029/2002jd002291, 1996.

Pope, C. A., and Dockery, D. W.: Health effects of fine particulate air pollution: Lines that connect, J Air Waste Manage, 56, 709-742, 2006.

Posfai, M., Simonics, R., Li, J., Hobbs, P. V., and Buseck, P. R.: Individual aerosol particles from biomass burning in southern Africa: 1. Compositions and size distributions of carbonaceous particles, J Geophys Res-Atmos, 108, 2003.

Posfai, M., Gelencser, A., Simonics, R., 5 Arato, K., Li, J., Hobbs, P. V., and Buseck, P. R.: Atmospheric tar balls: Particles from biomass and biofuel burning, J. Geophys. Res.-Atmos.109, D22302, doi:10.1029/2008jd010216, 2004.

Rader, D. J. and McMurry, P. H.: Application of the Tandem Differential Mobility Analyzer to studies of droplet growth and evaporation, J. Aerosol Sci., 17, 771–788, 1986.

Reid, J. S., Koppmann, R., Eck, T. F., and Eleuterio, D. P.: A review of biomass burning emissions part II: intensive physical properties of biomass burning particles, Atmos Chem and Phys, 5, 799-825, 2005.

Stober, W. A., A note on the aerodynamic diameter and the mobility of non-spherical aerosol particles, J. Aerosol Sci., 2:453–456 , 1971.

Sullivan, A. P., Holden, A. S., Patterson, L. A., McMeeking, G. R., Kreidenweis, S. M., Malm, W. C., Hao, W. M., Wold, C. E., and Collett, J. L.: A method for smoke marker measurements and its potential application for determining the contribution of biomass burning from wildfires and prescribed fires to ambient PM2.5 organic carbon, J Geophys Res-Atmos, 113, 2008.

Susott, R. A.: Characterization of the thermal properties of forest fuels by combustible gas analysis., Forest Sci, 28, 404 1982

Wang, H., John, W.: Particle Density Correction for the Aerodynamic Particle Sizer, Aerosol Science and Technology, 6, 191-198, 1987.

Ward, D. E., Hao, W. M., Susott, R. A., Babbitt, R. E., Shea, R. W., Kauffman, J. B., and Justice, C. O.: Effect of fuel composition on combustion efficiency and emission factors for African savanna ecosystems, J Geophys Res-Atmos, 101, 23569-23576, 1996.

Ward, D. E. and Radke, L. E.: Emission measurements from vegetation fires: a comparative evaluation of methods and results, in: Fire in Environment. The Ecological, Atmospheric and Climatic Importance of Vegetation Fires, edited by: Crutzen, P. J. and Goldammer, J. G.,John Wiley and Sons, New York, pp. 53–76, 1993.

Weise, D. R., Zhou, X. Y., Sun, L. L., and Mahalingam, S.: Fire spread in chaparral - 'go or no-go?', Int J. Wildland Fire, 14, 99-106, 2005.

Yokelson, R. J., D. E. Ward, R. A. Susott, J. Reardon, and D. W. T. Griffith, Emissions from smoldering combustion of biomass measured by Open-Path Fourier Transform InfraRed spectroscopy, J. Geophys. Res., 102, 18,865– 18,877, 1997.

Table 3.1. Fuel type species composition and abbreviations

Fuel type	Fuel Code	Plant Species
Chamise/scrub oak	CHS	Adenostomafasciculatum, Quercusberberidifolia
Ceanothus	CEA	Ceanothusleucodermis
Coastal sage scrub	COS	Salvia mellifera, Ericameriaericoides, Artemisia californica
California sagebrush	CAS	Artemisia californica, Ericameriaericoides
Manzanita	MAN	Arctostaphylosrudis, Arctostaphylospurissima
Oak savanna	OAS	Quercusemoryi, Eragrostislehmanniana
Oak woodland	OAW	Quercusemoryi, Arctostaphylospungens
Masticated mesquite	MES	Prosopisvelutina, Baccharissarothroides

Table 3.2. Fuel and bed properties

Fuel type	*n*	Moisture content (%)	Fuel bed dry mass (g)	Bulk density (kg/m^3)	Packing ratio[a]	Consumption (%)
Southwestern U.S. Chamise/Scrub Oak **(CHS)**	6	11.9	2079	8.6	0.015	38
Ceanothus **(CEA)**	6	10.2	2007	5.8	0.010	54
Coastal Sage Scrub **(COS)**	5	9.3	2299	6.0	0.010	95
California Sagebrush **(CAS)**	6	9.0	2460	6.4	0.011	93
Manzanita **(MAN)**	6	12.6	2906	7.6	0.013	94
Oak Savanna **(OAS)**	5	14.3	2788	7.3	0.012	91
Oak Woodland **(OAW)**	5	32.8	2054	5.3	0.009	95
Masticated Mesquite **(MES)**	5	4.3	1831	14.3	0.024	92

[a] Packing ratio = bulk density/particle density. Assumed particle density of 593 $kg\,m^{-3}$ (average from Countryman, 1982)

Table 3.3. Geometric mean diameter and the geometric standard deviations

Fuel type	In total	
	Dg(nm)	σ
California Sagebrush (CAS)	50.72	1.66
Ceanothus (CEA)	39.67	1.64
Chamise/Scrub Oak (CHS)	52.30	1.62
Coastal Sage Scrub (COS)	45.30	1.62
Manzanita (MAN)	39.20	1.62
Masticated Mesquite (MES)	34.00	1.58
Oak Savanna (OAS)	25.00	1.76
Oak Woodland (OAW)	29.00	1.67

Table 3.4. Species effects on particle size distribution

Fuel Type	CAS	CEA	CHS	COS	MAN	MES	OAS	OAW
CAS		N[2]	Y	Y	N	N	N	N
CEA			N	Y	Y	Y	N	N
CHS				N	N	N	N	N
COS					Y	N	N	N
MAN						Y	N	N
MES							N	Y
OAS								Y

[2] Y indicates mean geometric diameter of fuel type 1 ± 2σ overlaps with mean geometric diameter of fuel type 2 ± 2σ.

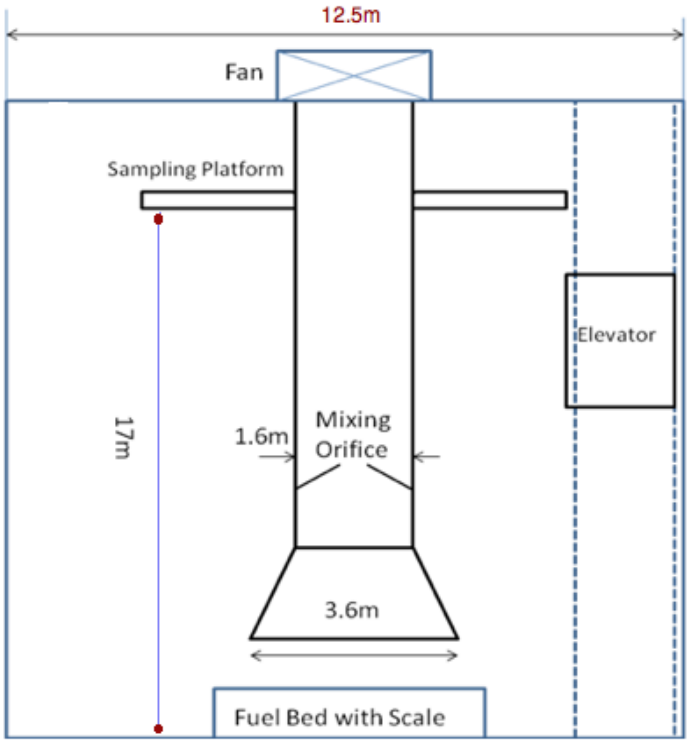

Figure 3.1. Schematic drawing of combustion laboratory, USDA Forest Service Fire Sciences Laboratory, Missoula, MT. Detailed characteristics of the facility are described in Christian et al. (2004).

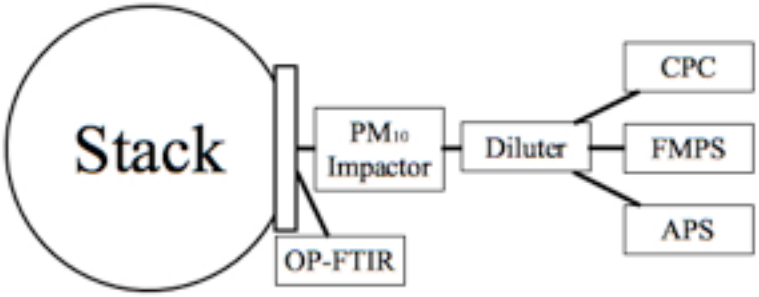

Figure 3.2. Schematic of measurement system.

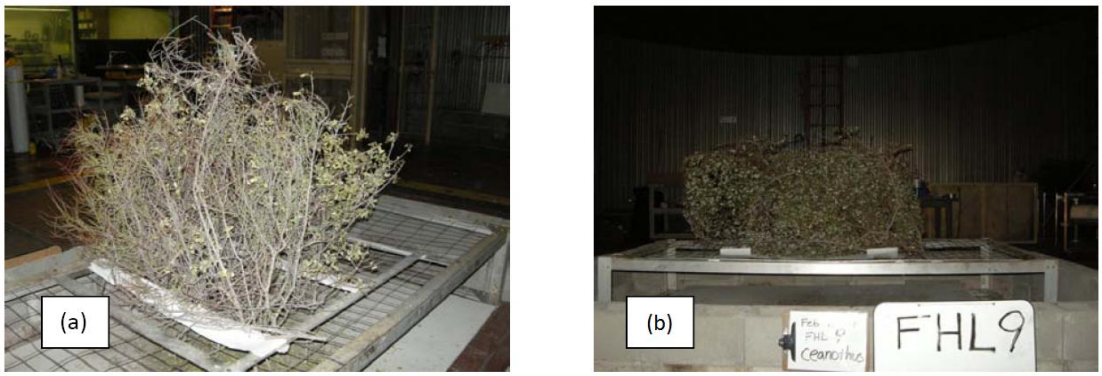

Figure 3.3. Two pictures showing fuel and fuel bed, before the fuel is lit on fire.

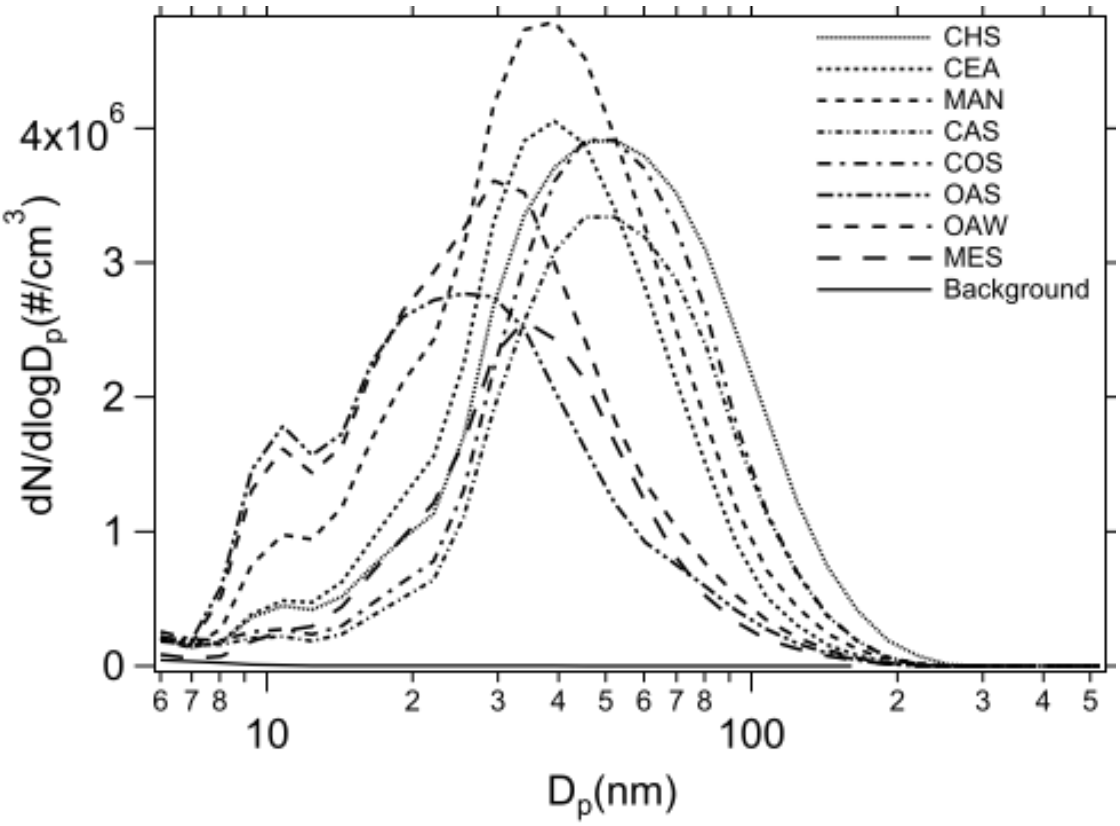

Figure 3.4-(a) Averaged burns- linear scale

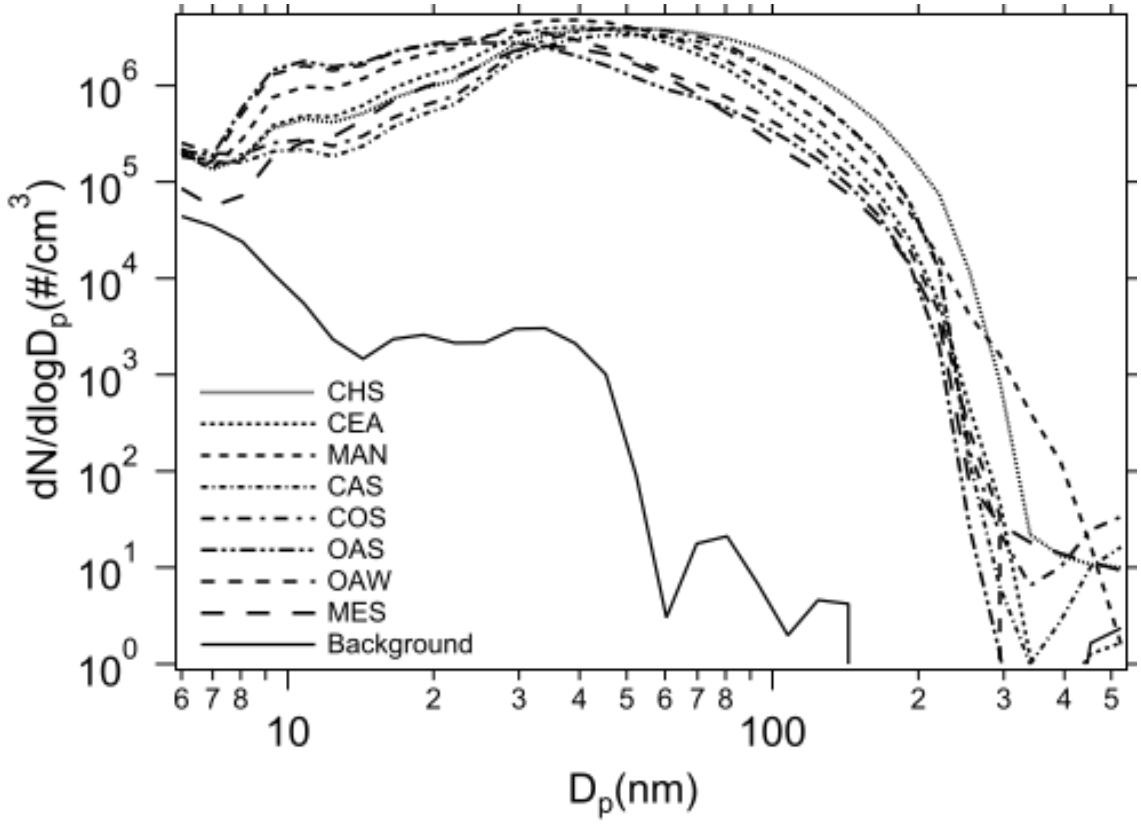

Figure 3.4-(b) Averaged burns- log scale

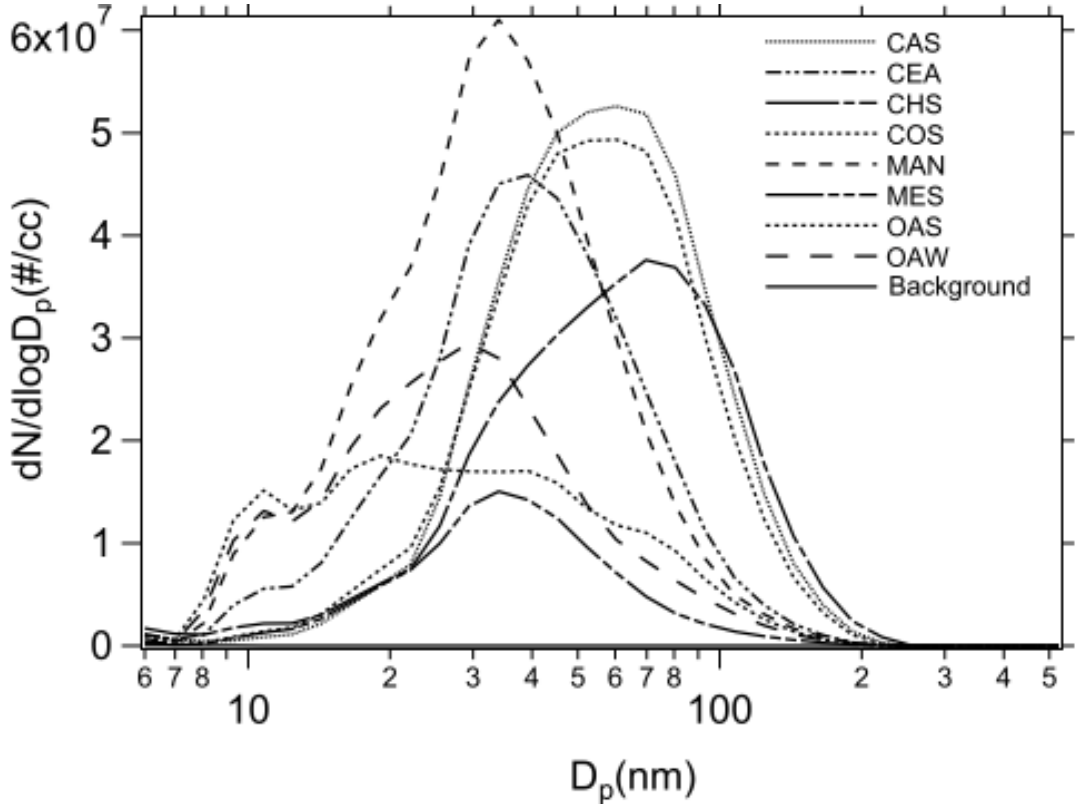

Figure 3.4-(c) Flaming phase

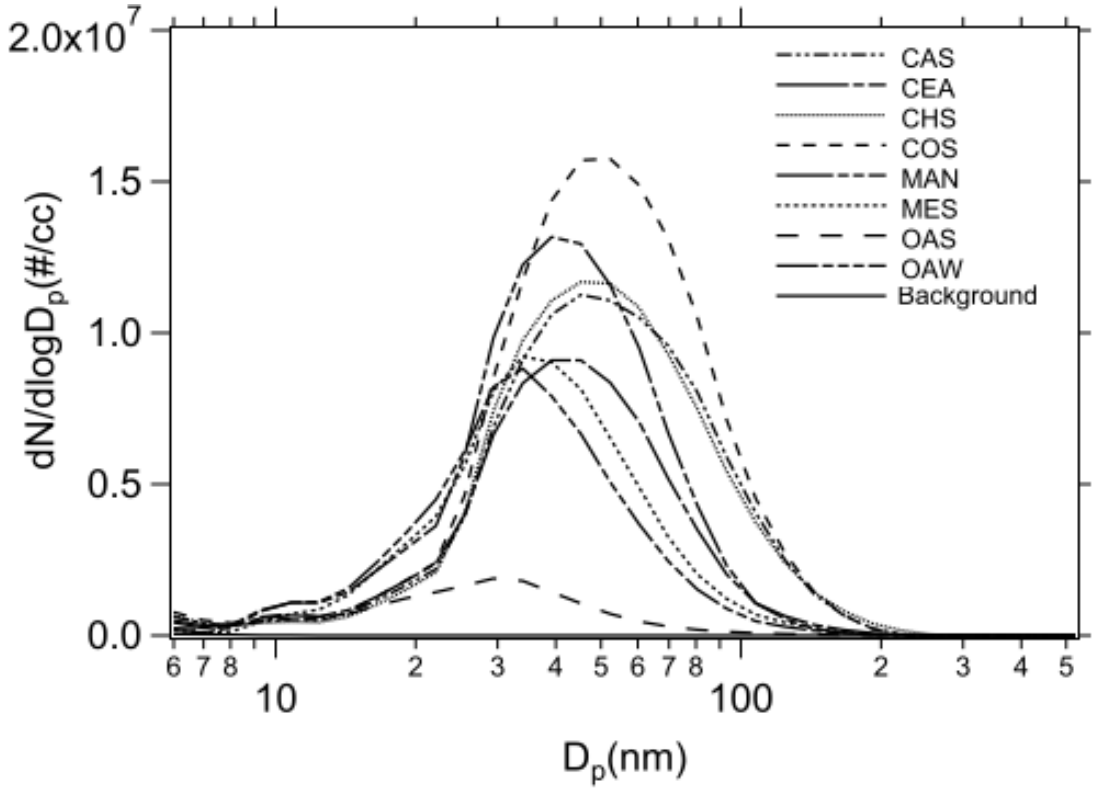

Figure 3.4-(d) Mixed phase

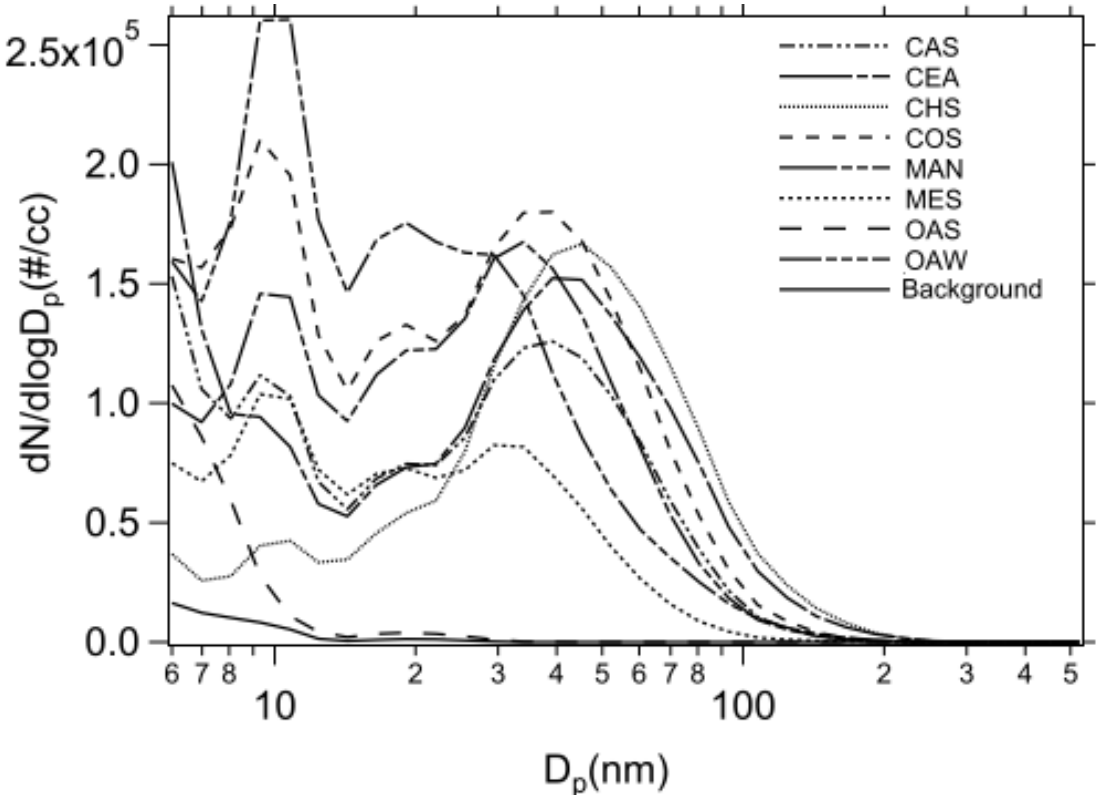

Figure 3.4-(e) Smoldering phase

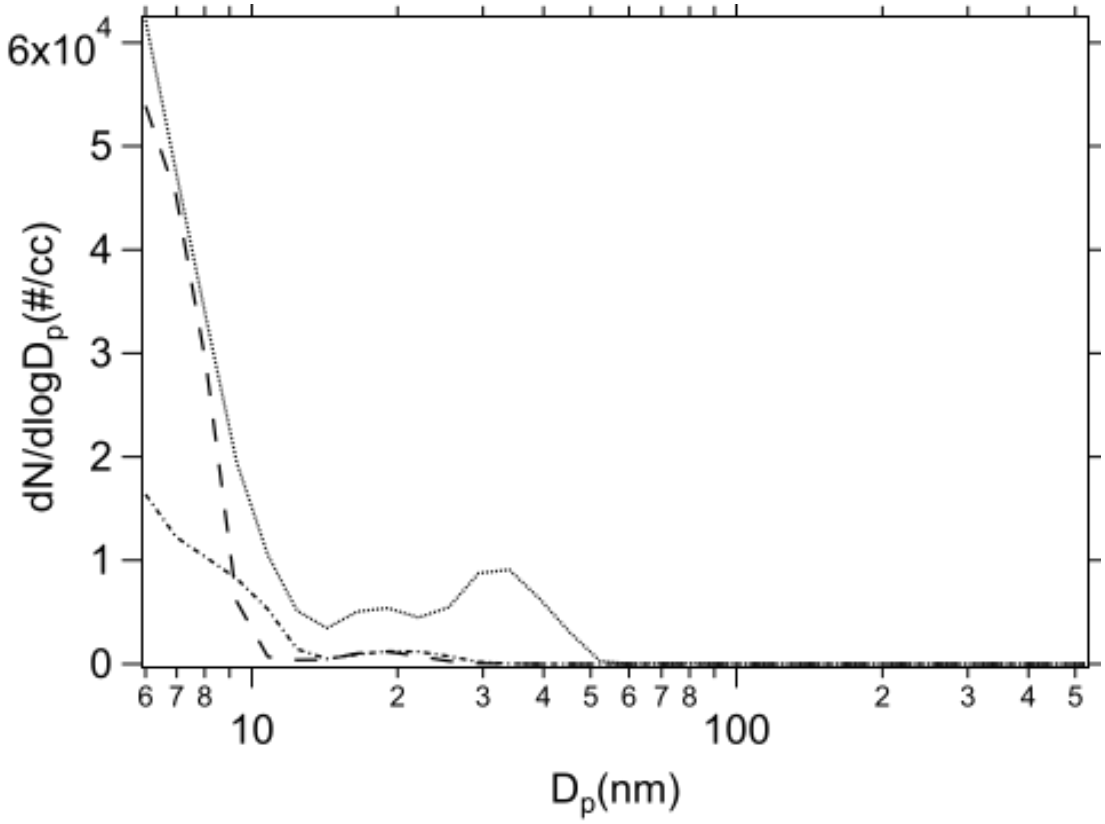

Figure 3.4-(f) Background level concentration

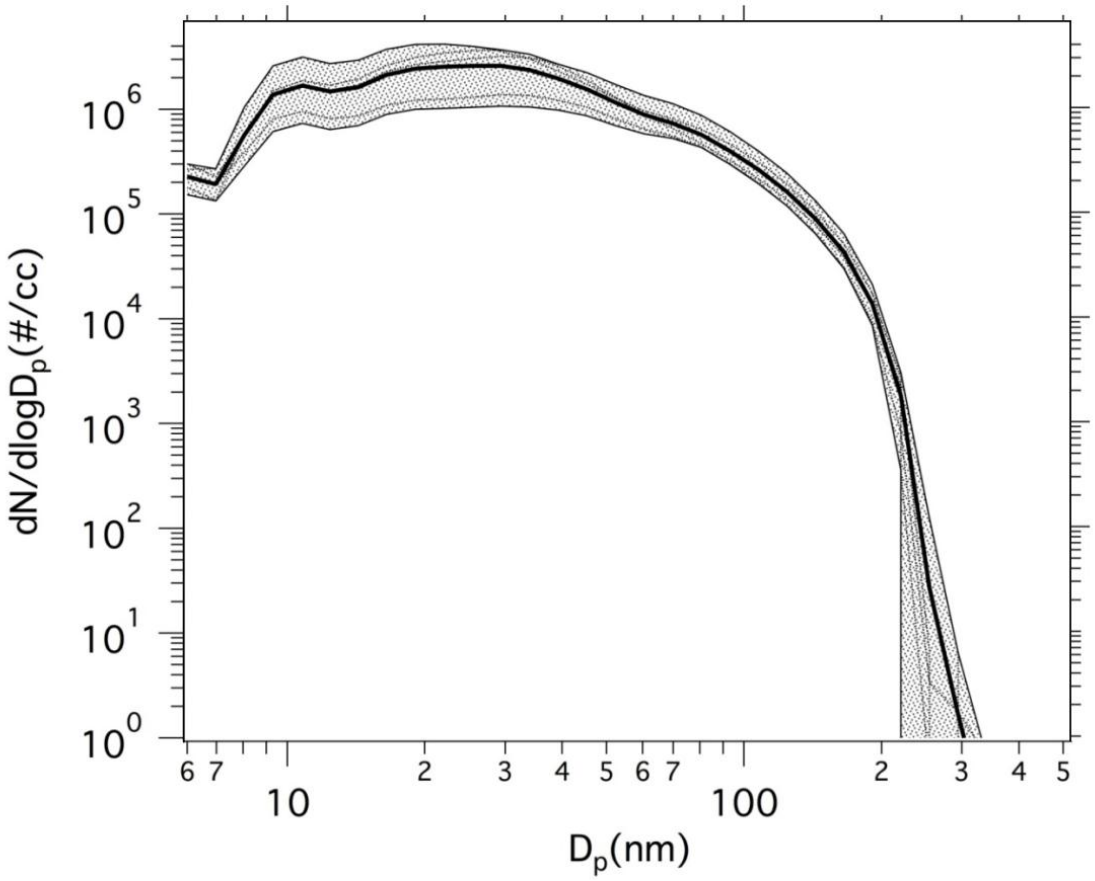

Figure 3.4-(g) Variation of measurements (Oak Savanna)

Figure 3.4. Particle size distributions corresponding to (a) whole burn(linear) (b) whole burn(log-log) (c) Flaming, (d) Mixed, and (e) Smoldering phases (f) presents background levels measured by FMPS (g) variation of measurements

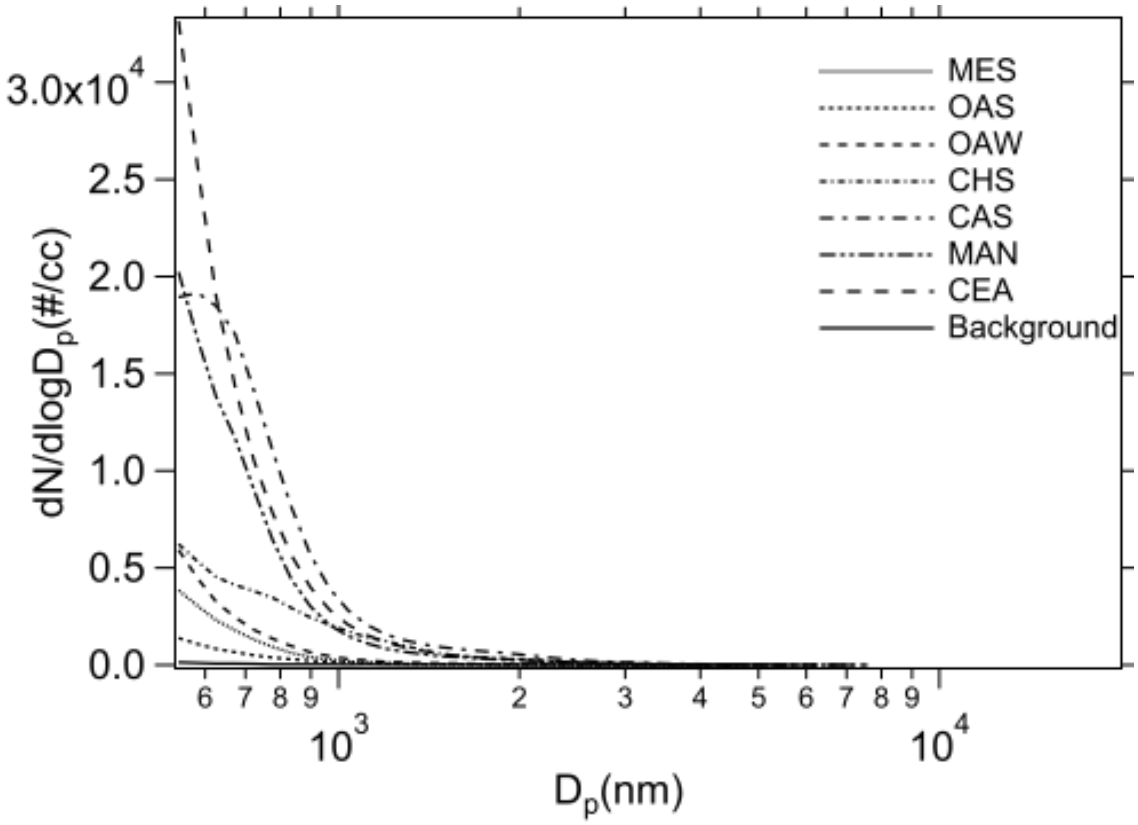

Figure 3.5- (a) Averaged- linear scale

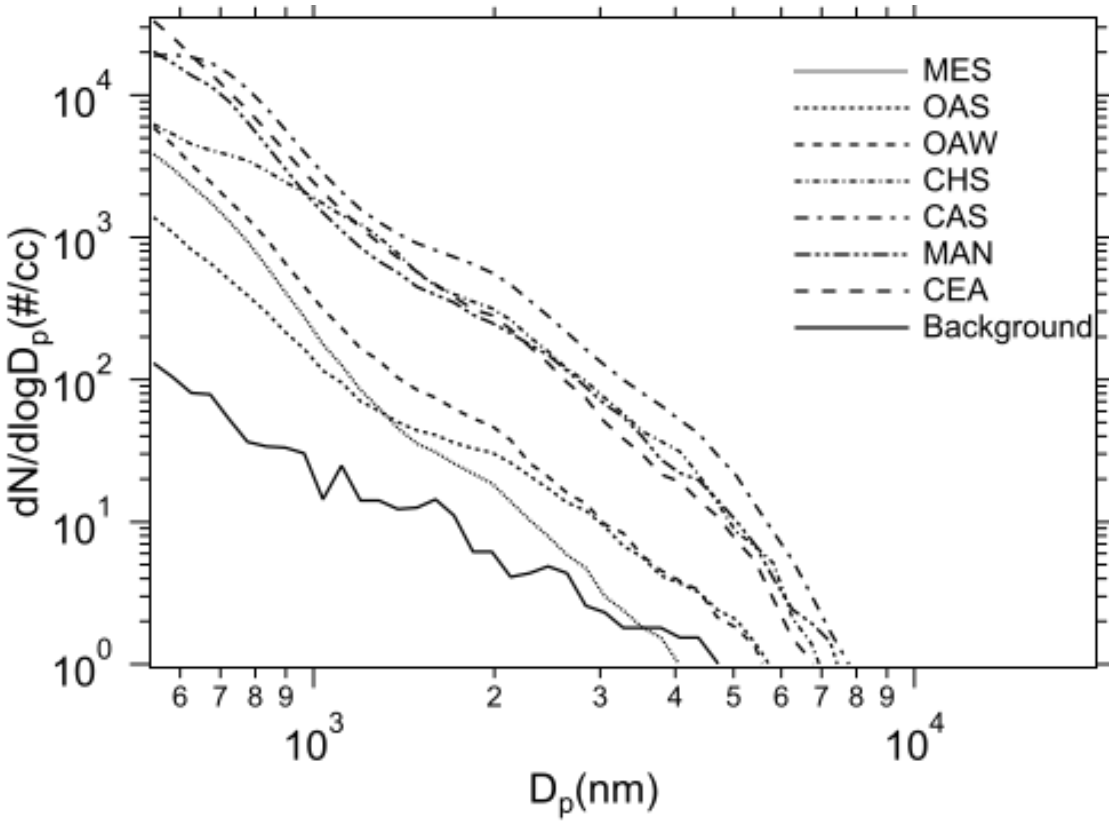

Figure 3.5- (b) Averaged- log scale

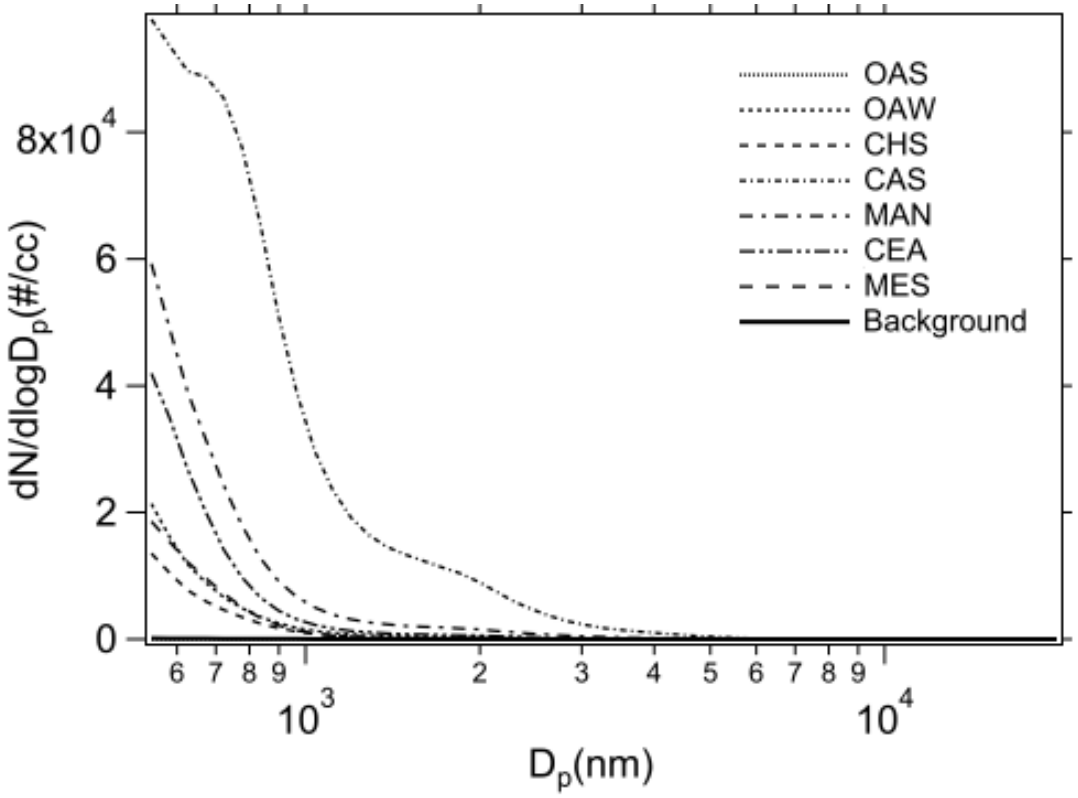

Figure 3.5- (c) Flaming phase

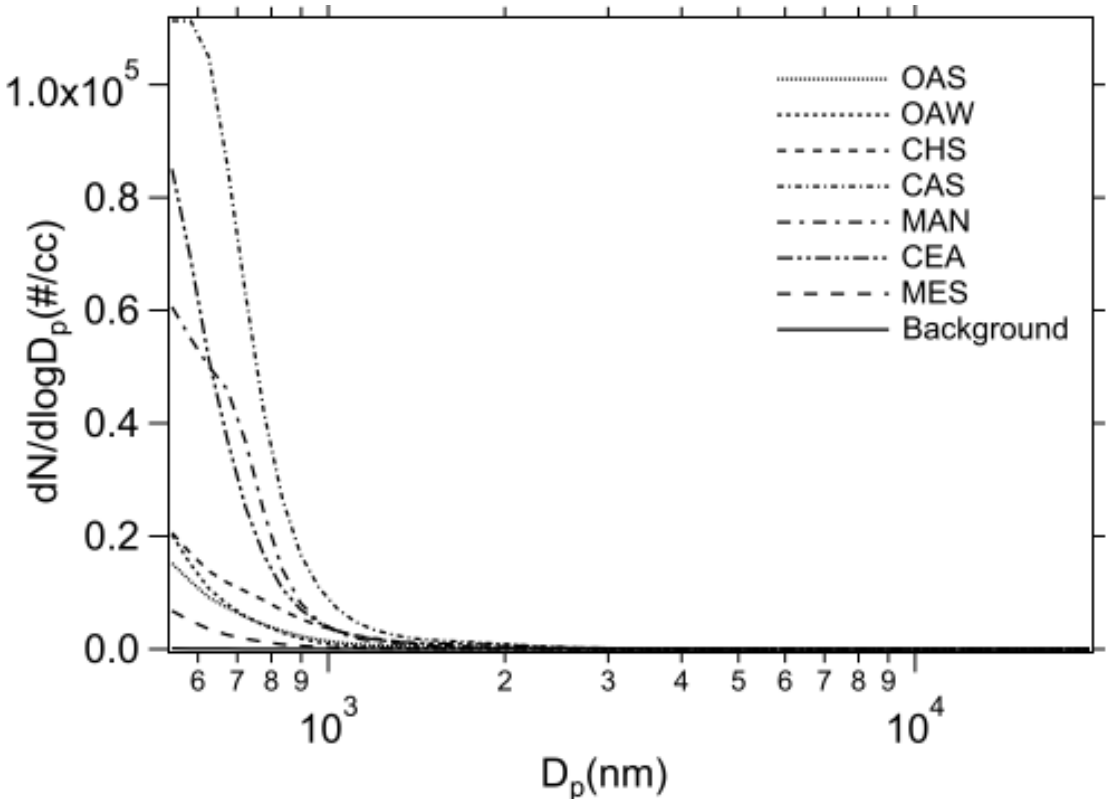

Figure 3.5- (d) Mixed phase

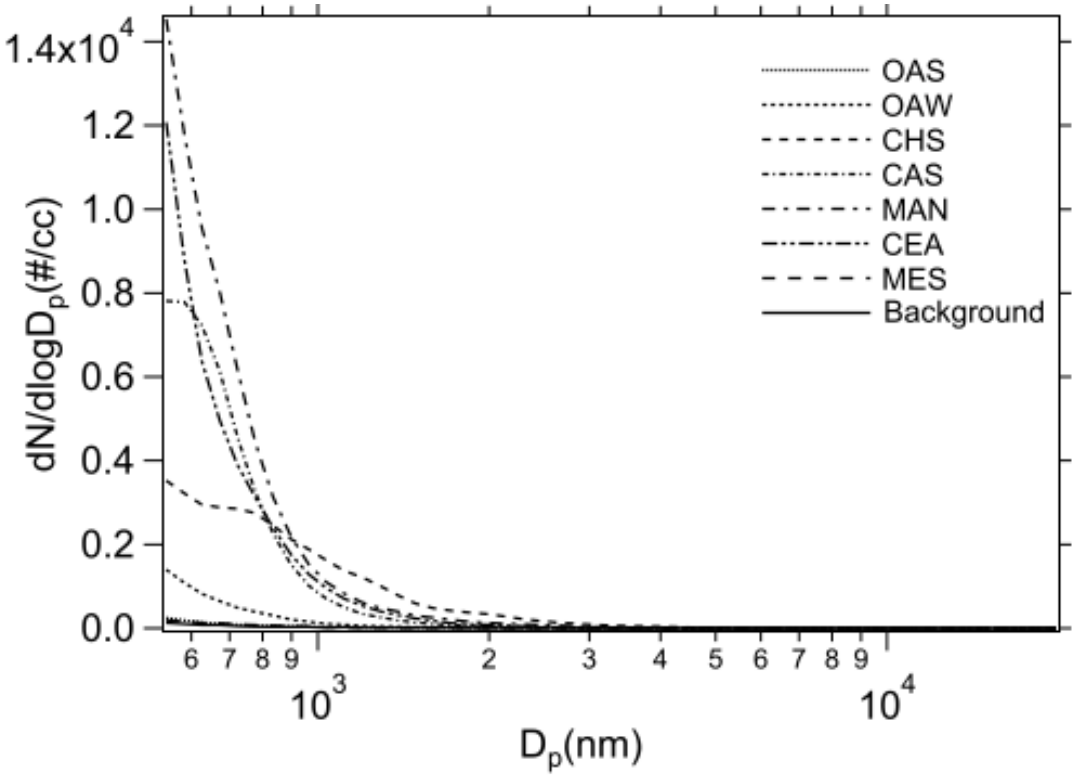

Figure 3.5- (e) Smoldering phase

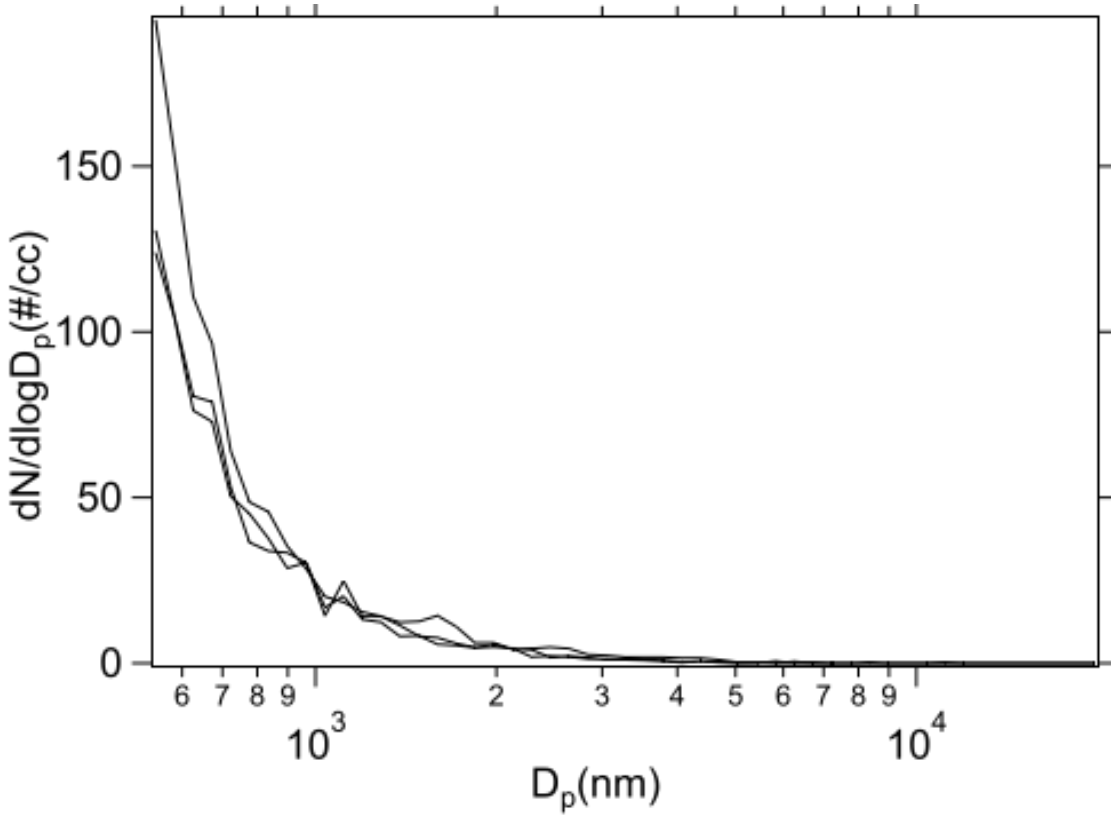

Figure 3.5-(f) Background level concentration

Figure 3.5. Aerodynamic particle size distribution measured by APS for different phases (a) whole burn(linear) (b) whole burn(log-log) (c) Flaming (d) Mixed (e) Smoldering, and (f) corresponds to background concentration

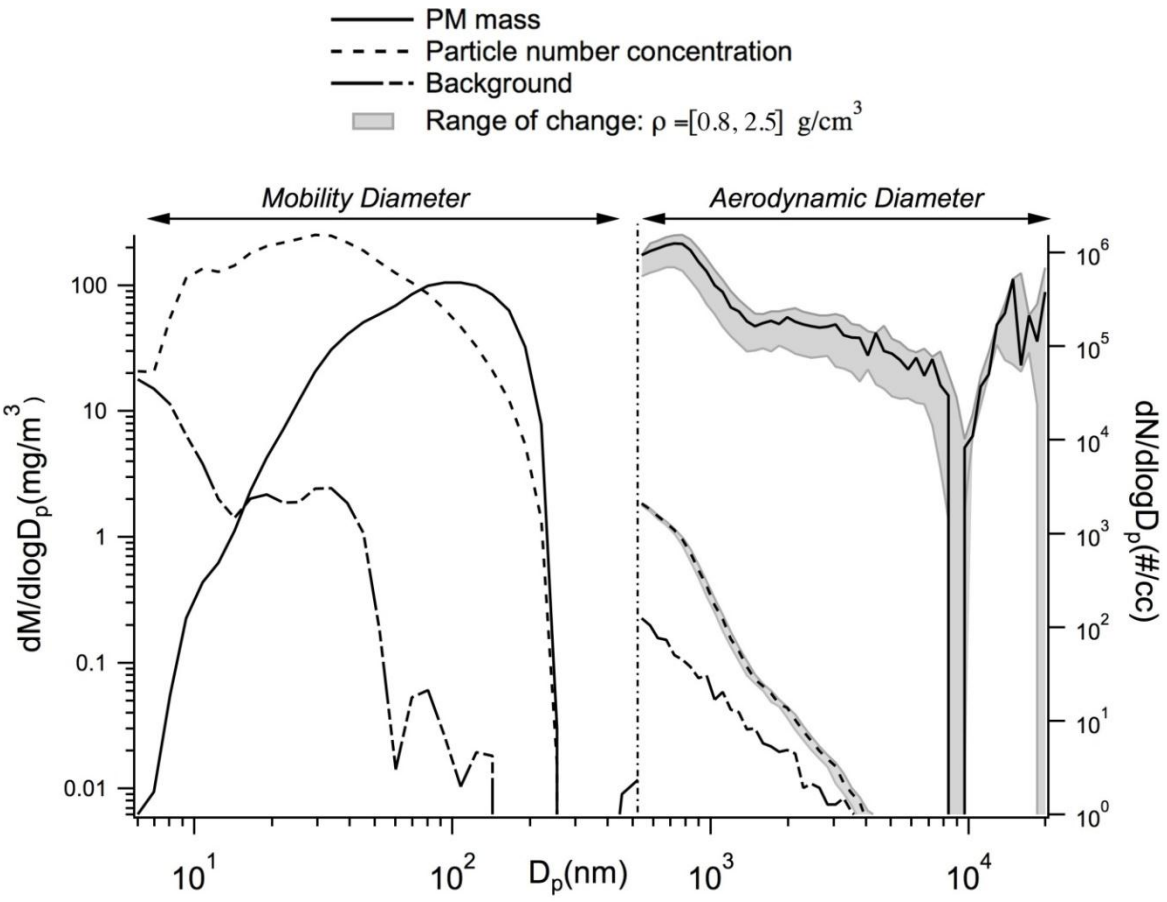

Figure 3.6. Particle number and mass size distributions corresponding to a typical burn, also the background concentration

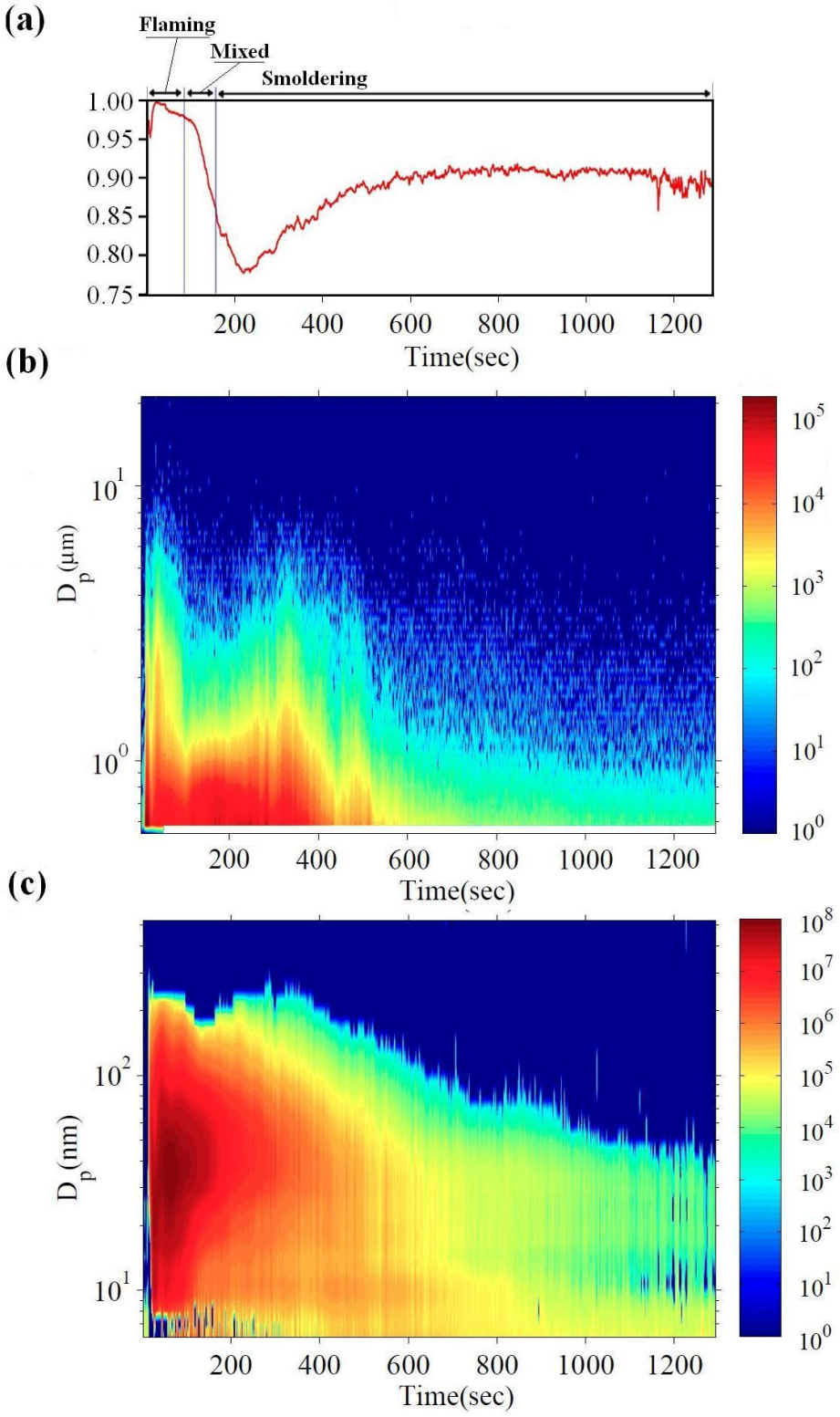
(a)
Flaming
Mixed
Smoldering
1.00
0.95
0.90
0.85
0.80
0.75
200
400
600
800
1000
1200
Time(sec)
(b)
10^1
10^0
D_p (μm)
10^5
10^4
10^3
10^2
10^1
10^0
200
400
600
800
1000
1200
Time(sec)
(c)
10^2
10^1
D_p (nm)
10^8
10^7
10^6
10^5
10^4
10^3
10^2
10^1
10^0
200
400
600
800
1000
1200
Time(sec)

Figure 3.7. (a) Modified Combustion Efficiency (MCE); Corresponding APS (a) and FMPS (b) contour graphs showing particle number size distributions

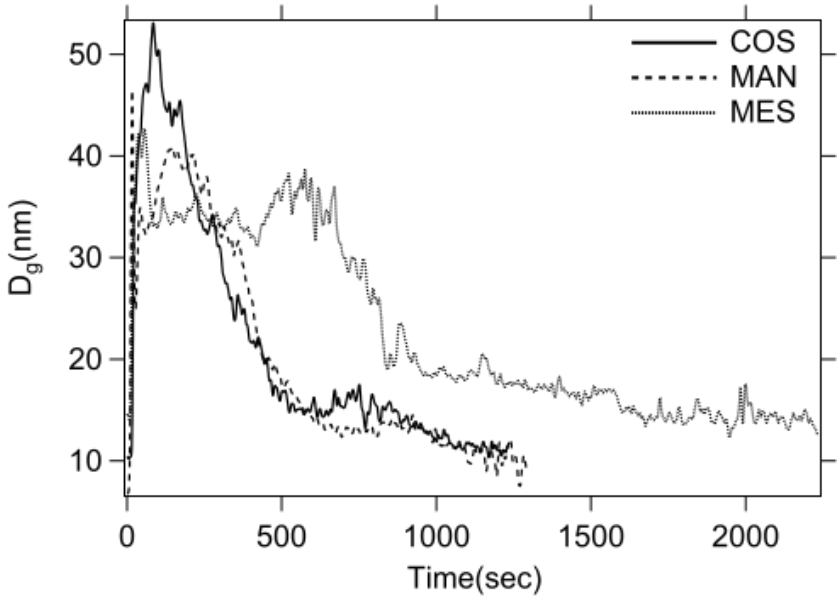

Figure 3.8. MCE vs. Geometric Mean Diameter for three typical burns

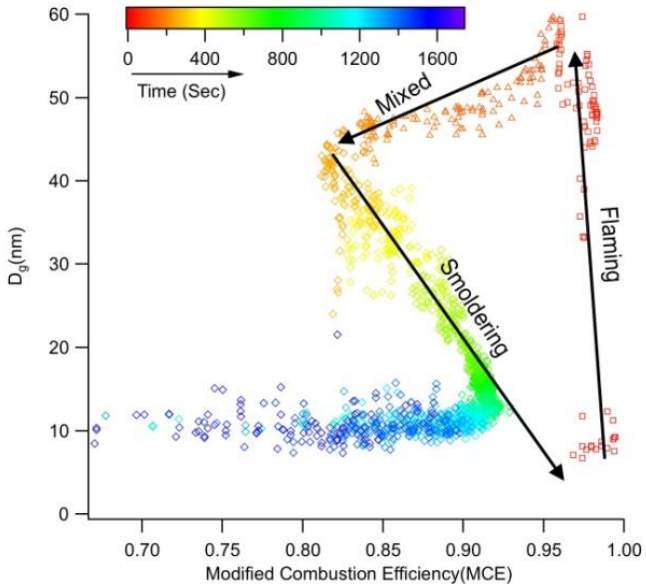

Figure 3.9- (a) CAS

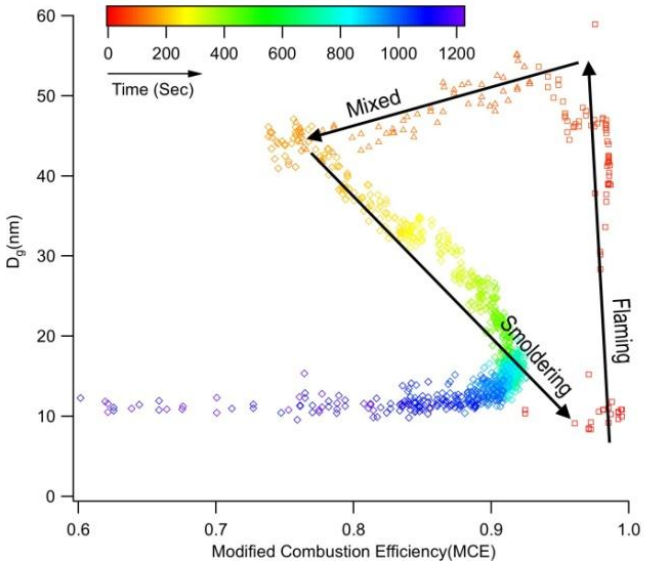

Figure 3.9- (b) COS

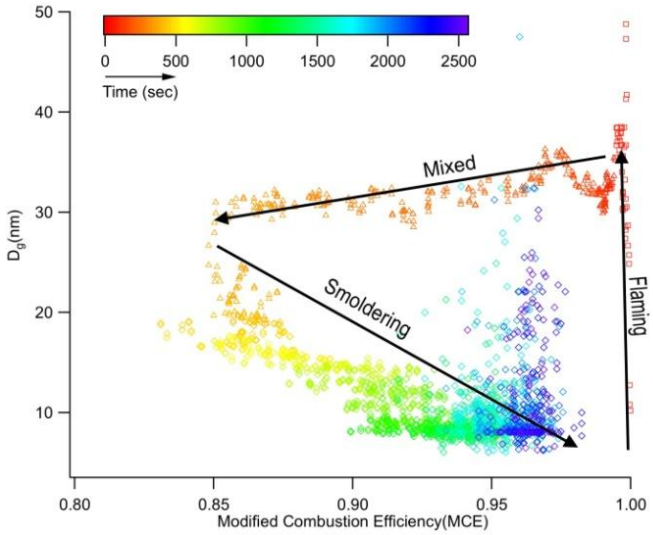

Figure 3.9-(c) OAW

Figure 3.9. MCE vs. Geometric Mean Diameter for three typical burns

Chapter Four: Laboratory characterization of PM emissions from combustion of wildland biomass fuels

4.1. Abstract

Particle emissions from open burning of southwestern (SW) and southeastern (SE) U.S. fuel types during 77 controlled laboratory burns are presented. The fuels include SW vegetation types: ceanothus, chamise/scrub oak, coastal sage scrub, California sagebrush, manzanita, maritime chaparral, masticated mesquite, oak savanna, and oak woodland as well as SE vegetation types: 1-year, 2-year rough, pocosin, chipped understory, understory hardwood, and pine litter. The SW fuels burned at a higher Modified Combustion Efficiency (MCE) than the SE fuels resulting in lower particulate matter (PM) mass emission factor (EF). Particle size distributions for six fuels and particle number emission or all fuels are reported. Excellent mass closure (slope = 1.00, $R^2 = 0.94$) between ions, metals, and carbon with total weight was obtained. Organic carbon emission factors inversely correlated (R^2= 0.72) with MCE, while elemental carbon (EC) had little correlation with MCE (R^2=0.10). The EC/total carbon (TC) ratio sharply increased with MCE for MCEs exceeding 0.94. The average levoglucosan and total Poly Aromatic Hydrocarbons (PAH) emissions factors ranged from 25-1272 mg/kg fuel and 1790-11300 μg/kg fuel, respectively. No correlation between MCE and emissions of PAHs/levoglucosan was found. Additionally, PAH diagnostic ratios were observed to be poor indicators of biomass burning. Large fuel-type

and regional dependency was observed in the emission rates of ammonium, nitrate, fluoride, chloride, sodium, and potassium.

4.2. Introduction

Fresh smoke from wildland biomass burning is a complex mixture of gases and aerosols. The amount and composition of fire emissions depend on a wide range of parameters related fuel type, packing ratio, fuel composition, chemical composition, fuel moisture, fire behavior (e.g. relative amount of smoldering and flaming) (Andreae and Merlet, 2001 Akagi et al., 2011). While wildland fuels are composed primarily of cellulose, hemicelluloses, and lignin, the composition and quantity of trace elements vary by plant species, soil type, and ambient air mass, deposition of sea-salt and anthropogenic nitrogen and sulfur deposition (Albini, 1976, Fenn 1991, Hardy et al., 1996, McKenzie et. al., 1996, Yokelson et al., 2011). Local climate and meteorological conditions influence both plant structure and moisture-conserving strategies, which in turn influence fire behavior and smoke emissions when these fuel types are burned.

While the mean June-August temperatures are similar (15-27 °C), the southwestern (SW)United States tends to be drier (34-69 cm annual precipitation) than the more humid southeastern (SE) United States (114-160 cm) and the seasonality of precipitation is different (23-30 cm December-February for both regions, < 3 cm and 30-42 cm June-August for the SW and SE, respectively[3]. However, some plants and plant communities have developed

[3] Climatological statistics derived from data developed by National Climatic Data Center using US Climate Division Dataset Mapping Page and 1981-2010 base period (http://www.esrl.noaa.gov/psd/data/usclimdivs/) accessed 24 Apr 2012.

similar structure and foliar characteristics such as chaparral in California and pocosin in North Carolina (Christensen 2000, Keeley 2000,). Prescribed burning is a vegetation management tool used to manage wildlife habitat, removee wildland fuel accumulation to reduce the potential for severe wildfire, and to mimic the natural role of fire (Chandler et al, 1983). Recent modeling studies have analyzed the potential use of prescribed burning as a tool to reduce carbon dioxide emissions (Narayan et al, 2007, Wiedinmyer and Hurteau, 2010). Due to a variety of reasons, prescribed burning is used extensively in the SE in contrast to limited use in chaparral and oak ecosystems in the SW. Between 2002 and 2011 the annual average area treated with prescribed burning was 599 kHa in the southeastern U.S. (SE: Alabama, Arkansas, Florida, Georgia, Louisiana, Mississippi, North Carolina, South Carolina, Tennessee, and Virginia) and 134 kHa in the southwestern U.S. (SW: Arizona, California, Colorado, New Mexico, Nevada, and Utah) (NIFC, 2012). During the same period, wildfires burned an average of 854 kHa yr-1 in the SW and 215 kHa yr-1 in the SE (NIFC, 2012).

While prescribed burning is an important land management tool, emissions from prescribed fires and wildfires can have a significant detrimental impact on air quality by degrading visibility and increasing ambient concentrations of fine particulate matter (PM2.5, aerosol with an aerodynamic diameter $\leq$ 2.5 μm), ozone (O_3) (ref) More generally, emissions from biomass combustion can have a substantial influence on local-to-global scale chemical and physical properties of the atmosphere through short- and long-range transport (Crutzen and Andreae (1990), Fishman et al. (1991)). Smoke aerosols can alter the radiation budget of the earth, cloud properties and climate (Reid et al. (1998), Haywood et al. (2003), Kaufman and

Fraser (1997), Hobbs et al. (1997)). Epidemiological studies have linked mass concentration of $PM_{2.5}$ to human morbidity and mortality (Pope III et al. (2009)). Wildland firefighter exposure studies have reported exposures to CO, particulates, and silica at levels near or higher than recommended occupational exposure levels (Materna et al 1992), other studies report that smoke exposure occasionally approaches legal and recommended exposure levels (Reinhardt and Ottmar 1997). Because of the different nature of the work, firefighters generally were exposed to more smoke on prescribed fires than on wildfires (Reinhardt and Ottmar 2004). Additionally, toxic gases (Roberts et al., 2011) are emitted and several PAHs present in wood-smoke are known to be carcinogenic and/or associated with mutagenicity (Roberts and Corkill (1998), Ramdahl and Becher (1982)). Wildland firefighter exposure studies have reported exposures to CO, particulates, and silica at levels near or higher than recommended occupational exposure levels (Materna et al 1992), other studies report that smoke exposure occasionally approaches legal and recommended exposure levels (Reinhardt and Ottmar 1997). Because of the different nature of the work, firefighters generally were exposed to more smoke on prescribed fires than on wildfires (Reinhardt and Ottmar 2004).

Limited data is available regarding particulate emissions from the combustion of fuels commonly burned by prescribe fires and wildfires in the U.S. Little emissions data exist for fuels common to the SW United States, specifically those classified as chaparral. The USFS has classified approximately 5.7 million hectares (17%) of the vegetation in California as brush, 1.62 million hectares of southern and central California are covered with the shrub complex known as chaparral. To assess the potential effects of biomass burning on the atmosphere, it is necessary to provide reliable emission factors (EF) and combustion

parameters to emission inventory algorithms that provide emission input to atmosphere – chemistry transport models and smoke dispersion models. The objective of our study is to determine particulate matter EF for the combustion of fuels representative of ecosystems commonly managed with prescribed burning in SW and SE U.S. EF were determined by measuring particulate and gas phase emissions from the burning of fuels in the large scale combustion facility at U.S. Forest Service (USFS) Missoula Fire Sciences Laboratory. The current study presents only a subset of results and the other results from lab and field components are published elsewhere (Burling et al. 2010, Hosseini et al. 2010, Burling et al. 2011, Veres et al. 2010, Roberts et al. 2010).

4.3. Experimental Methods

4.3.1. Fuel type description

Samples of vegetation representing important wildland fuel types on Department of Defense installations in the southwestern and southeastern U.S. were harvested in the field and shipped to the U.S. Forest Service Fire Sciences Laboratory (FSL) in Missoula, MT in January 2009. These fuel types commonly occur in these two regions. The fuels were stored and then burned in the FSL combustion facility in February 2009.

Table 4.1 describes the species composition and chemistry of vegetation comprising each fuel type studied and provides the three-letter fuel code used for fuel type in this paper. This list encompasses 9 and 4 fuel types from the SW and SE that were provided by the United States Forest Service (USFS). Further details regarding the fuels are provided in Burling et al. (2010).

Fuels were analyzed for chemical composition by first grinding the plant tissues (wood and foliage) into a uniform coarse material using a Thomas Model 4 Wiley® Mill[4]. The samples were further ground to extremely fine particles using a mortar grinder. Approximately 5g of each fuel sample was analyzed for C, H, N, S, and O using a combustion technique (McGeehan and Naylor (1988)) on a Thermo Fisher Scientific FlashEA 1112 Series Elemental Analyzer (Table 4.1). The vegetation components comprising the fuel beds were also analyzed by an outside laboratory (University of Idaho Analytical Sciences Laboratory) for Cl, K, and Na content (Table 1). The content of Cl, K, and Na varied greatly with location of origin and plant type (see Table 1). Because we did not measure fuel consumption by vegetation component, we cannot quantitatively link element loss in the fuels to the particle and gas-phase emissions. However, we have estimated lower and upper limits on element release for each fuel type and aggregated these limits to provide a representative value for each location (see Table 1). The purpose of these representative values is to illuminate the role of fuel chemistry in aerosol element emissions they are not intended for developing quantitative relationships.

4.3.2. Combustion Facility and Burn procedure

Experiments were conducted at the U.S. Forest Service's combustion facility at the Fire Sciences Laboratory (FSL) in Missoula, MT. The facility is a large air-conditioned chamber that measures $12.5\,m \times 12.5\,m \times 22m$ in height (Figure 4.1). A 3.6 m inverted funnel opening approximately 2 m above the floor captures the smoke from fires on a continuously

[4] The use of trade names is provided for informational purposes only and does not constitute endorsement by the U.S. Department of Agriculture.

weighed fuel bed. The smoke is then directed through a 1.6 m diameter exhaust stack that exhausts through the ceiling. The room is pressurized slightly to ensure complete entrainment of fire emissions. A large sampling platform surrounds the stack at 17 m elevation where an Open Path Fourier Transform Infrared Spectrometer (OP-FTIR) and a suite of particle instrumentation were located (Figure 4.2). The smoke at the height of sampling platform is well-mixed and has the same temperature and mixing ratios across the stack diameter (Christian et al., 2003, Christian et al., 2004). The fuel bed was an aluminum frame with wire mesh and removable heat-resistant 1.27 cm Kaowool M Board that was removed depending on the physical characteristics of the vegetation. Two electronic balances continuously recorded the mass of the fuel. The stack exhaust fan speed was 1.5 and 3.0 m/s for majority of the burns. Nearly all of the fires were ignited with a propane torch, a small number were ignited using isopropyl alcohol in addition to the torch. Additional information on the FSL combustion facility may be found in (Christian et al., 2004).

4.3.3. Measurement system and sample analysis

Three filter sampling systems (FS1, FS2, UCR) simultaneously pulled the smoke sample from the exhaust stack through a cyclone, and then onto quartz and Teflon filters (Figure 4.2). The cut-off sizes and set flow rates are as follows: two cyclones with cut-off diameters of 2.5 and 3.5 μm were installed on the FS1 and FS2 lines operating at 30 and 28 lpm, respectively. A 2.5 μm impactor ($PM_{2.5}$) distributed the smoke samples between filter samplers QF1,2 and TF1,2 at 25, 23, 27, and 22 lpm (UCR), respectively. For 43 of the 77 burns, FS2 was loaded with Teflon filters while FS1 was loaded with a quartz filter.

However, for 24 of the burns FS1 and FS2 were loaded with Teflon filters. QF1,2 and TF1,2 were always loaded with quartz and Teflon filters, respectively. Since duplicate measurements were made by UCR and the USFS (FS1 and FS2), the two subsets were ultimately combined to form the larger data set that is used in this study. UCR used 47 mm Quartz (2500QAT-UP Tissuquartz™, Pall Corporation, NY) preconditioned at 600 °C for 5 hours and pre-weighed 47 mm Teflo® (2μm pore, Pall Corporation, NY) filters.

In addition to the sampler system described previously, several particulate phase instruments were also located on the platform: an Aerodyne High Resolution Time of Flight Aerosol Mass Spectrometer (HR-TOF-AMS), an Ultrafine Condensation Particle Counter (UCPC Model 3776, TSI Inc.), a Scanning Mobility Particle Sizer (SMPS), a Fast Mobility Particle Sizer (FMPS Model 3091, TSI Inc.), Aerodynamic Particle Sizer (APS Model 3321, TSI Inc.), a Micro-Orifice Uniform Deposit Impactor (MOUDI), and a Dekati® Mass Monitor (DMM).

A single 1.0 cm × 1.5 cm punch from each quartz filter was analyzed for elemental and organic carbon by both UCR and the USFS with a Sunset Laboratory (Forest Grove, OR) Thermal/Optical Analyzer following NIOSH 5040 reference method (1996) (Birch and Cary, 1996). Pre- and Post-experiment Teflon filter weights were obtained following Code of Federal Regulations (CFR40 1065, 2005).

Following gravimetric analysis, elemental composition of the deposited material on the Teflon filters was determined using by X-ray fluorescence (XRF). The USFS samples were analyzed by Chester Labnet (Tigard, OR) using U.S. EPA Method IO-3.3. The UCR samples

were analyzed by the South Coast Air Quality Management District (SCAQMD, Diamond Bar, CA) using a PANalytical Epsilon 5® Energy Dispersion X-Ray Fluoresce (EDXRF) equipped with dual anode (Scandium/Tungsten) X-ray tube. Each filter was analyzed ten separate times using ten different excitation conditions under vacuum. The instrument software deconvoluted and calculated the concentration for each element in μg/m3. For the EDXRF technique, Analytical quality control was determined by testing NIST Standard Reference Material 2783. Most USFS Teflon filters were analyzed by XRF method for 29 burns, while UCR analyzed one filter for each fuel type.

A set of 47-mm Teflon substrates was used for Ion Chromatography (IC) analysis following California Air Resources Board Method MLD 142. The filters were extracted by sonication into deionized water and small amount of isopropyl alcohol. Aliquots of the extract were then filtered and analyzed on a Dionex DX-120 ion chromatograph. The analysis yielded concentrations of the following ions: sulfate, nitrite, fluorite, chloride, bromide, sodium, ammonium, potassium and calcium.

The 47-mm quartz substrates were spiked with 13C labeled levoglucosan (purchased from Cambridge Isotope Laboratories Inc., Andover, MA) and select deuterated PAHs. The ^{13}C spike volume was calculated based on the organic carbon content of each filter (μg/filter), whereas the PAH spike volume was maintained constant at 100 μL on each filter. The filters were extracted using dichloromethane and acetone (50:50) by a Dionex® Automated Solvent Extractor 200 (ASE). Half of the extracted volume was used for levoglucosan analysis and the other half for the PAH analysis.

The half of the extracted sample used for PAH analysis was concentrated to 5 mL by rotary evaporation using a BUCHI-3000 evaporator. The sample was further concentrated to 1.5 mL with a nitrogen stream. This final volume was transferred to amber wide crimp top vials, sealed and analyzed on a Agilent® 5973 GC-MS equipped with a Programmable Temperature Vaporizer (PTV) large volume inlet (7683 Series).

The other half of the extracted sample was concentrated to 5 mL by rotary evaporation using a Buchi® R-3000 Rotary evaporator. This sample was further evaporated to 250µL aliquot using nitrovap. 50 µL of the aliquot was carefully transferred into an amber vial and nitrovaped to dryness. The sample was then derivatized for 2 hours at 70°C with 50µL of N,O-bis(trimethylsilyl) trifluoroacetamide and 25µL of pyridine (obtained from Sigma-Aldrich Chemle GmbH, Switzerland). The sample was subsequently re-diluted to a specific calculated volume based on expected LV concentration, transferred to an amber wide crimp top vial, sealed and analyzed on the GC-MS. The mass spectrum of levoglucosan tritrimethylsilyl ether exhibited only a small molecular ion (m/z 378) with fragments due to loss of CH_3 (m/z 363), CH_5Si (m/z 333), $C_6H_{17}OSi_2$ (m/z 217) and $C_7H_{18}OSi_2$ (m/z 204, base peak). Fragments 217 and 333 were used for quantification.

The general fire behavior (i.e. the relative amount of flaming and smoldering combustion) was characterized using Modified Combustion Efficiency (MCE) based on CO and CO_2 concentrations measured by OP-FTIR (further details in Burling et al. (2010)). The MCE is defined as the fire-integrated excess ratio of CO_2 to CO plus CO_2 (Ward, D. E. and Radke (1993): $= \frac{\Delta CO_2}{\Delta CO + \Delta CO_2}$). It was assumed that the background concentrations of CO and CO_2

were constant during the burns and were equal to their 1-min averaged concentration prior to ignition.

4.4. Results and Discussion

77 fuel beds were burned in an 18 day period in February 2009. Mean temperature and relative humidity in the facility during this period were 23.7 °C (s.d. = 2.0) and 15.2% (s.d. = 3.5), respectively. While in storage, the samples lost much of the moisture normally contained in the plant tissues so the samples that were burned did not represent the moisture content of the living vegetation when normally burned during either a prescribed burn or wildfire. Moisture content of the SW fuels ranged from 4 to 33%; moisture content in living chaparral ranges from 70-160% over the normal growing cycle (Countryman and Dean, 1979). Similarly, moisture content of the SE fuels ranged from 3 to 32%; moisture content in living evergreen pocosin shrubs ranged from about 70 to 250% (Blackmarr and Flanner 1975). The arrangement of the fuels significantly affected the fuel consumption. Initially, five chamise/scrub oak and three ceanothus fuel beds were arranged vertically; however, the fire failed to spread well resulting in low fuel consumptions of 3% to 52% (average: 26%). The remaining fuel beds were arranged horizontally, which greatly increased fuel consumption to ~90% for the rest of the burns. A total of 77 fires (71 from SE and SW fuel beds) were conducted at the Missoula FSL combustion facility in February 2009.

4.4.1. Determination of the mix of Combustion Processes

Modified Combustion Efficiency (MCE) (Ward, D. E. and Radke (1993), Yokelson et al (1996)), calculated for each burn, was used to ascertain the relative amount of combustion

processes (e.g., smoldering, and flaming; average MCE is shown in Table 4.1). The average of fire-integrated MCE values for all burns is 0.94±0.002 (median: 0.942; range: 0.868 - 0.975) indicating that all the burns had a mix of flaming and smoldering with high MCE indicating relatively more flaming. The coefficient of variation of MCE in this study is much smaller than some previous studies (e.g. 0.5% vs. 3.1% McMeeking 2009).

4.4.2. Fuel Moisture versus MCE

Fuel Moisture (FM) may weakly affect the average burn MCE (Figure 4.3). Figure 4.3 was produced combining data from this study with a selected other lab studies: Weise et al. (1991) for California chaparral, Keene et al. (2006) for African savanna, and McMeeking et al. (2009) for a wide variety of U.S. domestic fuels. The plot shows that all these studies have consistent MCE-FM results. The upper bound of MCE for FM>20% stays relatively flat around 0.95 while the lower bound decreases with increasing FM. Upper and lower bounds both sharply converge to MCE=1, when FM<20%. The downward and upward triangles in Figure 4.3 indicate heading and backing fires, respectively (Keene et al., 2006). As can be seen for FM up to 20%, MCE appears to be bound by the fire propagation dynamics (backing/heading fire). Backing/heading fires represent two limiting combustion cases: A heading fire has larger flames, spreads faster and leaves more un-burned fuel behind while a backing fire has smaller flames, slower propagation rates and has higher combustion completeness (Ward, 1998, Peterson and Leenhouts, 1997). For example, Lobert et al., 1991 observed a 40% increase in the CO/CO_2 ratio going from a backing fire to a heading fire for laboratory savanna grass burns. The propagation factor (heading/backing fire) does not

seem to be the dominant factor in MCE values for FM>30%, since after this point the MCE is seemingly not bound by backing/heading fire data points.

4.4.3. Total Particulate Emissions

4.4.3.1. Particle Matter Mass Emission Factors

The EFs in the current study are calculated based on the carbon mass-balance method (Ward et al., 1979, Yokelson et al., 1999, and Burling et al., 2011). Table 4.1 presents average particle emissions factors for each fuel type studied. The average emission factors for PM2.5 (g PM2.5 per kg dry biomass burned EFPM2.5) measured in this study are plotted versus average MCE (Figure 4.4). Also included are data points from previous studies that examined similar fuels, as well as trend lines from earlier lab and airborne studies. Hereafter, we will use notation of EF g/kg< MCE> for reporting emission factor and MCE.

The laboratory study of McMeeking 2009 reported an average EFPM2.5 for chaparral fuels of 11.6±15.1 g kg-1<0.909±0.029> that includes 7.8±1.2 g kg^{-1} <0.913±0.012> , 6.5±4.2 g kg^{-1} <0.914±0.030>, and 23.5±25.9 g kg^{-1} <0.899±0.030> for cea, chs, and man, respectively. The current study has lower PM emissions for chs and man, mainly attributed to the higher MCEs (for these specific fuels) in this study. However, cea is higher in the current study, likely due to lower combustion temperatures from the poorly combusted fuel bed. The EFPM2.5 response to MCE in our study (slope = 248.8, Figure 4.4) is 80% of that reported by McMeeking (2009) (slope = 311.1, Figure 9 of McMeeking et al. (2009) for EFPM2.5).

Size-resolved PM mass speciation using a micro-orifice uniform deposit impactor (MOUDI) was obtained for 6 burns (Figure 4.5). The size distribution of PM peaked in the particle accumulation mode with an aerodynamic diameter that ranged (depending on fuel type shown in parentheses) between the 8th stage (2yr/CL and 1 yr/CL; 0.18 μm cut-size) and 10th stage (oas, cea, cuh, and mes; 0.056 μm cut-size). The PM mass in the size range 3.2-18μm varied between 2-18% of the PM3.2 mass with an average of 10%±6%. The ratio of EFPM3.5 to EFPM10 was 1.00-1.07; this is consistent with the PM10 to PM2.5 mass ratio of 1.09 of McMeeking et al. (2009). For quality control purposes, we correlated the total accumulated mass on the MOUDI stages against the Teflon filter mass on the same fire. The total accumulated MOUDI mass was 27% higher than the Teflon filters mass (the correlation is shown in Figure 4.5-(g), r^2=0.99). According to Reid et al. 2005, coarse-mode particles can contribute to 10-20% of the total collected PM mass consistent with the current study.

4.4.3.2. Particulate Matter Number Emission Factors

Figure 4.7 and Table 4.3 present the fire average particle number emission factors for SW and SE fuel types. The number emission factor was measured and reported separately for two instruments: the ultra-fine CPC Model 3772, TSI Inc. (measuring size range: 2.5nm-3μm) and the Dekati® Mass Monitor (DMM) (measuring size range: 0-1.2μm). CPC Average EFPN were calculated to be (5.2±2.7)×1015, (4.7±1.3)×1015, and (7.8±1.9)×1015 for fuels from the chaparral group, FHUA (SW), and camp Lejeune (SE), respectively. Similarly, average DMM EFPN were (5.3±1.6)×1015, (3.7±1.2)×1015, (6.5±2.2)×1015 for fuels from chaparral group, FHUA (SW), and camp Lejeune (SE), respectively. These EFPN

are in agreement with the estimate of Andreae and Merlet (2001) that suggest an EFPN of 3.4×1015 particles per kg of fuel burned for Aitken nuclei/condensation nuclei aerosol. Differences between particle number emission factors from different fuel types in the current study are explained based by their respective MCEs (Figure 4.8). In general, the lower SE MCE values compared with higher SW MCE values result in the higher SE particle number emission factors compared with SW fuels.

The airborne EFPN3μm of (3.0±1.7)×1016 of Sinha et al. (2003) (CPC TSI 3025A) from 10 savanna fire smoke plumes in Africa with very little aging was an order of magnitude higher than this study. The rapid production of ozone and organic acids observed in their airborne FTIR measurements indicate ongoing photochemistry in the plume suggesting the possibility of new particle formation. An airborne study of Amazonian deforestation, Guyon et al. (2005), measured an EFPN3μm of 4.6×1014-1.1×1016 particles/kg fuel burned covering the wide range of lab and field study values.

Figure 4.6 presents the EFPN by the CPC versus the EFPN by the DMM. As shown, there is a relatively large coefficient of variation (with r^2=0.63) in comparing the CPC and DMM. The overall particle number emission factor of CPC is observed to be about 82% of the DMM. As shown in a previously published article from this study (Hosseini et al., 2010), the geometric mean diameter of particles decreases as the fire evolves from flaming phase into smoldering phase. It is noted that the DMM requires a robust size distribution to accurately invert the electronic signals to number concentrations leading to greater variability in number count and possible biases in absolute number concentrations. Therefore, varying PN size distributions and different particle size ranges of the two instruments gave rise to

the discrepancy; the ultrafine CPC 3776 has a particle size lower detection limit of 2.5 nm and the DMM has a size range of 0 to 1.2 μm.

Similar to the observed dependency of PM mass on MCE, the linear correlation of EFPN of CPC and DMM with MCE is obtained (Figure 4.8). As shown, MCE and EFPN are weakly anti-correlated (rCPC2=0.27, rDMM2=0.33) which shows some natural variability and may reflect the wide range of fuel types of this study. The regression lines in this study are comparable to previous field studies. The airborne study of Guyon et al. (2005) who observed biomass burning of Amazonian forests reported a regression line of EFPN=(-2.80×MCE+2.76)×1016 that is 37% of the EFPN observed in this study. The Janhall et al. (2010) review paper, based on airborne measurements of biomass burning of three fuel types (forest, savanna, and grass), estimates a regression line of EFPN=(-3.46× MCE+3.44)×1016, about half the EFPN measured in the current study. These differences are easily attributed to coagulation losses of nucleation mode particles on short time scales (Reid et al., 1998, Akagi et al., 2012; Reid et al., 2005a, b). Moreover, the regression line calculated by Janhall et al. (2010) uses data points acquired from a Passive Cavity Aerosol Spectrometer Probe (PCASP), which has a lower cut-size of 100nm compared to the cut-size of 2.5 nm in the current study.

4.4.4. Particle Component Emission Factors

4.4.4.1. Organic and Elemental Carbon Thermal Optical Analysis

Integrated EFOC, g carbon/kg fuel burned, for all the burns is plotted as function of MCE (Figure 4.9-b). EF OC is observed to negatively correlate with MCE (r^2=0.72). lit/FB from

SE fuels emitted the highest amount of OC per kg fuel burned (10.60±3.64 g kg-1 <0.894±0.017>), and oas/FHUA from SW the lowest (0.44±0.10 g kg-1 <0.971±0.004>). Comparisons of literature EFOC must account for MCE since OC emission factors are highly dependent on MCE. McMeeking et al. (2009) reports EFOC of 1.8 <0.913>, 1.5 <0.914> , and 7.1 <0.899> g/kg dry fuel for chaparrals cea, chs, man, respectively, similar to values in Table 4.2 but slightly overestimated by the proposed EFOC vs. MCE line (Figure 4.9-b). Andreae and Merlet (2001) suggest EFOC of 3.4 g kg-1 <0.94> for savanna and grassland that agrees well with the given EFOC-MCE linear fit. Overall, SE fuels generally led to higher EFOC compared to SW fuels at similar MCEs. The only exception is cuh/CL of SE, which was similar to SW fuels.

Integrated EFEC as a function of MCE is plotted in Figure 4.9-a. The EFEC (g/kg) ranged from 0.47 g kg-1 <0.965> to 1.54 g kg-1 <0.944> for SW fuels and from 0.41 g kg-1 <0.954> to 1.51 g kg-1 <0.945> for SE fuels, respectively. The highest EFOC in SE and SW group is from cas/FHL and uh/CL, respectively; the lowest EFEC for SE and SW were cuh/CL and oaw/FHUA. No EFEC ecosystem dependency was observed. Further, Andreae and Merlet (2001) suggest an EFEC of ~ 0.48 g kg-1 <~0.94> for savanna and grassland fuels that is comparable with the average of chaparral fuels in this study 1.08 g kg-1 <0.945>. Check Akagi et al 2011 EFEC. The correlation between EFEC and MCE is much weaker (r^2=0.10) than correlation between EFOC and MCE.

Intense flaming significantly increases the fraction of elemental carbon (EC) emissions in the total PM carbon emissions (TC). Figure 4.10 illustrates the relationship between the EC/TC ratio and average MCE. EC/TC was lower than 0.15 for MCEs smaller than 0.93, while this

value strongly rose to 0.7 for MCEs larger than 0.95. The results are consistent with previous studies (e.g. as shown in the figure: McMeeking et al. (2009), Christian et al. (2003)). Reid et al. (2005) suggests values between 0.05 and 0.18 for flaming, and 0.03 to 0.075 for smoldering. However, Reid et al. define smoldering as MCE<0.9; furthermore, their EC/TC numbers mostly originate from field studies, which rarely achieve MCE<0.95 compared to up to 0.98 achieved in the lab where EC/TC rises quickly. Even accounting for MCE, field EC/TC values are lower than lab EC/TC. For example, the airborne study of Sinha et al. (2004) sampled fires from African savannah grasses. They measured EC/TC ratios of 0.135 <0.959> and 0.255 <0.976> for miombo woodland and dambo grass gland fires, respectively. During the flaming phase in our experiment, we observed temperatures up to ~70 °C at the instrumentation platform level; it is possible that the NMOC require more time to condense to the particle phase, as indicated by the lower EC/TC ratios of airborne studies.

EC/TC ratio increases rapidly as MCE increases past 0.94 (Figure 4.10). The same fact can be seen in Figure 9 (a)-(b) of McMeeking et al. (2009). Reid et al. (2005) also noted through investigation of previous studies on fires from savanna/grass/cerrado, tropical forest, etc. for phases of flaming/smoldering set forth that the black carbon content of PM during flaming can be a factor of 5 higher than during smoldering.

Compared to McMeeking et al., 2009, current study has nearly seven times higher adsorption artifacts for OC >500 $\mu g/m^3$ and almost twice higher for 0-100 $\mu g/m^3$ (Figure 4.12), and the data is more scattered as well. The mass fraction of artifact exponentially, 0.146+0.355e−0.004x and 0.021+0.173e-0.012x, decreased with increase in concentration of

smoke for the current and McMeeking et al. studies, respectively. McMeeking et al., 2009 used significantly less amount of fuel for each burn and this might have led to cooler diluted smoke, enhanced partitioning of gas into particle phase, and subsequently less artifacts, while in the current study the weight of the fuel bed varied between 250 and 5,500 grams averaging 2470±1090 g.

McMeeking et al. 2009 reported an exponential function for the ratio of carbon artifacts (SVOCs) collected on the back filter to front filter OC. a plot of artifacts (SVOC) collected on the back shows

4.4.5. Particle Inorganic Content

4.4.5.1. Particle Inorganic Content Metals: X-ray Fluorescence (XRF) Analysis

Teflon filters collected on 50 different burns were analyzed for Cl, Br, Si, P, S, and metals (atomic mass number Na-Pb). The dominant elements, by mass fraction, in order of decreasing median ranking by burn were K, Cl, Na, S, Zn, Mg, Si, and Ca with potassium the dominant element in 47 of the 50 filters analyzed. In the vast majority of burns with XRF data (28 of 50) the elements K, Cl, Na, and S comprised >90% of the inorganic elemental mass. As discussed in Akagi et al. (2011), the properties of particles emitted by biomass burning can change rapidly after emission. The cooling/dilution regime experienced by emissions in the laboratory may be very different from that realized by emissions of a "real fire" burning in the natural environment. It is possible the contribution of semi-volatile organic compounds to organic particle formation and growth is not as efficient in the lab environment. However, the amount of elemental carbon and metals cannot change after

emission. Therefore, the EF of inorganic elements measured in our laboratory burns are applicable to fires in the natural environment; however, the mass percentages are likely overestimated due to incomplete condensation of gas-phase SVOC.

The mass of all inorganic elements as a percent of total PM2.5 mass ranged from 1-56% and varied strongly with fuel type and source location. The mass percent for K, Cl, Na, and S are shown in Figure 4.13. Fuels harvested from SW consistently produced particles with higher K and Cl mass fractions than the fuels from SE (Figure 4.13). By source location, the average K and Cl mass percent for SW fuels was: VAFB: K = 17.1(± 4.0)%; Cl = 16.4(± 5.3)%, FHL: K = 10.5(± 5.1)%; Cl = 4.9(± 3.4)%, and FHUA: K = 13.7(± 3.0)%; Cl = 6.9(± 1.3)% for FHUA. The particulate mass fractions of these elements are higher than in previous reports, which may be due to incomplete condensation of gas-phase NMOC as plume cools. However, Chang-Graham et al. (2011) noted unusual metallo-organic species noted detected previously in biomass burning aerosol and hypothesized that land use practice on the military bases where the fuels were collected could contribute. Further, the ratios between metals and metals and EC should not be affected by any possible temperature artifacts.

The PM mass fractions of Cl, K, (and also Na for VAFB), and the sum of all inorganics produced by the southwestern fuels are on the upper end of values found in the literature. The studies reviewed by Reid et al. (2005), which covered a wide-range of biomass (South American grassland, African savanna, Cerrado, and North American temperate forest, and tropical broadleaf forest) reported that inorganic trace species emissions were highly variable and accounted for ~5-15% of PM mass. Of 10 studies reviewed by Reid et al. (2005), the

percent of PM mass consisting of K ranged from 0.4-18% and the Cl mass percent ranged from 0.2-11%. Andreae and Merlet (2001) recommend particulate K emission factors that correspond to 6%, 3%, and 1-3% of their recommended EFPM2.5 for savanna/grassland, tropical forest, and extra-tropical forest biomass, respectively. In the laboratory study of McMeeking (2009), results for a large variety of fuels, classified according to five broad vegetation groups (montane, rangeland, chaparral, southeast U.S. coastal plain, boreal) produced average mass percents of K and Cl that each ranged from ~0.3-6%. At the less generalized classification of fuel type, the results of McMeeking (2009) differ widely, with the mass percentages of K and Cl varying between 0.1-19.4% and 0.1–18.4%, respectively. In a laboratory study of fuels from Indonesia and Africa, the sum of K and Cl typically accounted for only a few percent of PM mass, with the exception of invasive fire-maintained alang-alang grass from Indonesia which generated PM that was ~28% Cl and ~19% K by mass Christian et al. (2003). Only two studies reported PM mass fractions of K and Cl for fuels similar to our southwestern fuels. McMeeking (2009) found that the fraction of PM2.5 mass comprised by K and Cl ranged from 1.6-9.5% and 0.4-6.1%, respectively for the chaparral varieties ceanothus, chamise, manzanita and sagebrush. In another laboratory study, K and Cl made up ~24% and ~10%, respectively, of total PM mass emitted by sagebrush combustion (Chen et al., 2007).

Emission factors for K, Cl, Na, and S in PM2.5 are provided in Table 4.3. EF for K, Cl, and Na varied significantly by fuel. Fuels from VAFB and FHL had the largest EFK, EFCl, and EFNa (with VAFB being significantly larger than FHL), while the fuels from the southeast had the smallest. EFK, EFCl, and EFNa were highest for the fuels from VAFB and FHL

and lowest for the southeast fuels. The oas and oaw fuels from FHUA had EFK, EFCl, and EFNa similar to the southeast fuels, while EFK and EFCl for mes was comparable to that measured for the Pacific coast fuels (VAFB and FHL). The differences can be explained largely by the chemical composition of the vegetation making up the fuels. The VAFB and FHL fuels had representative Cl, K, and Na (Table 4.1). In contrast, the SE fuels and FHUA oas and oaw had concentrations of these elements that were very low (Table 4.1). The chemistry of the mes from FHUA was an outlier, high in Cl and K, but low in Na. The high Cl and K for the mes fuel were largely due to the desert broom component, a shrub species that has been identified as a possible element hyper-accumulator.

We may compare our chaparral metal/halogen results with McMeeking et al. (2009) which reports chaparral emissions for K, Cl, Na, and S. Our chaparral average EFK of 0.652 g kg-1 is similar to McMeeking et al. (EFK = 0.50 g kg-1), while our EFCl is about three times as large (0.471 g kg-1 vs. 0.20 g kg-1) and our EFNa differs greatly (0.143 g kg-1 vs. 0 g kg-1). Considering the strong link we observed between the element content of the fuels and their respective particle EF, it is likely the differences in EF are due to fuel chemistry. McMeeking et al. do not report fuel chemistry; however, it is possible the Cl and Na content of the fuel samples burned their study was significantly less than that in our study. Among the southwestern fuels, those with an 'oak' wood component (chs of California, oas and oaw of Arizona) produced particles with K (9.4±3.2%) and Cl (2.4±1.1%) mass fractions that were significantly lower that of the other 6 fuels types studied from this region (average 18.0±4.4% and 11.9±5.5%) – see Figure 4.13. Inter-fuel differences for both elements are significant at the $p < 0.001$ level. These observations, along with the lack of a significant

correlation with MCE, indicate that location and vegetation composition both influence the chemical composition of fuels. We believe both factors are responsible for the difference in EFCl and EFNa observed between our study and McMeeking et al. The Cl content in vegetation and chloride deposition has been observed to show a strong gradient with distance from the Pacific coast (McKenzie et al., 1996). Since our chaparral fuels were sampled at coastal sites, while, McMeeking et al. studied chaparral harvested 150 km east of Los Angeles, the fuels used in the later study would be expected have a lower content of Cl, Na, and other sea-salt elements.

The percentage of particulate mass as K or S was weakly correlated with MCE (r^2 = 0.20 for K and r^2 = 0.40 for S), while the Cl and Na mass fractions had no correlation. The lack of a significant correlation between inorganic particulate emissions and MCE is consistent with the findings of McMeeking (2009) and Christian et al. (2003) although Ward and Hardy et al. (1996) found EFK (flaming) was roughly 10× higher than EFK (smoldering). The Ward and Hardy (1991) study were all from fires of the same fuel type; whereas this and the other studies cited were across many different fuel types. It is possible that the fuel variations may mask any MCE dependence for these studies.

The particulate emissions of Cl and gas-phase HCl (EFHCl) were not correlated with MCE and we suspect their variability is driven by fuel composition. Any underlying dependence of PM Cl and HCl emissions on combustion behavior, in particular the partitioning of evolved fuel Cl between the gas and particulate phase, if present, may be masked by wide variations in fuel Cl content. The EFs of particulate Cl to HCl as a function of MCE was observed to account for the variability of the fuel Cl content. No significant correlation between the ratio

EFPMCl/EFPMHCl and MCE (plot not shown) was observed, a result that indicates combustion behavior (as represented by MCE) is not an important factor in Cl partitioning between these two species.

4.4.5.2. Ionic Inorganic species

Inorganic ion species emission factors are provided in Table 4.4. Similar to the emission factor of crustal elements, potassium and chloride were the most abundant ions and were strongly correlated with each other (slope=1.03; r^2=0.89). Fuels from southwest, compared to the fuels from southeast, emitted much higher amounts of Cl^-, K^+, SO_4^{2-}, Na^+ per unit mass of fuel burned. This is consistent with our results from the previous section. The mass concentration of nitrite, nitrate, and ammonium for most of filters was below detection limit. These species grow rapidly post emission as reported elsewhere (Yokelson et al., 2009, Akagi et al., 2012).

Chlorine was the most abundant inorganic species in the PM2.5 aerosol, accounting for 0.4-24.5% of the soluble inorganic mass concentration. McMeeking et al. (2009) found that chlorine accounted for 2-9% of PM2.5 mass for several of the same fuels burned in this study including chaparral and sagebrush. Similar to our study, they observed high Cl^- mass fraction (60% of inorganics). $EFCl^-$ varied from 0 to 1.23 g/kg of fuel burned depending on the fuel type and source location. The study average was 0.34±0.35 g/kg. The $EFCl^-$ reported were 1-2 g/kg, 0-1.8 g/kg, 0-1.8 g/kg, and 0-3.2 g/kg from Andreae and Merlet (2001), Christian et al. (2003), Keene et al. (2006), and McMeeking et al. (2009), respectively.

Sulfate emission factors ranged from 0 to 0.22 g SO_4^{2-}/kg fuel and were weakly correlated with MCE (r^2=0.48). Also comparing XRF to IC results, it can be inferred that ~89% of the particulate sulfur element is in the form of SO_4^{2-}. Sinha et al. (2003) estimated an average 0.16 g sulfate per kg of fuel burned for savanna fires, while Andreae and Merlet (2001) recommended 0.37 g/kg. $EFSO_4^{2-}$ is affected by the age of smoke and the nutrient content of the fuel (Yokelson et al. (2009)). As a smoke plume ages, the SO_2(g) oxidizes in aqueous phase to $H2SO_4$ and then partners with positive ions such as potassium and ammonium in the particles, thereby increasing aerosol SO_4^{2-} percent mass over time. In the airborne studies of northern tropics deforestation, Yokelson et al. (2009) showed that sulfate mass concentration can increase 3 times during a time interval of ~1hr. In their study, sulfate made up to 1.5% of PM1 mass from nascent smoke, while in our study it made up to 7.5% of PM2.5 mass for very fresh smoke. The sulfate content differences are attributed to the different sulfur content of the fuel. In our study, sulfate was also weakly correlated with MCE (r^2=0.48).

Non-soil, non-sea-salt Potassium (often denoted "nsnss-K") is an important tracer of biomass burning aerosol (Andreae and Merlet, 2001). Potassium was the second-most abundant ionic species in this study varying between 0.03 to 1.40 g/kg fuel burned. The emission factor of potassium from XRF was 12% higher than the ionic K from Ion Chromatography (IC) (r^2=0.83) indicating the vast majority of potassium is in ionic form. Our results are consistent with the laboratory studies of McMeeking et al. (2009) and Christian et al. (2003) that reported emission factor of 0.03 to 1.50 g/kg for a variety of US

domestic fuels, and 0.02 to 1.29 g/kg for African, Indonesian fuels. However, we report EFK^+ that is twice the EFK^+ that McMeeking et al. (2009) obtained for chaparral.

Among all the southeastern and southwestern fuels, fuels from VAFB had the highest mass percent of ionic inorganic species ranging from ~9-62%, while emissions from Camp Lejeune fuels had the lowest amount of inorganic PM (~2-15%). Other than fuel source location, fuel type also affected the ionic species emissions. For example, among the fuel from VAFB, fuel code 'man' has the least amount of Cl^- (301.03±97.73 mg/kg fuel burned), while fuel code 'cas' from the same location has the greatest amount (1405.99±457.22 mg/kg fuel burned). These observations coupled with the lack of significant correlation with MCE suggest that fuel composition and vegetation type play the dominant role in emissions of ionic species. Very little to lower than detection limit amounts of calcium, ammonium, bromide, and nitrite were found. These species plus fluoride comprise the remainder of the inorganic ions. No dependency on MCE was observed for any these ions. A slight correlation between Na+ and MCE (r^2=0.19) without any regional dependency was observed.

4.5. Elemental Analysis of the PM filters

4.5.1. Mass Balance

PM2.5 mass was reconstructed based on OC, EC, metals, and water-soluble ions from Ion Chromatography (IC) analysis. The relation that is considered here is as follows:

$$EF_{PM_{2.5}} = EF_{EC} + EF_{OM} + \sum EF_{XRF} + \sum EF_{IC} \qquad \text{Eq. 4.1}$$

where the terms of the right hand side are the sum of emission factors of elemental carbon (EFEC), organic mass (EFOM=factor×EFOC), elemental crustal material($\sum EF_{XRF}$), and inorganic salts ($\sum EF_{IC}$) for the ith burn.

Mass reconstruction followed Levin et al. (2010); Cl^- was paired to K^+ as KCl, excess K^+ was then balanced with K_2SO_4 and KNO_3, whereas, excess Cl^- was balanced with NH_4Cl and NaCl. Any remaining ions were explicitly accounted for in the salt group. Following the IMPROVE protocol (Pitchford et al., 2007), an assumption was made to consider all Ca and Al from XRF analysis as CaO and Al_2O_3 .

The EF of organic matter (EFOM) was estimated by multiplying the organic carbon emission factor by a factor of 1.52 to account for associated O, H, and N. This OM/OC value minimizes the difference between the actual and the constructed PM masses, is within the range recommended by Reid et al. (2005), and is consistent with the OM/OC ratio acquired by the AMS in this study (Qi et al., 2012). Additionally, the value is similar to the factors of 1.5 and 1.55 used by Levin et al. (2010) and McMeeking et al. (2009), respectively. A coefficient of determination of 0.94 is observed.

4.6. Emission Factors of Levoglucosan

Levoglucosan (1,6-anhydro-β-D-glucose), a tarry anhydro sugar and by-product of pyrolysis of cellulose, is a well-established biomass burning marker (Shafizadeh and Fu, 1973, Shafizadeh et al., 1979, Shafizadeh, 1984, Simoneit et al., 1999). Cellulose itself accounts for 40-45% of wood's dry weight and is composed of linear chains of D-glucose linked by ß-1,4-glycosidic bonds with a degree of polymerization of up to ~15000 unit (Pettersen, 1984).

Emission factors of levoglucosan (LG) versus MCE are listed in (Table 4.5). This subset of data encompasses 43 burns. Measured emission factors for levoglucosan vary substantially with fuel type. For the 15 fuel types of this study, EFLG varied over two orders of magnitude (Table 4.5). On average, fuels from 'Camp Lejeune' emitted the highest amount of levoglucosan per kg fuel burned, while the lowest per mass LG emissions were from the Chaparral fuels. The reported values from the current study are within the range reported by Schauer et al. (2001) for residential wood burning, average EFs of 1375, 706, and 1940 mg/kg fuel for pine, oak, and eucalyptus, respectively. The LG/OC ratios for the three fuel groups were 4.24±0.90, 4.30±1.41, and 5.73±0.83 mg/g for Chaparral, FHUA, and CL, respectively. Sullivan et al. (2008) during the FLAME studies measured an average LG/OC value of 520 mg/g for their 73 burns. Engling et al. (2006) reported values from 36 to 1368 μg/mg OC. The current study values are 2-3 times lower than reported LG/OC ratios for 'man' and 'chs' (Sullivan et al. (2008)) of 8.8-11.4 and 6.3-10.6 mg/g, respectively. In general, fuels from SE emitted more LG per unit weight of fuel compared to the SW fuels. MCE alone is unable to account for the differences observed between these studies. Lab experiments suggest that presence of salts, specially salts containing K, Li, Ca significantly reduces LG pyrolysis yields (Richards & Zheng, 1991, Eom et al., 2012). Thus, higher K/PM ratios in this study suggest lower EFLG. As shown in Figure 4.11, a sharp decrease in LG production is observed at K/PM ratio of ~0.03. Moreover, Ward & Hardy, 1991 found that potassium emissions were high during high temperature flaming phase. Hence, potassium could not be identified a predictive factor for determining EFLG that varied two orders of magnitude.

The PM mass fractions of levoglucosan in this study were 1.56±0.50 (FHL), 1.76±0.44 (FHUA), 5.73±0.83 (CL), and varied largely between burns from 0.3 for 'cos' (lowest) to 9.5% for 'cuh' (highest). SE fuels had the highest levoglucosan PM mass fraction ranging from 3% ('cuh') to 9.5% ('2yr'), while SW fuels varied between 0.3% ('cos') and 3.2% ('cea'). No correlation between mass fraction of levoglucosan in PM and MCE was found in contrast to previous findings of Dhammapala et al. (2007) for wheat and Kentucky blue grass (only based on three samples).

4.7. Emission Factor of Particle-Phase PAHs

The major emissions of particle-phase PAHs from southwestern fuels are benzo[k] fluoranthene, pyrene, benzo[a] fluoranthene, chrysene, benzo[a] pyrene, fluoranthene, phenanthrene, and fluorene, which contribute approximately 80% of total particle-phase PAHs for both chaparral and FHUA groups. Pyrene and benzo[k] flouranthene alone made up 13-20% of PAH emissions. Chaparral and FHUA had a mean emission factor of 6550 and 1720 μg/kg . The highest observed amount of total PAHs per kg fuel burned was 11300 μg/kg from 'cos' and the lowest was 1300 μg/kg from 'oas'. In general, Chaparral fuels emitted approximately 4 times higher amount of PAHs than FHUA fuels.

The mass fraction of PAH in the PM varied from 0.03%(chs) to 0.54%(cos) and averaged 0.20% and 0.26% mass of PM for chaparral and FHUA fuels, respectively. Despite having less PAH per kg fuel burned, FHUA resulted in higher fraction of PM in PAHs compared to the Chaparral group.

It has been suggested that the ratio of certain diagnostic ratios for PAHs are useful in determining combustion source (Gonkalves et al., 2011, Wang et al., 2009, Alves et al., 2010). The ratios of Fla/(Py+Fla) and Ph/(Ph+Ant) as suggested by Wang et al. (2009) and Ind/(Ind+Benzo[ghi]P) by Gonkalves et al. (2011)are shown in the bottom of Table 4.6 for all the fuel types and the two fuel groups. The ratio Fla/(Py+Fla) was 0.40±0.04 for Chaparral group and 0.20±0.10 for FHUA group. The FHUA ratios are similar to those reported from combustion of cereal straw (0.50-0.53)(Hays et al., 2005), shrubs (0.54-0.60) (Wang et al., 2009), and agricultural residue (0.46-0.63) (Gonkalves et al., 2011). 'mes' and 'oas' did not fall within the range of suggested ratios for the ratio of Fla/(Py+Fla). The Ph/(Ph+Ant) ratio averaged 0.72±0.17 (except for 'mch') and was consistent with the range reported by above-mentioned studies. 'mes' and 'oas' from FHUA significantly has higher Ph/(Ph+Ant) ratios (~0.9) close to the values seen cooking emissions/engine exhaust (He et al., 2004, Rogge et al., 1993, Schauer et al., 1999), which in addition to a differing fuel type, the disparity might be due to the high MCE values. Most of the studies used by (Wang et al., 2009) are combustion processes involving mostly smoldering (based on small EC/TC ratios). Therefore, the range of suggested diagnostic ratios might not be robust due to the overlap of suggested ranges between different emission sources (Goncalves et al., 2011) and also not covering the wider range of possible MCE values (e.g. higher MCEs were observed in the current study). Ind/(Ind+Benzo[ghi]P) was 0.40±0.04 for both fuel groups. Our data is close to lower end of evaluated values from the study of (Hays et al., 2005) for cereal straw. Chinese cooking (He et al., 2004) and automobile and trucks (Rogge et al., 1993) have ratios of 0.19 and 0.04-0.09, respectively.

4.8. Conclusions

We report detailed particle-phase emission measurements from combustion of different vegetation types typically managed with fire on military bases in the southwest US. Since these fuels burn periodically (prescribed or wildfire), the results of this study will help to better understand and manage air quality impacts in neighboring areas. Emission factors for numerous species are provided as a function of MCE. At a certain FM, all observed MCEs were limited between two heading and backing fire MCEs. Due to lack of sufficient data, it was impossible to model the fire behavior; more effort is needed for characterizing the MCE.

On average, the SE fuels emitted more PM mass (10.8 g/kg fuel burned) compared to SW fuels (3.83 g/kg fuel burned) consistent with lower MCE for SE fuels. No regional trend was observed after accounting for MCE. Some of the observed differences between field and lab results for similar MCE may be attributable to the smoke temperature, fuel bed differences as discussed in more detail elsewhere (Yokelson et al., in preparation) and also timescale of the MCE measurement (field is on order of hours, laboratory on order of a few minutes). Due to the non-linear emissions behavior with MCE, comparison of fire-integrated values from lab and field studies might result in unexpected and unexplainable differences.

The SE and SW fuels showed large regional dependency in their emission factors for particle inorganics. The PM mass fraction of chlorine and potassium in the SW fuels was on the high end of values reported in the literature. Any correlation between these emission rates with MCE was masked by large variations due to fuel composition. Chlorine alone accounted for

0.4-24.5% of the water-soluble mass fraction. Sulfate correlated weakly with MCE. Comparison of XRF and IC results indicates the vast majority (~88%) of sulfur and potassium are present as $SO_4$2- and K+, respectively. Inorganic species contributed 9-62% and 2-15% of PM mass for SW and SE fuels, respectively. No correlation was observed between MCE and calcium, ammonium, bromide, and nitrate.

Levoglucosan/OC ratios were observed to be a function of the fuel type with little to no correlation with MCE. Finally, the emission factor of 15 PAHs totaled 1 - 11 mg/kg burned for SW. 80% of measured particle phase PAHs was attributed to benzo[k] fluoranthene, pyrene, benzo[a] fluoranthene, chrysene, benzo[a] pyrene, fluoranthene, phenanthrene, fluorene. Pyrene and benzo[k] flouranthene constituted 13-20% of particle-phase PAHs emissions. Previously published PAH diagnostic ratios were not observed to be good markers for our biomass burning samples.

4.9. References

Code of Federal Regulations (2005). 40CFR Part 1065, 2005. Washington DC.

Akagi, S. K., Yokelson, R. J., Wiedinmyer, C., Alvarado, M. J., Reid, J. S., Karl, T., Crounse, J. D., and Wennberg, P. O.: Emission factors for open and domestic biomass burning for use in atmospheric models, Atmos. Chem. Phys., 11, 4039-4072, doi:10.5194/acp-11-4039-2011, 2011.

Akagi, S. K., Craven, J. S., Taylor, J. W., McMeeking, G. R., Yokelson, R. J., Burling, I. R., Urbanski, S. P., Wold, C. E., Seinfeld, J. H., Coe, H., Alvarado, M. J., and Weise, D. R.: Evolution of trace gases and particles emitted by a chaparral fire in California, Atmos. Chem. Phys., 12, 1397-1421, doi:10.5194/acp-12-1397-2012, 2012

Albini, F. (1976). Estimating wildfire behavior and effects. USDA Forest Service General Technical Report INT, 30.

Alves, C., Goncalves, C., Evtyugina, M., Pio, C., Mirante, F., & Puxbaum, H. (2010). Particulate organic compounds emitted from experimental wildland fires in a Mediterranean ecosystem. Atmospheric Environment, 44(23), 2750– 2759.

Andreae, M. & Merlet, P. (2001a,b). Emission of trace gases and aerosols from biomass burning. Global Biogeochemical Cycles, 15(4), 955–966.

Bertschi, I., Yokelson, R., Ward, D., Babbitt, R., Susott, R., Goode, J., & Hao, W. (2003). Trace gas and particle emissions from fires in large diameter and belowground biomass fuels. J. Geophys. Res, 108, 8472.

Birch, M. & Cary, R. (1996). Elemental carbon-based method for monitoring occupational exposures to particulate diesel exhaust. Aerosol Science and Technology, 25(3), 221–241.

Blackmarr, W.H., Flanner, W.B. (1975). Moisture variation in selected pocosin shrubs of eastern North Carolina. Res. Pap. SE-124, Asheville, NC: USDA Forest Service, Southeastern Forest Experiment Station. 10 p.

Burling, I., Yokelson, R., Akagi, S., Urbanski, S., Wold, C., Griffith, D., Johnson, T., Reardon, J., & Weise, D. (2011). Airborne and ground-based measurements of the trace gases and particles emitted by prescribed fires in the united states. Atmos. Chem. Phys, 11, 12197–12216.

Burling, I., Yokelson, R., Griffith, D., Johnson, T., Veres, P., Roberts, J., Warneke, C., Urbanski, S., Reardon, J., Weise, D., et al. (2010). Laboratory measurements of trace gas emissions from biomass burning of fuel types from the southeastern and southwestern united states. Atmos. Chem. Phys, 10, 11115–11130.

Cassinelli, M. & O'Connor, P. (1996). NIOSH Manual of Analytical Methods (NMAM). National Institute for Occupational Safety and Health (NIOSH), Washington, DC, http://www.cdc.gov/niosh/docs/2003-154/, 4th ed. edition.

Chang-Graham, A. L., Profeta, L. T. M., Johnson, T. J., Yokelson, R. J., Laskin, A., and Laskin, J.: A case study of water soluble metal containing organic constituents of biomass burning aerosol, Environ. Sci. Technol., 45, 1257–1263, doi:10.1021/es103010j, 2011.

Chen, L. W. A., Moosmüller, H., Arnott, W. P., Chow, J. C., Watson, J. G., Susott, R. A., Babbitt, R. E., Wold, C. E., Lincoln, E. N., and Hao, W. M.: Emissions from laboratory combustion of wildland fuels: Emission factors and source profiles - environmental science & technology (ACS publications), Environmental Science & Technology, 47, 4317-4325, 10.1021/es062364i, (Web): May 10, 2007.

Christian, T., Kleiss, B., Yokelson, R., Holzinger, R., Crutzen, P., Hao, W., Saharjo, B., & Ward, D. (2003a,b). Comprehensive laboratory measurements of biomass-burning emissions: 1. emissions from Indonesian, African, and other fuels. J. Geophys. Res, 108, 4719.

Christian, T., Kleiss, B., Yokelson, R., Holzinger, R., Crutzen, P., Hao, W., Shirai, T., & Blake, D. (2004). Comprehensive laboratory measurements of biomass-burning emissions: 2. First intercomparison of open-path FTIR, PTR-MS. Technical report, and GC-MS/FID/ECD, J. Geophys. Res., 109, D02311.

Cochrane, M. A., Moran, C. J., Wimberly, M. C., Baer, A. D., Finney, M. A., Beckendorf, K. L., Eidenshink, J., and Zhu, Z.: Estimation of wildfire size and risk changes due to fuels treatments, Int. J. Wildland Fire

Countryman, C.M., Dean, W.A. (1979). Measuring moisture content in living chaparral: a field user's manual. Gen. Tech. Rep. PSW-36. Berkeley, CA: USDA Forest Service, Pacific Southwest Research Station. 28 p. http://treesearch.fs.fed.us/pubs/24092

Crutzen, P. & Andreae, M. (1990). Biomass burning in the tropics: Impact on atmospheric chemistry and biogeochemical cycles. Science, 250(4988), 1669.

Dhammapala, R., Claiborn, C., Jimenez, J., Corkill, J., Gullett, B., Simpson, C., & Paulsen, M. (2007). Emission factors of pahs, methoxyphenols, levoglucosan, elemental carbon and organic carbon from simulated wheat and kentucky bluegrass stubble burns. 41(12), 2660–2669.

Engling, G., Carrico, C., Kreidenweis, S., Collett Jr, J., Day, D., Malm, W., Lincoln, E., Min Hao, W., Iinuma, Y., & Herrmann, H. (2006). Determination of levoglucosan in biomass combustion aerosol by high-performance anion-exchange chromatography with pulsed amperometric detection. Atmospheric Environment, 40, 299–311.

Eom, I.-Y., Kim, J.-Y., Kim, T.-S., Lee, S.-M., Choi, D., Choi, I.-G., & Choi, J.-W. (2012). Effect of essential inorganic metals on primary thermal degradation of lignocellulosic biomass. Bioresource Technology, 104(0), 687-694. doi: 10.1016/j.biortech.2011.10.035

Fenn, M. (1991) Increased Site Fertility and Litter Decomposition Rate in High-Pollution Sites in the San Bernardino Mountains, Forest Science, 37(4), pp. 1163-1181(19).

Ferek, R., Reid, J., Hobbs, P., Blake, D., & Liousse, C. (1998). Emission factors of hydrocarbons, halocarbons, trace gases and particles from biomass burning in brazil. Journal of Geophysical Research, 103(D24), 32107.

Fishman, J., Fakhruzzaman, K., Cros, B., & Nganga, D. (1991). Identification of widespread pollution in the southern hemisphere deduced from satellite analyses. Science, 252(5013), 1693.

Gonkalves, C., Evtyugina, M., Alves, C., Monteiro, C., Pio, C., & Tomé, M. (2011). Organic particulate emissions from field burning of garden and agriculture residues. Atmospheric Research.

Guyon, P., Frank, G., Welling, M., Chand, D., Artaxo, P., Rizzo, L., Nishioka, G., Kolle, O., Fritsch, H., Dias, S., et al. (2005). Airborne measurements of trace gas and aerosol particle emissions from biomass burning in amazonia. Atmospheric Chemistry and Physics Discussions, 5(3), 2791–2831.

Hardy, C., Conard, S., Regelbrugge, J., & Teesdale, D. (1996). Smoke emissions from prescribed burning of southern California chaparral. 1996.

Hays, M., Fine, P., Geron, C., Kleeman, M., & Gullett, B. (2005). Open burning of agricultural biomass: Physical and chemical properties of particle-phase emissions. Atmospheric Environment, 39(36), 6747–6764.

Haywood, J., Osborne, S., Francis, P., Keil, A., Formenti, P., Andreae, M., & Kaye, P. (2003). The mean physical and optical properties of regional haze dominated by biomass burning aerosol measured from the c-130 aircraft during safari 2000. J. Geophys. Res, 108, 8473.

He, L., Hu, M., Huang, X., Yu, B., Zhang, Y., & Liu, D. (2004). Measurement of emissions of fine particulate organic matter from Chinese cooking. Atmospheric Environment, 38(38), 6557–6564.

Hobbs, P., Reid, J., Kotchenruther, R., Ferek, R., & Weiss, R. (1997). Direct radiative forcing by smoke from biomass burning. Science, 275(5307), 1777.

Hosseini, S., Li, Q., Cocker, D., Weise, D., Miller, A., Shrivastava, M., Miller, J., Mahalingam, S., Princevac, M., & Jung, H. (2010). Particle size distributions from laboratory-scale biomass fires using fast response instruments. Atmos. Chem. Phys, 10, 8065–8076.

Janhall, S., Andreae, M., & Poschl, U. (2010). Biomass burning aerosol emissions from vegetation fires: particle number and mass emission factors and size distributions. 10(3), 1427–1439.

Kaufman, Y. & Fraser, R. (1997). The effect of smoke particles on clouds and climate forcing. Science, 277(5332), 1636.

Keene, W., Lobert, R., Crutzen, P., Maben, J., Scharffe, D., Landmann, T., Hély, C., & Brain, C. (2006). Emissions of major gaseous and particulate species during experimental burns of southern African biomass.

Levin, E., McMeeking, G., Carrico, C., Mack, L., Kreidenweis, S., Wold, C., Moosm "uller, H., Arnott, W., Hao, W., Collett Jr, J., et al. (2010). Biomass burning smoke aerosol properties measured during fire laboratory at Missoula experiments (flame). Journal of Geophysical Research, 115(D18), D18210.

Lobert, J., Scharffe, D., & Hao, W. (1991). Experimental evaluation of biomass burning emissions- nitrogen and carbon containing compounds. Global biomass burning-

Atmospheric, climatic, and biospheric implications(A 92-37626 15-42). Cambridge, MA, MIT Press, 1991,, (pp. 289–304).

McGeehan, S. & Naylor, D. (1988). Automated instrumental analysis of carbon and nitrogen in plant and soil samples 1. Communications in Soil Science & Plant Analysis, 19(4), 493–505.

McMeeking, G., Kreidenweis, S., Baker, S., Carrico, C., Chow, J., Collett Jr, J., Hao, W., Holden, A., Kirchstetter, T., & Malm, W. (2009). Emissions of trace gases and aerosols during the open combustion of biomass in the laboratory. Journal of Geophysical Research, 114(D19), D19210.

Peterson, J. & Leenhouts, B. (1997). What wildland fire conditions minimize emissions and hazardous air pollutants and can land management goals still be met? Unpublished support document to the EPA Interim Air Quality Policy on Wildland and Prescribed Fires.

Pettersen, R. (1984). The chemical composition of wood. Advances in chemistry series, (207), 57–126.

Pitchford, M., Malm, W., Schichtel, B., Kumar, N., Lowenthal, D., & Hand, J. (2007). Revised algorithm for estimating light extinction from improve particle speciation data. Journal of the Air & Waste Management Association, 57(11), 1326–1336.

Pope III, C., Ezzati, M., & Dockery, D. (2009). Fine-particulate air pollution and life expectancy in the united states. New England Journal of Medicine, 360(4), 376–386.

Qi, L., Hosseini, S., Jung, H., Yokelson, R., Weise, D., Cocker, D., Huang, Y. (2012). Chemical Characterization of Particle Emissions from Controlled Burns of Biomass Fuels using a High Resolution Time-of-Flight Aerosol Mass Spectrometer. Atmospheric Chemistry and Physics Discuss., 12, 8397-8432, doi:10.5194/acpd-12-8397-2012, 2012

Richards, G. N., & Zheng, G. (1991). Influence of metal ions and of salts on products from pyrolysis of wood: Applications to thermochemical processing of newsprint and biomass. Journal of Analytical and Applied Pyrolysis, 21(1–2), 133-146. doi: 10.1016/0165-2370(91)80021-y

Radke, L., Hegg, D., Hobbs, P., Nance, J., Lyons, J., Lursen, K., Weiss, R., R., Riggan, P., P., & Ward, D. (1991). Particulate and trace gas emissions from large biomass fires in North America. Global biomass burning- Atmospheric, climatic, and biospheric implications(A 92-37626 15-42). Cambridge, MA, MIT Press, 1991,, (pp. 209–224).

Ramdahl, T. & Becher, G. (1982). Characterization of polynuclear aromatic hydrocarbon derivatives in emissions from wood and cereal straw combustion. Analytica Chimica Acta, 144, 83–91.

Reid, J. S., Hobbs, P. V., Ferek, R. J., Blake, D. R., Martins, J. V., Dunlap, M. R., and Liousse, C.: Physical, chemical, and optical properties of regional hazes dominated by smoke in brazil, Journal of Geophysical Research, 103, 32059-32032, 1998.

Reid, J., Koppmann, R., Eck, T., & Eleuterio, D. (2005a,b). A review of biomass burning emissions part ii: intensive physical properties of biomass burning particles. Atmos. Chem. Phys, 5(3), 799–825.

Roberts, J. M., Veres, P. R., Cochran, A. K., Warneke, C., Burling, I. R., Yokelson, R. J., Lerner, B., Holloway, J. S., Fall, R., and de Gouw, J.: Isocyanic acid in the atmosphere: Sources, concentrations and sinks, and potential health effects, PNAS, 108, 8966-8971, doi: 10.1073/pnas.1103352108, 2011.

Roberts, J., Veres, P., Warneke, C., Neuman, J., Washenfelder, R., Brown, S., Baasandorj, M., Burkholder, J., Burling, I., Johnson, T., et al. (2010). Measurement of HONO, HNCO, and other inorganic acids by negative-ion proton-transfer chemical-ionization mass spectrometry (NI-PT-CIMS): application to biomass burning emissions, atmos. Meas. Tech, 3, 981–990.

Roberts, R. & Corkill, J. (1998). Grass seed field smoke and its impact on respiratory health. Journal of environmental health, 60, 1–8.

Rogge, W., Hildemann, L., Mazurek, M., Cass, G., & Simoneit, B. (1993). Sources of fine organic aerosol. 2. Noncatalyst and catalyst-equipped automobiles and heavy-duty diesel trucks. Environmental science & technology, 27(4), 636–651.

Schauer, J., Kleeman, M., Cass, G., & Simoneit, B. (1999). Measurement of emissions from air pollution sources. 1. C1 through C29 organic compounds from meat charbroiling. Environmental Science & Technology, 33(10), 1566–1577.

Schauer, J. J., Kleeman, M. J., Cass, G. R., & Simoneit, B. R. T. (2001). Measurement of emissions from air pollution sources. 3. C1-C29 organic compounds from fireplace combustion of wood. Environmental Science & Technology, 35(9), 1716–1728. PMID: 11355184.

Shafizadeh, F. (1984). The chemistry of pyrolysis and combustion. Chemistry of Solid Wood, edited by: Rowell, R., Advances in Chemistry Series, 207, 489–529.

Shafizadeh, F. & Fu, Y. (1973). Pyrolysis of cellulose. Carbohydrate Research, 29(1), 113–122. Shafizadeh, F., Furneaux, R., Cochran, T., Scholl, J., & Sakai, Y. (1979). Production of levoglucosan and glucose from pyrolysis of cellulosic materials. Journal of Applied Polymer Science, 23(12), 3525–3539.

Simoneit, B., Schauer, J., Nolte, C., Oros, D., Elias, V., Fraser, M., Rogge, W., & Cass, G. (1999). Levoglucosan, a tracer for cellulose in biomass burning and atmospheric particles. Atmospheric Environment, 33(2), 173–182.

Sinha, P., Hobbs, P., Yokelson, R., Bertschi, I., Blake, D., Simpson, I., Gao, S., Kirchstetter, T., & Novakov, T. (2003). Emissions of trace gases and particles from savanna fires in Southern Africa. Journal of Geophysical Research, 108(D13), 8487.

Sinha, P., Hobbs, P., Yokelson, R., Blake, D., Gao, S., & Kirchstetter, T. (2004). Emissions from miombo woodland and dambo grassland savanna fires. J. Geophys. Res, 109.

Sullivan, A., Holden, A., Patterson, L., McMeeking, G., Kreidenweis, S., Malm, W., Hao, W., Wold, C., & Collett Jr, J. (2008). A method for smoke marker measurements and its potential application for determining the contribution of biomass burning from wildfires and prescribed fires to ambient PM2. 5 organic carbon. J. Geophys. Res, 113, D22302.

Urbanski, S. P., H. W. M. & Baker, S. (2009). Chemical composition of wildland fire emissions. In R. A. Bytnerowicz A., Arbaugh M. & A. C. (Eds.), Wildland Fires and Air Pollution, number 8 (pp. 79–107). Developments in Environmental Science.

Veres, P., Roberts, J., Burling, I., Warneke, C., de Gouw, J., & Yokelson, R. (2010). Measurements of gas-phase inorganic and organic acids from biomass fires by negative-ion proton-transfer chemical-ionization mass spectrometry. J. Geophys. Res, 115, D23302.

Wang, Z., Bi, X., Sheng, G., & Fu, J. (2009). Characterization of organic compounds and molecular tracers from biomass burning smoke in south china i: Broad-leaf trees and shrubs. Atmospheric Environment, 43(19), 3096–3102.

Ward, D. E., Nelson, R. M., Adams, D. F. (1979), Forest Fire Smoke Plume Documentation, 72nd Annual Meeting of Air Pollution Control Association, Cincinnati, Ohio

Ward, D. (1998). Smoke from wildland fires. Health Guidelines for Vegetation Fire Events, Lima, Peru, (pp. 6–9).

Ward, D. & Hardy, C. (1991). Smoke emissions from wildland fires. Environment International, 17(2-3), 117–134.

Ward, D. E. & Radke, L. (1993). Chapter 4: Emission measurements from vegetation fires: A comparative evaluation of methods and results In Crutzen, P.J. & Goldammer, J.G. (eds) Fire in the Environment: The Ecological, Atmospheric, and Climatic Importance of Vegetation Fires. John Wiley & Sons.

Weise, D., Ward, D., Paysen, T., & Koonce, A. (1991). Burning California chaparral-an exploratory study of some common shrubs and their combustion characteristics. International Journal of Wildland Fire, 1(3), 153–158.

Wiedinmyer, C. & Hurteau, M. (2010). Prescribed fire as a means of reducing forest carbon emissions in the western united states. Environmental science & technology, 44(6), 1926–1932.

Yokelson, R., Clarke, A., Weinheimer, A., Knapp, D., Montzka, D., Holloway, J., Weibring, P., Flocke, F., & Zheng, W. (2009). Emissions from biomass burning in the Yucatan. Atmospheric Chemistry and Physics, 9(15), 5785–5812.

Yokelson, R. J., Burling, I. R., Urbanski, S. P., Atlas, E. L., Adachi, K., Buseck, P. R., Wiedinmyer, C., Akagi, S. K., Toohey, D. W., and Wold, C. E.: Trace gas and particle emissions from open biomass burning in Mexico, Atmos. Chem. Phys., 11, 6787-6808, doi:10.5194/acp-11-6787-2011,2011.

Table 4.1. Elemental composition of fuel types used in this work (left) and summary of fuel types, codes, and number of burns for each burn (right)

Fuel type	Fuel code	Species names	# of Burns	N wt%	C wt%	S wt%	O wt%	H wt%	Cl mg/kg	K mg/kg	Na mg/kg
Southwestern Fuels											
Ceanothus	cea	Ceanothus leucodermis	6	1.05	43.46	0.01	42.34	6.04	2000	4000	500
Chamise/Scrub oak	chs	Adenostoma fasciculatum, Quercus berberidifolia	6	0.92	47.49	0.00	41.17	6.60	< 50	1100	< 80
California sage	cas	Artemisia californica, Ericameria ericoides	6	1.12	48.11	0.22	40.59	6.69	3000	11000	1600
Coastal sage	cos	Salvia mellifera, Ericameria ericoides, Artemisia Californica	5	1.00	47.92	0.44	41.90	6.66	3000	6900	4100
Maritime chaparral	mch	Ceanothus impressus var. impressus, C. cuneatus var. fascicularis, Salvia mellifera	5	1.10	46.90	0.03	44.18	6.51	3850	6900	1450
Manzanita	man	Arctostaphylos rudis, Acrtostaphylos purissima	6	1.00	41.33	0.20	42.07	5.74	580	4200	460
Masticated mesquite	mes	Prosopis velutina,	5	1.25	50.96	0.03	44.29	7.08	860	6350	<80

Fuel type	Fuel code	Species names	# of Burns	N wt%	C wt%	S wt%	O wt%	H wt%	Cl mg/kg	K mg/kg	Na mg/kg
		Baccharis sarothroides									
Oak savanna	oas	Quercus emoryi, Eragrostis lehmanniana	5	0.78	52.47	0.03	46.51	7.29	53	2800	< 80
Oak woodland	oaw	Quercus emoryi, Arctostaphylos pungens	5	0.59	43.40	0.00	43.31	6.03	110	4700	< 80
Southeastern fuels											
1 year herbaceous	1yr	Lyonia lucida, Ilex glabra	3	0.82	53.27	0.06	40.00	7.40	160	2000	150
2 year herbaceous	2yr	Lyonia lucida, Ilex glabra	4	1.07	49.68	0.10	39.55	6.90	320	2500	300
Chipped understory hardwood	cuh	Acer rubrum, Persea borbonia, Gardonia lasianthus	3	-	-	-	-	-	-	-	-
Understory hardwood	uh	Acer rubrum, Persea borbonia, Gardonia lasianthus	3	-	-	-	-	-	-	-	-
Pocosin	poc	Lyonia lucida, Ilex glabra	3	-.	-	-	-	-	280	1200	120

Fuel type	Fuel code	Species names	# of Burns	N wt%	C wt%	S wt%	O wt%	H wt%	Cl mg/kg	K mg/kg	Na mg/kg
Pine litter	lit	Pnus taeda, Pinus echinata, Pinus elliottii, Pinus palustris	5	0.77	49.05	0.02	42.31	6.81	130	1100	< 80

Table 4.2. Emission factors for total PM2.5, EC, OC, K, Cl, Na, S in g/kg fuel burned, and EC/TC ratio. Numbers in parentheses represent one standard deviation.

Species/group	MCE	EC/TC	PM2.5	EC	OC	K	Cl	Na	S
Southwest									
cea/FHL	0.953(0.008)	0.40(0.22)	4.62(2.08)	0.64(0.29)	1.16(0.86)	0.607(.065)	0.345(.034)	0.016(.011)	0.025(.004)
chs/FHL	0.941(0.011)	0.39(0.07)	7.38(2.11)	1.36(0.44)	2.18(0.63)	0.535(.245)	0.171(.058)	0.034(.014)	0.061(.031)
cas/VAFB	0.944(0.004)	0.58(0.07)	6.87(0.83)	1.54(0.14)	1.16(0.38)	0.725(.057)	0.633(.015)	0.195(.014)	0.049(.001)
cos/VAFB	0.939(0.004)	0.62(0.07)	6.36(0.72)	1.54(0.17)	0.97(0.35)	0.664(.575)	0.585(.509)	0.169(.239)	0.053(.046)
man/VAFB	0.948(0.007)	0.42(0.14)	3.61(1.17)	0.51(0.18)	0.85(0.71)	0.525(.061)	0.323(.063)	0.218(.043)	0.044(.007)
mch/VAFB	0.952(0.002)	0.43(0.15)	4.10(0.34)	0.57(0.12)	0.81(0.35)	0.918(.143)	0.922(.105)	0.253(.042)	0.033(.003)
Chaparral ave.	0.946(0.006)	0.49(0.11)	5.46(1.31)	1.08(0.21)	1.17(0.54)	0.652(.269)	0.471(.320)	0.143(.119)	0.045(.024)
mes/FHUA	0.954(0.002)	0.44(0.01)	2.97(0.42)	0.57(0.09)	0.72(0.13)	0.625(.173)	0.472(.121)	0.001(.000)	0.035(.008)
oas/FHUA	0.971(0.004)	0.52(0.08)	1.61(0.38)	0.50(0.17)	0.44(0.10)	0.169(.039)	0.048(.013)	0.005(.004)	0.027(.009)
oaw/FHUA	0.965(0.003)	0.44(0.14)	2.01(0.47)	0.47(0.13)	0.67(0.33)	0.147(.100)	0.026(.021)	0.007(.006)	0.029(.020)
FHUA ave.	0.963(0.003)	0.48(0.08)	2.21(0.42)	0.49(0.15)	0.58(0.18)	0.297(.248)	0.166(.219)	0.005(.005)	0.030(.013)
Southeast									
lit/FB	0.894(0.016)	0.10(0.06)	19.06(6.78)	1.06(0.63)	10.60(3.64)	0.048(.040)	0.018(.019)	0.039(.015)	0.024(.009)

Species/group	MCE	EC/TC	PM2.5	EC	OC	K	Cl	Na	S
1yr/CL	0.942(0.001)	0.08(0.03)	11.35(4.99)	0.46(0.17)	5.70(1.04)	0.279(.126)	0.063(.041)	0.054(.020)	0.040(.013)
2yr/CL	0.928(0.007)	0.07(0.03)	13.78(6.19)	0.48(0.18)	6.88(2.63)	0.248(.171)	0.085(.040)	0.089(.072)	0.039(.015)
poc/CL	0.953(0.010)	0.18(0.06)	4.91(2.12)	0.44(0.16)	2.22(1.02)	0.042(.009)	0.011(.003)	0.018(.002)	0.008(.002)
cuh/CL	0.958(0.003)	0.36(0.04)	1.69(0.16)	0.41(0.03)	0.75(0.16)	0.159(.018)	0.108(.027)	0.034(.005)	0.015(.003)
uh/CL	0.954(0.011)	0.32(0.09)	7.46(2.04)	1.51(0.66)	3.07(0.73)	0.282(.073)	0.095(.025)	0.046(.009)	0.047(.015)
Camp Lejeune ave.	0.938(0.008)	0.17(0.06)	10.79(4.12)	0.81(0.37)	5.66(1.85)	0.172(.136)	0.060(.045)	0.047(.037)	0.029(.017)

Table 4.3 Weighted average PM number emission factors for the southwest and southeast fuels measured by CPC and Dekati Mass Monitor (DMM).

Species/group	CPC (#/kg)×10^{15}	DMM (#/kg)×10^{15}
Southwest		
cea	10.5 ± 6.7	8.1 ± 6.3
chs	5.1	4.8
cas	4.4 ± 0.9	3.9 ± 0.8
cos	3.2 ± 0.2	3.8 ± 0.1
man	4.3 ± 2.0	6.0 ± 3.9
mch	3.6 ± 0.1	4.9 ± 0.3
Chaparral ave.	5.2 ± 2.7	5.3 ± 1.6
mes	6.1 ± 1.5	5.1 ± 2.0
oas	3.9 ± 0.7	3.5 ± 0.6
oaw	4.0 ± 0.9	2.6 ± 0.3
FHUA ave.	4.7 ± 1.3	3.7 ± 1.2
Southeast		
lit	6.3 ± 2.1	3.3 ± 1.0
1yr	8.5	7.2
2yr	10.9 ± 1.3	9.7 ± 3.5
poc	6.7 ± 2.3	6.8 ± 2.8

Species/group	CPC (#/kg)×10^{15}	DMM (#/kg)×10^{15}
cuh	7.0 ± 1.3	4.3 ± 2.8
uh	6.2 ± 1.8	4.6 ± 0.1
Camp Lejeune ave.	7.8 ± 1.9	6.5 ± 2.2

Table 4.4. Aerosol-phase emission factors of cations and anions (mg/kg fuel burned)

Species/ group	Sulfate	Nitrite	Fluorite	Chloride	Bromide	Sodium	Ammonium	Potassium	Calcium
Southwest									
cea/FHL	-	-	20.29 ± 10.19	481.00 ± 174.81	-	712.99 ± 953.99	-	391.88 ± 93.71	103.24
chs/FHL	140.96 ± 51.17	-	21.67 ± 3.78	177.72 ± 35.86	-	243.26 ± 228.80	-	364.93 ± 160.18	-
cas/VAFB	207.65 ± 59.04	-	20.56	1405.99 ± 457.22	-	457.92 ± 177.65	130.3	1192.62 ± 340.16	-
cos/VAFB	248.51 ± 26.73	59.96	22.12	1071.73 ± 119.09	-	332.07 ± 44.55	-	1279.42 ± 196.65	-
man/VAFB	102.44 ± 18.33	27.32	12.27 ± 8.49	301.03 ± 97.73	8.11	143.00 ± 58.56	-	408.67 ± 101.55	-
mch/VAFB	92.50 ± 24.60	-	11.89 ± 4.44	873.76 ± 102.96	-	213.24 ± 47.19	91.44	822.85 ± 86.26	-
mes/FHUA	117.80 ± 15.72	-	16.99 (1)	589.75 ± 124.61	-	186.74 (5) ± 79.91	167.12 ± 7.13	622.48 ± 145.77	-
oas/FHUA	78.97 ± 10.05	-	-	61.40 ± 4.16	-	95.59 (5) ± 17.05	-	119.49 ± 28.40	-
oaw/FHUA	85.24 ± 6.14	-	6.98 ± 2.58	43.41 ± 10.80	-	64.56 (5) ± 13.65	-	143.20 ± 71.74	-
Southeast									
lit/FB	-	-	60.34 ± 29.35	125.43 ± 39.61	-	378.65 ± 149.53	-	-	-

Species/ group	Sulfate	Nitrite	Fluorite	Chloride	Bromide	Sodium	Ammonium	Potassium	Calcium
1yr/CL	-	-	-	125.49 ± 14.96	-	402.52 ± 76.58	-	-	-
2yr/CL	-	-	63.04	174.81 ± 60.32	-	356.92 ± 63.81	-	-	-
poc/CL	-	-	12.67 ± 4.99	114.06 ± 12.13	-	116.72 ± 62.64	-	101.47 ± 51.39	-
cuh/CL	-	-	-	33.76 ± 11.11	-	97.48	-	-	-
uh/CL	141.81 ± 10.04	231.32	17.60 ± 1.38	161.29 ± 39.44	-	194.78 ± 36.58	-	245.89 ± 147.55	187.76

Table 4.5 presents levoglucosan (LG) emission factors (mg/kg fuel burned), and also fraction of LG in the PM, Organic Carbon (OC) and Organic Mass (OM) (wt%)

Fuel type	EF_{LG}	LG/PM	LG/OM	LG/OC	EC/TC
Southwest					
cea	187.4±172.2	3.19±2.42	6.24±3.14	4.1±2.1	36±23
chs	234.0±117.7	3.03±1.24	6.44±3.05	4.2±2.0	38±8
cas	25.2±9.3	0.37±0.17	1.46±0.13	1.0±0.1	58±7
cos	19.7±6.4	0.31±0.08	1.53±0.47	1.0±0.3	63±9
man	30.2±10.3	0.79±0.21	3.71±1.13	2.4±0.7	47±9
mch	79.2±42.7	1.64±1.18	6.05±2.86	4.0±1.9	44±18
Chaparral ave.	95.9±35.6	1.56±0.50	4.24±0.90	2.8±0.6	48±6
mes	28.9±10.9	0.75±0.08	2.07±0.37	1.4±0.2	44±1
oas	29.1±13.6	1.80±0.67	4.31±0.91	2.8±0.6	52±8
oaw	58.6±35.1	2.74±1.12	6.53±4.12	4.3±2.7	42±15
FHUA ave.	38.9±13.1	1.76±0.44	4.30±1.41	2.8±0.9	46±6
Southeast					
lit	1089.8±507.2	5.76±1.65	5.76±1.65	3.8±1.1	10±6
1yr	888.0±521.7	6.92±0.33	6.92±0.33	4.5±0.2	8±4
2yr	1272.5±545.9	9.52±1.04	9.52±1.04	6.2±0.7	6±4
poc	208.3±142.2	4.03±1.11	4.03±1.11	2.6±0.7	17±8
cuh	50.2±6.8	3.02	3.02	2.0±0.0	37
uh	337.0±135.7	5.14±3.46	5.14±3.46	3.4±2.3	32±9
Camp Lejeune ave.	641.0±155.1	5.73±0.83	5.73±0.83	3.7±0.5	18±3

Table 4.6. PAH presents emission factors in μg per kg fuel burned and diagnostic ratios for particle phase PAHs

Fuel type	cea	chs	cas	cos	man	mch	**Chaparral Ave.**	mes	oas	oaw	**FHUA Ave.**
Acy {2}[a,b]	297.2 ± 338.6	144.3 ± 137.5	77.8 ± 42.1	270.8 ± 149.9	19.2 ± 12.6	27.9	139.5 ± 66.2	35.5 ± 26.6	36.1 ± 49.0	82.2 ± 84.3	51.2 ± 33.7
Ace {2}	144.0 ± 97.7	126.8 ± 146.3	26.6 ± 26.9	7.4 ± 4.2	11.0 ± 13.9	3.7	53.2 ± 29.8	25.2±17.7	29.6±39.4	37.9±45.2	30.9±20.8
Fle {2}	329.7±350.1	391.4±476.0	84.2±81.9	20.8±5.2	43.9±53.0	97.4	161.2±99.8	68.4±77.8	145.5±134.5	128.6±156.8	114.2±73.6
Ph {3}	1434.5±1270.8	1055.1±1045.7	301.1±201.6	234.4±53.5	244.6±171.8	133.6	567.2±278.0	116.3±89.9	214.6±160.9	113.5±193.1	148.2±89.0
An {3}	197.5±283.1	78.0±74.5	148.1±166.6	94.5±59.3	156.7±230.4	136.7	135.2±68.7	11.1±9.0	8.7±5.1	79.3±128.9	33.0±43.1
Fla {3}	492.2 ± 171.7	558.3 ± 549.5	1041.9 ± 343.5	1156.1 ± 17.1	176.7 ± 124.8	257.8	613.8 ± 113.7	103.6 ± 96.6	88.5 ± 36.2	181.8 ± 309.3	124.6 ± 108.7
Py {4}	664.2 ± 426.6	738.0 ± 976.6	1480.4 ± 170.2	1433.2 ± 121.3	345.8 ± 162.3	447	851.4 ± 183.0	418.1 ± 420.1	256.3 ± 149.7	273.3 ± 243.0	315.9 ± 169.3
B[a]A {4}	778.9 ± 430.0	338.2 ± 302.4	1524.2 ± 707.5	1550.7 ± 74.4	223.8 ± 119.8	432.5	808.1 ± 148.8	280.1 ± 283.4	134.0 ± 71.6	172.7 ± 161.5	195.6 ± 111.3
Chr {4}	269.6 ± 273.5	225.9 ± 202.9	1478.4 ± 686.8	1425.2 ± 225.6	238.4 ± 167.8	432.5	678.3 ± 136.1	258.1 ± 213.4	133.8 ± 70.2	171.6 ± 159.7	187.8 ± 91.9
B[b]F {4}	216.3 ± 213.1	164.5 ± 182.2	591.8 ± 341.9	823.7 ± 213.2	145.4 ± 108.1	151.9	348.9 ± 83.8	107.8 ± 98.6	37.0 ± 13.8	105.1 ± 116.0	83.3 ± 51.0
B[k]F {4}	1164.6 ± 809.6	256.8 ± 241.8	3232.0 ± 3144.1	2156.5 ± 135.6	537.6 ± 563.0	612.4	1326.7 ± 551.1	228.4 ± 182.6	145.9 ± 43.1	266.6 ± 461.8	213.6 ± 166.2
B[a]P {5}	130.2 ± 80.4	59.9 ± 52.9	713.2 ± 937.3	433.0 ± 37.8	28.2 ± 10.0	75.2	240.0 ± 157.2	29.6 ± 25.8	22.7 ± 1.9	405.7 ± 682.1	152.7 ± 227.5
Ind {5}	104.4 ± 163.9	118.3 ± 123.7	342.5 ± 110.2	582.1 ± 167.1	42.4 ± 28.2	102.3	215.3 ± 48.0	37.3 ± 27.5	23.2 ± 5.3	8.2 ± 12.0	22.9 ± 10.2

Fuel type	cea	chs	cas	cos	man	mch	**Chaparral Ave.**	mes	oas	oaw	**FHUA Ave.**
D[ah]A {5}	59.0 ± 68.8	12.1 ± 10.5	113.7 ± 59.4	149.9 ± 44.8	13.4 ± 7.5	26.5	62.5 ± 17.0	13.5 ± 9.1	10.7 ± 3.5	8.7 ± 7.8	11.0 ± 4.1
B[ghi]P {4}	199.6 ± 276.0	136.8 ± 119.1	534.2 ± 172.2	993.2 ± 268.1	47.5 ± 31.7	164.6	346.0 ± 73.2	53.9 ± 39.3	34.1 ± 10.7	12.5 ± 20.6	33.5 ± 15.2
Sum	6481.9	4404.4	11690.1	11331.5	2274.6	3102	6547.3	1786.9	1320.7	2047.7	1718.4
Diagnostic ratios											
Fla/(Py+Fla)	0.43	0.43	0.41	0.45	0.34	0.37	0.40	0.2	0.26	0.40	0.28
Ph/(Ph+Ant)	0.88	0.93	0.67	0.71	0.61	0.49	0.72	0.91	0.96	0.59	0.82
Ind/(Ind+Benzo[ghi]P)	0.34	0.46	0.39	0.37	0.47	0.38	0.40	0.41	0.40	0.40	0.40

[a] Abbreviations: Acy(acenaphthylene), Ace(acenaphthene), Fle(fluorene), Ph (phenanthrene), An (anthracene), Fla (fluoranthene), Py (pyrene), B[a]A (benz[a]anthracene), Chr (chyrsene), B[b]F (benzo[b]fluoranthene), B[k]F (benzo[k]fluoranthene), B[a]P (benzo[a]pyrene), B[ghi]P (benzo[ghi]perylene), Ind (indeno[1,2,3-cd]pyrene), D[ah]A (dibenz[ah]anthracene) [b] No. of fused aromatic rings

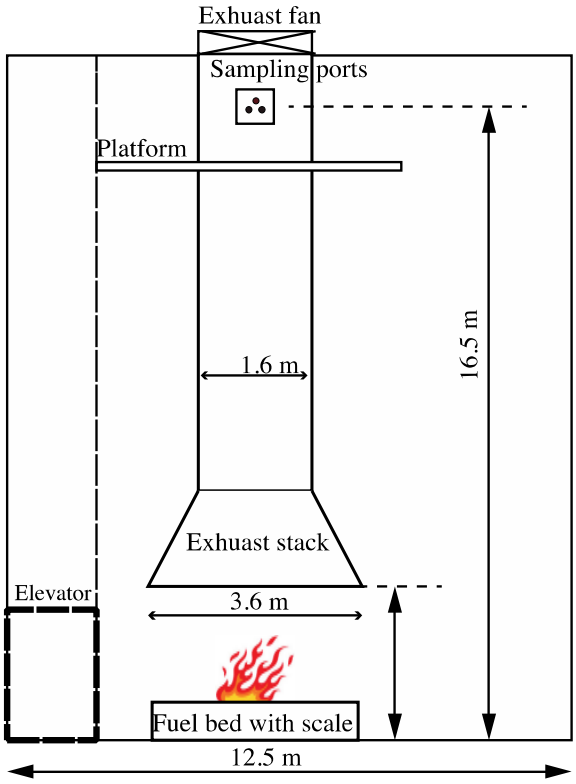

Figure 4.1. Schematic drawing of combustion laboratory, USDA's forest service fire sciences laboratory, Missoula, MT. Detailed characteristics of the facility are explained in Christian et al. (2004).

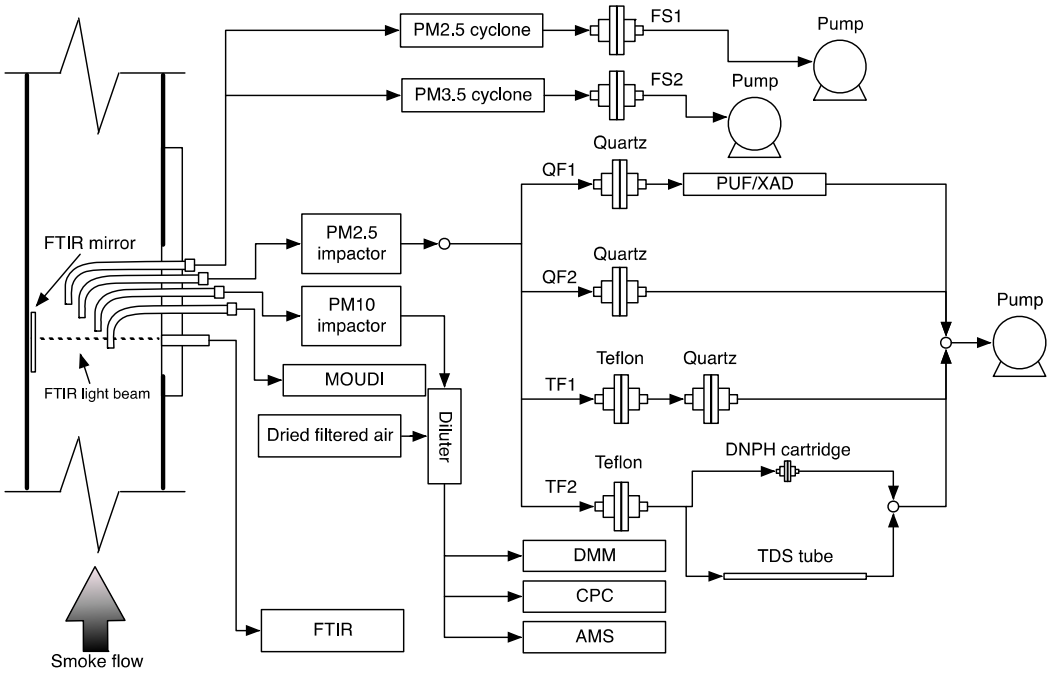

Figure 4.2. Schematic graph of the sampling system used to measure the emissions; a PM2.5 impactor was applied before the filter sampler system, and a PM10 impactor was used for other instruments.

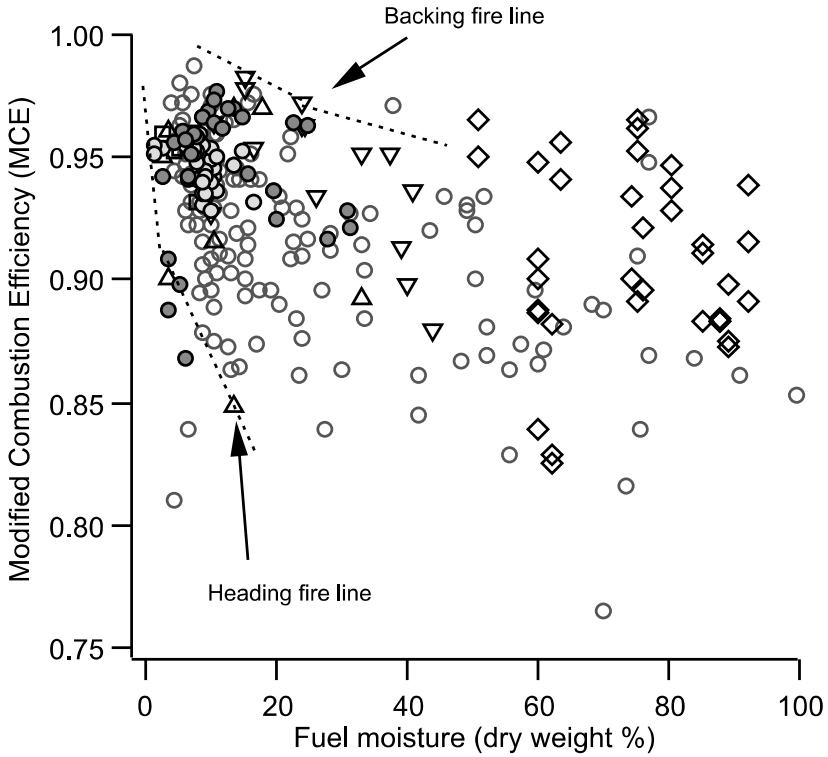

Figure 4.3. Fire integrated MCE versus fuel moisture content from this study (solid light (SE) and dark (SW) gray circles); from Weise et al., 1991 for California chaparral (diamonds); from McMeeking et al., 2009 for a wide variety of US domestic fuel types including Chaparral (cea, chs, and man) (circles); from Keene et al. 2006, for in-lab open burning of African savanna grassland: backing (downward triangle), mixed(square), and heading (upward triangle) fires. The dashed lines show the upper and lower limits of heading and backing fires.

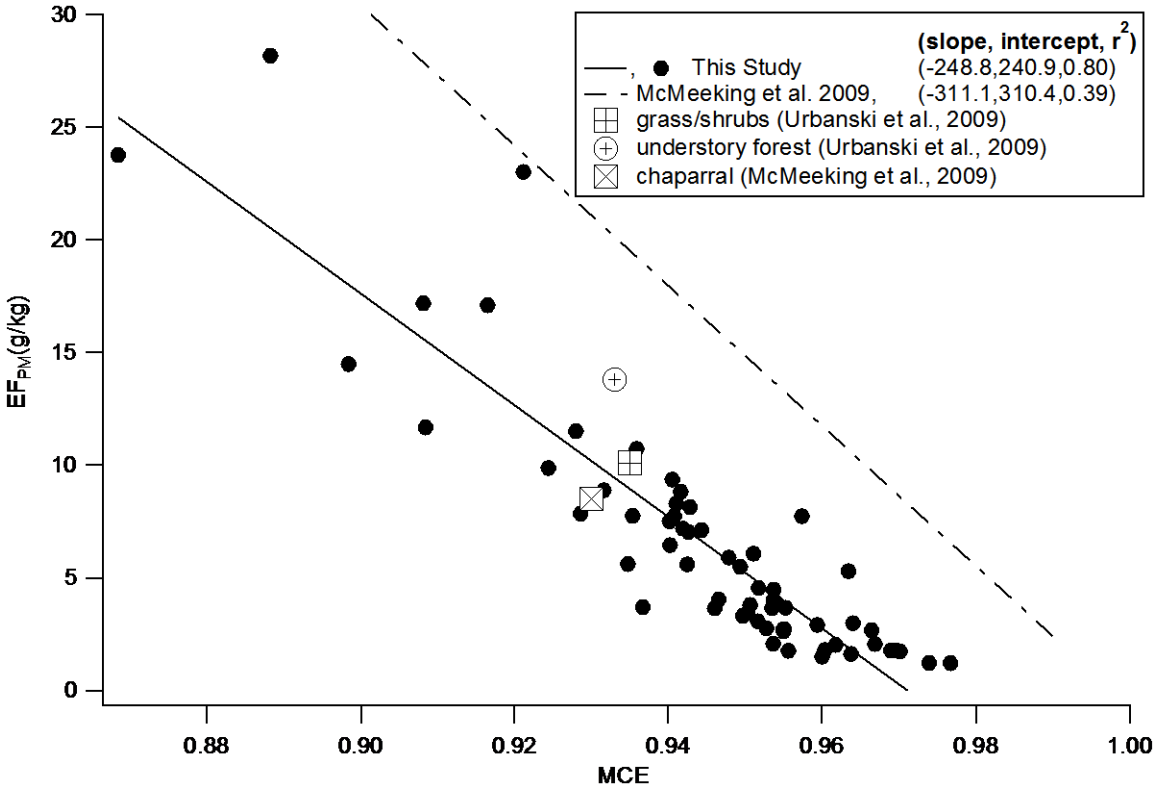

Figure 4.4. Particulate Matter (PM2.5) as a function of Modified Combustion Efficiency (MCE). Black solid circles are EF for PM2.5 measured for this study. Solid and dashed lines represent the linear regression of PM2.5 onto MCE for this and other studies, respectively indicated on the plot for laboratory, ground-based and airborne field measurements.

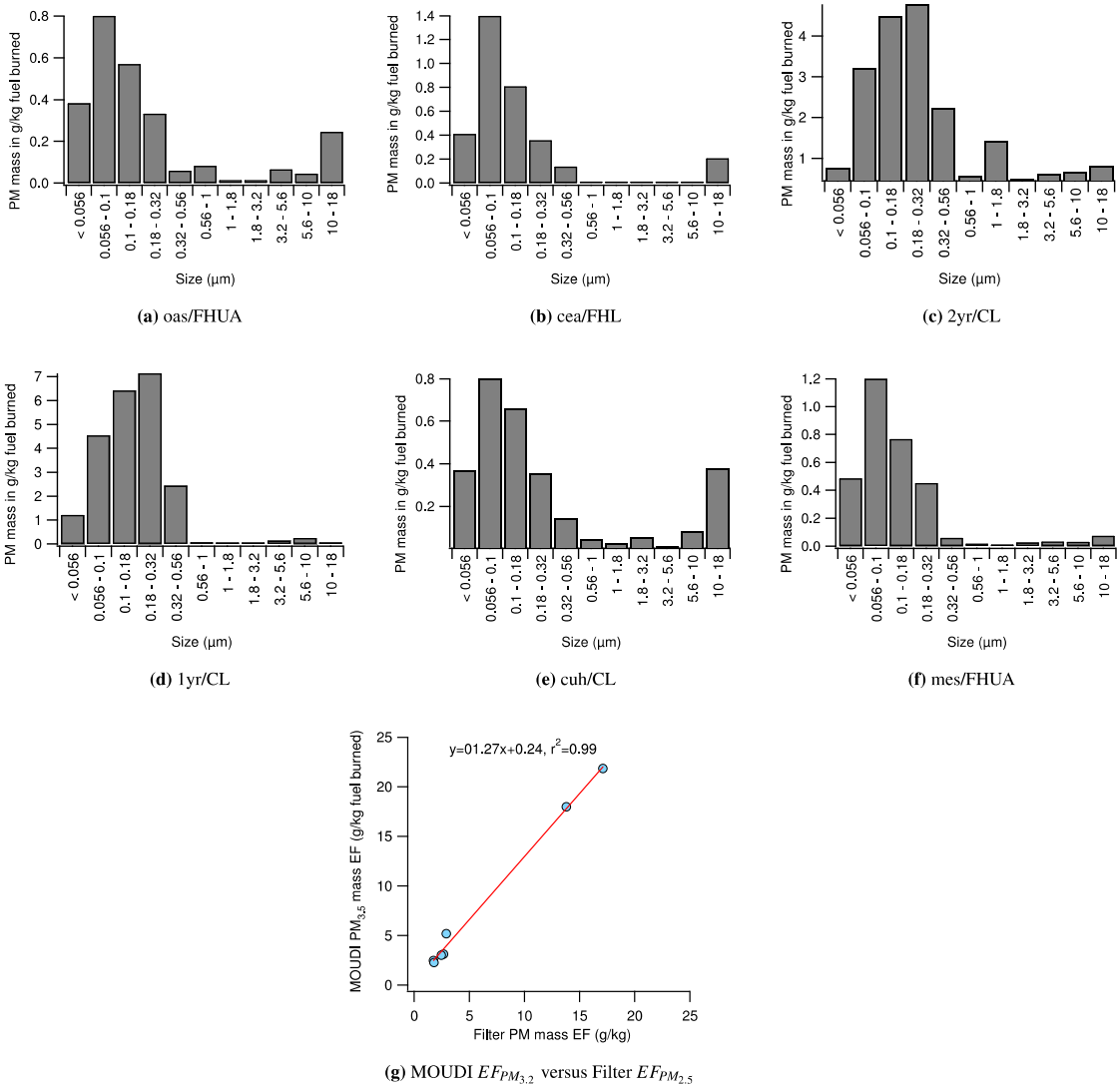

(a) oas/FHUA **(b)** cea/FHL **(c)** 2yr/CL

(d) 1yr/CL **(e)** cuh/CL **(f)** mes/FHUA

(g) MOUDI $EF_{PM_{3.2}}$ versus Filter $EF_{PM_{2.5}}$

Figure 4.5. Size-resolved mass emission factors obtained through the MOUDI/filter setup (a)-(f); in sub-figure (g) the mass emission factors of PM3.5 from the six sampled MOUDIs are graphed versus their corresponding mass emission factors acquired from the filter measurements

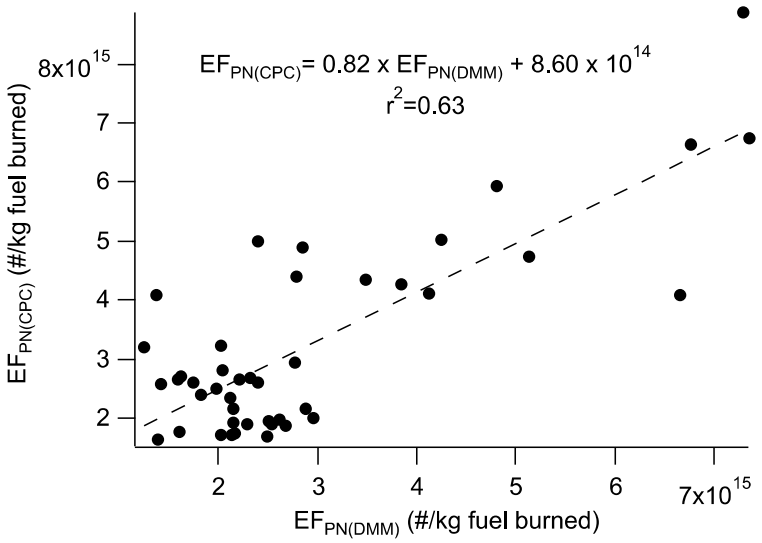

Figure 4.6. This graph illustrates the difference between measured particle number emission factors of butanol-based CPC and DMM; the slope is 0.82 and as shown DMM gives ~20% higher EFPN

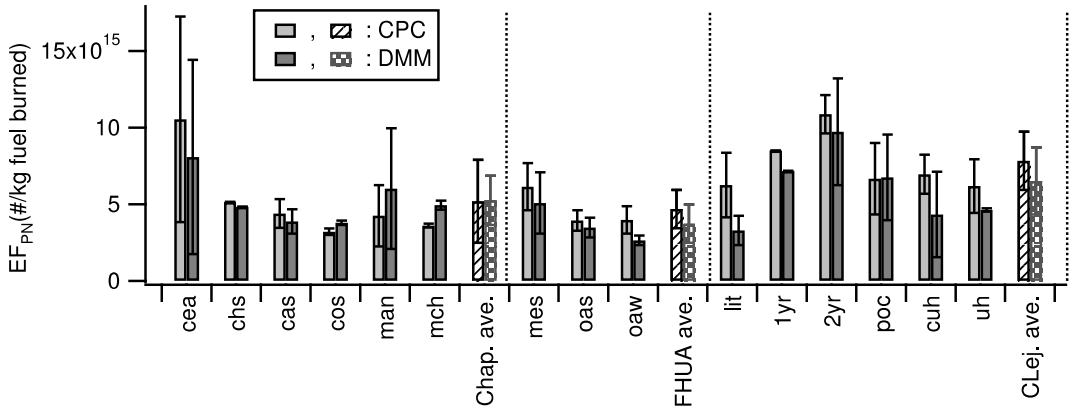

Figure 4.7. Particle number emission factors measured by CPC and DMM as function of fuel type

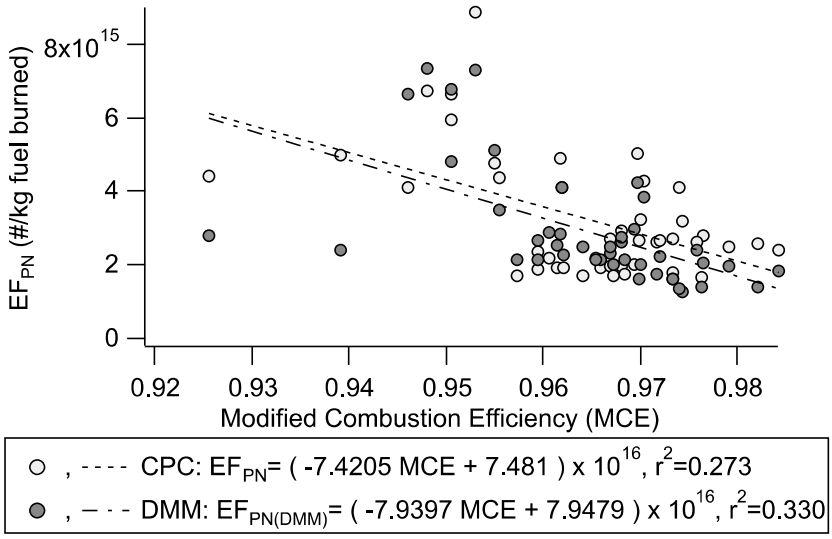

Figure 4.8. Particle number emission factors −EFPN (#/kg fuel burned) vs. Modified Combustion Efficiency (MCE) for all southwestern and southeastern fuel types acquired by two different working principal instruments, butanol-based CPC (solid dark gray circles) and particle-charge based DMM (solid light gray circles) are shown here. The best linear fit also is depicted using the dashed lines.

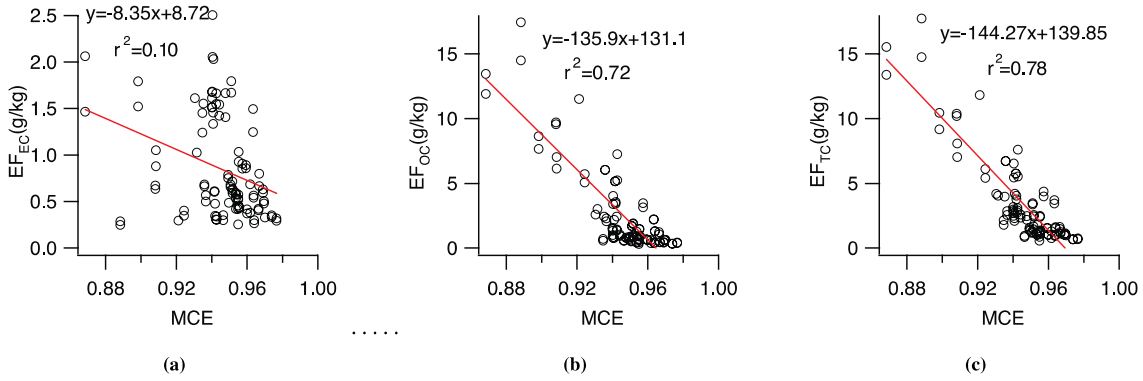

Figure 4.9. Fire-integrate PM2.5 emission factors plotted versus MCE for (a) elemental carbon(EC) (b) organic carbon(OC) (c) total carbon(TC)

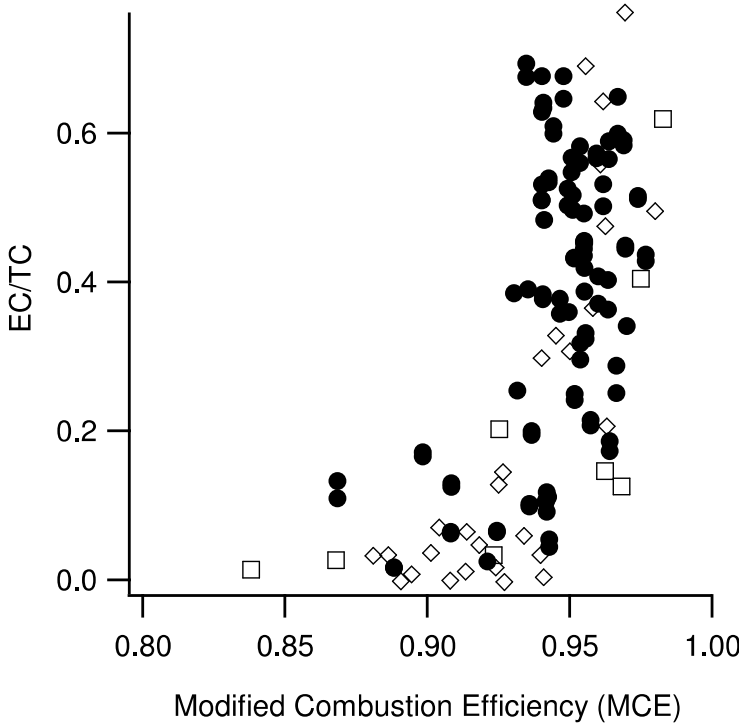

Figure 4.10. Particle elemental carbon to total carbon ratio (EC/TC) plotted versus modified combustion efficiency (MCE). Solid circles represent EC/TC measured in this study. Also shown are: open diamond, McMeeking et al. 2009, and open box, Christian et al. 2003

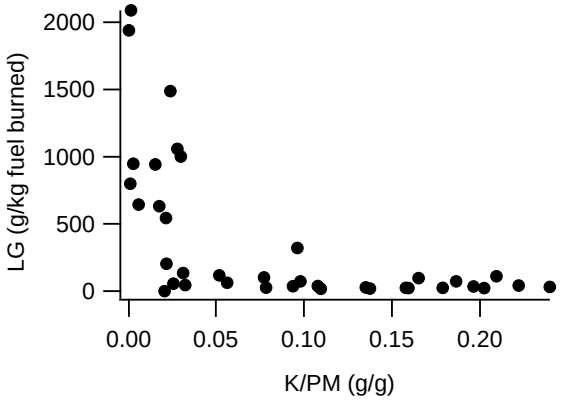

Figure 4.11. Levoglucosan emission factor (g/kg fuel burned) plotted versus potassium to PM mass ratio (g/g) for the SW and SE fuels

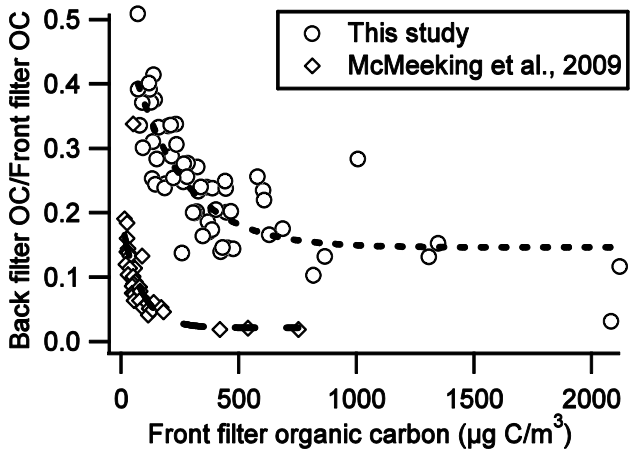

Figure 4.12. Mass fraction of semi-volatile organic compounds (SVOCs) in total collected Organic Carbon (OC); Open circles are data from this study (best exponential fit: 0.146+0.355e−0.004x), and open diamonds from McMeeking et al., 2009 (best exponential fit: $0.021 + 0.173e^{-0.012x}$).

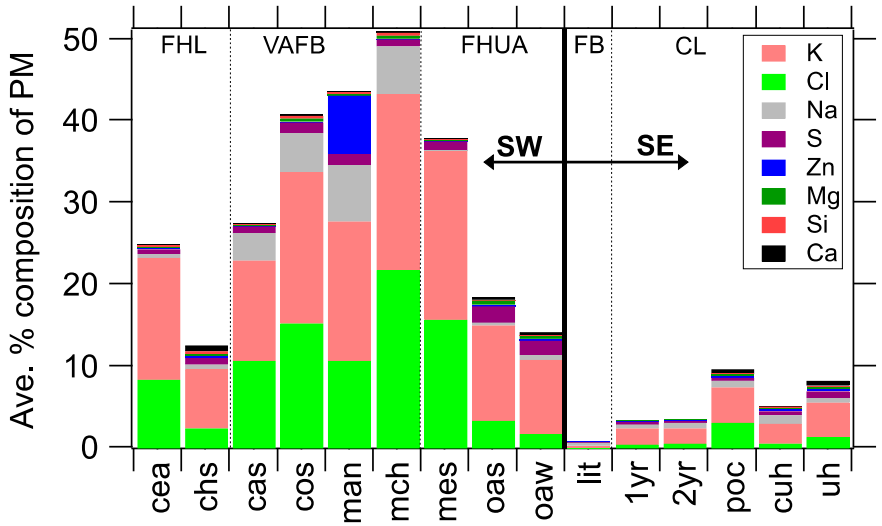

Figure 4.13. Percentage composition of PM mass comprised by the elements K, Cl, Na, S, Zn, Mg, Si, Ca for 41 burns, segregated by fuel type and site origin

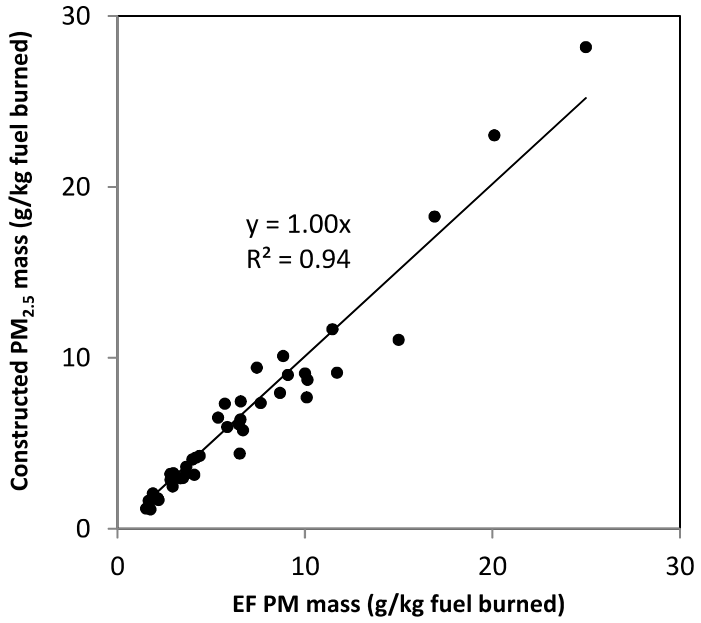

Figure 4.14. Reconstructed PM2.5 mass emission factor (g/kg fuel burned) versus gravimetric PM2.5 mass emission factor. Solid line represents the regression line with slope of 1 and correlation coefficient of 0.94.

Chapter Five: Chemical characterization of gas phase emissions from US vegetation

5.1. Abstract

Emissions factors of gas-phase polyaromatic hydrocarbons, carbonyls, and select volatile organic compounds from open combustion of southwestern (SW) and southeastern (SE) U.S. vegetation types commonly managed by prescribed burns during 77 controlled laboratory burns are presented. The fuels were burned under controlled laboratory conditions at the US Forest Service Fire Sciences Laboratory in Missoula, MT. Effect of vegetation type, regional dependency, and combustion efficiency on emissions are investigated. In general, emission factors anticorrelated with fire combustion efficiency. We suggest that emission factors are better segregated using Elemental Carbon to Total Carbon ratio (EC/TC) compared to the Modified Combustion Efficiency (MCE). MCE fails to conserve linearity of emission factors for MCE>0.94. Emission factors of most compounds showed exponential decay with EC/TC ratio, e.g. formaldehyde, acetaldehyde, acetone, benzene, ethylbenzene, toluene, and xylenes. The Pearson coefficient for emission factors of these compounds vs. MCE increased when plotted against EC/TC ratio. PAHs in the gas exponentially decreased with EC/TC ratio up to 0.3 and then again seemed to grow. MCE appears to compress a large portion of system response to flaming combustion regime, i.e. 0.2<EC/TC ratio<0.6, into small position of MCE, i.e. 0.94<MCE<1.0, and thus leading to false impression of linearity for all combustion regimes.

5.2. Introduction

Biomass burning is recognized as the second largest source of trace gases in the atmosphere (Crutzen and Andreae, 1990, Yokelson et al., 1996, Akagi et al., 2011). A significant fraction of biomass burning emissions in the U.S. belongs to emission from prescribed burns. Prescribed burning is a land management tool used to maintain/restore ecosystem health and resiliency and mitigate wildfire risk by reducing hazardous fuels (Wade et al., 1989, Biswell, 1999). However, prescribed burning can significantly affect the regional air quality and through long-range transport can influence areas distant from fire (Warneke et al., 2009, Warneke et al., 2010). Between 2002 and 2011 the annual average area treated with prescribed burning was 599 kHa in the southeastern U.S. (SE: Alabama, Arkansas, Florida, Georgia, Louisiana, Mississippi, North Carolina, South Carolina, Tennessee, and Virginia) and 134 kHa in the southwestern U.S. (SW: Arizona, California, Colorado, New Mexico, Nevada, and Utah) (NIFC, 2012). During the same period, wildfires burned an average of 854 kHa yr-1 in the SW and 215 kHa yr-1 in the SE (NIFC, 2012).

Similar to combustion of any hydrocarbon fuel, emissions from combustion of biomass is dominated by emissions of carbon dioxide (CO_2), carbon monoxide (CO), and water (H_2O). Previous studies indicate that Oxygenated Volatile Organic Carbons (OVOCs) account for the majority of non-methane hydrocarbons (NMHC) (Christian et al., 2003; Christian et al., 2004). Emission Factors (EF) of NMOC compounds are found to be dependent on phase of combustion (flaming vs. smoldering) - modified combustion efficiency (MCE), fuel moisture, chemical composition of the fuel, etc. (Andreae and Merlet, 2001). However, the reported EFs suffer from large variability from one study to another.

Online instruments such as Proton-transfer-Reaction mass spectrometry (PTR-MS) and Open Path Fourier Transform Infrared (OP-FTIR) spectrometer have been extensively used in laboratory and field experiments for speciation of NMOCs (Yokelson et al., 1996, Yokelson et al., 1997, Yokelson et al., 1999, Christian et al., 2003, Yokelson et al., 2007, Burling et al., 2010). These online methods have advantages over the offline methods including high sensitivity, no storage or sampling artifacts, high temporal resolution (Warneke et al., 2011). Because of the difficulties in using offline analysis methods (e.g. gas chromatography methods) such methods have not been often used in laboratory and field experiments (Jenkins et al., 1996b,Jenkins et al., 1996a: U.S. agricultural and forest biomass fuels, Oros and Simoneit, 2001: temperate and polar region trees, Hays et al., 2005: US foliar fuels). However, the offline methods were not a limiting factor in the current study, because of sampling during the whole fire and high mixing ratios observed in the laboratory (Burling et al., 2010).

Extensive measurements of gas-phase emissions were conducted at the U.S. Department of Agriculture (USDA) Forest Service Fire Sciences Laboratory in Missoula, MT through offline analysis methods for better characterization of emissions from fuels representative of vegetation types managed by prescribed burning on several U.S. Department of Defense bases located in southwestern and southeastern U.S. This laboratory study let us use a sophisticated suite of instrumentation that is hard to deploy in the field. The emission factors of aldehydes and ketones, polyaromatic hydrocarbons and select volatile organic compounds from 77 fires that burned 18 fuel types are reported. We also investigated how Modified Combustion Efficiency (MCE) can alter the EFs. Moreover, we explored the

Elemental Carbon to Total Carbon ratio (EC/TC ratio)-obtained from the particle phase- as a better predictor of emission factors in comparison with MCE. This publication only represents a subset of results; other results from lab and field components from this study are published elsewhere (Burling et al., 2010, Burling et al., 2011, Hosseini et al., 2010,Veres et al., 2009, Roberts et al., 2010, Veres et al., 2010, Akagi et al., 2012, Yokelson et al., 2012, Hosseini et al., 2012b).

5.3. Methods

5.3.1. Missoula Fire Lab

The combustion facility at the U.S Department of Agriculture (USDA) Forest Service, Forest Sciences Laboratory (FSL) at Missoula, MT is described in more detailed by Christian et al., 2004. Briefly, the facility is a large burn chamber that measures 12.5m×12.5m×22m high (show in Figure 5.1). The fuel bed is located under a large 3.6m inverted funnel connected to a 1.6 m diameter exhaust stack that extends through the ceiling. The room is pressurized with temperature and humidity controlled air in order to capture all the emissions from the fire. The exhaust is vented through the ceiling. A sampling platform surrounds the stack at the height of 17m where instruments are located and temperature and pressure are measured. Previous studies showed that the smoke sample at the height of the sampling platform and across the stack is well mixed (Christian et al., 2003b;Christian et al., 2004).

5.3.2. Fuel Description

The laboratory fire experiments were conducted for 18 major vegetation types with 3-6 replicates for each vegetation type. The fuels are commonly managed by prescribed burning/military bases and were collected from Southwestern (SW) and Southeastern (SE) U.S. Detailed description for each vegetation type burned in this study can be found in Burling et al., 2010. Here, we briefly list the fuels and the fuel codes used in the current study (Table 5.1). Vegetation types were collected in January 2009 from Vandenberg Air Force Base, California (regional code shown as 'VAFB' in the tables and figures), Fort Hunter-Ligget, CA ('FHL'), Fort Huachuca, AZ ('FHUA'), and Fort Benning, GA ('FB'). The SW fuels included manzanita (fuel code shown as 'man' in the tables and figures), California sage ('cas'), coastal sage ('cos'), maritime chaparral ('mch'), Chamise scrub oak ('chs'), chaparral grass ('chg'). SE vegetation types included oak savanna('oas'), oak woodland('oaw'), mesquite('mes'), one-year-rough and two year rough ('1yr' and '2yr') referring to understory vegetation collected a year after burning, pocosin ('poc'), understory hardwood('uh'), chipped understory hardwood('cuh'), chipped understory litter from various southern pine stands ('lit').

5.3.3. Measurement System and Analytical Methods

The Open-Path Fourier Transform Infrared (OP-FTIR) instrument was placed on the sampling platform approximately 17 m above the height of fuel bed so that the open white cell spanned the diameter of the stack directly in the rising smoke stream for continuous 1.5 sec measurement. In the current work, we used the CO and CO_2 from OP-FTIR results to calculate phase of combustion (MCE) (more details on OP-FTIR can be found in Burling et

al., 2010). The analysis and sampling of Elemental Carbon(EC)/Organic Carbon(OC) is explained in the companion paper of the current study (Hosseini et al., 2012b). Carbonyls were collected at 0.7 lpm onto 2,4-dinitrophenylhydrazine (DNPH) coated silica cartridges (Water Corp., Milford, MA) . Volatile organic compounds (VOC) were collected at 0.8 lpm onto pre-baked 6 mm OD Gerstel Carbotrap™ 300 Multi Bed glass thermal desorption (TDS) tubes (GERSTEL). Both the DNPH cartridge and TDS tube were located downstream of a Teflon® filter. PAHs were collected sequentially; first on a quartz filter and then into a column packed with polyurethane foam (PUF) and XAD-4 resin. The quartz filters were preconditioned at 600°C for 5 hours in an oven. The flow rates through Teflon and quartz filters were measured to be 22 and 25 lpm, respectively. All the samples were taken at the top of the sampling platform where OP-FTIR and the rest of the instrumentation were located. Samples collected at the FSL facility were kept cold and away from light and returned to UCR laboratory for subsequent analysis of carbonyls, VOCs, and PAHs following the below protocols:

Analysis of Carbonyls: DNPH cartridges were analyzed for carbonyls following a modified SAE 930142 HP protocol (Siegel et al., 1993). The cartridges were extracted using 5mL of acetonitrile and injected into Agilent 1200 series high performance liquid chromatograph (HPLC) equipped with a 5 mm Deltabond AK Resolution (200 cm"4.6mm ID) with upstream guard column and a Diode array detector. The HPLC analysis followed the SAE 930142HP protocol (Siegl et al., 1993).

Analysis of BTEX: CarboTrap™ 300 Multi Bed tubes were injected into an Agilent® 6980 GC-FID system via a Gerstel® Thermal Desorption System (TDS) that was setup according

to the specifications of SAE 930142HP Method 2 for C4-C12 hydrocarbons (Siegl et al 1993). The unit ramps from -40 to 250 °C at a rate of 6 °C/min to desorb the sample from the tubes.

Analysis of PAHs and C10-C30 hydrocarbons: PUF/XAD resins were analyzed according to a modified EPA TO-13A protocol (ASE). PUF-XAD cartridges were spiked with deuterated standards and extracted with methylene chloride using a Dionex® Automated Solvent Extractor (ASE-200) (60 min, 250 °C). The extract is then concentrated to approximately 5ml using a Roto-Evaporator. The eluent was further concentrated by evaporation using ultra high purity nitrogen or helium, and then analyzed by an Agilent® 5973 GC-MS.

5.4. Results and discussion

77 fires were sampled during an 18-day period at the FSL facility in Missoula, MT. Immediately after ignition the CO_2 concentration sharply increased which is attributable to the flaming phase. Shortly, the CO concentration started increasing. At this stage, there was no clear distinction between the flaming and smoldering. However, the relative amount of flaming to smoldering combustion was calculated using the concept of Modified Combustion Efficiency (MCE), which is defined as the fire-integrated excess concentration of CO_2, divided by the excess concentration of CO_2 plus CO measured by the OP-FTIR (Ward and Radke, 1993). We assumed that the background concentrations of CO and CO_2 for the burns were constant and equal to their 1-min averaged concentration prior to ignition. The arrangement of the fuels on the fuel bed - whether it is horizontally or

vertically- considerably affected the fuel consumption (for more detail see Hosseini et al., 2012b)

5.4.1. Polycyclic Aromatic Hydrocarbons (PAHs)

PUF/XAD cartridges from 41 burns were analyzed for 16 PAH species including naphthalene (Nap), acenaphthylene (Acy), acenaphthene (Ace), fluorene (Fle), phenanthrene (Ph), anthracene (Ant), fluoranthene (Fla), pyrene (Py), benzo[a]anthracene(B[a]A), chrysene(Chr), benzo[b]fluoranthene (B[b]F), benzo[k]fluoranthene (B[k]F), benzo[a]pyrene (B[a]P), indeno[1,2,3-c,d]pyrene (Ind), dibenzo[a,h]anthracene (D[a,h]A), benzo[g,h,i]perylene (B[ghi]P). Emission factors of these PAHs for all the SW/SE fuels are provided in Table 5.2 in mg/kg dry fuel burned. The variability of measurements is shown with one standard deviation (σ).

Only a few articles have investigated the emissions of PAHs from wood burning (cited below) and all suffer from large variability (unlike PM mass/EC/OC). This is mostly because researcher have been trying to characterize the PAH EFs based on fuel type/combustion methods. As shown in Table 5.2, the EFs in the current study varied largely between fuel types/regions. The Coefficient of Variation (CV) of PAHs except for a few cases varied between 10-270% with the lowest CV of 35% belonging to Nap among all fuel types. Generally, heavier PAHs with a higher number of aromatic rings led to higher CV, e.g. 90% for Fle or 110% in case of B[a]A, which might be due to lower vapor pressure of heavier Molecular Weight (MW) PAHs and therefore more gas-to-particle phase partitioning and/or differing yields of PAHs at various burning conditions.

Table 5.2 represents the average ± standard deviation ($\mu \pm \sigma$) for all regions and fuel types. The study average EF of total PAH was 75.09±62.74 mg kg-1. Among all fuel types of SW/SE, duf/AK, lit/GA, fir/MT emitted the highest PAH EFs of 344, 136, and 191 mg/kg fuel burned, respectively and poc/CL emitted the lowest (18.4 mg kg-1 fuel burned) consistent with previous studies (McDonald et al., 2000, Jenkins et al., 1996, Schauer et al., 2001, Hedberg et al., 2002).

On average, dominant PAH species by mass fraction in the order of decreasing average ranking were Nap, Acy, Ant, Ph, Py, Fla, Fle. These species comprised nearly 99% of total gas phase PAHs. In general, the lower the MW of the PAH, the higher the yield was. Hedberg et al., 2002 combusted birch wood in wood stove and reported that Fle, Ph, Ant, Fla, Py contributed to 70% of the total PAHs (Nap was not analyzed). The same species comprised 61-63% of the total PAH (excluding Nap) in VAFB, FHUA, FHL, CL, AK regional group but for fuels from FB, and MT it was only 36% and 92%, respectively.

Acy was the second highest produced PAH and showed the same trend as Nap. EF of Acy was 79% of the EF of Nap for all of the burns (R^2=0.35). Although the plot of Ph vs. MCE seems linear (Figure 5.3), the plot of Ant vs. Ph (not shown) is more scattered compared to the previous plots (R^2=0.36). Comparing the plots of Acy and Ph vs. EC/TC, it is clear that Ph is somewhat less produced for EC/TC<0.3 compared to Nap and Acy. Ant, Py, Fle, and Fla were all similar to Acy. Three outliers (outside of the mean 95% confidence intervals) were observed for Py/VAFB for which these fuels emitted unexpectedly high Acy.

A Tukey's posthoc test showed that there is no statically significant difference between EF of PAH species among various SW/SE fuel types. Similarly, using the same test it turned out that regional dependency was not a significant factor as well. Moreover, comparing the gas-phase PAH EFs with the particle-phase PAH EFs (Hosseini et al., 2012), the lower MW PAH were in the gas phase (MW≤200) and heavier ones (MW>200) were present in the particle phase, consistent with Zou et al., 2003 (see Figure 5.2).

Nap was the highest contributor in the total gas-phase PAH, ~(56±13) except for duf that emitted 17% more Acy compared to Nap. McDonald et al., 2000 (residential wood burning) reported (average ± standard error) Nap EFs of 21.42 ± 5.13 [EC/TC=0.20], 54.62 ± 18.32 [EC/TC=0.09], and 28.06 ± 19.06 [EC/TC=0.11] for softwood in fireplace, hardwood in fireplace and wood stove, respectively. These paired values are in good agreement with our results when plotted on Figure 5.3, i.e. on average the burns with smaller EC/TC values led to higher amounts of Nap. The EFs of Ant reported by Hedberg et al., 2002 varied largely between 0.1 and 102 averaging 19.3 mg/kg. In agreement with their results, Ant EFs turned out to be 3.42±1.03 (FHUA), 5.66±3.80 (FHL, CA), 6.58±3.88 (CL), 8.56±1.95 (FB), 9.22±4.20 (VAFB), 24.46 (MT), and 47.99 (AK) mg/kg fuel burned. No field study could be found that has reported EFs of gas-phase PAHs. However, if measured, reaction of O_3, OH radical, NO_3 with PAHs in smoke plumes can significantly lower the concentration of PAHs downwind of a fire. The main daytime loss process for PAHs in the troposphere is the reaction with OH radicals that takes hours to days (Calvert, 2002). Since the nighttime reaction with NO_3 is on the scale of days to months, the reaction of PAH with NO_3 can be ignored, similarly the reaction with ozone (Atkinson et al., 1992). PM can play an important

factor. Alebic-Juretic et al., 1990 investigated the degradation of PAHs on a solid carrier. They estimated the lifetime of B[a]P, Py, and Fle in 50 ppb O_3 to be 0.5-3.5 hr, 12 hr, and 6 days, respectively. Therefore, primary/secondary PM may provide suitable sites for continuous conversion of PAHs to secondary OC.

The relation between the emission factors of the highest ranked PAHs and Modified Combustion Efficiency (MCE) is represented in Figure 5.3. The total gas phase PAHs strongly correlated with MCE (R^2=0.77). The Pearson coefficient (R^2) was good with 0.50, 0.64, and 0.59 for Nap, Acy, and Ph, respectively. However, when focusing on the flaming side of the plots, a sudden drop in total PAHs, Nap, Acy, Ph, and Ant can be observed at MCE=~0.94. The same behavior was reported by McMeeking et al., 2009 and Hosseini et al., 2012a for EF of OC. They showed that MCE was exponentially correlated with EC/TC ratio and MCE>0.94 produced a sharp increase in the EC/TC ratio. Based on the evidence, it seems that MCE compresses a large portion of system changes (EC/TC=0.2-0.6) into only a small fraction of MCE range (i.e. MCE=0.94-1.00) (Figure 5.4). The plot of PAHs vs. MCE gives the impression of linearity because the high range MCE region (MCE>0.94) compresses system changes and low MCE region expands the system response. The data points in MCE plots are denser at MCE>0.94 because more burns or data points are available at this range mostly due to burning dry fuel in the laboratory experiments.

Total PAHs also showed a dual behavior with respect to MCE and EC/TC ratio (Figure 5.3). Based on definition of MCE, a more vigorous fire should results in less PAH (more complete combustion), while looking at the PAH vs. EC/TC ratio plots, the gas phase PAHs at first exponentially decreased and then started increasing (EC/TC>0.35). As

shown in Figure 5.3, Nap EF and the data scatter reaches to a min when the EC/TC ratio is ~0.25-0.35. Lowest amount of Nap in this range was produced by cuh/CL (34.3 mg/kg [0.33]), oaw/FHUA (34.5 mg/kg [0.34] and 46.2 mg/kg {0.26]). From 0.35 up to 0.7 a slight rise in production of Nap can be observed. In the post-harvest (Kentucky blue grass/wheat) study of Dhammapala et al., 2007 the individual values for emission factors of gas phase PAH were not reported, only the total (gas+particle) PAHs. What they showed was in contrast to values observed in this study. For the particle-phase, the total PAH in their study correlated with MCE (R^2=0.62) but not for the gas-phase PAH (R^2=0.06). They state that this could be due to largely variable temperature of the combustion chamber (28-50 °C) that led to more particle-phase compounds to be present in the gas phase. Jenkins et al., 1996a investigated the effect of stack temperature on gas-to-particle partitioning, referring to their plot, 20-50 °C can make up to 100% change in the partition of PAHs in the gas-to-particle phase.

Fraction of total PAHs in the particle-phase in the current study varied 2 to 17% and averaged 8±4% (filter surface temperature 27-29 °C). This is consistent with the values suggested by Jenkins et al., 1996a for filters collected at 25-30 °C. PAHs with molecular weight of above 200 were mostly captured on the filter, less than this MW the PAH were found in the tubing rinsate. Less than 1% and 2.8% of Nap and Ant ended up on the filter consistent with the results of rice straw from Jenkins et al., 1996a, respectively. Compared to their study, we found relatively higher amount of lighter and lower amount of heavier species consistent with Jenkins et al., 1996a, their woody fuels led to lower fractions in the higher MW PAHs as well. We can also compare our particle-phase fraction of total PAHs

with the results of McDonald et al., 2000 study (reported using standard error not standard deviation) which were significantly different and largely variable compared to the current study: 50% for softwood in fireplace, 33% for hardwood in fireplace, and 25% for hardwood in woodstove (based on their average values).

It should be noted here that lab studies should have higher EC/TC ratio primarily due to condensation of SOA and SVOCs on primary particulate matter from fires as the particle ages (Akagi, 2012a). Hosseini et al., 2012a proposed a way to correct for the ratio based on the amount of levoglucosan EF measured using online/offline methods.

An open-burning laboratory study of stubble of post-harvest wheat and Kentucky blue grass, Dhammapala et al., 2007 suggested implementing methods of increasing the combustion efficiency to lower emissions of PAH in agricultural burning. However, considering the results of current study, more factors have to be taken into account to minimize PAH emissions.

5.4.2. Carbonyls

Emission factor of the carbonyls are presented in Table 5.4. We analyzed the DNPH cartridges for formaldehyde, acetaldehyde, acetone, acrolein, propionaldehyde, crotonaldehyde, methyl ethyl ketone (MEK), methacrolein, benzaldehyde, valeraldehyde, tolualdehyde, and hexaldehyde. Measurement uncertainties in Table 5.4 are shown using average ± one standard deviation ($\mu \pm \sigma$). Based on the variability calculated for all the burns and individual aldehydes and ketones, the Coefficient of Variation (CV) ranged between 10% and 59% corresponding to mes/FHUA and cea/FHL fuel codes, respectively. Overall,

fuels from CL, NC had the highest CV of 65% and the lowest was from VAFB, CA with 26%. No trend in CV relative to the weight of aldehydes and ketones, unlike PAHs, was observed. Moreover, the variability of individual compounds of this group is similar to sum of aldehydes and ketones.

The most abundant aldehyde was formaldehyde being 27.2±5.0% of total aldehyde emissions. The study average EF of formaldehyde was 466.6±461.1 mg/kg fuel burned at average MCE of 0.942 and average EC/TC ratio of 0.367466.6±461.1 mg/kg fuel burned ⟨0.942⟩{0.367}. The min formaldehyde EF was 100 mg/kg fuel burned ⟨0.964⟩{0.589} emitted by oaw/FHUA, for which both MCE and ET/TC ratio indicated a very high burning rate. 'lit'/FB emitted the highest rate of formaldehyde EF of 2026 mg/(kg fuel burned) ⟨0.898⟩{0.165} with very low burning rate. The next highest-ranked carbonyls were acetaldehyde, hexaldehyde, valeraldehyde, acetone with 19.1±3.1%, 15.4±4.5%, 14.4±4.4%, 13.2±4.8%, respectively. These six compounds accounted for 89% of total aldehyde emissions. Methacrolein and tolualdehyde were below detection limit. A one-way between subjects ANOVA was conducted to compared the effect of fuel type on emission factor of aldehydes. There was a significant effect of fuel type at the $p<0.05$ level for the fuel types. A Tukey's posthoc test along with homogenous subset results provided three subsets for the aldehydes for which their means were not significantly different from each other. The largest group included all fuel types except 1yr and lit, the second group had cea, 1yr, and 2yr, and the third cea, 1yr, 2yr, very similar to the homogenous subsets of EC/TC ratio, however very different compared to MCE with seven subsets. However, based on the figures discussed below the differences can be attributed to quality of combustion, not the fuel type.

Average study EFs of SW fuels for formaldehyde, acetaldehyde, and acetone were 254.1±146.8, 170.7±98.1, 133.8±84.1 mg/kg fuel burned and for SE fuels were 891.5±578.4, 702.6±429.9, and 434.6±238.8 mg/kg fuel burned, respectively. Aldehydes summed 298±612 and 3775±2422 mg/kg fuel burned for SW and SE, respectively. The fuels from SE emitted nearly 1.8-6.1 times higher aldehydes compared to SW fuels. The highest ratio of 6.1 belonged to hexaldehyde; MEK had the lowest ratio of 1.8. An independent samples t-test revealed that there is significant difference in the EFs of SE and SE fuels (p-value<0.01). However, the large discrepancy between the EF of SE and SW fuels is largely due to EC/TC ratio growing from 0.168 for SE to 0.472 for SW fuel and MCE from 0.925 to 0.951 resulting in hotter flames of SW and thus less aldehyde formation (Figure 5.5). As can be seen, only 3% decrease in MCE resulted in 200-800% growth in aldehyde formation, this formation rate is better described by means of 64% decrease in EC/TC ratio.

SVOCs constitute a major fraction of non-methane hydrocarbons (NMOC) from biomass burning (Yokelson et al., 1996, Yokelson et al., 1997, Yokelson et al., 1999). It has been found that the OVOCs may constitute the majority of total hydrocarbons from biomass burning. For example, Yokelson et al., 2003 measured 5.3 g/kg of OVOCs and 3.6 g/kg of hydrocarbons including methane from an aircraft for a fire burning in savanna. Aldehydes, main fraction of OVOCs, can be emitted through combustion processes or formed in the biomass burning plumes by photochemical degradation of organic hydrocarbons, destroyed by photolysis, and reaction with OH or NO_3 radicals. However, reaction with NO_3 is of minor importance as a consumption process for aldehydes (Seinfeld and Pandis, 2006).

Therefore, concentration of aldehydes depends on the equilibrium state of the driving forces i.e. photolysis, OH reaction, OH formation. For example, in William fire plume ΔHCHO/ΔCO increased 47% over 1-hr period and then leveled off or ΔHCHO/ΔCO grew 7.3 times over a period of 4-hr, or as another example, in African savanna fire plumes a 40 min ageing led to a 9 fold increase in ΔHCHO/ΔCO ratio (Yokelson et al., 2003b). Cloud processing can also significantly increase the mixing ratio of HCHO as discussed in Yokelson et al., 2003a through faster photochemistry on the outer layer of clouds and/or heterogeneous conversion of methanol to formaldehyde. The accurate measurement of oxygenated VOCs (OVOCS) from biomass burning is a crucial step in estimation of products of photochemical reactions, since OVOCs are a major source of OH radical in the system of equations for the predictive models. Photolysis of HCHO and CH_3CHO can deliver 81.3% and 7.9% of locally-produced OH_x radicals in a biomass burning plume (Jenkin and Clemitshaw, 2000, Crutzen and Andreae, 1990).

The study average formaldehyde EF of 466 mg/kg fuel burned is consistent with the value of 440 mg/kg fuel at MCE=0.961 from savanna and grassland as reported by Andreae and Merlet, 2001. For tropical forest fuels at MCE=0.938 the reported EF of HCHO is comparable to our EF of lit fuel code produced at low MCE of 0.898. The average acetaldehyde and acetone EFs from the current study are also within their ranges of 0.50±0.39 and 0.25-0.62 of savanna and grassland burns, respectively. Extratropical forest at MCE=0.936 produced 2.2±1.4 g/kg HCHO, a value that is 3.8 times higher than the emission factor calculated based on our best linear fit (see Figure 5.5).

Our regression line at MCE=0.91 gives an EFHCHO of 990 mg/kg fuel burned, half of 1660 mg/kg fuel burned from the airborne study of Yokelson et al., 2007 in tropical forests. Their laboratory average of FTIR and PTR-MS mixing ratios led to an EFHCHO of 0.66 g/kg compared to our model at MCE=0.949 which is 54% less. We observed 57% and 77% less acetaldehyde compared to both airborne (Yokelson et al., 2007) and laboratory (Yokelson et al., 2007) studies at MCE=0.91 and 0.949, respectively. One of the reasons for such high EFs in addition to photochemistry might be the significant biogenic emissions of such compounds from tropical forests (Yokelson et al., 2008). Christian et al., 2007 reported a ground based EFHCHO of 1.8 g/kg fuel burned from tropical forest burns in Brazil that is unusually low at a MCE of 0.788. Our regression line gives 2.95 g/kg fuel burned. The reason is that ground-based measurement should lead to a higher EF since the cold smoldering plume drifts near the ground in contrast to airborne measurements with more flaming phase components.

Yokelson et al., 2008 suggested that their average airborne gas-phase VOC excluding formaldehyde and acetic acid should be multiplied by a factor of 1.12 and 2 for deforestation and pasture fires to account for separation of flaming/smoldering phase emissions in the rising smoke plume. The reasons that the suggested equation did not work for formaldehyde and acetic acid was that these two compounds are highly affected (increased) by post-emission photochemistry and radical reactions. One might expect laboratory EF of HCHO be higher compared to airborne studies due to airborne measurements being inclined towards flaming phase emissions and due to formaldehyde being mainly emitted by smoldering. As a result, the formation rate of HCHO in the plume might be underestimated.

A possible source of error might be use of MCE as a mean of comparison. MCE is not a linear function of combustion; thus, partial (short) sampling of airborne studies might not lead to a representative MCE comparable with laboratory MCEs calculated during the whole burn.

Christian et al., 2003b Investigated Indonesian fuels in the same laboratory as the current study. Their formaldehyde emission factors varied from 0.54 g/kg for alang-alang (MCE=0.953) to 3.17 (MCE=0.901) g/kg fuel burned for forest litter; their acetaldehyde ranged between 0.13 (MCE=0.953) for alang-alang and 1.25 (MCE=0.838) for peat fuel. The mixing ratios were measured by PTR-MS. Comparing the slope of regression line of formaldehyde and acetone from their study with the current study (no Acetaldehyde was measured in their study), it turns out that the formaldehyde and acetone from the current study were 10% and 30% lower, respectively. Since proton affinity of HCHO is close to water, measurement of HCHO requires detailed calibration of PTR-MS, which was not performed for their study. Instead, they used a rough rate constant correction method suggested by Hansel et al., 1995. They mentioned that PTR-MS is the only way to measure aldehydes continuously due to high noise-to-signal ratio of the FTIR.

There are only a few publications on airborne measurement of emissions from fire of chaparral fuels (Hardy et al., 1996 and Radke et al., 1991). However, to our knowledge except the work of Burling et al., 2011 there are no previous field measurement reporting emission factors of formaldehyde from chaparral fuels. The MCE from the study of Burling et al., 2011 reporting EFs of chaparral burns averaged 0.935±0.017 and varied between 0.903 and 0.950. They could not find any correlation between MCE and EF of HCHO due

to one of the points at MCE=~0.9 being unexpectedly low (~1.2 g/kg fuel burned), and due to lack of enough data points to be able to draw a conclusion. However, the average chaparral HCHO EF of their study was 2-4 higher compared to the current study using the regression line at their MCE (MCE=0.951±0.011). For the two fires of conifer understory burns in Camp Lejeune (CL in this study), Burling et al., 2011 reported EFs of 1.27 and 1.28 g/kg fuel burned at MCE of 0.944 and 0.947. At these two MCEs, our regression line predicts 0.439 and 0.407 g/kg HCHO that is nearly 3 times less that their value. The best linear fit of EFHCHO vs. MCE presented by Yokelson et al., 2003a based a number previous airborne and laboratory measurements had slope that was 2.74 times higher than the EFs of this study. Figure 5.5 shows plots of select aldehydes against both MCE and EC/TC ratio. Formaldehyde is one of the products of the smoldering phase that is shown linearly correlated with CO emission factors (Goode et al., 2000). Since most of the carbon released from a fire is released in form CO and CO_2, therefore MCE can be approximated using the following equation

$$MCE = \frac{\Delta CO_2}{\Delta CO + \Delta CO_2}$$

$$= \frac{MW_{CO_2}[C]_{CO_2}}{MW_{CO_2}[C]_{CO_2} + MW_{CO}[C]_{CO}}$$

$$= \left(1 + \frac{MW_{CO}[C]_{CO}}{MW_{CO_2}[C]_{CO_2}}\right)^{-1}$$

alternatively, inversely the fraction of fuel total carbon converted into CO:

$$EF_{CO} \approx k\frac{[C]_{CO}}{[C]_{total}} = k\left(\left(\frac{MCE}{1-MCE}\right)\frac{MW_{CO}}{MW_{CO_2}} + 1\right)^{-1}$$
$$= k\left(\left(\frac{MCE}{1-MCE}\right)\frac{7}{11} + 1\right)^{-1} = k\left(\frac{1-MCE}{1-\frac{4}{11}MCE}\right) \quad \text{Eq. 5.1}$$

where k is the proportionality constant, and $[C]_{CO}$, $[C]_{total}$ are the excess measured molar carbon concentration of CO and total carbon, respectively. This function is illustrated in Figure 5.4 for the entire range of MCE i.e. [0,1]. Although the function is not linear, it can be reasonably substituted with a linear function. It has been shown that formaldehyde and acetaldehyde are all products of smoldering phase and are correlated with CO. Since CO is linearly correlated with MCE, therefore, all other products of smoldering phase that correlate with CO will linearly correlate with MCE as well. MCE fails to represent the EF of flaming phase products, because the above-mentioned products are not correlated with CO during mixed and specially flaming phase (MCE>0.94).

Plots of formaldehydes, acetaldehyde, and acetone against MCE and EC/TC ratio are shown in Figure 5.5. Best linear regression for all these compounds along with the pseudo Pearson coefficient (r^2) are calculated and shown in the corresponding figures. EFs of aldehydes linearly decreased with increasing MCE in the range of 0.84 and 0.98. However, MCE appeared to fail for EFs of MCEs>0.94: a sudden drop in the EF of formaldehyde, acetaldehyde, and acetone and contraction of data points in the small range of MCE=[0.94-0.98]. The same plots are again shown in Figure 5.5. against EC/TC ratio. Compared to MCE plots, data shown in EC/TC plots are equally spread across the range of EC/TC=[0,0.7] on a logarithmic y-axis. Data show linearity in their entire range. The best

regression line for formaldehyde is calculated as log(EFformaldhyde)=-1.52+2.95 with a psudo-R^2 of 0.48 close to the R^2=0.52 of the MCE plot. The log transformation led to a better linear representation of acetaldehyde and acetone EFs vs. EC/TC ratio of Psudo-R^2=0.49 vs. R^2=0.22 and Psudo-R^2=0.56 vs. R^2=0.22, respectively, compared to the corresponding MCE plots.

5.4.3. Other Volatile Organic Carbons (VOCs)

A total of 34 thermal desorption tubes (TDS) tubes were analyzed for benzene, ethyl benzene, toluene, 1,3-butadiene, m,p-xylene, o-xylene, and. The average emission factors for each fuel type of SW and SE along with the calculated standard deviation (ave±stdev) are shown in Table 5.3. The coefficient of variation (CV) varied largely between 73-108% and 85-116% for SW and SE groups with Ethylbenzene and m-p-xylene being the lowest and o-xylene and toluene being the highest, respectively. The CV for MCE and EC/TC corresponding to the burns of analyzed samples were 1 and 4% for MCE and 28% and 77% for EC/TC ratio. It seems the large variability in these EFs based on region is more consistent with EC/TC. CV calculated within the fuel types decreased significantly compared to regional CVs. CV of benzene, toluene, ethylbenzene, xylenes, and 1,3-butadiene reduced to 6-65% except for oaw/FHUA that consistently had CV of 100-140%. No distinct pattern was identified in CVs with respect to fuel type categorization or fuel type location.

The study average EFs of VOCs in order of decreasing abundance were 169.4±179.87, 94.8±148.7, 30.4±45.2, 14.1±15.3, 12.2±18.38, 10.4±20.6 mg/kg fuel burned for benzene, toluene, m,p-xylene, 1,3-butadiene, ethylbenzene, and o-xylene at the corresponding average

MCE of 0.942±0.026 and EC/TC ratio of 0.693±0.196. Benzene EF in this study is close to 230±110 mg/kg of savanna and grassland number reported by Andreae and Merlet, 2001. However, taking into account their MCE, their benzene EF of 230±110 mg/kg at MCE=0.961 is nearly twice as the EF reported in this study. For tropical forests and Extratropical forest at their reported MCE, EFs of benzene of the current are ~4 times higher. This could be due to depletion of benzene in the atmosphere. Ethylbenzene at the report MCE=0.938 and 0.936 for Extratropical forest estimated to be 11 mg/kg which is close to the lower range of 13-35 mg/kg.

Sinha et al., 2003 during their 10 field campaign in Africa measured the airborne EFs of benzene and toluene. We calculated the MCE based on their reported CO and CO_2 values. Their MCE ranged between 0.931 and 0.987, and averaged 0.961±0.018. EF of benzene and toluene varied between 47 and 280 with an ave of 177.5± 86 mg/kg and between 0.56 and 330 mg/kg with an average of 94±105 mg/kg. These reported EFs are close to our average study reported EFs. However, their reported EFs were not acceptably anti-correlated with MCE. Therefore, we could not compare the slope with the current study.

Christian et al., 2003b performed laboratory measurements of emissions from a number of African and Indonesian fuels. Their EF of benzene and toluene averaged 1060±1266 mg/kg and 796±570 mg/kg (approximately 5-6 times higher than the current study). Calculating the best linear fit for their published data, we report that their benzene and toluene EF responses with respect to MCE were 4 times higher than this study. The 4-times difference could be attributed the difference in fuel types and type of combustion/sampling. For example, the peat sample smoldered for 2.5 hr while sampling. This specific sample

produced a significantly large amount of benzene (3190 mg/kg). Excluding this data point makes the slope only 50% more. The other reason might be the amount of mass burned, 0.6 kg, in comparison to ~2 kg fuel of this study.

As a part of TROFFEE study, laboratory EFs of benzene, toluene, ethylbenzene, and sum of xylenes measured by PTR-MS were reported for 16 tropical forest fuel species by Yokelson et al., 2008. We calculated the best fit using their published data. Compared to their EFs, our EFs were ~1.2 times lower except for ethylbenzene which was 2.4 times lower (R^2=12%). However, for their Strawberry guava a plant native to South America, the EFs of aforementioned species were unexpectedly lower. Excluding that data points, our EFs are ~3.7 lower (R^2=49%).

Yokelson et al., 2007 investigated the airborne EFs of the aforementioned VOCs as another part of their TROFFEE study for experiments for which the MCE ranged over a range of 0.882-0.947 and averaged 0.910±0.021. Plotting their EFs for the benzene, toluene, xylenes, ethylbenzene vs. MCE do not show any upward or downward trend over the entire range (Figure 5.6). However, compared to their average reported values, the EFs of benzene, toluene, and xylenes of the current study at the same MCE are 30%, 5%, and 12% higher. Ethylbenzene turned out to be 60% lower. Excluding ethylbenzene, the rest of the EFs are in good agreement.

In the SW group, the lowest and highest EFs belonged to oaw/FHUA and cea/FHL, and were 4.1, 728.2 mg/kg respectively. For SE the lowest and highest benzene EFs were 20.8, 702 mg/kg for 1yr/CL and duf/AK, respectively. There were significant differences (p-value<5%) among EFs of SW and SE for toluene (SW: 54.5±52.6 g/kg, SE: 225.6±262.5

g/kg), m,p-xylene (SW:14.1±11.0 g/kg, SE:83.4±70.7 g/kg), ethylbenzene (SW: 6.1±4.4 g/kg, SE:31.9±30.6 g/kg), o-xylene (SW:3.73±4.0 g/kg, SE:32.07±33.7 g/kg). No significant differences were observed for benzene (SW: 150.8±160.1 g/kg, SE: 229.4±235.8 g/kg) and 1,3-butadiene (SW:11.3±9.1 g/kg, SE:23.3±26.1 g/kg). However, these differences can be attributed to efficiency of combustion as explained for PAHs and aldehydes.

Among the fuels collected from SW, FHL had the highest emission rate of benzene, 429.4 g/kg. FHL constantly emitted the highest rate of emissions for all the species due to its lowest MCE and EC/TC ratio of 0.944±0.10 and 0.402±0.142 in this group. The most vigorous burns of SW fuel were from VAFB category with MCE and EC/TC ratio of 0.946±0.006 and 0.520±0.135, respectively. EFs of VOC were significantly affected by intensity of the fires. The 0.2% increase in MCE and 23% in EC/TC ratio resulted in 134, 95, 89, 38, 24, and 17% decrease in the average EFs of benzene, 1,3-butadiene, o-xylene, ethylbenzene, m,p-xylene, toluene in this group. From the other hand for the fuels from SE, CL had the lowest EFs due to its high ave. MCE compared to other fuel locations in this group, e.g. EFbenzene=101.2 g/kg with MCE=0.944 or EC/TC=0.193. The effect of fire intensities can be clearly seen here as well. For example, going from AK with benzene EF of 703.3 g/kg to CL with 8 time increase in EC/TC ratio and 14% increase in MCE, average EFs of benzene, 1,3-butadiene, o-xylene, ethylbenzene, m,p-xylene, toluene reduced 89, 86, 87, 83, 79%, respectively.

5.5. Conclusion

We investigated detailed gas-phase emission measurements from combustion of different vegetation types typically managed using prescribed burning on department of defense lands in the southeastern and southwestern US. We report emission factors for many gas-phase species including carbonyls, polyaromatic hydrocarbons and select volatile organic compounds. The coefficient of variation of PAHs, carbonyls, and volatile organic carbons varied between 10-270%, 10-50%, and 6-140% among all fuel types. Higher fuel moisture of SE resulted in considerably higher emission factors for SE fuels compared to SW. Therefore, except for PAHs, the statistical analysis of emission factors revealed fuel type/regional dependency. Generally, heavier PAHs resulted in higher variably due to their increased vapor pressure and increased gas-to-particle phase partitioning. For all fuel types, naphthalene was the highest accounted for the most of gas phase PAHs, 56±13%, except for duff that emitted 17% more acetylene compared to naphthalene. On average, formaldehyde accounted for 27±5% of total carbonyls emissions ranging between 100 and 2026 mg/kg from oaw/FHUA and lit/FB, respectively. EF of formaldehyde correlated linearly with MCE (R^2=0.53). The study average EFs of VOCs in order of decreasing abundance were 169.4±179.87, 94.8±148.7, 30.4±45.2, 14.1±15.3, 12.2±18.38, 10.4±20.6 mg/kg fuel burned for benzene, toluene, m,p-xylene, 1,3-butadiene, ethylbenzene, and o-xylene at the corresponding average MCE of 0.942±0.026 and EC/TC ratio of 0.693±0.196, respectively.

We proved that EF CO can be approximated using a linear function of MCE, and showed that the EF of most of the compounds showed a sudden change in behavior at MCE=0.94 consistent with the past reported behavior of EF OC by McMeeking et al., 2009 and

Hosseini et al., 2012b. The same type of behavior change at MCE=0.94 can be traced in the emission factors of PAHs, carbonyls, and other VOCs from the current study. We believe that the problem is due to definition of MCE; when the fire regime changes to flaming, the combustion pathways no longer support linearity of emissions with EF of CO. In the smoldering phase, many products of incomplete combustion such as formaldehyde correlate well with CO, thus correlate well with MCE too. As long as smoldering dominates the combustion process, all EFs lie on a line. However, when the flaming dominates (MCE>0.94), the emission factor of same compounds in terms of MCE fails to conserve linearity with respect to MCE. It seems that MCE significantly compresses a large portion of system changes, i.e. EC/TC ratio of 0.2-0.6, into a small fraction of MCE range, i.e. 0.94<MCE<1.0, thus giving the false impression of linearity for most compounds. For example, only 3% decrease in MCE resulted in 200-800% growth in aldehyde formation, this formation rate is better described by means of 64% decrease in EC/TC ratio. As shown, EF of most compounds showed exponential decay with EC/TC ratio, e.g. formaldehyde, acetaldehyde, acetone, benzene, ethylbenzene, toluene, and xylenes. The Pearson coefficient for EF of these compounds vs. EC/TC showed significant increase when plotted vs. EC/TC ratio. PAHs in the gas phase showed a different behavior meaning exponential decay up to EC/TC ratio of 0.3 and then scattered increase.

5.6. Acknowledgements

Funding for this study was provided by the US Department of Defense Strategic Environmental Research and Development Program (SERDP) as projects SI-1647, SI-1648, and SI-1649. We appreciate the efforts of UCR staff, Kathy Cocker, and UCR students,

Varalakshmi Jayaram and Poornima Dixit for analysis of samples and the assistance of personnel at USMC Camp Lejuene, US Army Ft. Huachuca, Ft. Hunter-Liggett, Ft. Benning, and Vandenberg Air Force Base in selecting fuel types for study and fuel samples for burning. We also would like to thank Joey Chong, Bonni Corcoran, Amy Olson, Violet Holly, Signe Leirfallom, and Emily Lincoln for harvesting the fuels and assembling the fuel beds for this study. Authors are grateful to Robert Yokelson and Ian Burling for FTIR data and Wei Min Hao, Shawn Urbanski, Cyle Wold.

5.7. Reference

Akagi, S. K., Yokelson, R. J., Wiedinmyer, C., Alvarado, M. J., Reid, J. S., Karl, T., Crounse, J. D., and Wennberg, P. O.: Emission factors for open and domestic biomass burning for use in atmospheric models, Atmos. Chem. Phys., 11, 4039-4072, 10.5194/acp-11-4039-2011, 2011.

Akagi, S. K., Craven, J. S., Taylor, J. W., McMeeking, G. R., Yokelson, R. J., Burling, I. R., Urbanski, S. P., Wold, C. E., Seinfeld, J. H., Coe, H., Alvarado, M. J., and Weise, D. R.: Evolution of trace gases and particles emitted by a chaparral fire in California, Atmos. Chem. Phys., 1397-1421, doi:10.5194/acp-12-1397-2012, 2012a.

ACP - Abstract - Evolution of trace gases and particles emitted by a chaparral fire in California: http://www.atmos-chem-phys.net/12/1397/2012/acp-12-1397-2012.html, 2012b.

Alebic-Juretic, A., Cvitas, T., and Klasinc, L.: Heterogeneous polycyclic aromatic hydrocarbon degradation with ozone on silica gel carrier, Environmental Science & Technology, 24, 62-66, 10.1021/es00071a005, 1990.

Andreae, M. O., and Merlet, P.: Emission of trace gases and aerosols from biomass burning, Global biogeochemical cycles, 15, 955-966, 2001.

Atkinson, R., Baulch, D. L., Cox, R. A., Hampson, J. R. F., Kerr, J. A., and Troe, J.: Evaluated Kinetic and Photochemical Data for Atmospheric Chemistry: Supplement IV. IUPAC Subcommittee on Gas Kinetic Data Evaluation for Atmospheric Chemistry, Journal of Physical and Chemical Reference Data, 21, 1125-1568, 1992.

Biswell, H.: Prescribed burning in California wildlands vegetation management, Univ of California Pr, 1999.

Burling, I., Yokelson, R., Griffith, D., Johnson, T., Veres, P., Roberts, J., Warneke, C., Urbanski, S., Reardon, J., Weise, D., and others: Laboratory measurements of trace gas emissions from biomass burning of fuel types from the southeastern and southwestern United States, Atmos. Chem. Phys, 10, 11115-11130, 2010.

Burling, I., Yokelson, R. J., Akagi, S., Urbanski, S., Wold, C. E., Griffith, D. W. T., Johnson, T. J., Reardon, J., and Weise, D.: Airborne and ground-based measurements of the trace gases and particles emitted by prescribed fires in the United States, Atmos. Chem. Phys, 11, 12197-12216, 2011.

Calvert, J. G.: The mechanisms of atmospheric oxidation of aromatic hydrocarbons, Oxford University Press, USA, 2002.

Christian, T., Kleiss, B., Yokelson, R., Holzinger, R., Crutzen, P., Hao, W., Saharjo, B., and Ward, D.: Comprehensive laboratory measurements of biomass-burning emissions: 1. Emissions from Indonesian, African, and other fuels, J. Geophys. Res, 108, 1-4719, 2003a.

Christian, T., Kleiss, B., Yokelson, R., Holzinger, R., Crutzen, P., Hao, W., Saharjo, B., and Ward, D.: Comprehensive laboratory measurements of biomass-burning emissions: 1. Emissions from Indonesian, African, and other fuels, J. Geophys. Res, 108, 4719, 2003b.

Christian, T., Kleiss, B., Yokelson, R., Holzinger, R., Crutzen, P., Hao, W., Shirai, T., and Blake, D.: Comprehensive laboratory measurements of biomass-burning emissions: 2. First intercomparison of open-path FTIR, PTR-MS, and GC-MS/FID/ECD, J. Geophys. Res., 109, D02311, 2004.

Christian, T. J., Yokelson, R. J., Carvalho Jr, J. A., Griffith, D. W. T., Alvarado, E. C., Santos, J. C., Neto, T. G. S., Veras, C. A. G., and Hao, W. M.: The tropical forest and fire emissions experiment: Trace gases emitted by smoldering logs and dung from deforestation and pasture fires in Brazil, Journal of Geophysical Research, 112, D18308, 2007.

Crutzen, P. J., and Andreae, M. O.: Biomass burning in the tropics: Impact on atmospheric chemistry and biogeochemical cycles, Science, 250, 1669-1678, 1990.

Dhammapala, R., Claiborn, C., Jimenez, J., Corkill, J., Gullett, B., Simpson, C., and Paulsen, M.: Emission factors of PAHs, methoxyphenols, levoglucosan, elemental carbon and organic

carbon from simulated wheat and Kentucky bluegrass stubble burns, Atmospheric Environment, 41, 2660-2669, DOI 10.1016/j.atmosenv.2006.11.023, 2007.

Goode, J. G., Yokelson, R. J., Ward, D. E., Susott, R. A., Babbitt, R. E., Davies, M. A., and Hao, W. M.: Measurements of excess O_3, CO_2, CO, CH_4, C_2H_4, C_2H_2, HCN, NO, NH_3, HCOOH, CH_3COOH, HCHO, and CH_3OH in 1997 Alaskan biomass burning plumes by airborne Fourier transform infrared spectroscopy (AFTIR), J. Geophys. Res., 105, 22147-22166, 10.1029/2000jd900287, 2000.

Hansel, A., Jordan, A., Holzinger, R., Prazeller, P., Vogel, W., and Lindinger, W.: Proton transfer reaction mass spectrometry: on-line trace gas analysis at the ppb level, International Journal of Mass Spectrometry and Ion Processes, 149, 609-619, 1995.

Hardy, C. C., Station, P. N. R., and Program, V. M.: Smoke emissions from prescribed burning of southern California chaparral, US Department of Agriculture, Forest Service, Pacific Northwest Research Station, 1996.

Hays, M. D., Fine, P. M., Geron, C. D., Kleeman, M. J., and Gullett, B. K.: Open burning of agricultural biomass: Physical and chemical properties of particle-phase emissions, Atmospheric Environment, 39, 6747-6764, DOI 10.1016/j.atmosenv.2005.07.072, 2005.

Hedberg, E., Kristensson, A., Ohlsson, M., Johansson, C., Johansson, P.-Å., Swietlicki, E., Vesely, V., Wideqvist, U., and Westerholm, R.: Chemical and physical characterization of emissions from birch wood combustion in a wood stove, Atmospheric Environment, 36, 4823-4837, 10.1016/s1352-2310(02)00417-x, 2002.

Hosseini, S., Li, Q., Cocker, D., Weise, D., Miller, A., Shrivastava, M., Miller, W., Mahalingam, S., Princevac, M., and Jung, H.: Study of Particle Size Distribution and Morphology Using Fast Response Particle Instruments and TEM, Western States Combustion Institue (WSSCI), University of Colorado at Boulder, 2010.

Hosseini, S., Li, Q., Yokelson, R., S., U., I., B., D., W., Miller, J. W., Jung, H., and Cocker, D.: Chemical characterization of gas phase emissions from combustion of various US vegetation types, Atmospheric Chemistry and Physics, 2012a.

Hosseini, S., Urbanski, S., Dixit, P., Li, Q., Burling, I., Yokelson, R., Johnson, T., Sharivastava, M., Jung, H., Weise, D., Miller, W., and Cocker, D.: Laboratory characterization of PM emissions from combustion of wildland biomass fuels, Atmospheric Chemistry and Physics, 2012b.

Jenkin, M. E., and Clemitshaw, K. C.: Ozone and other secondary photochemical pollutants: chemical processes governing their formation in the planetary boundary layer, Atmospheric Environment, 34, 2499-2527, 2000.

Jenkins, B. M., Daniel Jones, A., Turn, S. Q., and Williams, R. B.: Particle concentrations, gas-particle partitioning, and species intercorrelations for Polycyclic Aromatic Hydrocarbons (PAH) emitted during biomass burning, Atmospheric Environment, 30, 3825-3835, 10.1016/1352-2310(96)00084-2, 1996a.

Jenkins, B. M., Jones, A. D., Turn, S. Q., and Williams, R. B.: Emission Factors for Polycyclic Aromatic Hydrocarbons from Biomass Burning, Environmental Science & Technology, 30, 2462-2469, 10.1021/es950699m, 1996b.

McDonald, J. D., Zielinska, B., Fujita, E. M., Sagebiel, J. C., Chow, J. C., and Watson, J. G.: Fine Particle and Gaseous Emission Rates from Residential Wood Combustion, Environmental Science & Technology, 34, 2080-2091, 10.1021/es9909632, 2000.

McMeeking, G. R., Kreidenweis, S. M., Baker, S., Carrico, C. M., Chow, J. C., Collett, J. L., Jr., Hao, W. M., Holden, A. S., Kirchstetter, T. W., Malm, W. C., Moosmüller, H., Sullivan, A. P., and Wold, C. E.: Emissions of trace gases and aerosols during the open combustion of biomass in the laboratory, J. Geophys. Res., 114, D19210, 10.1029/2009jd011836, 2009.

Oros, D. R., and Simoneit, B. R. T.: Identification and emission factors of molecular tracers in organic aerosols from biomass burning Part 2. Deciduous trees, Applied Geochemistry, 16, 1545-1565, 10.1016/s0883-2927(01)00022-1, 2001.

Radke, L., Hegg, D., Hobbs, P., Nance, J. D., Lyons, J., Laursen, K., Weiss, R., Riggan, P., and Ward, D.: Particulate and trace gas emissions from large biomass fires in North America, Global biomass burning- Atmospheric, climatic, and biospheric implications(A 92-37626 15-42). Cambridge, MA, MIT Press, 1991, 209-224, 1991.

Roberts, J. M., Veres, P., Warneke, C., Neuman, J., Washenfelder, R., Brown, S., Baasandorj, M., Burkholder, J., Burling, I., Johnson, T. J., and others: Measurement of HONO, HNCO, and other inorganic acids by negative-ion proton-transfer chemical-ionization mass spectrometry (NI-PT-CIMS): application to biomass burning emissions, Atmos, Meas. Tech, 3, 981-990, 2010.

Schauer, J. J., Kleeman, M. J., Cass, G. R., and Simoneit, B. R. T.: Measurement of Emissions from Air Pollution Sources. 3. C1-C29 Organic Compounds from Fireplace Combustion of Wood, Environmental Science & Technology, 35, 1716-1728, 2001.

Seinfeld, J. H., and Pandis, S. N.: Atmospheric Chemistry and Physics - From Air Pollution to Climate Change (2nd Edition), John Wiley & Sons, 2006.

Sinha, P., Hobbs, P., Yokelson, R., Bertschi, I., Blake, D., Simpson, I., Gao, S., Kirchstetter, T., and Novakov, T.: Emissions of trace gases and particles from savanna fires in southern Africa, Journal of Geophysical Research, 108, 8487, 2003.

Veres, P., Roberts, J. M., Burling, I. R., Warneke, C., de Gouw, J., and Yokelson, R. J.: Measurements of gas-phase inorganic and organic acids from biomass fires by negative-ion proton-transfer chemical-ionization mass spectrometry, J. Geophys. Res, 115, D23302, 2010.

Veres, P. R., Roberts, J. M., de Gouw, J. A., Warneke, C., Burling, I. R., and Yokelson, R. J.: Measurements of gas-phase inorganic and organic acids in biomass fires by negative-ion proton-transfer chemical-ionization mass spectrometry (NI-PT-CIMS), J. Geophys. Res., D165+, 2009.

Wade, D. D., Lunsford, J. D., Dixon, M. J., and Mobley, H. E.: A guide for prescribed fire in southern forests, Technical publication R8-TP-US Department of Agriculture, Forest Service, Southern Region, 1989.

Ward, D. E. & Radke, L.: Chapter 4: Emission measurements from vegetation fires: A comparative evaluation of methods and results In Crutzen, P.J. & Goldammer, J.G. (eds)

Fire in the Environment: The Ecological, Atmospheric, and Climatic Importance of Vegetation Fires. John Wiley & Sons, 1993.

Warneke, C., Bahreini, R., Brioude, J., Brock, C. A., de Gouw, J. A., Fahey, D. W., Froyd, K. D., Holloway, J. S., Middlebrook, A., Miller, L., Montzka, S., Murphy, D. M., Peischl, J., Ryerson, T. B., Schwarz, J. P., Spackman, J. R., and Veres, P.: Biomass burning in Siberia and Kazakhstan as an important source for haze over the Alaskan Arctic in April 2008, Geophys. Res. Lett., 36, L02813, 10.1029/2008gl036194, 2009.

Warneke, C., Froyd, K. D., Brioude, J., Bahreini, R., Brock, C. A., Cozic, J., de Gouw, J. A., Fahey, D. W., Ferrare, R., Holloway, J. S., Middlebrook, A. M., Miller, L., Montzka, S., Schwarz, J. P., Sodemann, H., Spackman, J. R., and Stohl, A.: An important contribution to springtime Arctic aerosol from biomass burning in Russia, Geophys. Res. Lett., 37, L01801, 10.1029/2009gl041816, 2010.

Warneke, C., Roberts, J. M., Veres, P., Gilman, J., Kuster, W. C., Burling, I., Yokelson, R., and de Gouw, J. A.: VOC identification and inter-comparison from laboratory biomass burning using PTR-MS and PIT-MS, International Journal of Mass Spectrometry, 303, 6-14, 10.1016/j.ijms.2010.12.002, 2011.

Yokelson, R., Goode, J., Ward, D., Susott, R., Babbitt, R., Wade, D., Bertschi, I., Griffith, D., and Hao, W.: Emissions of formaldehyde, acetic acid, methanol, and other trace gases from biomass fires in North Carolina measured by airborne Fourier transform infrared spectroscopy, Journal of geophysical research, 104, 30109-30130, 1999.

Yokelson, R., Karl, T., Artaxo, P., Blake, D., Christian, T., Griffith, D., Guenther, A., and Hao, W.: The Tropical Forest and Fire Emissions Experiment: overview and airborne fire emission factor measurements, Atmospheric Chemistry and Physics Discussions, 7, 6903-6958, 2007.

Yokelson, R., Christian, T., Karl, T., and Guenther, A.: The tropical forest and fire emissions experiment: laboratory fire measurements and synthesis of campaign data, Atmospheric Chemistry and Physics Discussions, 8, 4221-4266, 2008.

Yokelson, R., Burling, I. R., Gilman, J., Warneke, C., Stockwell, C., Hosseini, S., Jung, H., Cocker, D., Miller, J. W., Gouw, J., Akagi, S. K., Urbanski, S., Veres, P., Roberts, J. M., Kuster, W., Reardon, J., Griffith, D. W. T., and Johnson, T. J.: Merging field and laboratory measurements to estimate the emission factors for known and unknown trace gases emitted by some prescribed fires in the US. , Atmospheric Chemistry and Physics, 2012.

Yokelson, R. J., Griffith, D. W. T., and Ward, D. E.: Open-path Fourier transform infrared studies of large-scale laboratory biomass fires, J. Geophys. Res, 101, 067-21080, 1996.

Yokelson, R. J., Susott, R., Ward, D. E., Reardon, J., and Griffith, D. W. T.: Emissions from smoldering combustion of biomass measured by open-path Fourier transform infrared spectroscopy, Journal of Geophysical Research-All Series, 102, 18-18, 1997.

Yokelson, R. J., Bertschi, I. T., Christian, T. J., Hobbs, P. V., Ward, D. E., and Hao, W. M.: Trace gas measurements in nascent, aged, and cloud-processed smoke from African savanna fires by airborne Fourier transform infrared spectroscopy (AFTIR), J. Geophys. Res., 108, 8478, 10.1029/2002jd002322, 2003a.

Yokelson, R. J., Bertschi, I. T., Christian, T. J., Hobbs, P. V., Ward, D. E., and Hao, W. M.: Trace gas measurements in nascent, aged, and cloud-processed smoke from African savanna fires by airborne Fourier transform infrared spectroscopy (AFTIR), Journal of Geophysical Research, 108, 8478, 2003b.

Zou, L. Y., Zhang, W., and Atkiston, S.: The characterisation of polycyclic aromatic hydrocarbons emissions from burning of different firewood species in Australia, Environmental Pollution, 124, 283-289, 10.1016/s0269-7491(02)00460-8, 2003.

Table 5.1 summary of vegetation burned, along with Modified Combustion Efficiency (MCE) vs. Elemental Carbon (EC) to Total Carbon (TC) ratio

Region	Fuel code	Fuel name	EC/TC ratio	MCE
Southwest Fuels				
FHL CA	cea	Ceanothus	0.346±0.227	0.946±0.011
	chg	Chaparral grass	0.541±0.011	0.952±0.001
	chs	Chamise ScrubOak	0.380±0.082	0.939±0.010
	ave.		0.367±0.138	0.942±0.011
VAFB CA	cas	CA sage	0.572±0.068	0.944±0.005
	cos	Coastal sage	0.635±0.088	0.939±0.004
	man	Manzanita	0.418±0.147	0.948±0.007
	mch	Maritime Chaparral	0.443±0.176	0.953±0.002
	ave.		0.520±0.135	0.946±0.006
FHUA AZ	mes	Mesquite	0.440±0.011	0.954±0.001
	oas	Oak Savanna	0.517±0.076	0.971±0.004
	oaw	Oak Woodland	0.421±0.153	0.965±0.004
	ave.		0.466±0.103	0.963±0.008
Southeast Fuels				
CL NC	1yr	1yrRough NC	0.080±0.036	0.934±0.015
	2yr	2yrRough NC	0.063±0.037	0.927±0.006
	poc	Pocosin NC	0.169±0.075	0.953±0.011
	cuh	Treated NC	0.351±0.028	0.959±0.003
	uh	Untreated NC	0.318±0.090	0.954±0.012
	ave.		0.193±0.132	0.944±0.016
FB GA	lit	FB GA litter	0.096±0.058	0.894±0.017
AK	duf	AK Duff	0.002	0.827

[1] Fuel collection regions: FHL: Fort Hunter Ligget, VAFB: Vandenberg Air Force Base, FHUA: Fort Huachuca, CL: Camp Lejeune, FB: Fort Benning

Table 5.2. Emission factors of Poly Aromatic Hydrocarbons (PAHs). The reported values are in the format of μ±σ (average±Stdev). The values shown in the parenthesis represent the number of valid data points. Blanks indicate below detection limit. The FHA, VAFB, FHUA categories belong to the southwest region, and CL, FB, and AK belong the southeast group.

Region	Fuel code	Nap	Acy	Ace	Fle	Ph	Ant	Fla	Py	B[a]A	Chr	B[b]F	B[k]F	B[a]P	Ind	D[a,h]A	B[ghi]P
VAFB CA	cas	38.26± 28.96	16.43± 8.17	1.02± 0.87	0.91± 0.76	9.84± 3.64	10.52± 4.01	3.66± 3.50	4.45± 3.28	0.01± 0.00	0.01± 0.01	0.01± 0.02	0.01± 0.01	0.07± 0.15	0.00± 0.00	0.01± 0.00	0.01± 0.01
	cos	31.67± 3.74	20.21± 0.27	0.63± 0.67	3.19± 3.43	12.65± 2.98	13.36± 3.43	7.42± 2.70	5.99± 6.17	0.01± 0.01	0.01± 0.01	0.01± 0.01	0.02± 0.02	0.01± 0.01	0.00± 0.00	0.00± 0.00	0.00± 0.00
	man	38.09± 31.93	14.17± 12.20	0.25± 0.11	0.21± 0.13	5.84± 1.75	6.32± 1.43	1.18± 0.21	1.06± 0.46	0.04± 0.06	0.04± 0.05	0.09± 0.12	0.02± 0.01	0.03± 0.03	0.03± 0.04	0.05± 0.07	0.00± 0.00
	mch	16.13± 0.71	6.50± 4.85	0.16± 0.06	0.30± 0.40	5.93± 5.04	5.50± 4.26	1.63± 1.27	1.75± 1.29	0.01± 0.00	0.03± 0.03	0.01± 0.01	0.01± 0.01	0.00± 0.00	0.00± 0.00	0.01± 0.00	0.00± 0.00
	Ave.	33.80± 24.25	14.96± 8.50	0.65± 0.71	1.01± 1.51	8.75± 3.93	9.22± 4.20	3.35± 3.22	3.49± 3.37	0.02± 0.03	0.02± 0.03	0.03± 0.06	0.01± 0.01	0.04± 0.10	0.01± 0.02	0.02± 0.04	0.01± 0.01
FHL CA	cea	38.22± 7.05	5.27± 1.43	0.25± 0.04	0.57± 0.17	3.44± 4.85	4.81± 3.09	0.01± 0.01	0.89± 0.27	0.03± 0.03	0.03± 0.03	0.07± 0.06	0.03± 0.02	0.04± 0.05	0.01± 0.00	0.01± 0.00	0.01± 0.00
	chs	24.34± 3.31	11.47± 1.81	0.44± 0.47	1.04± 1.15	8.48± 2.10	8.83± 2.24	1.25± 1.18	1.29± 1.22	0.00± 0.00	0.01± 0.01	0.11± 0.14	0.11± 0.13	0.01± 0.00	0.03± 0.04	0.02± 0.03	0.01± 0.00
	chg	20.47	0.96	0.16	0.15	0.99	1.02	0.14	0.16			0.03			0.01	0.04	0.01
	Ave.	29.12± 9.31	6.89± 4.68	0.31± 0.27	0.67± 0.69	4.97± 4.28	5.66± 3.80	0.53± 0.89	0.91± 0.78	0.01± 0.02	0.02± 0.02	0.08± 0.08	0.06± 0.08	0.02± 0.03	0.02± 0.02	0.02± 0.02	0.01± 0.00
FHUA AZ	mes	23.90± 1.81	3.84± 0.44	0.19± 0.13	0.13± 0.01	1.59± 2.72	3.98± 0.83	0.46± 0.78	1.22± 0.39	0.46± 0.79	0.30± 0.51	0.03± 0.01	0.07± 0.09	0.01± 0.01	0.00± 0.00	0.01± 0.00	0.00± 0.00
	oas	19.33± 9.32	2.24± 1.50	0.20± 0.09	0.29± 0.29	2.75± 1.05	2.91± 1.06	0.53± 0.60	0.84± 0.47	0.03± 0.05	0.02± 0.04	0.06± 0.08	0.01± 0.00	0.02± 0.03	0.03± 0.04	0.04± 0.07	0.00± 0.00
	oaw	24.11±	8.32±	0.66±	0.16±	2.20±	3.84±	0.53±	0.79±	0.01±	0.01±	0.02±	0.00±	0.01±	0.00±	0.00±	0.00±

Region	Fuel code	Nap	Acy	Ace	Fle	Ph	Ant	Fla	Py	B[a]A	Chr	B[b]F	B[k]F	B[a]P	Ind	D[a,h]A	B[ghi]P
		3.86	2.22	0.10	0.22	3.07	1.05	0.74	0.61	0.01	0.01	0.01	0.01	0.00	0.00	0.00	0.00
	Ave	21.66± 6.85	3.93± 2.73	0.29± 0.21	0.22± 0.22	2.29± 1.86	3.42± 1.03	0.51± 0.60	0.94± 0.46	0.16± 0.43	0.10± 0.28	0.04± 0.05	0.03± 0.05	0.01± 0.02	0.02± 0.03	0.02± 0.05	0.00± 0.00
CL NC	1yr	54.2	11.96	1.16	0.43	7.28	7.66	1.77	2.22	0.03	0.03	0.05	0.02	0.11		0.01	0.01
	2yr	56.26± 10.71	16.33± 13.59	1.13± 0.91	1.78± 0.80	8.88± 4.03	9.20± 4.14	2.10± 0.80	1.24± 0.53	0.01± 0.02	0.01± 0.01	0.02± 0.00	0.02± 0.01	0.05± 0.05	0.00± 0.00	0.01± 0.00	0.01± 0.00
	poc	11.75	1.56	0.08	0.47	1.8	1.87	0.47	0.36		0.01			0.01			
	cuh	15.05	3.99	0.38	0.13	3.11	3.22	0.65	0.34			0.01		0.01			
	uh	28.91	6.04	0.57	0.2	0.07	5.71	0.01	0.04	0.03	0.02	0.02	0.05	0.03	0.01	0.02	0.01
	Ave	39.81± 21.48	10.36± 10.13	0.80± 0.69	0.94± 0.92	5.56± 4.45	6.58± 3.88	1.31± 1.02	0.95± 0.82	0.01± 0.02	0.01± 0.01	0.02± 0.01	0.02± 0.02	0.04± 0.04	0.00± 0.00	0.01± 0.01	0.01± 0.00
FB GA	lit	62.44± 23.43	48.25± 31.19	1.80± 1.43	3.05± 2.72	8.37± 1.84	8.56± 1.95	0.94± 1.07	2.41± 1.35	0.03± 0.01	0.03± 0.03	0.04± 0.01	0.02± 0.01	0.16± 0.09	0.01± 0.00	0.01± 0.01	0.02± 0.02
AK	duf	88.74	103.4	2.31	7.68	46.46	47.99	22.44	24.97	0.03	0.04	0	0.01	0.04	0.02	0.01	0.01
MT	fir	126.09	4.47	0.49	2.21	23.3	24.46	9.47	0.34	0.01	0.02	0.01	0.02	0.02		0.01	

The full name and the abbreviation of analyzed PAHs are as follows: Naphthalene (Nap), Acenaphthylene (Acy), Acenaphthene (Ace), Fluorene(Fle), Phenanthrene (Ph), Anthracene (Ant), Fluoranthene (Fla), Pyrene (Py), Benzo[a]anthracene(B[a]A), Chrysene(Chr), Benzo[b]fluoranthene (B[b]F), Benzo[k]fluoranthene (B[k]F), Benzo[a]pyrene (B[a]P), Indeno[1,2,3-c,d]pyrene (Ind), Dibenzo[a,h]anthracene (D[a,h]A), Benzo[g,h,i]perylene (B[ghi]P). Empty cells represent below detection limit.

Table 5.3 represents emission factor of a number of volatile organic compounds (VOCs) for all the southwest and southeast fuel types in mg/kg dry fuel. The FHA, VAFB, FHUA categories belong to the southwest region, and CL, FB, and AK belong the southeast group.

Region	Fuel type	1,3- Butadiene	Benzene	Toluene	m,p-xylene	Ethylbenzene	o-xylene
FHL CA	cea	25.93	728.24	99.32	21.01	10.60	7.18
	chs	24.86	130.66	66.65	22.11	9.00	7.98
	ave.	25.40±0.76	429.45±422.55	82.99±23.11	21.56±0.78	9.80±1.14	7.58±0.57
VAFB CA	cas	15.81±9.51	219.90±134.37	71.65±53.38	24.56±17.70	9.52±7.50	5.71±8.30
	cos	8.54±3.04	279.32±117.85	128.47±108.09	20.78±6.44	6.68±1.62	3.29±0.65
	man	9.12±8.36	92.35±21.78	33.28±7.12	7.77±1.40	4.15±1.12	1.98±0.86
	mch	32.19	170.08	80.98	19.54	11.23	7.85
	ave.	13.03±9.62	183.52±116.95	70.79±63.30	17.40±12.72	7.11±5.00	4.01±5.05
FHUA AZ	mes	5.63±1.70	56.28±34.46	29.56±16.07	10.41±6.49	5.01±3.03	3.81±2.43
	oas	6.72±5.90	37.76±13.51	19.59±12.35	6.16±3.94	2.67±1.79	1.83±0.79
	oaw	5.62±6.24	59.08±77.75	31.54±41.24	7.33±9.47	3.88±5.17	1.58±1.42
	ave.	6.07±4.15	49.43±35.08	25.97±18.88	8.10±5.77	3.85±2.88	2.57±1.88
CL NC	1yr	3.42	20.81	20.92	43.59	11.27	4.55
	2yr	13.10	242.07	215.23	121.40	47.81	46.98
	poc	7.19	85.44	42.92	33.54	8.09	4.31
	cuh	6.73±3.32	78.88±11.01	43.01±2.66	15.22±0.04	7.11±0.13	8.69±1.80
	ave.	7.43±3.88	101.22±83.18	73.02±80.08	45.79±43.99	16.28±17.71	14.64±18.23
FB GA	lit	45.64±35.60	313.05±202.49	389.65±306.28	142.96±91.42	47.46±36.87	48.68±40.67
AK	duf	57.75	703.30	662.53	152.20	79.18	86.01

Table 5.4. Emission factor of aldehydes and ketones in mg/kg fuel burned. The values are reported in this format: mean±stdev (number of data points). Blanks indicate below detection limit.

Region	Fuel type	Form-aldehyde	Acet-aldehyde	Acetone	Acrolein	Propion-aldehyde	Croton-aldehyde	MEK	Butyr-aldehyde	Benz-aldehyde	Valer-aldehyde	Hex-aldehyde
CL NC	1yr	1185.4± 644.2	842.0± 500.3	466.0± 140.3					350.5± 143.6		905.2± 625.9	700.5± 343.7
	2yr	818.2± 81.9	805.0± 239.5	661.5± 84.4		185.2± 62.6		251.5± 32.6	232.1± 29.3		892.7± 353.5	1029.0± 299.2
	poc	558.9	379.5	210.0		73.4		87.3	79.3		500.8	480.0
	cuh	194.1± 42.8	157.3± 49.7	125.7± 7.7		32.6		44.7	64.9		92.1± 29.0	109.9± 32.8
	uh	449.7± 118.5	360.2± 111.6	224.3± 53.7	38.5	79.4± 25.7		98.8± 5.5	123.3± 18.2		294.4± 22.8	393.1± 91.2
	ave.	647.4± 407.5	534.0± 346.5	368.3± 228.4	38.5	105.9± 70.7		138.8± 90.8	186.6± 121.6		550.6± 432.0	597.4± 402.7
FB GA	Lit	1542.9± 576.9	1203.9± 277.4	653.3± 155.9		291.6± 68.5		340.1± 71.4	241.4± 49.5		908.0± 360.0	1485.3± 590.1
FHL CA	cea	368.0± 305.6	244.3± 209.5	189.6± 180.2					162.5± 90.0		291.9± 238.9	255.8± 215.4
	chs	409.3± 135.2	268.9± 25.5	214.4± 31.1		86.6	57.5	314.5	124.9± 41.2		345.4± 48.9	230.5± 93.8
	chg	167.4± 13.0	171.8± 13.6	135.4± 7.2		30.8			71.8± 8.8	47.3± 1.3	56.6± 24.5	72.7± 7.2
	ave.	346.5± 226.0	240.1± 138.0	188.8± 118.8		58.7± 39.5	57.5	314.5	129.8± 69.7	47.3± 1.3	260.9± 195.3	213.3± 161.8
FHUA AZ	mes	220.6± 34.9	147.3± 13.1	117.8± 15.8				44.6± 0.7	65.4± 3.4		88.5± 30.9	106.1± 42.8

Region	Fuel type	Form-aldehyde	Acet-aldehyde	Acetone	Acrolein	Propion-aldehyde	Croton-aldehyde	MEK	Butyr-aldehyde	Benz-aldehyde	Valer-aldehyde	Hex-aldehyde
	oas	132.1± 37.1	89.7± 33.6	61.7± 9.2					36.9± 4.7		48.3± 4.5	61.4± 18.2
	oaw	150.2± 71.0	101.0± 42.0	74.9± 31.8					58.0± 30.5		52.1± 36.3	66.6± 40.2
	ave.	185.3± 56.6	124.2± 34.8	95.8± 31.0				44.6± 0.7	56.4± 17.2		71.5± 32.5	87.4± 40.7
MT	fir	971.3	551.9	289.4					294.8		226.2	253.6± 0.0
VAFB CA	cas	228.6± 53.8	141.7± 54.8	106.1± 51.0					72.6± 19.8		76.6± 17.7	76.8± 23.2
	cos	215.7	126.8	115.4					69.6		75.5	85.9
	man	178.9± 33.5	97.0± 21.7	76.8± 12.2		29.4			52.4± 12.2		88.7± 32.4	91.8± 31.8
	mch	174.5± 28.6	169.3± 98.7	141.2± 103.4				63.2	74.0± 18.0	71.6	86.4± 12.1	105.8± 57.6
	ave.	204.0± 47.2	131.0± 53.6	103.2± 50.0		29.4		63.2	66.4± 18.0	71.6	82.2± 21.2	86.6± 29.5

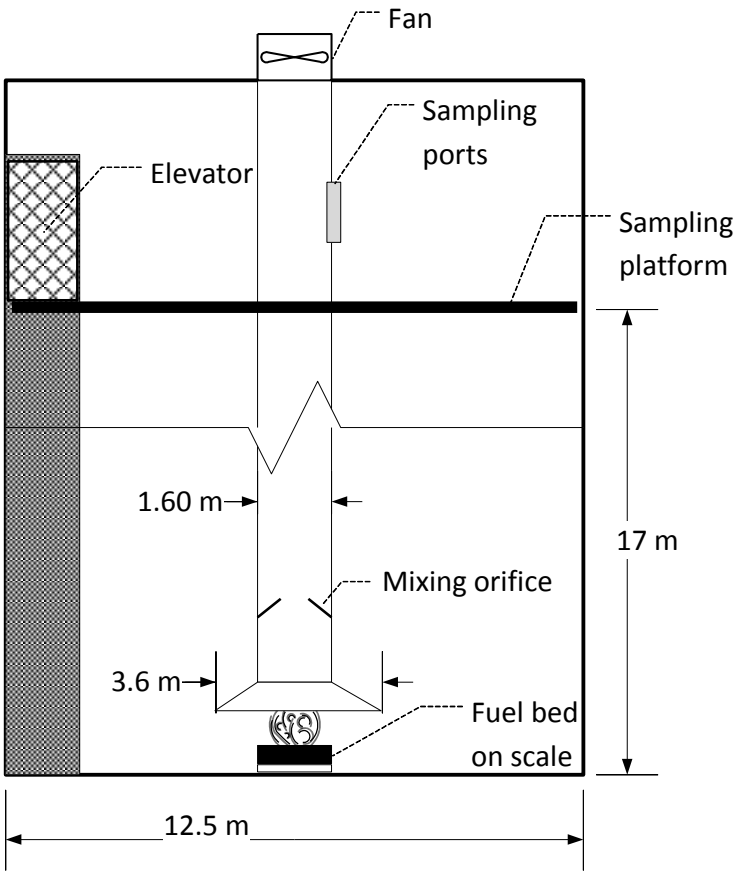

Figure 5.1. Schematic of combustion laboratory at Missoula Forest Service Laboratory

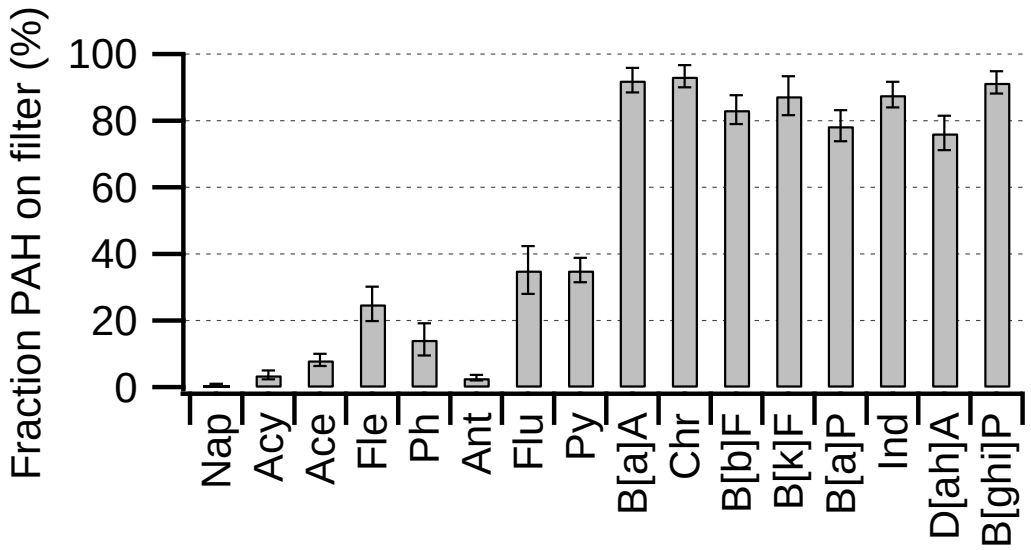

Figure 5.2. Average particle-phase mass fraction of PAH species of all different fuel types in the current study. The error bars represent the standard error of the calculated emission factors.

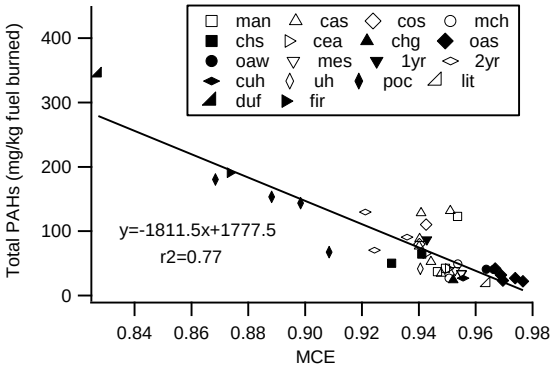
man cas cos mch
chs cea chg oas
oaw mes 1yr 2yr
cuh uh poc lit
duf fir
y=-1811.5x+1777.5
r2=0.77
Total PAHs (mg/kg fuel burned)
MCE

(a)

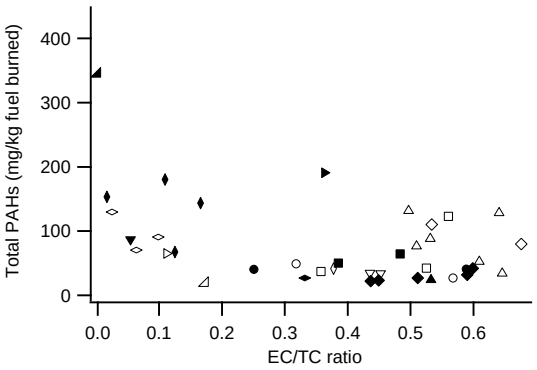
Total PAHs (mg/kg fuel burned)
EC/TC ratio

(b)

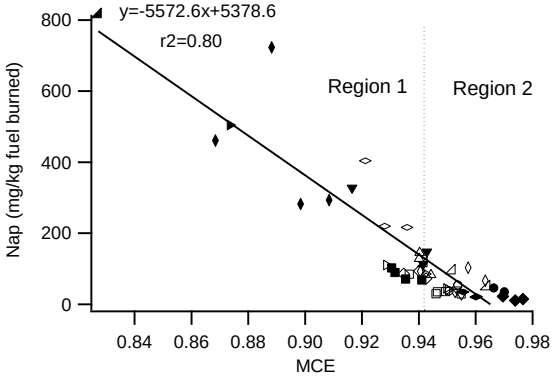
y=-5572.6x+5378.6
r2=0.80
Region 1
Region 2
Nap (mg/kg fuel burned)
MCE

(c)

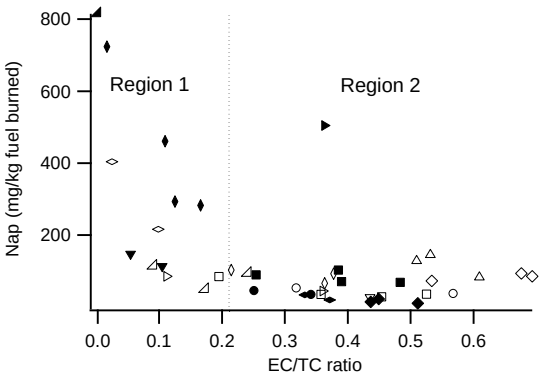
Region 1
Region 2
Nap (mg/kg fuel burned)
EC/TC ratio

(d)

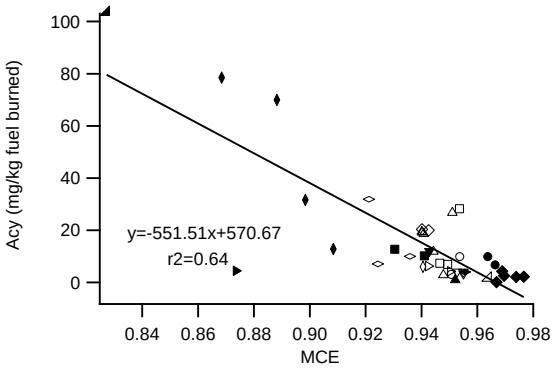
y=-551.51x+570.67
r2=0.64
Acy (mg/kg fuel burned)
MCE

(e)

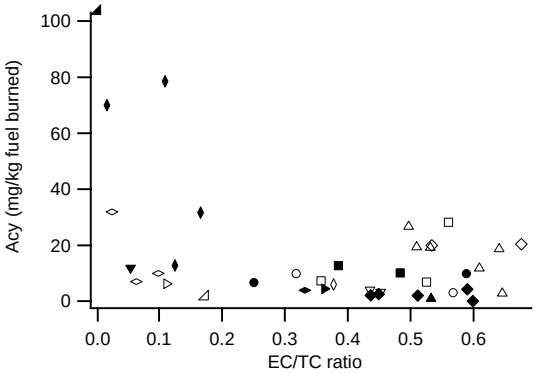
Acy (mg/kg fuel burned)
EC/TC ratio

(f)

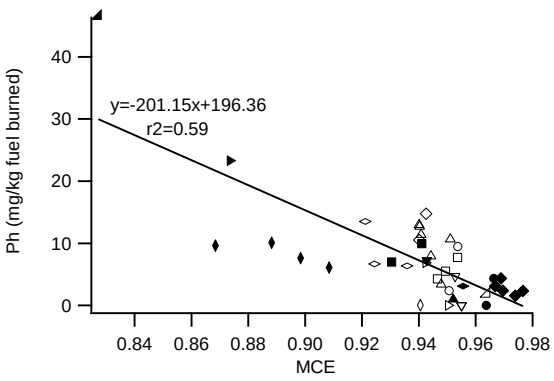
y=-201.15x+196.36
r2=0.59
Ph (mg/kg fuel burned)
MCE

(g)

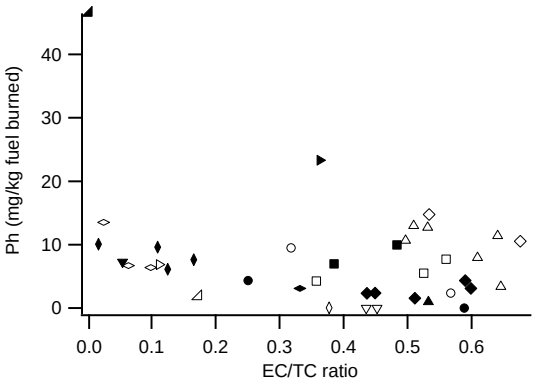
Ph (mg/kg fuel burned)
EC/TC ratio

(h)

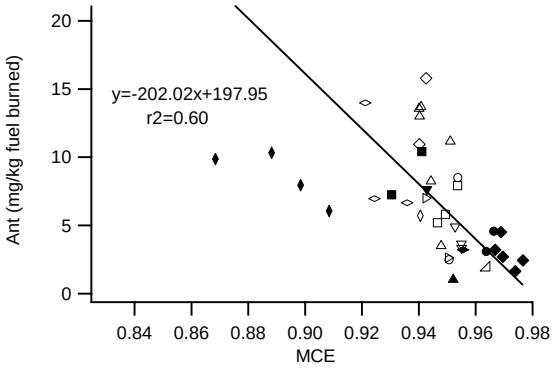
y=-202.02x+197.95
r2=0.60
Ant (mg/kg fuel burned)
MCE

(i)

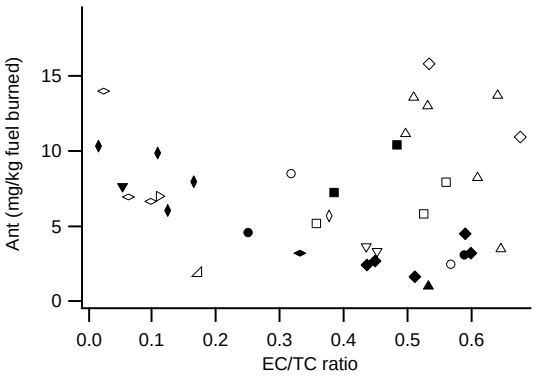
Ant (mg/kg fuel burned)
EC/TC ratio

(j)

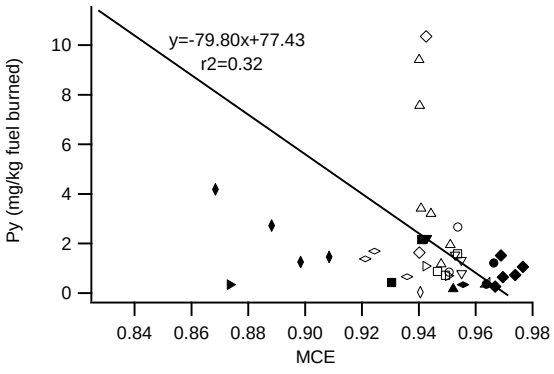
y=-79.80x+77.43
r2=0.32
Py (mg/kg fuel burned)
MCE

(k)

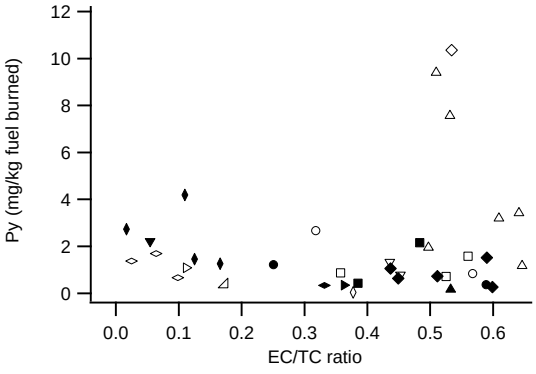
Py (mg/kg fuel burned)
EC/TC ratio

(l)

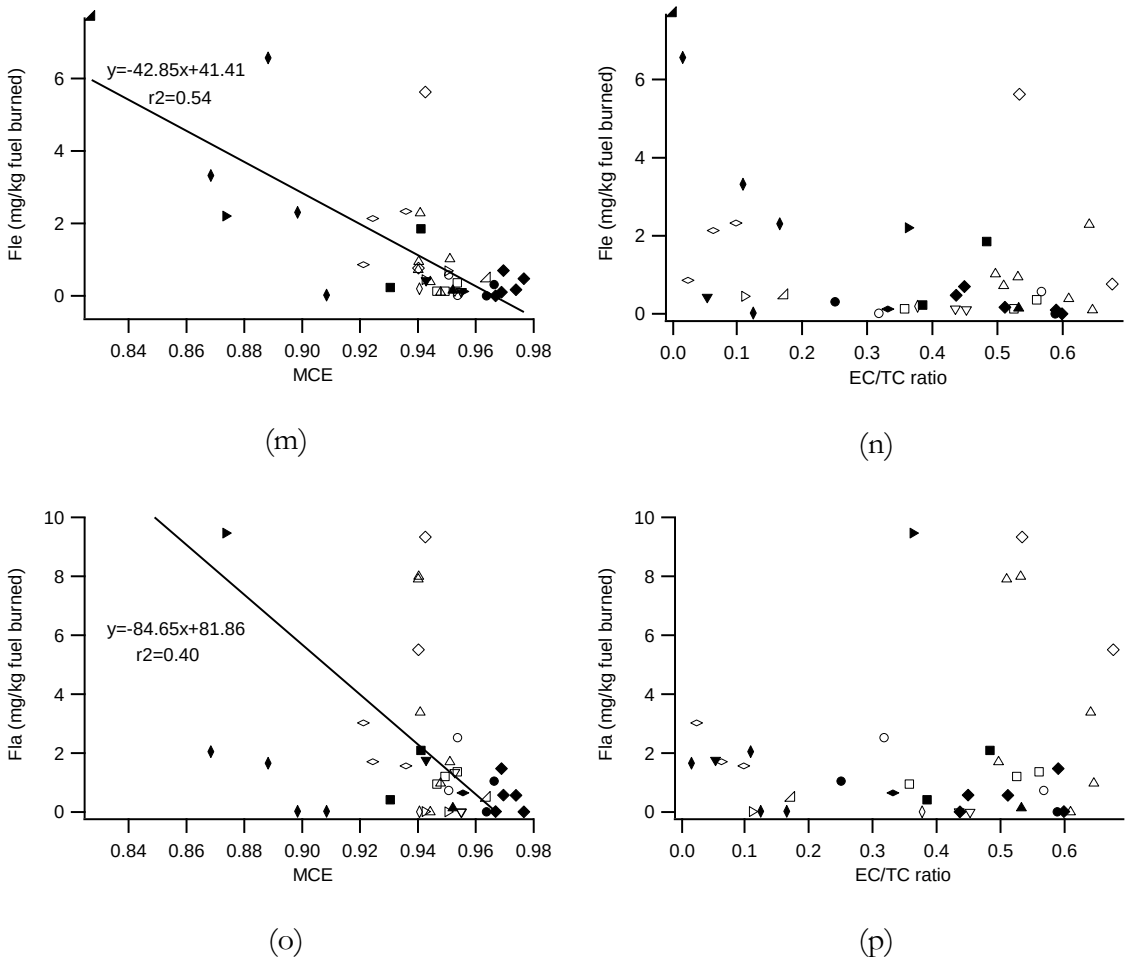

Figure 5.3. Plots of emission factors of Nap, Acy, Ph, Ant, Py, Fle, Fla, and total PAHs as a function of MCE and EC/TC ratio. Each fuel type is shown with a distinct symbol, and symbols are the same for all the sub-plots.

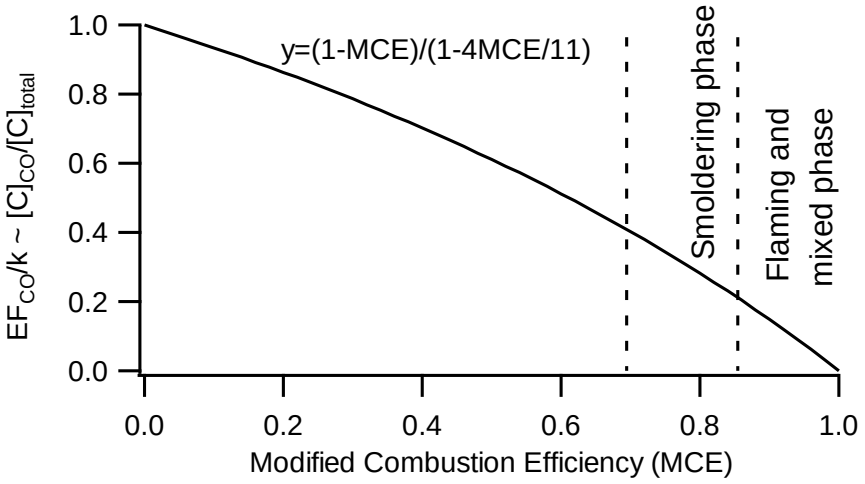

Figure 5.4. This plot shows theoretical emission factor of CO vs. MCE; the equation is formulated based on MCE and a proportionality factor; this proves that CO and all other co-emitted compounds such as formaldehyde, acetaldehyde, etc. can be linearly represented by MCE since they are all correlated with CO in the smoldering phase, but not during the flaming phase since the combustion regime changes.

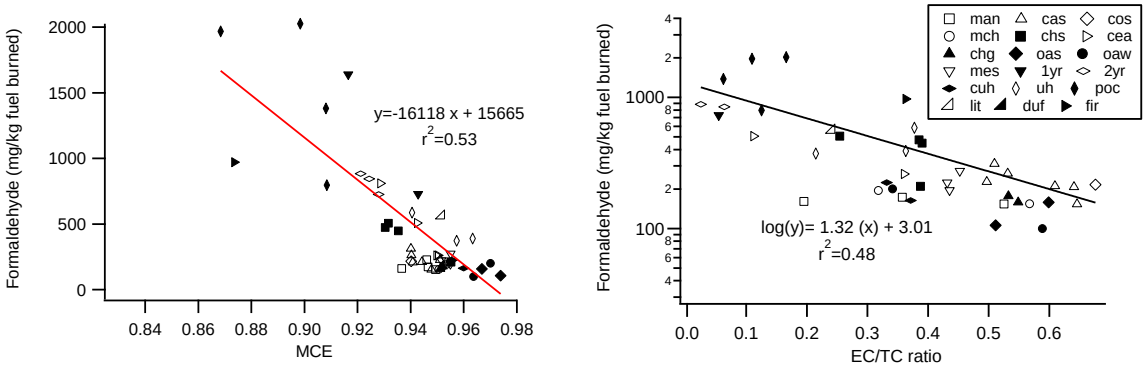

(a) (b)

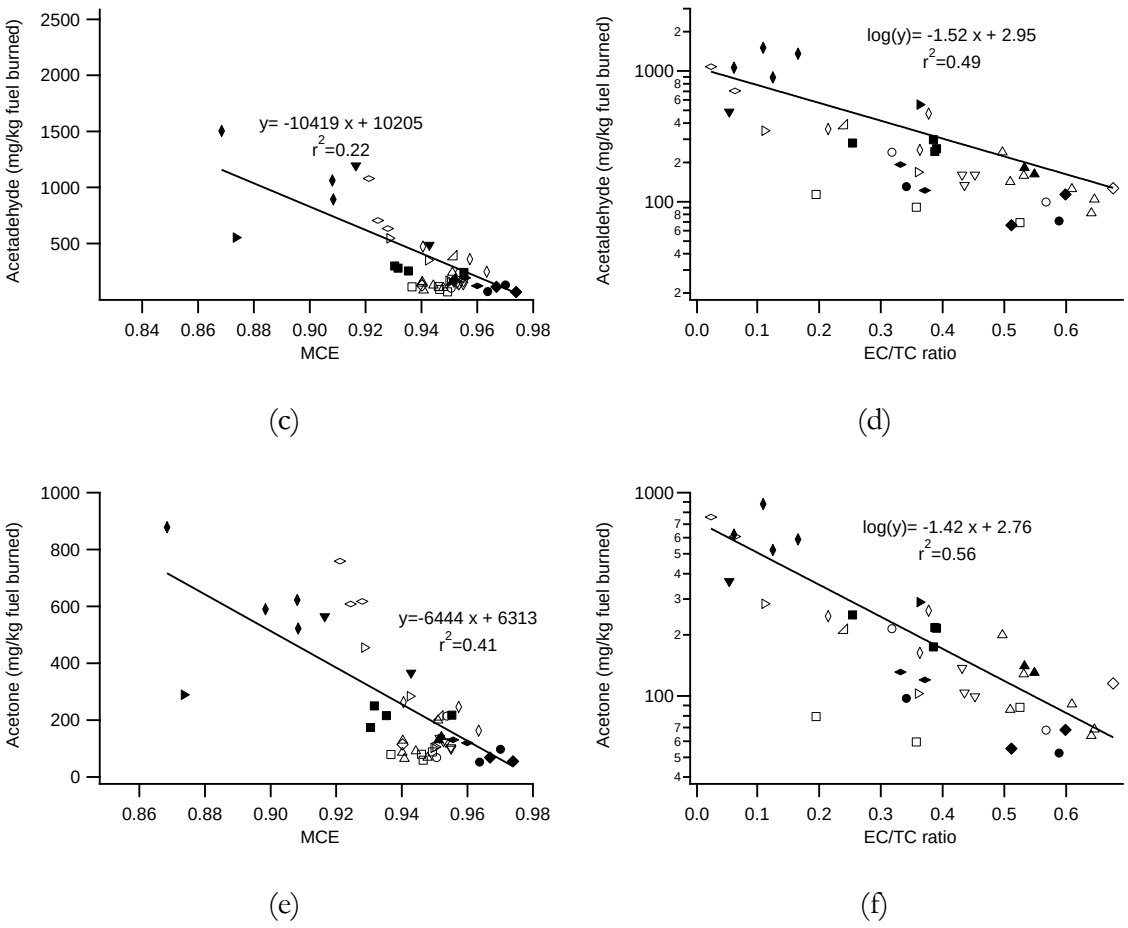

Figure 5.5. Plots of emission factors of formaldehyde, acetaldehyde and acetone as shown side by side a function of MCE and EC/TC ratio. Each fuel type is shown with a distinct symbol, and symbols are the same for all the sub-plots.

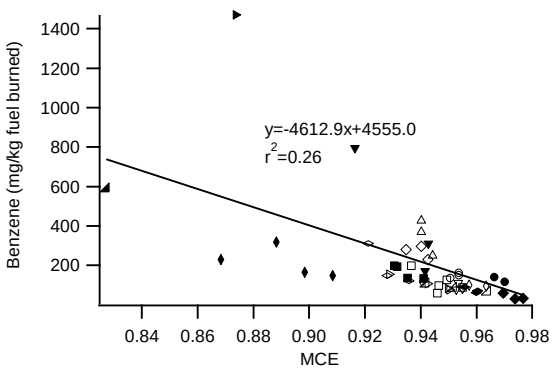
Benzene (mg/kg fuel burned)
y=-4612.9x+4555.0
r2=0.26
MCE

(a)

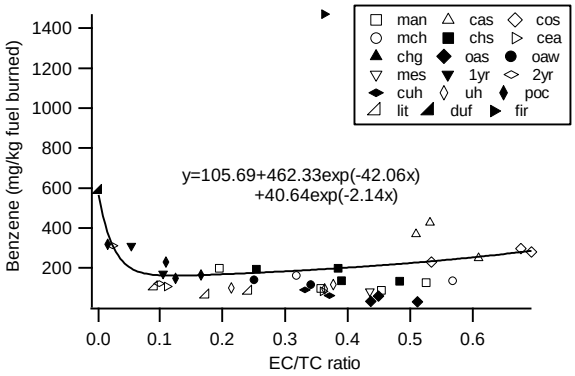
man cas cos
mch chs cea
chg oas oaw
mes 1yr 2yr
cuh uh poc
lit duf fir
Benzene (mg/kg fuel burned)
y=105.69+462.33exp(-42.06x)
+40.64exp(-2.14x)
EC/TC ratio

(b)

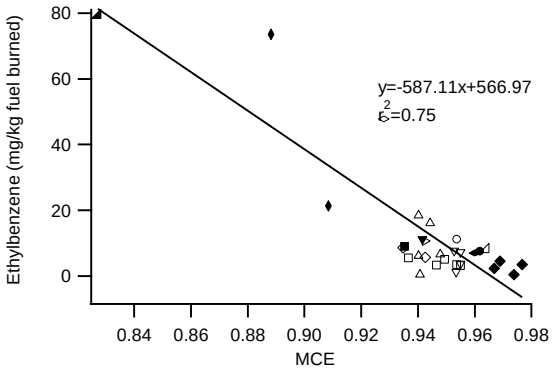
Ethylbenzene (mg/kg fuel burned)
y=-587.11x+566.97
r2=0.75
MCE

(c)

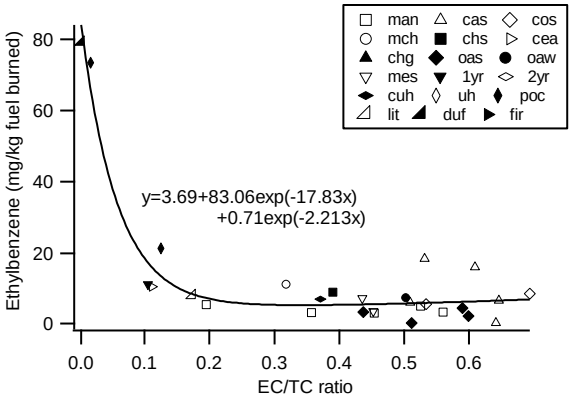
man cas cos
mch chs cea
chg oas oaw
mes 1yr 2yr
cuh uh poc
lit duf fir
Ethylbenzene (mg/kg fuel burned)
y=3.69+83.06exp(-17.83x)
+0.71exp(-2.213x)
EC/TC ratio

(d)

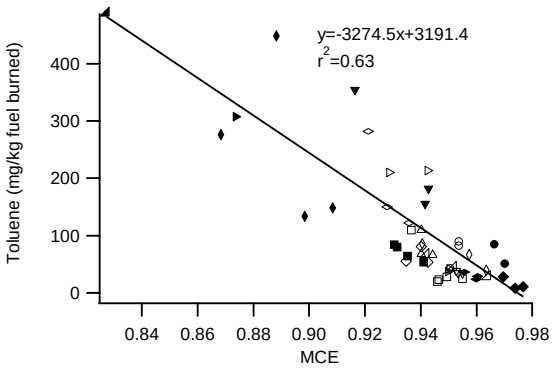
Toluene (mg/kg fuel burned)
y=-3274.5x+3191.4
r2=0.63
MCE

(e)

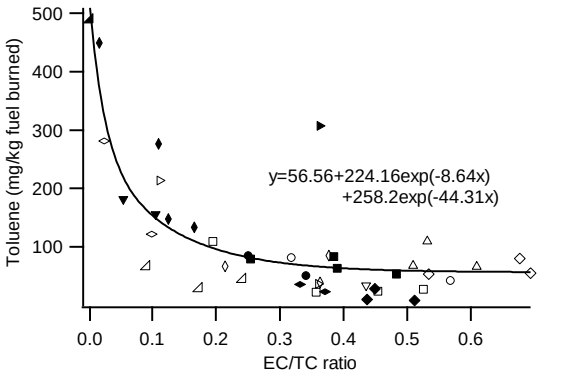
Toluene (mg/kg fuel burned)
y=56.56+224.16exp(-8.64x)
+258.2exp(-44.31x)
EC/TC ratio

(f)

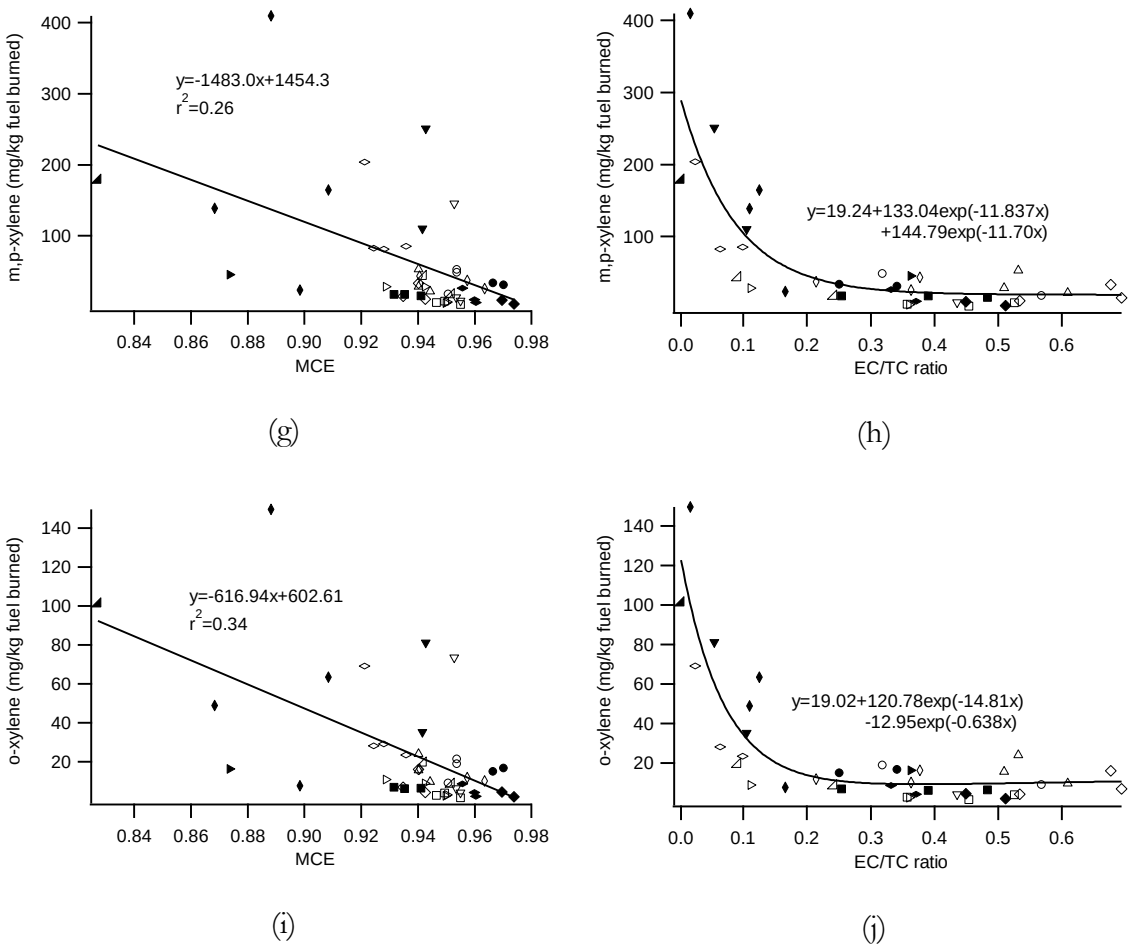

Figure 5.6. Plots of emission factors of benzene, ethylbenzene, o- and m,p-xylene as functions of MCE and EC/TC ratio shown side by side. Each fuel type is shown with a distinct symbol, and symbols are the same for all the sub-plots.

Chapter Six: A new biomass burning model for determining the fire intensity based carbon ratios

6.1. Abstract

Modified Combustion Efficiency has been widely used as an independent variable in the field of biomass burning. To study prescribed burns and wild fires, we developed a new model capable of determining degree of fire intensity and emission rates as a replacement for MCE based on laboratory tests of 22 SW/SE U.S. vegetation types. We suggest the ratio of elemental (EC) to total organic (TC) carbon, as a measure to correlate levoglucosan and polyaromatic hydrocarbons with fire intensity.

6.2. Introduction

Biomass burning is a dynamic process during which large concentrations of Particulate Matter (PM) and trace gases are released into the atmosphere (Andreae & Merlet, 2001; Guenther et al., 2006). Greenhouse gases, indirect formation of ozone (Pfister, Wiedinmyer, & Emmons, 2008, Sudo & Akimoto, 2007), and primary/secondary organic aerosols can result in local to global climatic air quality changes (Rosenfeld, 1999, Wiedinmyer et al., 2011). Prediction of these influences requires existence of an inventory of correct emission factors categorized based on *correct characterization of fire* and simulation packages *based on efficient models*.

Ward & Hardy, 1991 introduced combustion efficiency (CE), the ratio of total carbon emitted as CO_2 to the total amount of carbon released by the fire (including gas and particle-phase emissions), as an independent variable to model the emission release rate for open burning. Since the measurement of total hydrocarbons was a major challenge, another easier-to-use meter, Modified Combustion Efficiency (MCE), was developed (Ward & Hao, 1991; Ward & Radke, 1993) and has become widely used by the scientific community. MCE was defined as the excess (molar) ratio of CO_2 to CO plus CO_2 ($MCE=CO_2/(CO + CO_2)$). However, considering that nearly 95% of carbon release from biomass burning is in the form of CO and CO_2, MCE is another representation of the emission factor (EF) of CO, i.e. $1\text{-}MCE=CO/(CO+CO_2)$. Thus, if a compound can correlate with MCE, it correlates with CO as well. For example, lab and field Particulate Matter (PM) mass correlate very well with MCE, so PM mass has to correlate with CO emission factor too, and it does. Although Ward et al. recognized that MCE provided insight into the completeness of the combustion process, but did not explain all of the observed variances. MCE does not explicitly describe an important factor: flame dynamics and intensity. In the following, we will show how carbon ratio (EC/TC ratio) from a fire can be used as a better indicator of fire intensity.

6.3. Results and discussion

We observed large variations in the measured amount of levoglucosan relative to total organic carbon for different fuel types and burn conditions in the current study (Burling et al 2010). As an example, transient measurements of levoglucosan fragments ($C_3H_5O_2^+$ and $C_2H_4O_2^+$) vs. total organics emitted for two California chaparral fuel types (ceanothus and coastal sage scrub) suggest different rates of release (Figure 6.1). Since the slope estimates

differed significantly between fuel types, we considered fuel type to be an important factor in addition to fire-averaged MCE, which integrates flaming, smoldering, and mixed phases (Yokelson et al 1996). Nonetheless, none of the two parameters was able to explain the large variability observed in the dataset.

Levoglucosan molecules released during pyrolysis of woody fuel have to either get oxidized or break down into smaller molecules in the more intense fire zones. If oxidation is the most important parameter in the high MCE rage, a better correlation between levoglucosan and MCE is expected. However, the emission factor of levoglucosan (EF_{LG}) does not correlate well with MCE or EF_{CO} for all of the lab fires and fuel types in the current study (Figure 6.2-(a)).

The energy requirement to break bonds of cellulose and form monomers of levoglucosan is low, thus large quantities of levoglucosan are released during combustion stages (Simoneit et al., 1999) accompanied by low EC and high OC emissions due to low combustion temperatures. However, for more energetic combustion stages, levoglucosan structure is expected to further break into C_3-C_5 decides, oxalic acid, acetic acid, and formic acid and/or to lose oxygen contributing to the large production of simple molecules such as CO_2 (Gao, 2003) accompanied by higher EC and lower OC fraction in the PM. Consistent with this description, a strong relationship between EF_{LG} and the EC/TC ratio was observed (Figure 6.2-(b)). Therefore, it is inferred that EC/TC is an indirect measure of fire intensity capable of destructing levoglucosan molecules. Fire intensity is a measure of heat release rate. It has been shown that a higher intensity fire has a larger flame size (Wade, 1986,

Chandler et al., 1993) consistent with our observations of higher EC/TC ratio and larger flame size (Figure 6.3). No dependency of levoglucosan emissions on fuel type was detected.

The EC/TC ratio is also strongly related to the emissions of other organic compounds (Figure 6.4). The fluoranthene/OC ratio increases exponentially with increase in EC/TC ratio ($Fla/OC=0.09 + (EC/TC)^{4.36}$, $R^2=0.80$). The same trend was identified for Py/OC shown in Figure 6.4-c ($Py/OC=0.28+9.61\ (EC/TC)^{3.78}$, $R^2=0.81$), and also for benz[a]anthracene, chrysene, benzo[b] fluoranthene, benzo[k] fluoranthene, benzo[a] pyrene, benzo[ghi] perylene, dibenz[ah] anthracene, and indeno[1,2,3-cd] pyrene (shown in Figure 6.4-d). Acenaphthylene, acenaphthene, fluorene, phenanthrene, and anthracene did not seem to be correlated with EC/TC. In contrast to the previous group that had four or more fused aromatic rings, the exceptions in the second group had two or three rings and consequently higher vapor pressure (as opposed to more aromatic rings and lower vapor pressure), so depending on various factors such fire intensity and concentrations more variability is introduced to EFs. No trend could be observed in Figure 6.4-f between **Σ**PAH/OC ratio vs. MCE, the reason mainly lies within the underlying concept of PAH formation, which is not dependent on CO formation. It should be noted here that similar to levoglucosan, PAH EFs have been always reported with large variability when categorized based on MCE or fuel type.

Combustion especially when considering wildfires/prescribed burns is even more of a complex process. The majority opinion at present, supported by numerous experimental and modeling studies, is that soot particles form via PAHs. In fact, PAHs are precursors of soot formation. Formation of PAHs requires high temperature O_2-deprevated regions within the

main combustion zone as is dependent on a multitude of different reaction (Frenklach, 2002). It is shown that larger PAHs are formed by growth of smaller PAHs through HACA reactions (H_2 abstraction- C_2H_2 addition) (Frenklach, Clary, Gardiner, & Stein, 1985, Stein & Fahr, 1985) and also through H-atom migration (Michael Frenklach, Moriarty, & Brown, 1998). At some size PAH species begin to stick to each other during collision, thus forming PAH dimers. PAH dimers collide with PAH molecules forming PAH trimers or with other dimers forming PAH tetramers, and so on. Individual PAH species keep increasing in size via molecular chemical growth reactions. In this manner the moderate-sized PAH clusters evolve into solid particles (M. Frenklach & Wang, 1994). Moreover, these small particles will later form soot with core-shell structures. The core is made of aromatic compounds nucleated and grown when the flame temperature is high, and the shell is made of aliphatic compounds condensed when the gas temperature becomes somewhat lower (Wang, 2011). So based on the relative residence time of primary PAH and soot products in the main combustion zones, and availability of high temperature zones, the fire can turn more particulate carbon to graphitic carbon, i.e. higher EC/TC ratio.

Furthermore, there are also a number of numerical studies that defined soot as the accumulated weight of PAHs above a certain molecular weight. These studies could successfully predict the amount of soot (e.g.Frenklach et al., 1985). In addition, soot nucleation is likely to involve moderately sized PAHs (e.g. (Frenklach & Wang, 1994)). Due to all the chain-reactions that starts from the formation of the first benzene ring and eventually ends up in formation of soot, a higher ratio of soot to total carbon (EC/TC) is expected to indicate there has to be more PAHs in the total available particulate carbon.

Although measured MCE from a laboratory study and a field measurement can be very close, still there could be large differences in their measured EF PM. The flames in wildfires and prescribed burns are much larger (10-20m in height) compared to laboratory flames (max. 2m). Therefore, within the flame zone, temperatures are significantly higher and O_2-deprevation zones are more effective. These conditions are favorable towards soot formation. In another words, the fire has higher capacity for converting particulate carbon into graphitic carbon and for destructing more pyrolysis products (such as levoglucosan). In contrast, laboratory combustion of biomass engages mostly small size flames with consequently lower flame temperatures and more diffusive and convective oxygen, thus less EC/TC ratio.

We did not investigate heading/backing fires; however, our model is capable to explain why heading fire produces more PAH per unit mass OC. Heading fires significantly produce more PM mass per unit mass of fuel burned. However, backing fires produce significantly higher amount of PAHs. For example, the yield of B[a]P in the reported values by McMahon & Tsoukalas, 1987 for heading and backing fires of slash pines ranged from 238 to 3,454 and from 38 to 97 μg/kg fuel, respectively. Additionally, the EC/OC emission factors reported by McMeeking, 2008 for Montana sage, and pine needles clearly indicates ~40% increase in EC and ~70% decrease in OC formation rates going from heading to backing fire. These changes translate to ~4 times increase in EC/TC ratio which is a significant change according to our model. However, MCE for the same two burns showed only a minuscule increase of ~1.5%. These observations are consistent with observations of McMohan & Tsoukalas, 1987.

Levoglucosan has been extensively used as a tracer of biomass burning and also in the source apportionment models (Simoneit et al 1999, Lanz, et al., 2007, Schauer & Cass, 2000; Zheng, et al, 2002). However, without the knowledge of intensity of a fire (EC/TC ratio) use of levoglucosan concentration in source apportionment models may not lead to correct results, because the values in the literature are based on a limited number of laboratory and field test measurements without quantitatively relating levoglucosan emissions with fire characteristics.

The assumption that levoglucosan and EC do not undergo any change over transport times of several days (Fraser, 2000) might be used to estimate the amount of secondary OC formed in an aged smoke plume. The ratio of $(EC/TC)_{fresh}$ can be acquired from Figure 6.2 using a known EF_{LG}. Subtracting the OC_{fresh} from OC_{aged}, one can calculate the amount of secondary organics. The EF_{LG} can be estimated based on the mass emission ratio of levoglucosan to CO_2 multiplied by fire-averaged CO_2 emission factor or based on total carbon CO and CO_2 excess emissions. Among all field studies other than Kim Oanh et al., 2011, no other study could be found that has reported EF_{LG} and EC/TC ratios. Based on a LG/OC ratio of 464 mg/g OC from their reported field values and using Figure 6.2, OC_{fresh} turns out to be 355-422 mg/g OC that infers 5-25% increase in the OC due to aging. However, in a recent study Hoffmann, Tilgner, Iinuma, & Herrmann, 2010 suggested that levoglucosan may not be stable in the atmosphere as it was thought to be earlier (see also chamber study of Hennigan et al., 2010). Based on model calculations, they proposed daytime degradation rates of 4.7 ng $m^{-3}h^{-1}$ and 4.7 ng $m^{-3}h^{-1}$ for polluted continental summer

and winter atmospheres, respectively. However, the suggested degradation rates can be incorporated into source apportionment models as a corrective approach.

6.4. Conclusion

We proposed that the EC/TC ratio is a good measure of fire intensity and a better surrogate for determining phase of combustion. Correlation of MCE with the fire most important factor i.e. heat release rate is overlooked by most studies. MCE is basically EF_{CO}. CO correlates very well with PM mass, CH_4, etc.; thus, these compounds correlate very well with emission factor of CO or MCE. Fire is a very complex process; due to different heat release rates, combustion of a block of fuel with known amount of mass and fuel characteristics and another block with twice as much mass and the same fuel characteristics will result in dissimilar emissions profiles. In the current study, EC/TC ratio correlated exponentially with the PAH/OC in the gas phase, and could perfectly explain why some burns lead to orders of magnitude higher levoglucosan emissions. Based on the results of this study, EC/TC ratio can be used as indirect measure of fire intensity. It was also shown that the amount of secondary organics in the particle phase of an aged smoke plume can be calculated using the estimated EF of aged levoglucosan and $(EC/TC)_{aged}$ and comparing these values with the values obtained from the plot of emission factor of levoglucosan against EC/TC ratio presented in the current study.

6.5. Acknowledgments

Funding for this study came from the US Department of Defense Strategic Environmental Research and Development Program projects RC-1647, RC-1648, and RC-1649. We

appreciate the assistance of personnel at USMC Camp Lejeune, US Army Ft. Huachuca, Ft. Hunter-Liggett, Ft. Benning, and Vandenberg Air Force Base in selecting fuel types for study. Authors are grateful to Robert Yokelson and Ian Burling for FTIR data and Wei Mein Hao, Shawn Urbanski, Cyle Wold, Joey Chong, Emily Lincoln, and Jim Reardon for their help.

6.6. References

40CFR Part 1065 (2205). Code of Federal Regulations, 2005, Washington DC.

Andreae, M. O., & Merlet, P. (2001). Emission of trace gases and aerosols from biomass burning. Global Biogeochemical Cycles, 15(4), 955-966.

Birch, M. E., & Cary, R. a. (1996). Elemental Carbon-Based Method for Monitoring Occupational Exposures to Particulate Diesel Exhaust. Aerosol Science and Technology, 25(3), 221-241. doi:10.1080/02786829608965393

Chandler, C. (1983). Fire in forestry. v. 1. New York: Wiley. 300 p.

Dobbins, R. A., & Subramaniasiavam, H. (1994). Soot precursor particles in flames. Soot Formation in Combustion: Mechanisms and Models (p. 290). Heidelberg: Springer-Verlag.

D'Anna, A., D'Alessio, A., & Minutolo, P. (1994). Spectroscopic and chemical characterization of soot inception processes in premixed laminar flames at atmospheric pressure. In H. Bockhorn (Ed.), Soot Formation in Combustion: Mechanisms and Models (p. 83). Heidelberg: Springer Verlag.

Fraser, M. P. (2000). Using Levoglucosan as a Molecular Marker for the Long-Range Transport of Biomass Combustion Aerosols. Environmental Science & Technology, 34(21), 4560-4564.

Frenklach, Michael, Clary, D. W., Gardiner, W. C., & Stein, S. E. (1985). Detailed kinetic modeling of soot formation in shock-tube pyrolysis of acetylene. Symposium (International) on Combustion, 20(1), 887-901. doi:10.1016/S0082-0784(85)80578-6

Frenklach, Michael, Moriarty, N. W., & Brown, N. J. (1998). Hydrogen migration in polyaromatic growth. Symposium (International) on Combustion, 27(2), 1655-1661. doi:10.1016/S0082-0784(98)80004-0

Frenklach, M., & Wang, H. (1994). Detailed Mechanism and Modeling of Soot Particle Formation. In H. Bockhorn (Ed.), Soot Formation in Combustion: Mechanisms and Models. Springer-Verlag.

Frenklach, M. (2002). Reaction mechanism of soot formation in flames. Physical Chemistry Chemical Physics, 4(11), 2028-2037. The Royal Society of Chemistry. doi:10.1039/b110045a

Gao, S. (2003). Water-soluble organic components in aerosols associated with savanna fires in southern Africa: Identification, evolution, and distribution. Journal of Geophysical Research, 108(D13). doi:10.1029/2002JD002324

Graham, S. C., Homer, J. B., & Rosenfeld, J. L. J. (1975). The Formation and Coagulation of Soot Aerosols Generated by the Pyrolysis of Aromatic Hydrocarbons. Proceedings of the Royal Society A: Mathematical, Physical and Engineering Sciences, 344(1637), 259-285. doi:10.1098/rspa.1975.0101

Guenther, A., Karl, T., Harley, P., Wiedinmyer, C., Palmer, P. I., & Geron, C. (2006). Estimates of global terrestrial isoprene emissions using MEGAN (Model of Emissions of Gases and Aerosols from Nature). Atmospheric Chemistry & Physics Discussions, 6, 107-173. Retrieved from http://adsabs.harvard.edu/abs/2006ACPD.6.107G

Haynes, B. S., & Wagner, H. G. (1982). The Surface Growth Phenomenon in Soot Formation. Zeitschrift für Physikalische Chemie, 133(2), 201-213. Akademische Verlagsgesellschaft. doi:10.1524/zpch.1982.133.2.201

Hennigan, C. J., Sullivan, A. P., Collett, J. L., & Robinson, A. L. (2010). Levoglucosan stability in biomass burning particles exposed to hydroxyl radicals. Geophys. Res. Lett, 37, L09806.

Hoffmann, D., Tilgner, A., Iinuma, Y., & Herrmann, H. (2010). Atmospheric Stability of Levoglucosan: A Detailed Laboratory and Modeling Study. Environmental Science and Technology, 44(2), 694-699. doi:10.1021/es902476f

Kim Oanh, N. T., Ly, B. T., Tipayarom, D., Manandhar, B. R., Prapat, P., Simpson, C. D., & Sally Liu, L. J. (2011). Characterization of particulate matter emission from open burning of rice straw. Atmospheric Environment, 45(2), 493-502. Elsevier.

Lanz, V. A., Alfarra, M. R., Baltensperger, U., Buchmann, B., Hueglin, C., & Prévôt, A. S. H. (2007). Source apportionment of submicron organic aerosols at an urban site by factor analytical modelling of aerosol mass spectra. Atmospheric Chemistry and Physics, 7(6). Retrieved from http://adsabs.harvard.edu/abs/2007ACP.7.1503L

McMahon, C. K., & Tsoukalas, S. N. (1987). Polynuclear aromatic hydrocarbons in forest fire smoke. In P. W. Jones & R. I. Freudenthal (Eds.), Carcinogenesis (pp. 61-73). Raven Press.

McMeeking, G. R. (2008). The optical, chemical, and physical properties of aerosols and gases emitted by the laboratory combustion of wildland fuels. Ph.D. dissertation, Colorado State University.

Pfister, G. G., Wiedinmyer, C., & Emmons, L. K. (2008). Impacts of the fall 2007 California wildfires on surface ozone: Integrating local observations with global model simulations. Geophysical Research Letters, 35(19), L19814. American Geophysical Union. doi:10.1029/2008GL034747

Qi, L., Hosseini, S., Jung, H., Yokelson, R., Weise, D., Cocker, D., Huang, Y. (2012). Chemical Characterization of Particle Emissions from Controlled Burns of Biomass Fuels using a High Resolution Time-of-Flight Aerosol Mass Spectrometer. Atmospheric Chemistry and Physics Discuss., 12, 8397-8432, doi:10.5194/acpd-12-8397-2012, 2012

Rosenfeld, D. (1999). TRMM observed first direct evidence of smoke from forest fires inhibiting rainfall. Geophysical Research Letters, 26(20), 3105. American Geophysical Union. doi:10.1029/1999GL006066

Schauer, J. J., & Cass, G. R. (2000). Source Apportionment of Wintertime Gas-Phase and Particle-Phase Air Pollutants Using Organic Compounds as Tracers. Environmental Science & Technology, 34(9), 1821-1832. American Chemical Society. doi:10.1021/es981312t

Simoneit, B.R.T., Schauer, J.J., Nolte, C.G., Oros, D.R., Elias, V.O., Fraser, M.P., Rogge, W.F., Cass, G.R. (1999) Levoglucosan, a tracer for cellulose in biomass burning and atmospheric particles, Atmospheric Environment, 33(2), 173-182, doi:10.1016/S1352-2310(98)00145-9.

Stein, S. E., & Fahr, A. (1985). High-temperature stabilities of hydrocarbons. The Journal of Physical Chemistry, 89(17), 3714-3725. American Chemical Society. doi:10.1021/j100263a027

Sudo, K., & Akimoto, H. (2007). Global source attribution of tropospheric ozone: Long-range transport from various source regions. Journal of Geophysical Research, 112(D12), D12302. American Geophysical Union. doi:10.1029/2006JD007992

Wade, D. D. (1986). Linking fire behavior to its effects on living plant tissue. In: Forests, the world, and the profession Proceeding: Society of american Foresters Annual Convention. Bethesda, MD: Society of American Foresters: 112-116.

Wang, H. (2011). Formation of nascent soot and other condensed-phase materials in flames. Proceedings of the Combustion Institute, 33(1), 41-67. doi:10.1016/j.proci.2010.09.009

Ward, D.E., & Hao, W.M. (1991) Projection of emissions from burning of biomass for use in studies of global climate and atmospheric chemistry. 84th Paper 91-128.4

Ward, D. E., & Hardy, C. C. (1991). Smoke emissions from wildland fires. Environment International, 17(2-3), 117-134. doi:10.1016/0160-4120(91)90095-8

Ward D. E., & Radke, L. F. (1993). Emission measurements from vegetation fires: comparative evaluation of methods and results. In P. J. Crutzen & J. G. Goldammer (Eds.), Fire in the Environment: The Ecological, Atmospheric and Climatic Importance of Vegetation Fires (pp. 53-76). John Wiley.

Wiedinmyer, C., Akagi, S. K., Yokelson, R. J., Emmons, L. K., Al-Saadi, J. A., Orlando, J. J., & Soja, A. J. (2011). The Fire Inventory from NCAR (FINN): a high resolution global model to estimate the emissions from open burning. Geoscientific Model Development, 4(3), 625-641. doi:10.5194/gmd-4-625-2011

Zheng, M., Cass, G. R., Schauer, J. J., & Edgerton, E. S. (2002). Source Apportionment of PM2.5 in the Southeastern United States Using Solvent-Extractable Organic Compounds as Tracers. Environmental Science & Technology, 36(11), 2361-2371. American Chemical Society.doi:10.1021/es011275x

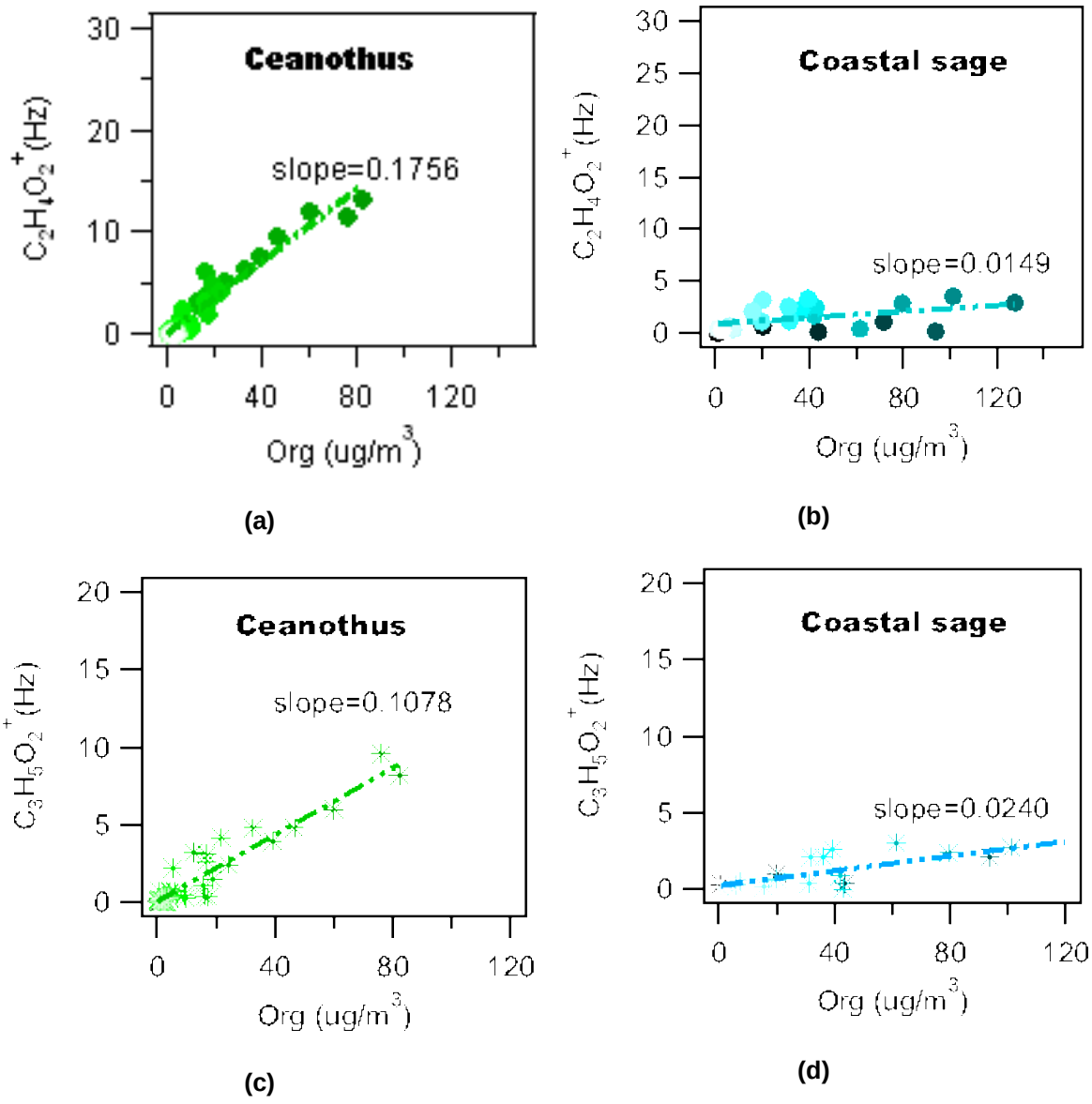

Figure 6.1. Transient measurement of (a),(b) $C_2H_4O_2^+$ and (c),(d) $C_3H_5O_2^+$ ions (levoglucosan fragments) against total organics of aerosol phase emissions for ceanothus and coastal sage; scrub fuel types (darker color represent the beginning of combustion and brighter means more towards the end of burns); levoglucosan fragments measured using AMS (Qi et al, 2012)

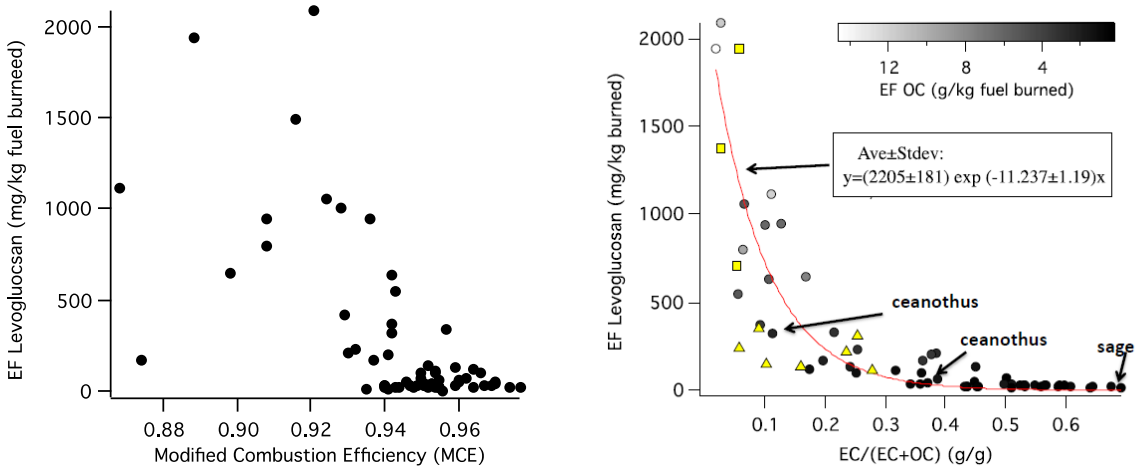

(a) (b)

Figure 6.2. Emission factor of levoglucosan plotted against (a) modified combustion efficiency (MCE) and (b) elemental carbon to total carbon ratio for all the burns; the amount of levoglucosan per kg fuel burned exponentially decreased with the increase in charring capacity (EC to TC ratio)

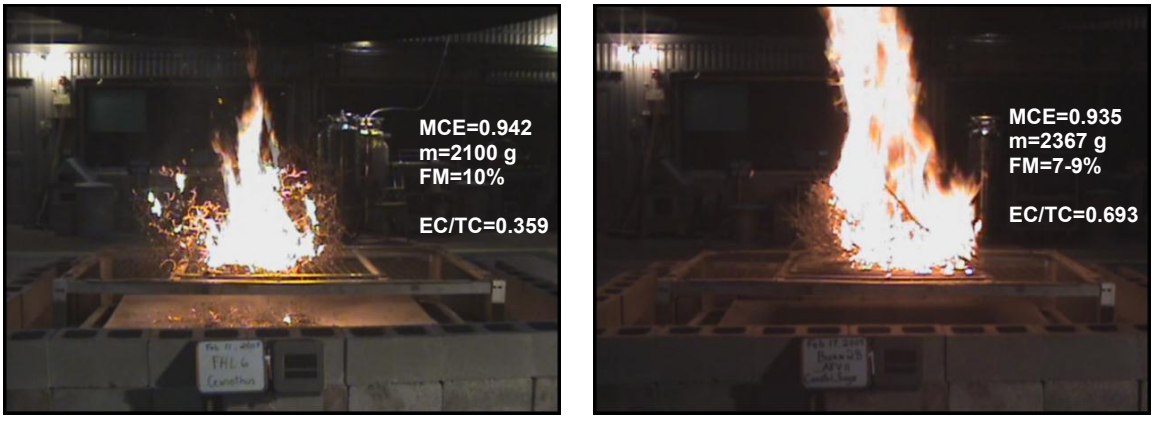

(a) Ceanothus (b) Coastal Sage

Figure 6.3. Comparison of flame sizes of (a) ceanothus and (b) coastal sage; more vigorous combustion of coastal sage led to larger flame size, i.e. more intense fire, and thus higher EC/TC ratio compared to ceanothus

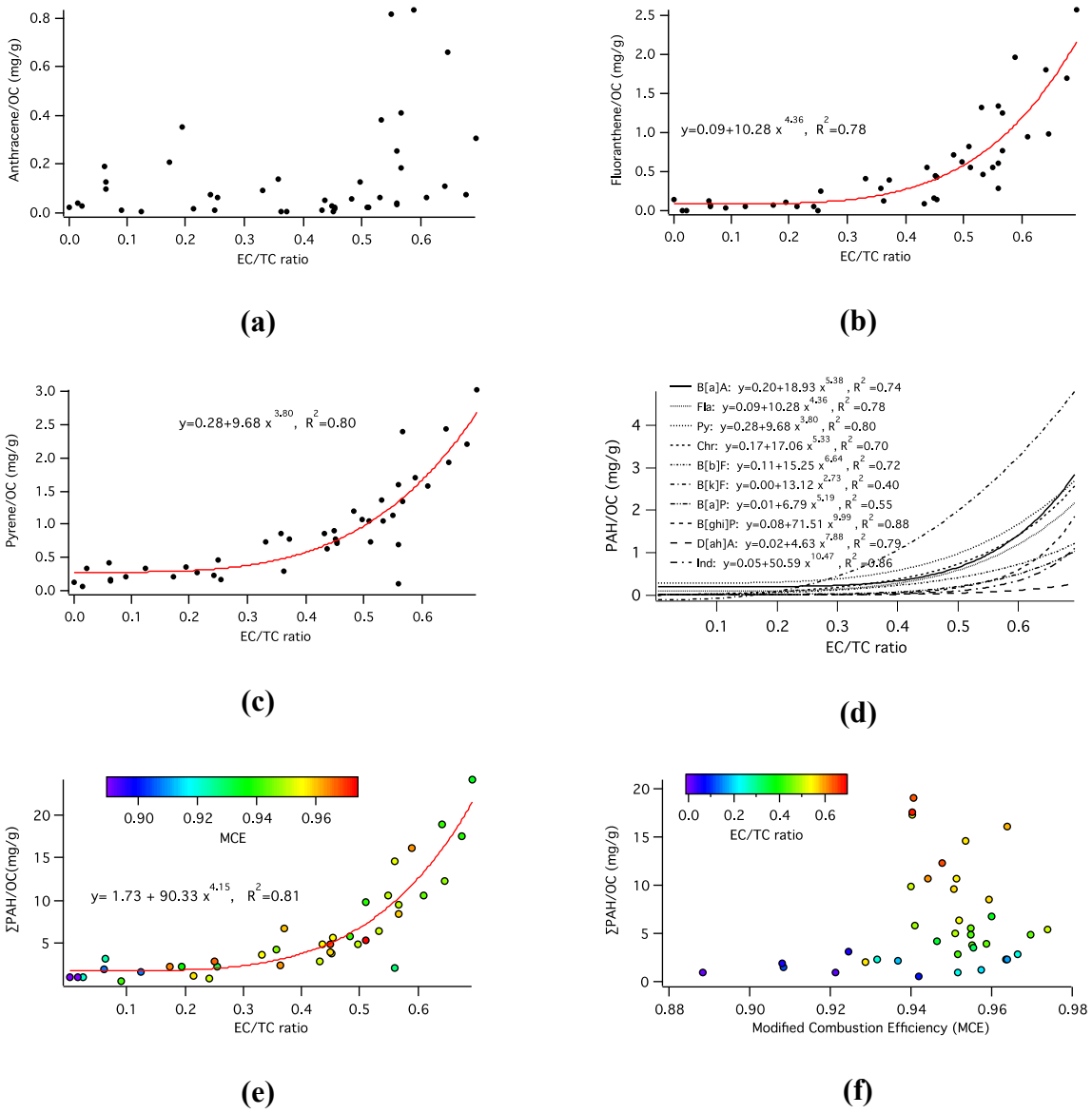

Figure 6.4. These figures represent the relation between formation rate of select PAHs versus elemental carbon to total carbon (EC/TC) ratio. An exponential growth with increase in charring capacity of the fire (EC/TC ratio) has been observed for PAHs with higher number of fused aromatic rings. No trend was identified for PAHs with lesser No. Aromatic rings such as Acy, Ace, Fle, Ph, An, etc.

Chapter Seven: Conclusions

The overall objective of this study was to improve characterization of emissions under flaming and smoldering with respect to volatile organic compounds and reactive gases, heavy metal and ions, and particulate matter. This goal was achieved through numerous laboratory combustion of wildland fuels from southeast and southwest US, and simulating the fires in a similar way to what happens in nature.

Chapter 2 investigates the effect of adding low-density polyethylene to piled silvicultural debris on smoke emissions. A series of experiments were conducted with varying amounts of polyethylene: 0.0, 0.25, and 2.50 wt% PE mixed with 2 kg of manzanita wood, and then the pile was ignited. Gaseous and particulate emissions were sampled during the entire flaming and mixed combustion phases and during a portion of the smoldering phase. An analysis of variance (ANOVA) coupled with general linear model accounting for effects of Modified Combustion Efficiency (MCE), polyethylene content and block effect was performed on 195 individually measured compounds. Results clearly showed that only 3M-Octane increased with increasing polyethylene content. Fluoranthene, pyrene, indeno(1,2,3-cd) pyrene, and M-cyclo pentane were also affected, however the statistical analysis could not identify any trend for these compounds.

Chapter 3 extends our knowledge of size of smoke particles from wildland fires and prescribed burns. 77 burns of SW and SE fuels were conducted at the FSL in Missoula, MT. Due to the smoke being fresh, major mode of size distribution was in the range of 29-52nm.

Most of the fuels resulted in unimodal size distribution during flaming phase and strong bimodal distribution during smoldering phase. Comparing the size and mass distribution, we reported that 61-68% of particle mass was in the range of 0.5 to 10 μm. Plots of geometric mean diameter of particles vs. instantaneous MCE were presented in which a triangular pattern was found that could better differentiate combustion phases. It was found that geometric mean diameter rapidly increases during flaming and gradually decreases during mixed and smoldering phase combustion, unlike previous studies reporting larger particle size during smoldering phase and smaller particles during flaming phase.

Chapter 4 represents detailed chemical and physical characterization of PM in smoke from combustion of SW and SE fuels. To determine relative amount of flaming and smoldering, we used Modified Combustion Efficiency of Ward, D.E. and Radke, 1993. In general, fuels from SW burned at a higher MCE compared to the fuel from SE resulting in lower PM emission factors. Fuel moisture greatly influenced the MCE. We observed that for fuel moistures less than 20%, the upper and lower bounds of fuel moisture vs. MCE plot sharply converged to MCE=1 and the bounds were defined by data points from backing/heading fires. However, the data presented in this study does not seem to be enough for drawing a definitive conclusion, and more experiments to relate fuel moisture, slope and wind is needed. The EC/TC ratio sharply increased as the MCE passed 0.94. This point might be in a turning point in the combustion characteristics, which cannot be captures using MCE. We also reported that PAH diagnostic ratios were observed to be poor indicators of biomass burning. Large fuel-type and regional dependency was observed in the emission rates of ammonium, nitrate, fluoride, chloride, sodium, ammonium, and potassium.

In continuation of chapter 4, chapter 5 investigates the emissions of gas-phase PAHs, carbonyls, and select volatile organic compounds. The statistical analysis showed that there is regional and fuel type dependency among the reported emission factors. However, considering the dependency of emissions on fuel moisture and effect of MCE on emissions, it may be concluded that fuel type and region have little effect on hydrocarbon emissions. We also showed that the EF CO can be approximated with a linear function based on a non-linear function of MCE. Similar to what is shown for EF OC in chapter 3, we observed a sudden change of behavior for many other compounds at MCE>0.94 in this chapter. We believe that the problem is due to definition of MCE; when the fire regime changes to flaming, the combustion pathways no longer support linearity of emissions with CO emissions. Therefore, emission factor of compounds (e.g. naphthalene) fails to conserve linearity with respect to MCE. It seems that MCE significantly compresses a large portion of system changes, i.e. EC/TC ratio of 0.2-0.6, into a small fraction of MCE range, i.e. 0.94<MCE<1.0, thus giving the false impression of linearity for most compounds. We suggested that emission factors are better segregated using Elemental Carbon to Total Carbon ratio (EC/TC) compared to the Modified Combustion Efficiency (MCE). More effort is still needed, to understand the underlying relation between different combustion parameters and the emission factors. Unfortunately, a very important fire parameter, the temperature, was not measured; this parameter needs to be accounted for in the future studies. Other than this, considering the fact that on-line instruments such as OP-FTIR and PTR-MS can measure instantaneous mixing ratios of

various compounds from a fire, measuring instantaneous EC and TC values to account for indirect measurement of fire intensity using instantaneous EC/TC ratio is beneficial.

In Chapter 6, MCE was shown to be a weak predictor of fire emission for compounds and species that weekly correlate with carbon monoxide; EC/TC ratio is proposed as a better surrogate of combustion intensity. Moreover, emissions of levoglucosan and PAHs in the particle phase were investigated, and it was turned out that the particle phase PAH/OC increases exponentially as the fire intensity (EC/TC ratio) increases and pyrolysis products such as levoglucosan decrease exponentially as the intensity decreases.